TECHNICAL REPORT STANDARD PAGE

1. Report No.	2. Government Accession No.	3. Recipient's Catalog No.
FHWA/LA-92/240		

4. Title and Subtitle	5. Report Date
PULL-OUT TESTING FACILITY FOR GEOSYNTHETICS	November 1992
	6. Performing Organization Code

7. Author(s)	8. Performing Organization Report No.
Khalid Farrag, Ph.D., Ilan Juran, Ph.D., and Yalcin Acar, Ph.D., P.E.	240

9. Performing Organization Name and Address	10. Work Unit No.
Civil Engineering Department Louisiana State University Baton Rouge, LA 70803	11. Contract or Grant No. 87-1GT

12. Sponsoring Agency Name and Address	13. Type of Report and Period Covered
Louisiana Transportation Research Center 4101 Gourrier Avenue Baton Rouge, LA 70808	Final Report (Second Edition)
	14. Sponsoring Agency Code

15. Supplementary Notes

Conducted in cooperation with the U.S. Department of Transportation, Federal Highway Administration.

16. Abstract

The considerable increase in using geosynthetics in soil reinforcement made it necessary to develop methods of measuring the interaction properties and modeling load transfer in reinforced-soil structures. The large number of factors that influence the interaction mechanism makes it difficult to standardize the equipment design, testing methodology and data interpretation procedure. The factors are mainly related to the equipment boundary effects, testing conditions, and soil and geosynthetics properties.

In order to develop a methodology for evaluating the interface properties of geogrids, a pull-out box and a direct shear box are constructed and instrumented. A testing program is conducted to evaluate the performance of the facility and the effect of different testing parameters (a.g. specimen dimensions, soil thickness, box boundary effects, pull-out rate, soil compaction and relative density, and confining pressure) on the pull-out interaction mechanism of geogrids. Standard equipment design and testing procedure are recommended to overcome most of the limitations in the current practice.

A data analysis procedure is established to determine the interface properties and the confined reinforcement characteristics from pull-out test results. The data analysis incorporates the effect of reinforcement extensibility on the soil-geogrid interface mechanism. The interface parameters are evaluated through comparison with the results from tests performed in the large direct shear box.

17. Key Words	18. Distribution Statement
pull-out testing, direct shear testing, geosynthetics, geogrids, reinforced soil, sand	No restriction. This document is available to the public through the National Technical Information Services, Springfield, VA 22161.

19. Security Classif. (of this report)	20. Security Classif. (of this page)	21. No. of Pages	22. Price
Unclassified	Unclassified	225	

Form DOT F1700.7 (1-92)

PULL-OUT TEST FACILITY FOR GEOSYNTHETICS

by

Khalid Farrag, Ph.D.
Geosynthetics Engineering Research Lab
Louisiana Transportation Research Center
4101 Gourrier Ave.
Baton Rouge, LA 70808

Ilan Juran, Ph.D.
Professor and Head, Civil Engineering Department
Polytechnic University
333 Jay Street, Brooklyn
N.Y., N.Y. 11201

and

Yalcin B. Acar, Ph.D., P.E.
Professor, Civil Engineering Department
Civil Engineering Department
Louisiana State University
Baton Rouge, LA 70803

LTRC PROJECT NO. 87-1GT
STATE PROJECT NO. 736-12-24
FEDERAL AID PROJECT NO. HPR-0010(14)

conducted for

LOUISIANA DEPARTMENT OF TRANSPORTATION AND DEVELOPMENT
LOUISIANA TRANSPORTATION RESEARCH CENTER

in cooperation with
U.S. DEPARTMENT OF TRANSPORTATION
FEDERAL HIGHWAY ADMINISTRATION

The contents of this report reflect the view of the authors who are responsible for the facts and accuracy of the data presented herein. The contents do not necessarily reflect the views or the policies of the state, the Louisiana Department of Transportation and Development, the Louisiana Transportation Research Center, or the Federal Highway Administration. This report does not constitute a standard, specification, or regulation.

November 1992

ACKNOWLEDGMENTS

Pull-out Testing Facility for Geosynthetics is supported by Louisiana Transportation Research Center (LTRC), the Federal Highway Administration, the Louisiana Department of Transportation and Development, the Board of Regents of the State of Louisiana and the Civil Engineering Department of Louisiana State University. The financial support, collaboration and cooperation provided by these agencies and institutes are gratefully acknowledged.

The authors are grateful to Professor Ara Arman, Ex-Director of LTRC, and Professor Roger K. Seals, Ex-Chairman of the Civil Engineering Department for the time and effort they have given in founding the Geosynthetic Engineering Research Laboratory at LTRC. Professor Peter Stopher, Director of LTRC, Professor Richard Avent, Chairman of the Civil Engineering Department, Mr. William Temple, Director of Research at LTRC, and Mr. Paul Griffin, Administrator of Geophysical Systems at LTRC, are acknowledged for their effective collaboration and cooperation.

The efforts of the former graduate research assistants: Mr. Grant Knochenmus, in contributing to the comprehensive review of the available testing equipment, and Mr. C.L. Chen in providing the preliminary structural design of the first pull-out box, are gratefully acknowledged. We also appreciate the assistance of Dr. Adnen Guermazi, former post-doctoral research associate in the Civil Engineering Department, in the implementation of the data acquisition for the first pull-out box.

Appreciations also extend to Mr. John Oglesby, Engineer Advanced at LTRC, for his technical discussions and contributions and to Mr. Kenneth Johnston and other LTRC personnel for their technical help in carrying out the testing program.

ABSTRACT

The considerable increase in using geosynthetics in soil reinforcement made it necessary to develop methods of measuring the interaction properties and modeling load transfer in reinforced-soil structures. The large number of factors that influence the soil-reinforcement interaction mechanism makes it difficult to standardize the equipment design, testing methodology, and data interpretation procedure. These factors are mainly related to the equipment boundary effects, testing conditions, and soil and geosynthetics properties.

In order to develop a methodology for evaluating the interface properties of geogrids, a large pull-out box and a direct shear box are constructed and instrumented. A testing program is conducted to evaluate the performance of the facility and the effect of different testing parameters (e.g. specimen dimensions, soil thickness, box boundary effects, pull-out rate, soil compaction and relative density, and confining pressure) on the pull-out interaction mechanism of geogrids. Standard equipment design and testing procedure are recommended in order to overcome most of the limitations in the current practice.

A data analysis procedure is established to determine the interface properties and the confined reinforcement characteristics from pull-out test results. The data analysis incorporates the effect of reinforcement extensibility on the soil-geogrid interface mechanism. The interface parameters obtained from the pull-out test results are evaluated through comparison with the results from tests performed in the large direct shear box.

IMPLEMENTATION STATEMENT

The testing methodology and procedure to determine the interface properties of geogrids in granular materials are established. The implementation of this research resulted in using the pull-out and direct shear boxes for evaluation studies and commercial research on several geogrids and granular soils. The results obtained from these testing equipment are accepted by the material manufacturers and outside firms as valid and usable.

The boxes are usable now to evaluate the confined behavior of geogrids under like conditions in highway construction practice and to establish Department specifications. Large direct shear tests, load-controlled, or displacement-controlled pull-out tests, can be conducted in performance asseement depending on the needs of the designers.

Further use of the boxes to establish design parameters for reinforced-soil structures will be achieved at the conclusion of the research project recently started. This project will provide data on the pull-out properties of geogrids in cohesive soils as well as verification by full scale pull-out testing in both granular and cohesive soils.

TABLE OF CONTENTS

		Page
ACKNOWLEDGEMENTS	. . . . .	iii
ABSTRACT	. . . . .	v
IMPLEMENTATION STATEMENT	. . . . .	vii
LIST OF TABLES	. . . . .	xi
LIST OF FIGURES	. . . . .	xiii
INTRODUCTION	. . . . .	1
OBJECTIVES OF THE RESEARCH	. . . . .	3
SCOPE OF THE RESEARCH	. . . . .	4
1 REVIEW OF THE EXISTING GEOSYNTHETIC TESTING PROCEDURES	. . . . .	5
1.1 IN-SOIL MECHANICAL PROPERTIES OF GEOSYNTHETICS	.	5
1.2 SOIL-GEOSYNTHETICS INTERFACE PROPERTIES	. . . . .	12
2 EQUIPMENT DESIGN AND INSTRUMENTATION	. . . . .	17
2.1 DESIGN CONSIDERATIONS	. . . . .	17
2.2 EQUIPMENT DESCRIPTION	. . . . .	19
2.2.A The Pull-out and Shear Box Details	. . . . .	19
2.2.B The Hydraulic Loading System	. . . . .	25
2.2.C The Sand Handling Facility	. . . . .	28
2.3 INSTRUMENTATION AND DATA ACQUISITION	. . . . .	30
2.3.A Load and Pressure Measurements	. . . . .	30
2.3.B Displacement Measurements	. . . . .	32
2.3.C Displacement-rate Measurements	. . . . .	32
2.3.D Data Acquisition System	. . . . .	35
3 TESTING PROCEDURE AND DATA INTERPRETATION	. . . . .	38
3.1 INTRODUCTION	. . . . .	38
3.2 SOIL COMPACTION AND SPECIMEN PREPARATION	. . . . .	39
3.2.A Soil Placement	. . . . .	39

		Page
	3.2.B Compaction Control	44
	3.2.C Reinforcement Preparation	48
3.3	DISPLACEMENT-RATE CONTROLLED TESTS	53
	3.3.A Unconfined Extension Tests	53
	3.3.B Pull-out Tests	55
	3.3.C Direct Shear Test	68
3.4	LOAD-CONTROLLED TESTS	74
4	**EFFECT OF TESTING PARAMETERS ON THE INTERACTION MECHANISM**	81
4.1	INTRODUCTION	81
4.2	EFFECT OF TESTING PARAMETERS ON PULL-OUT RESPONSE	84
	4.2.A Effect of Reinforcement Dimensions	84
	4.2.B Effect of Sleeve Length	91
	4.2.C Effect of Soil Thickness	101
	4.2.D Effect of Displacement-Rate	105
	4.2.E Effect of Soil Density	111
	4.2.F Effect of Confining Pressure	116
5	**ANALYSIS OF PULL-OUT TEST RESULTS**	122
5.1	INTRODUCTION	122
5.2	MODELING LOAD TRANSFER IN PULL-OUT TESTS	129
6	**CONCLUSIONS AND RECOMMENDATIONS**	137
6.1	CONCLUSIONS	137
6.2	RECOMMENDATIONS FOR A STANDARD TESTING METHOD FOR GEOGRID PULL-OUT IN GRANULAR SOILS	139
REFERENCES		145
APPENDIX A	**EQUIPMENT DETAILS**	151
APPENDIX B	**INSTRUMENTS SPECIFICATIONS**	163
APPENDIX C	**PULL-OUT TEST RESULTS**	175

LIST OF TABLES

Table		Page
3.1	UNCONFINED EXTENSION TESTS ON GEOGRID	53
3.2	TESTING PARAMETERS IN PULL-OUT TESTING SET NO. 1 . .	56
3.3	TESTING PARAMETERS IN PULL-OUT TESTING SET NO. 2 . .	60
3.4	TESTING PARAMETERS IN DIRECT SHEAR TESTS	69
3.5	STEPPED LOAD-CONTROLLED TESTS	78
4.1	PULL-OUT TESTING PARAMETERS FOR EVALUATION OF GEOGRID DIMENSIONS	86
4.2	PULL-OUT TESTING PARAMETERS FOR EVALUATION OF SLEEVE LENGTH	93
4.3	PULL-OUT TESTING PARAMETERS FOR EVALUATION OF SOIL THICKNESS	102
4.4	COMPARISON BETWEEN DISPLACEMENT-RATES IN DIFFERENT PULL-OUT BOXES	106
4.5	PULL-OUT TESTING PARAMETERS FOR EVALUATION OF DISPLACEMENT-RATE	107
4.6	PULL-OUT TESTING PARAMETERS FOR EVALUATION OF SOIL DENSITY	112
4.7	PULL-OUT TESTING PARAMETERS FOR EVALUATION OF CONFINING PRESSURE	117

LIST OF FIGURES

Figure		Page
1.1	Results of unconfined and confined extension tests on geotextiles	6
1.2	Confined extension testing devices on geotextiles	7
1.3	Confined extension testing apparatus	9
1.4	Confined extension testing apparatus	10
1.5	'Zero Span' confined extension apparatus	11
1.6	Triaxial cell with reinforced soil sample	11
1.7	Soil-geosynthetic direct shear test devices	13
1.8	Geosynthetic pull-out test devices	14
2.1	Side view of the pull-out box	20
2.2	Top view of the pull-out box	21
2.3	View of the large direct shear box	22
2.4-a	Longitudinal cross-section of the pull-out box	23
2.4-b	Cross-section of the pull-out box	23
2.5	Longitudinal cross-section of the direct shear box	24
2.6	View of the hydraulic ram and the loading frame	26
2.7	View of the hydraulic loading system	27
2.8	View of the sand handling facility	29
2.9	Data acquisition supporting instruments	31
2.10	Detail of the LVDT connection at the rear table	33
2.11	Displacement instrumentation of the geogrid	34
2.12	Schematic view of the data acquisition system	36
2.13	View of the data control system	37
3.1	Grain size distribution of the blasting sand	40
3.2	Results of direct shear tests on the sand	41
3.3	View of the elevated hopper and the two boxes	42
3.4	Sand placement scheme in the pull-out box	43
3.5	Soil density measurements in the pull-out box	45

Figure		Page
3.6	Locations of soil density measurements	46
3.7	Relationship between sand density and compaction	47
3.8	Geometric configuration and specifications of Tensar-SR2	49
3.9	Placement of the geogrid in pull-out box	50
3.10	Placement of the geogrid in the direct shear box	51
3.11	Locations of displacement measurement along the geogrid in pull-out box	52
3.12	Unconfined extension test results on the geogrid	54
3.13	Frictional resistance of the clamping plates in the pull-out box	57
3.14	Pull-out test results on geogrids, Set No. 1	58
3.15	Pull-out Test results on geogrids, Set No. 1	59
3.16	Pull-out Test results on geogrids, Set No. 2	61
3.17	Typical time-nodal displacements measurements in Set No. 1 tests	63
3.18	Time-nodal displacements measurements in Set No. 1 tests	64
3.19	Displacements along the geogrid nodes in pull-out	65
3.20	Normalized displacements along geogrids in Set No. 1 tests	67
3.21	Frictional resistance of upper box in direct shear test	70
3.22	Results of direct shear tests on sand-sand interface	71
3.23	Results of direct shear tests on geogrid-sand interface	72
3.24	Effect of reinforcement on the frictional resistance in direct shear test	73
3.25	Illustration of creep concept	75
3.26	Determination of the critical creep load	75
3.27	Loading scheme in load-controlled extension tests	76
3.28	Axial strains versus time in unconfined load-controlled tests	76
3.29	Concept of strain superposition in stepped loading tests	77
3.30	Loading scheme in stepped load-controlled pull-out test	79
3.31	Front displacement versus time in load-controlled pull-out test	80
4.1	Load transfer mechanism between soil and geogrid	82
4.2	Soil-reinforcement interaction mechanism for geosynthetics	83
4.3	Locations of the pressure cells in the pull-out box	85

Figure		Page
4.4	Effect of side wall friction on confining pressure	85
4.5	Placement of 2.5 ft wide geogrid specimen in the box	87
4.6	Pull-out test results on geogrids of different widths	88
4.7	Pull-out test results on geogrids of different lengths	90
4.8	Effect of wall roughness on pull-out test results	92
4.9	Effect of sleeve length on the pull-out resistance of geogrid	94
4.10	Effect of sleeve length on the pull-out resistance of geogrid	95
4.11	Schematic diagram of the locations of earth pressure cells	96
4.12-a	Earth pressure on the front wall [no-sleeves]	98
4.12-b	Earth pressure on the front wall [sleeve length 8-inches]	98
4.12-c	Earth pressure on the front wall [sleeve length 12-inches]	99
4.13	Effect of sleeve length on lateral earth pressure	100
4.14	Effect of sleeve length on the normalized displacement along the geogrid	100
4.15	Effect of soil thickness on pull-out resistance	103
4.16	Effect of soil thickness on the normalized displacement along the geogrid	104
4.17	Effect of displacement-rate on pull-out response	108
4.18	Effect of displacement-rate on pull-out response	109
4.19	Effect of displacement-rate on pull-out resistance	110
4.20	Effect of displacement-rate on normalized displacement along the geogrid	110
4.21	Effect of soil density on the pull-out resistance of geogrid	113
4.22	Effect of soil density on the pull-out resistance of geogrid	113
4.23	Variation of pull-out response with soil density	114
4.24	Effect of soil density on displacement distribution along the geogrid . .	115
4.25	Effect of confining pressure on the extension properties of geotextiles . .	118
4.26	Relationship between the efficiency factor and confining pressure . .	119
4.27	Effect of confining pressure on the pull-out resistance of geogrid . .	120
4.28	Effect of confining pressure on the pull-out resistance of geogrid . .	120
4.29	Effect of confining pressure on displacement distribution along the geogrid	121
5.1	Displacement measurements along the geogrid in pull-out	123

Figure		Page
5.2	Displacement distribution along the geogrid	124
5.3	Computed pull-out displacements along the reinforcement	128
5.4	Numerical simulation of pull-out test on woven strips	128
5.5	Displacement distribution along geogrid nodes	130
5.6	Schematic diagram of the discretized geogrid	131
5.7	Confined stress-strain relationship of the geogrid	131
5.8	Interface shear stress-displacement relationship for the geogrid	133
5.9	Interface shear stress-displacement relationship for the geogrid	134
5.10	Analytical and experimental shear stress-displacement relationship . .	135
5.11	Analytical and experimental displacement distribution along the geogrid	136
5.12	Analytical pull-out load distribution along the geogrid	136

INTRODUCTION

The considerable development of local and interstate highway systems in Louisiana has stimulated a growing interest in using geosynthetics for reinforcement of highway embankments and slopes. The use of geosynthetics as reinforcement elements in such structures imposes an economical and practical solution against the increasing costs of construction and the necessity to construct embankments on marginal sites with the available poor backfill soils. In view of the growing use of these materials, the Louisiana Department of Transportation and Development (LADOTD) and Louisiana Transportation Research Center (LTRC) have found it necessary to construct an adequate testing facility and develop an appropriate procedure for evaluating short and long term performance of geosynthetic reinforcement.

A wide variety of geosynthetic materials are now available for civil engineering applications (1,2,3). In selecting a specific geotextile or geogrid for reinforcement of embankments and slopes, the following aspects of performance should be considered:

i) stress-strain relationship and creep behavior of the reinforcement when placed in the soil,

ii) pull-out performance of the reinforcement and its load transfer mechanism.

Studies on the stress-strain and creep properties of geotextiles and geogrids are primarily conducted on unconfined samples (4,5,6,7,8). A testing procedure for determining the tensile properties of unconfined geotextile samples has been established (9). However, geosynthetics exhibit a more complex soil-interaction mechanism which raises major difficulty in interpreting unconfined test results to the actual behavior of these materials in soil. When geosynthetics are embedded in the soil, their stress-strain properties are significantly affected by soil confinement (10,11). Non-uniform shear stress-strain distributions are developed along the soil-geosynthetic interface with a large portion of shear strains being mobilized near the loading application point (12,13). Consequently, results from unconfined tests differ from those obtained under confined conditions and can not be used to determine the appropriate design parameters for the soil-reinforcement systems.

Various modified direct shear and pull-out boxes have been utilized to investigate the confined material properties, interface shear stress-strain relationships and pull-out resistance of geosynthetics (14,15,16,17,18). However, standard testing procedure for the determination of the confined reinforcement properties does not, yet, exist. The large number of factors that

affect the interface properties of the confined reinforcement raises major difficulties in comparing test results, and results in a wide scatter in the available results (11,19). These differences in results are primarily due to the use of different testing devices, the associated boundary effects, testing procedures, and soil placement and compaction schemes.

The Geosynthetic Engineering Research Lab (GERL) at LTRC was developed to provide a methodology for evaluation of the interaction properties of the geosynthetic reinforcement. For this purpose, a large pull-out box and a large direct shear box are constructed, the effect of various testing conditions are evaluated, and a testing procedures and data interpretation scheme are established. The report presents the design details, testing procedure and performance evaluation of the pull-out/direct shear testing facility. An interpretation scheme and analysis of test results are developed in order to determine the interface properties and shear parameters at the soil-geosynthetic interface.

The report contains a summarized review of the existing testing equipment and procedures in order to assess the limitations of the current testing procedures and the effect of testing parameters on the results. A detailed review of the state of testing and practice of geosynthetic reinforcement has been previously conducted (19) in order to provide guidelines for the design of the GERL testing facility. The report presents a description and specifications of the equipment, instrumentation, data acquisition system, and testing procedure and methodology. A parametric study on the effect of various testing parameters on the interaction mechanism and the interpretation of test results are also presented.

OBJECTIVES OF THE RESEARCH

In order to develop a methodology for evaluation of the in-soil mechanical characteristics and interface properties of geosynthetic reinforcement, it is necessary to establish reliable testing equipment, procedure, and appropriate interpretation scheme. The specific objectives of this research are:

i) to design, construct and calibrate pull-out box and a large direct shear box which will provide the capability of evaluating the confined behavior of different types of geogrids and geotextiles,

ii) to develop a reliable testing procedure and data interpretation method for evaluation of the short term and long term pull-out performance of geosynthetic reinforcements,

iii) to evaluate the effect of various testing parameters on the interaction mechanism of geosynthetic reinforcement and on the performance of the testing facility,

iv) to develop a data analysis procedure for interpretation of test results and determination of the interface properties and the in-soil material characteristics,

v) to establish guidelines for technical evaluation of geosynthetics performance.

SCOPE OF RESEARCH

The scope of this research focuses on testing and performance evaluation of geogrid reinforcement in dense granular soils. The selected type of geogrid, commonly used in soil reinforcement applications, is "Tensar SR2". The soil used, a uniform grain size blasting sand, is selected for relatively ease of handling. The research involves four tasks:

1. Review of the existing testing Procedures: A comprehensive review of the available testing equipment, procedures, and data interpretation methods was previously conducted (19) in order to evaluate the limitations of the current state of practice and to provide guidelines for the design of the testing facility.
2. Design of large pull-out and large direct shear boxes: These boxes are designed, constructed, and instrumented for evaluation of both short term and long term geogrid performance. The testing facility is designed to provide the capability of conducting two basic testing modes: (a) displacement-rate controlled and (b) load controlled modes. In the displacement-rate controlled mode, the geogrid is subjected to a constant pull-out displacement-rate during the test and the pull-out load is recorded. This testing procedure (which is most commonly used) provides the interface parameters related to the short term performance of the reinforcement such as peak and residual pull-out resistance and front displacement at the peak pull-out load. In the load controlled mode, pull-out loads are applied incrementally to the inclusion and maintained constant during a specified period. The displacements along the inclusion are recorded and data interpretation yields time-dependent response parameters related to the long term performance of the geogrids.
3. Performance evaluation study: Pull-out and direct shear testing programs are developed in order to evaluate the performance of the facility (i.e. the reproducibility of the results and accuracy of the monitoring system), to assess the effect of the rigid boundaries on test results, and to provide a data base for development of testing procedures (e.g. soil compaction, loading mode and displacement rate).
4. Development of data analysis procedure: A data interpretation scheme is developed in order to determine the interface properties of geogrid reinforcements.

CHAPTER 1

REVIEW OF THE EXISTING GEOSYNTHETIC TESTING PROCEDURES

The in-soil mechanical characteristics and interface properties of geosynthetics have been experimentally modelled by monitoring:

i) the in-soil mechanical properties of the geosynthetic (i.e. its confined stress-strain relationship and creep behavior),

ii) the soil-geosynthetic interface properties (i.e. shear stress-strain relationship and pull-out resistance).

Research on these parameters was conducted using various equipment and testing procedures which made it difficult to consistently compare the performance of different geosynthetic specimens. An evaluation of these equipment and testing procedures was previously conducted (19,20). The fundamental aspects of the state of testing of geosynthetics were reviewed in order to establish guidelines for the design of the testing facility.

1.1 IN-SOIL MECHANICAL PROPERTIES OF GEOSYNTHETICS

The unconfined stress-strain properties of geotextiles can be determined by testing the geotextile specimen in a wide width strip test (9). However, when the geosynthetic materials are embedded in the soil, their stress-strain properties are significantly affected by soil confinement (10,11). Results of confined extension tests (10,21) show that the confining pressure increases the tensile strength and deformation modulus of the geotextile material. Figure 1.1 demonstrates the effect of confining pressures on the deformation modulus and tensile strength of geotextiles. The effect of confinement can be more significant on geogrids; since, in addition to interface shear resistance, lateral earth resistance on the transversal elements restricts geogrid elongation and increases its deformation modulus.

Currently, no standard testing procedure or apparatus exists for measuring the "in-soil" stress-strain material properties. Several investigators have determined these properties by testing geotextiles in modified direct shear boxes (Figure 1.2). In these boxes, the rear end of the specimen is clamped to the back of the box; while the front of the specimen is subjected to an extension force. Most of the modified direct shear boxes have dimensions similar to the

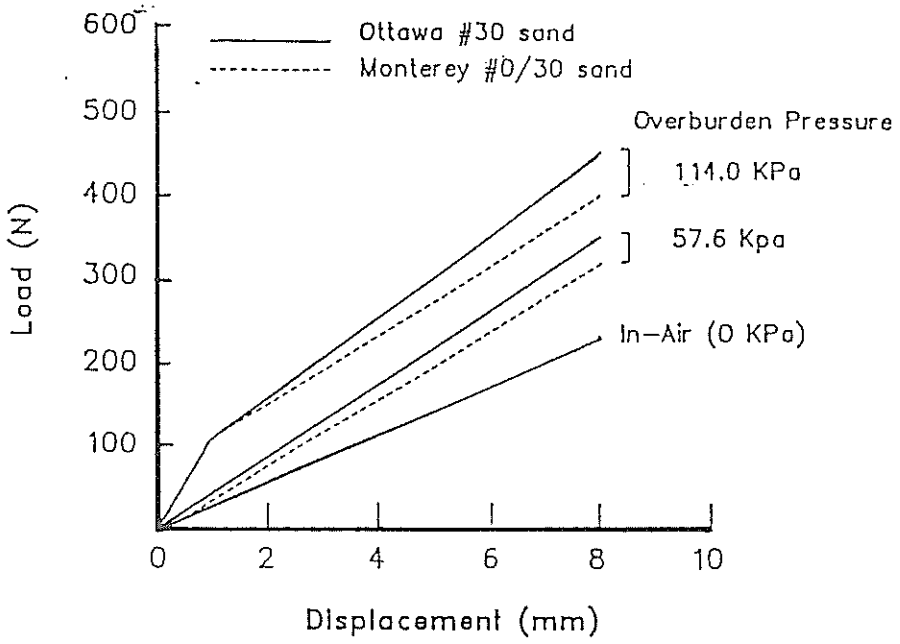

(a) After Siel et al. (21)

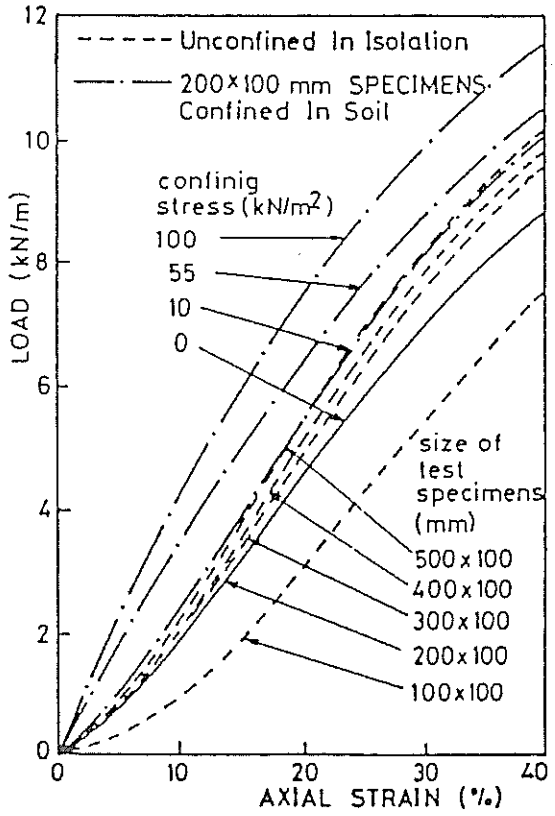

(b) After McGown et al. (10)

Figure 1.1 Results of unconfined and confined extension tests on geotextiles

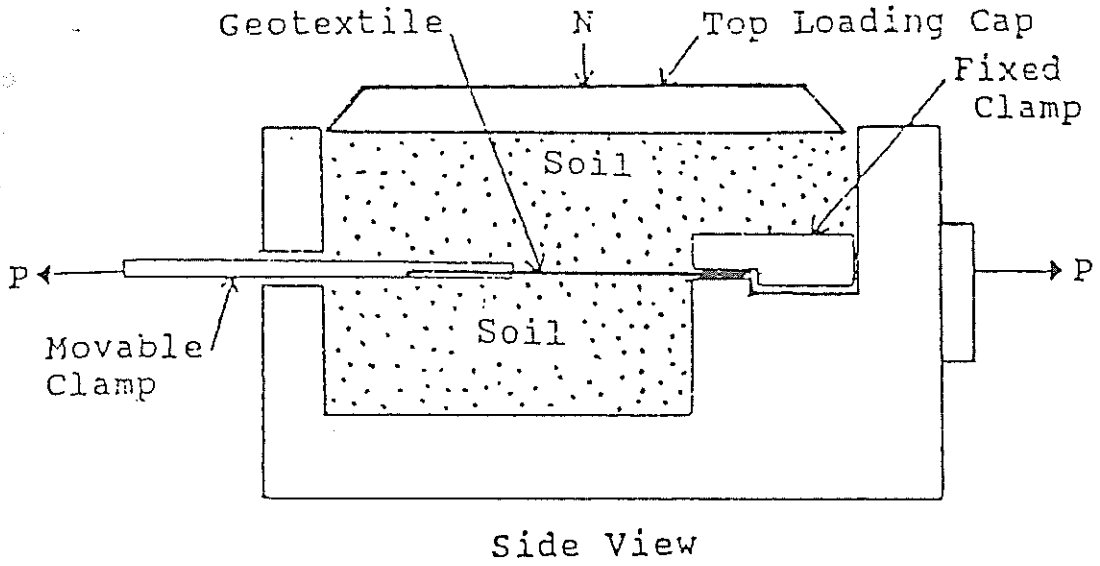

(a) After Siel et al. (21)

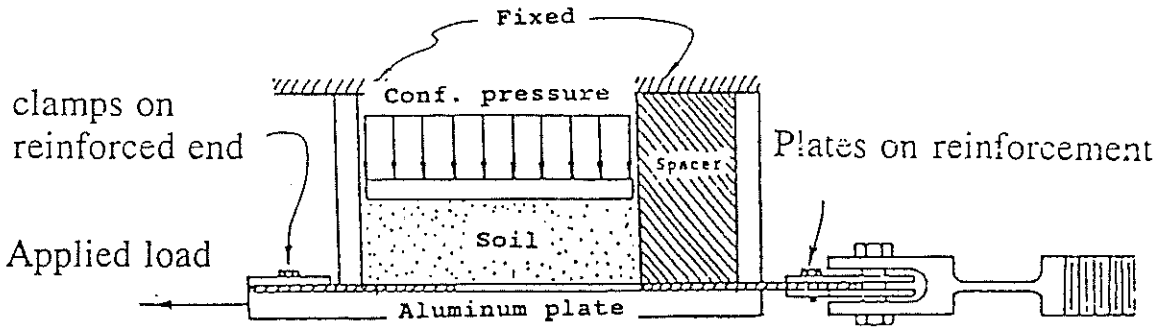

(b) After Leshchinsky and Field (22)

Figure 1.2 Confined extension testing devices on geotextiles

conventional ones (21, 22), where boundary effects on the interaction properties need to be investigated. Moreover, the elongation properties of large representative samples requires the use of relatively larger boxes (17,19).

McGown et al. (10) developed a custom-built apparatus (Figure 1.3) to evaluate the effect of confining pressure and specimen size on the confined extension properties of geotextiles. Their apparatus consists of two air pressure diaphragms, which are placed on each side of the geotextiles. A soil layer can be compacted between the diaphragm and the geotextile. Their results, shown in Figure 1.1, demonstrate the effect of confinement and sample dimensions on the confined properties of the geotextiles. In confined extension tests, shear strains are combined with material elongation along the specimen. Additional instrumentations to measure the displacement distribution along the specimen and load at the rear are necessary to de-couple the shear-extension effect. Knochenmus (23) developed a confined extension testing device (Figure 1.4) in which extension loads on both sides of the specimen and the developed pore pressures in the soil sample can be monitored.

Attempts have also been made to determine the confined stress-strain properties of the geotextiles using other devices. A 'zero span' confined tension test has been proposed (24) in which the specimen is confined by means of pressure controlled metal clamps. The apparatus is shown in Figure 1.5. Surface treatments were used on the clamp faces to simulate granular soil conditions. Several shortcomings of this apparatus are related to the difficulty in simulating the frictional conditions of the wide range of granular soils on the clamp surfaces. Moreover, the device does not account for many parameters influencing the confined extension properties such as soil dilatancy and soil particle interlocking on the specimen surface.

Triaxial tests have also been carried out to investigate the stress-strain properties and time-dependent behavior of samples reinforced with horizontal disks of fabrics (25,26). Figure 1.6 shows the reinforced soil sample in the triaxial test. In this test, strains in the fabric are difficult to be monitored and they are associated with different boundary conditions than those encountered in the field.

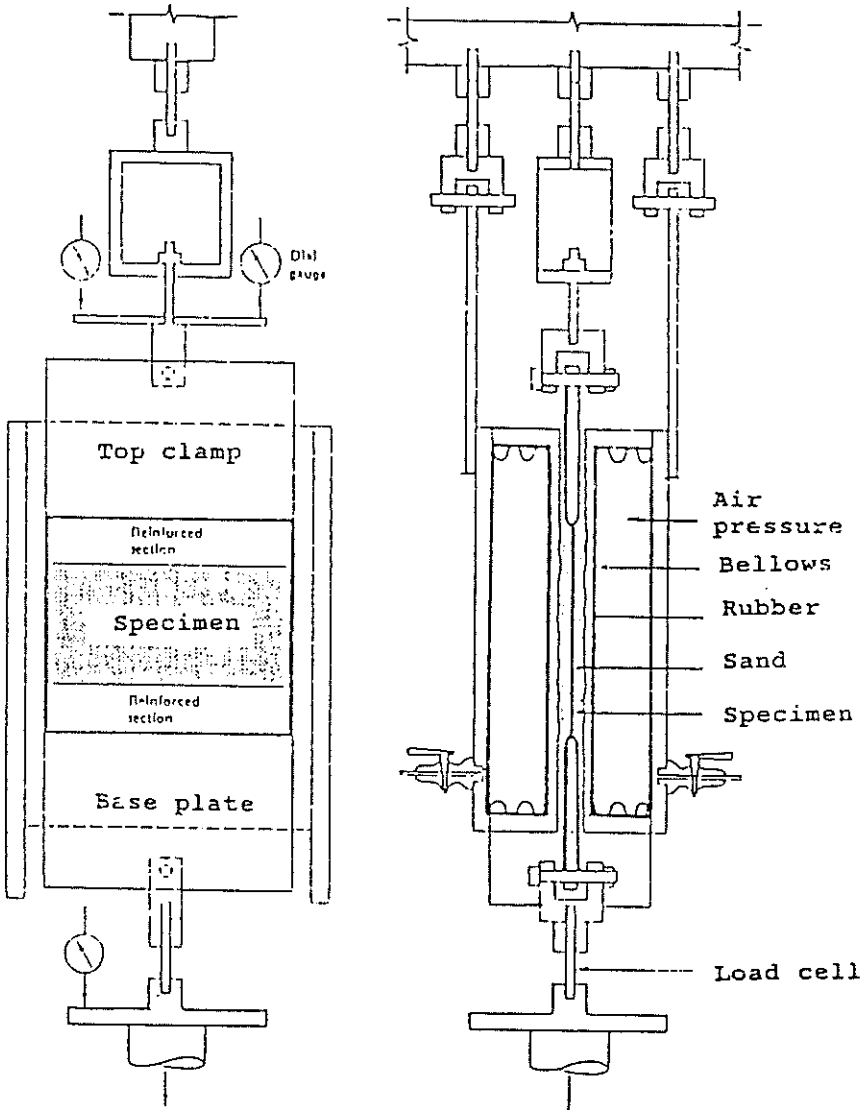

Figure 1.3 Confined extension testing apparatus (10)

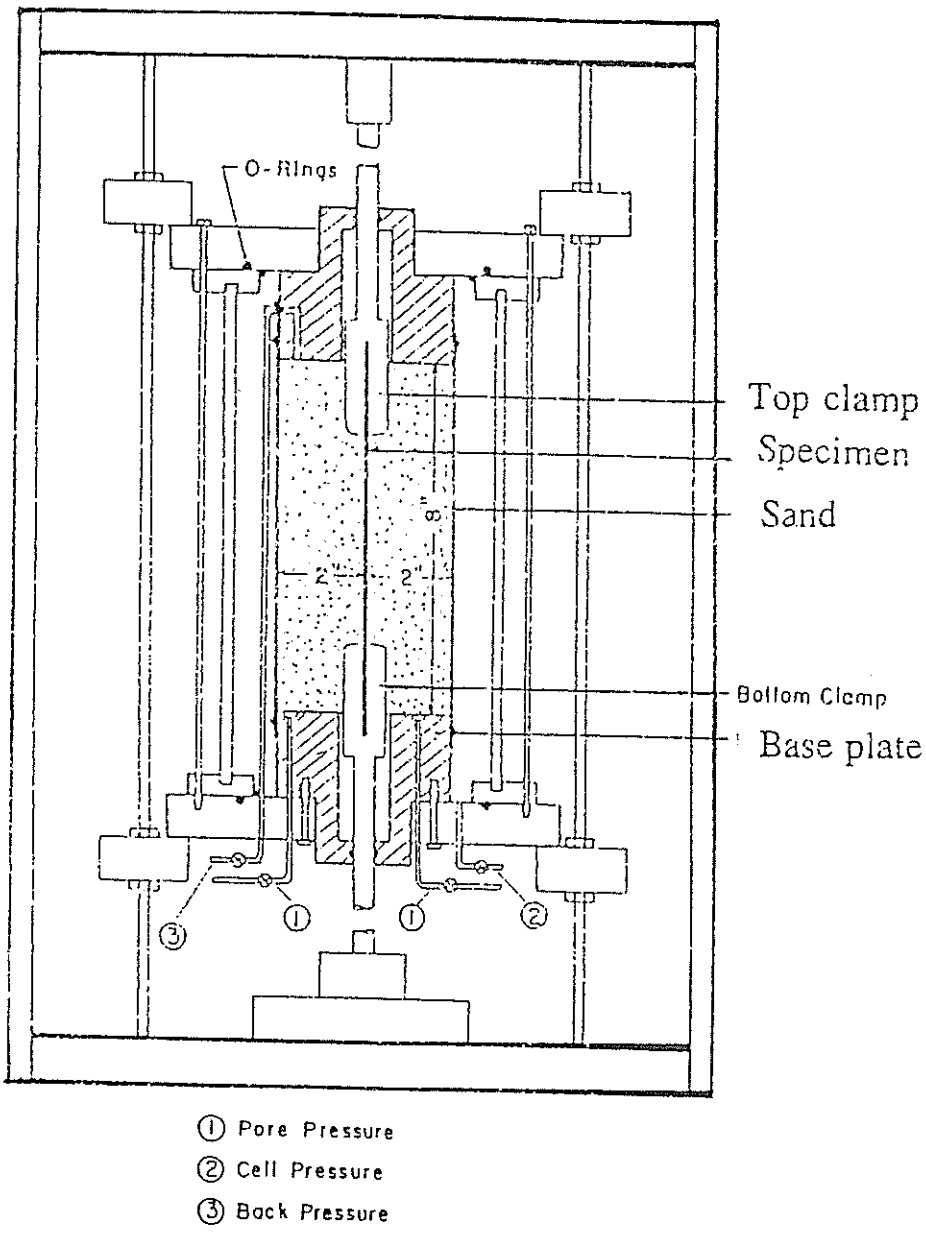

Figure 1.4 Confined extension testing apparatus (23)

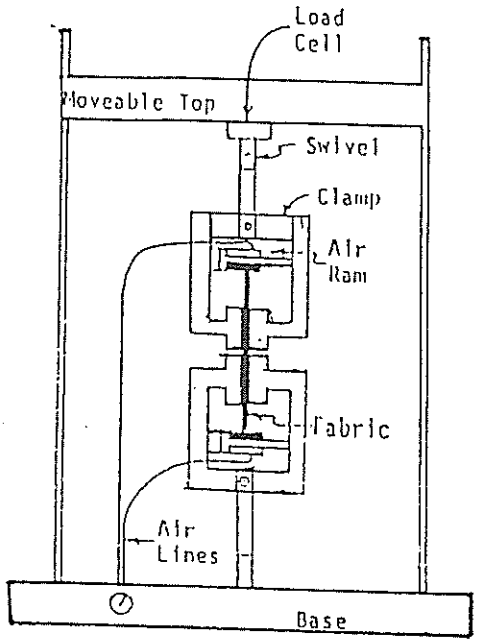

Figure 1.5 'Zero Span' confined extension apparatus (24)

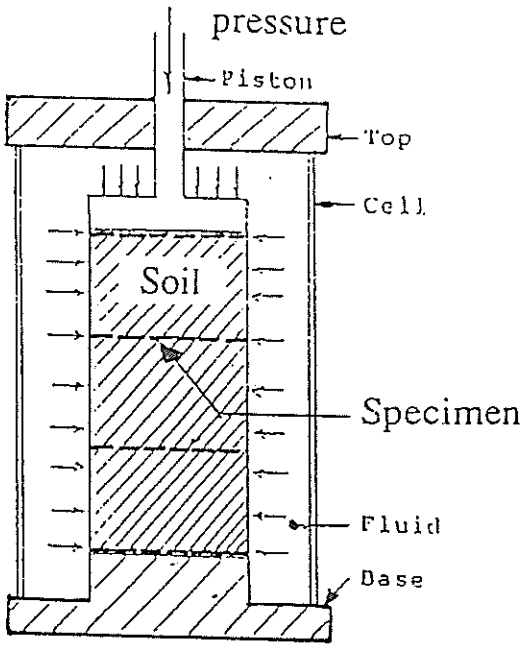

Figure 1.6 Triaxial cell with reinforced-soil sample (25)

1.2 SOIL-GEOSYNTHETIC INTERFACE PROPERTIES

The shear stress-strain developed at the soil-reinforcement interface can be monitored in both direct shear and pull-out boxes. In the direct shear box, tests are usually conducted in accordance with the conventional procedure of tests on un-reinforced soil samples. The horizontal displacement required to mobilize the shearing stresses are measured along with the vertical displacements of top plates. Typical shear boxes, used in determining the soil-geosynthetic frictional properties, are shown in Figure 1.7. Test results are usually expressed as the efficiency factor which is the ratio between the soil-reinforcement interface friction angle (tan δ) and the soil friction angle (tan ϕ).

Different shear boxes have been utilized to evaluate the shear strength at the soil-reinforcement interface. The sizes of shear boxes range from the conventional ones (27) and small boxes of four inches in length by four inches in width (28) to very large shear boxes of 40 inches by 40 inches (17). Relatively large shear boxes of 10 to 12 inches in width are often used (29,30,31) in order to adapt the large deformations required to mobilize the interface friction between soil and geosynthetics. Modified direct shear devices, with the lower boxes of bigger dimensions than the upper ones, are also utilized (16,32). The advantage of using bigger dimensions in the lower box is the ability in mobilizing higher shear strain levels in the reinforcement without loss of the shear area.

In the pull-out tests, the rear end of the specimen is free while the front end is clamped to the pull-out loading machine. Pull-out tests are used to provide the load-displacement relationship at the facing of the geosynthetic specimen and its pull-out resistance. Since no standard design for pull-out testing devices exists, box dimensions and testing procedures differ for every box. The dimensions of the box are usually chosen to reduce the boundary effects. Figure 1.8 shows typical pull-out testing equipment.

Direct shear and pull-out tests are associated with different testing procedures, loading paths, and boundary conditions. Consequently, the interface frictional parameters obtained from both tests can vary. The fundamental difference between the two tests is that the soil-inclusion interaction mechanism is different. In direct shear tests the mobilized shear strain is uniformly distributed along the soil-inclusion interface. While in the pull-out box, mobilized strain is a combination of the interface shear strain and the reinforcement extension.

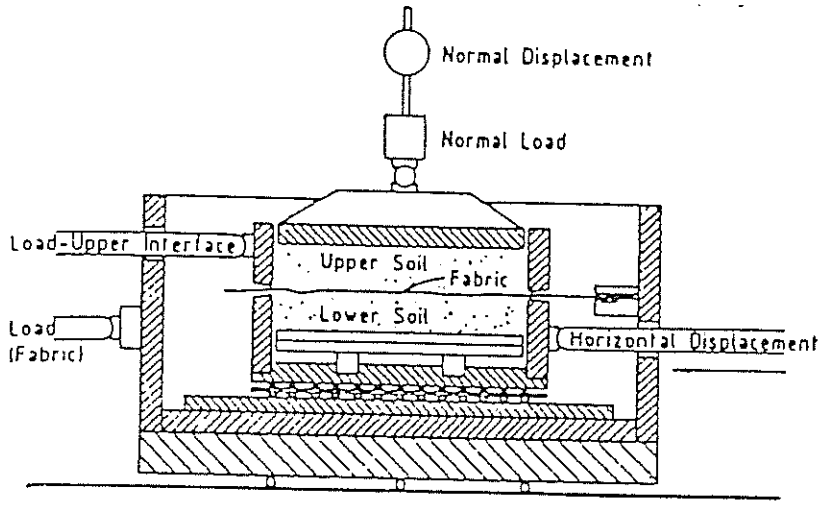

(a) After Rowe et al. (14)

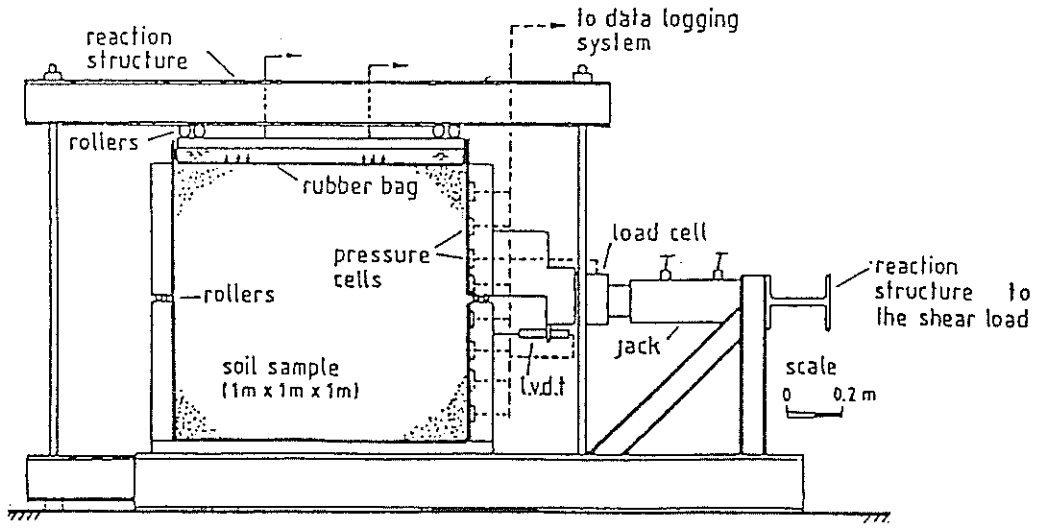

(b) After Palmeira and Milligan (17)

Figure 1.7 Soil-geosynthetic direct shear test devices

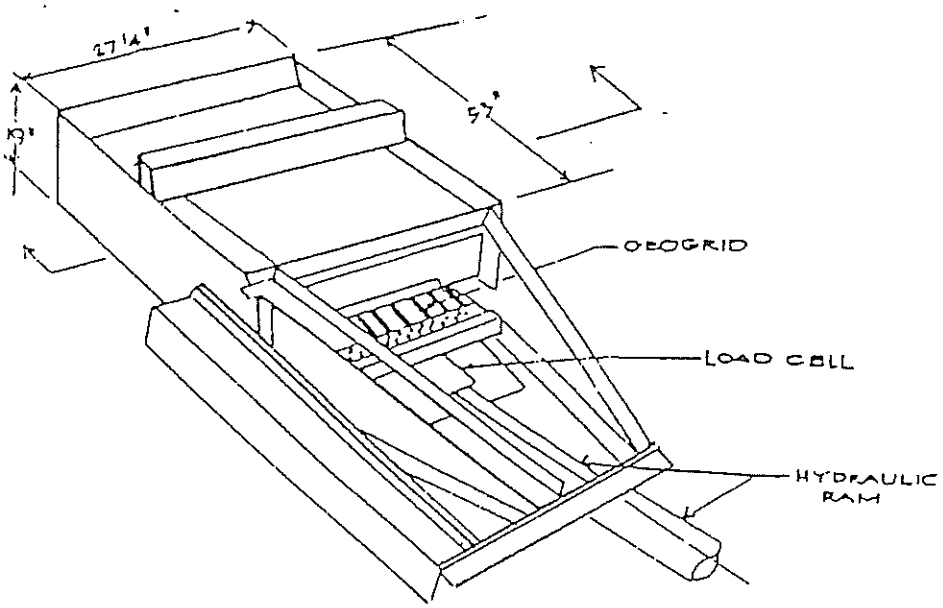

(a) STS Pull-out Box, after (13)

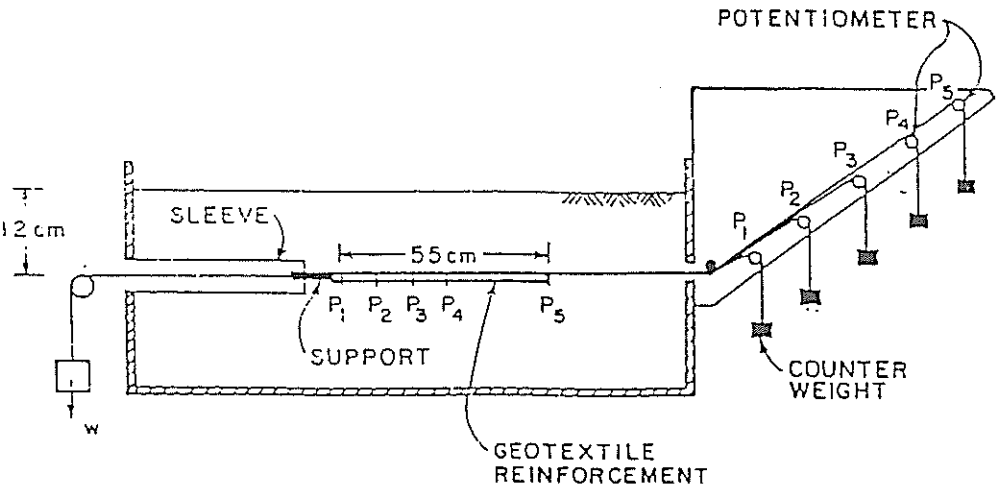

(b) After Juran and Christopher, (33)

Figure 1.8 Geosynthetic pull-out test devices

The coupled mechanism-of interface shear strain and reinforcement extension results in a non-uniform shear strain-stress distribution along the reinforcement. A realistic experimental model should incorporate the reinforcement extensibility which makes it more appropriate to perform pull-out tests for determining the interface parameters of extensible reinforcements.

The review of the existing pull-out tests (3,11,19,20) shows a large variety of testing equipment and procedures which makes it difficult to compare test results. It also signifies the influential effect of different testing parameters on the results. Most of these parameters are related to:

1. The pull-out tests reported are often conducted at controlled displacement-rate. Few pull-out tests are conducted under load-controlled mode (34). Pull-out testing equipment should have the capability of providing load-controlled tests in order to permit evaluation of long term pull-out behavior.
2. In displacement-rate controlled tests, a range of pull-out rates are reported varying from 0.004 inch/min (0.1 mm/min) to 0.8 inch/min (20 mm/min). Studies on the frictional resistance of the geotextile interface in direct shear tests (16) showed little sensitivity to variations in strain rates. However, in wide strip tests, geogrid tension strength varies with the applied rate of strain (6). The testing facility should have the capability of performing tests under different displacement rates to evaluate this effect.
3. The interaction between the soil and the box side walls can affect the pull-out test results. Soil confinement is usually applied by means of flexible air-bags to insure uniform distribution of normal stresses (15,17). The applied confining stresses can be partially carried out by the side wall friction causing a reduction in the normal pressure applied at the reinforcement level. This effect can be minimized by keeping the edge of the specimen far from the side walls (35). Some investigators covered the walls with lubricated membranes to provide low friction boundary (36). Alternatively, the specimen width/box width ratio may be chosen so as to minimize the effect of side wall friction.
4. The interaction between the reinforcement-soil system and the rigid front wall can also influence test results (37). As the reinforcement is pulled out from the box, the lateral earth pressure developed at the front face can result in an increase in pull-out resistance. Results of pull-out tests in boxes with different front walls show that pull-out resistance

increases as the degree of roughness of the front wall increases (37). Sleeves around the pull-out slot are incorporated to transfer the pull-out application point far behind the rigid front wall (13). The effect of sleeve length on minimizing the effect of front wall should be investigated.

5. The thickness of soil above and below the reinforcement differs in each box according to its clear height. If soil thickness is small, the interaction between the soil-reinforcement system and the boundaries may restrain soil dilatancy and affect the mobilized shear resistance at the interface. Results of pull-out tests on geogrids in various soil thickness (38) show that as the soil thickness increases, pull-out resistance decreases until a minimum force state is reached.
6. Different sample preparation and compaction procedures were utilized to ensure uniform soil density. Soil compaction is achieved by means of electric jack hammer (39), standard proctor hammer (29), hand tamping devices (40) and by mechanical tamping (35). A hopper with a flexible tube is also used to ensure uniform soil placement in the box (36).
7. Several investigators (13,18,38) clamped the reinforcement outside the box. This technique results in an unconfined front portion of the reinforcement and, consequently, in a variation of the effective interface area during the test.
8. For extensible geosynthetics, it is essential to monitor the displacements along the inclusion in order to interpret the confined elongation behavior of the reinforcement and, consequently, evaluate the pull-out resistance of the reinforcement in the field. Extensometers are used (12,13,33) to measure the displacements at various locations along the inclusion.

The measured soil-geosynthetic interaction parameters are also influenced by other factors such as the type and geometry of the reinforcement (37), soil grain size distribution and the state of overburden pressure (11,19). The pull-out and direct shear boxes are constructed to evaluate the effect of equipment, procedure and testing parameters on the interaction mechanism. A testing program is implemented for the performance evaluation of the boxes.

CHAPTER 2
EQUIPMENT DESIGN AND INSTRUMENTATION

2.1 DESIGN CONSIDERATIONS

Several testing facilities have been designed and used to determine the interaction parameters of soil-geosynthetic systems. The review of these facilities demonstrated the significant effect of different design parameters on the test results and led to the following design considerations:

1. Loading scheme: The testing equipment should provide the capability of conducting tests in both displacement-rate controlled and load-controlled modes. In the displacement-rate controlled mode, tests under various displacement rates are performed. Load-controlled tests are required in order to assess the confined time-deformation characteristics of the soil-reinforcement system.
2. Rigid wall boundary effects: The rigid walls of the box influence test results by imposing boundary conditions on the soil-reinforcement interface. The side wall friction can partially carry out the applied normal pressure and, thereby, affecting the confinement at the interface. Side wall friction can be minimized by either minimizing the friction along the box walls or by increasing the box dimensions to keep the confined specimen far from box walls. Moreover, the equipment should provide, through modular design, the flexibility to control sample and box dimensions in order to evaluate these boundary effects. Sleeves should be incorporated into the design to ensure that the soil-reinforcement interaction is carried out far from the interfering effect of the front wall. Soil pressure at the facing should be measured in order to determine the sleeve length at which this effect is minimal. Tests with different soil thickness above and under the reinforcement are also necessary in order to evaluate the effect of top and bottom plates on the interaction mechanism.
3. Soil placement and compaction: The frictional resistance of the inclusion is influenced by the relative density of the soil. When interface shear stresses are mobilized, dense soils tend to dilate. As this dilation is restrained in the box, normal stresses increase at

the vicinity of the inclusion. Furthermore, soil densification increases particle interlocking in geotextiles and passive resistance of the soil on the transversal elements of geogrids. A compaction procedure should be developed in order to ensure that the soil density is compacted uniformly to the desired density throughout the box.

4. The specimen clamping mechanism: In pull-out tests, the clamping of the reinforcement to the loading device outside the box leads to an unconfinement of the front portion of the reinforcement. The unconfined elongation of the front part implies variation of the interface area of the reinforcement during the test. The clamping mechanism should insure in-soil clamping of the specimen to maintain uniform confinement and a constant interface area of the specimen during pull-out.

5. Instrumentation: The soil-reinforcement interaction mechanism in pull-out tests is influenced by the reinforcement extensibility (12,37). In order to evaluate the frictional resistance along extensible reinforcement, an interpretation method that incorporates the inclusion extensibility should be adopted. Accordingly, the instrumentation must be capable of measuring the relative displacements at different locations along the confined reinforcement.

In order to satisfy the design criteria of the testing facility, the following objectives are considered in the design:

i) provide the capability of conducting both load-controlled and displacement-rate controlled pull-out tests,

ii) provide, through modular design of the pull-out box, flexibility in testing with various sample/box dimensions for evaluation of boundary effects,

iii) minimize the effect of the rigid front boundary by incorporating sleeves of appropriate lengths in the front wall,

iv) facilitate sample preparation, using a specially designed sand loading facility, and minimize operator's effort in testing and data monitoring by implementing the proper data acquisition system,

v) ensure in-soil clamping of the geosynthetic specimen in order to maintain a uniform confinement and a constant effective interface area of the specimen in pull-out tests,

vi) achieve a standard testing procedure through control of testing parameters and

reproducibility of test results,.

vii) establish a reliable instrumentation scheme for monitoring displacement at different locations along the geosynthetic specimen and soil pressure at the box walls.

2.2 EQUIPMENT DESCRIPTION

The testing facility consists mainly of the following:

1. Large pull-out box; the inside dimensions of the box are 60 inches (1.52 m) long, 36 inches (0.92 m) wide and 30 inches (0.76 m) high.
2. Large direct shear box; the dimensions of the lower box are 60 inches long, 36 inches wide and 15 inches (0.38 m) high. The dimensions of the upper box are 27 inches (0.68 m) long, 27 inches wide and 15 inches high.
3. Hydraulic loading system for each box. The loading system is capable of performing displacement-rate controlled and load-controlled tests.
4. Sand handling system. It consists of an elevated sand hopper and a sand vacuum machine in order to facilitate sand placement, removal and compaction control.
5. Instrumentation and data acquisition system to control and monitor the input testing and response parameters (e.g. displacement-rate, pull-out load and displacements at different locations along the reinforcement).

Figure 2.1 shows the pull-out box, the loading frame and the sand handling equipment. Figure 2.2 displays the top view of the box. The direct shear box is shown in Figure 2.3. Both boxes are constructed with ASTM A36 mild steel. The construction details of the testing equipment are presented in Appendix A.

2.2.A The Pull-out and Shear box Details

Schematic diagrams of the pull-out box and direct shear box are displayed in Figures 2.4 and 2.5, respectively. The main elements of the boxes are:

1. bottom and side wall steel plates of ¼-inch thick. The boxes are assembled in bolted modular units to permit increasing the box length, if necessary. For the tests performed in this study, box length is kept at 60 inches.

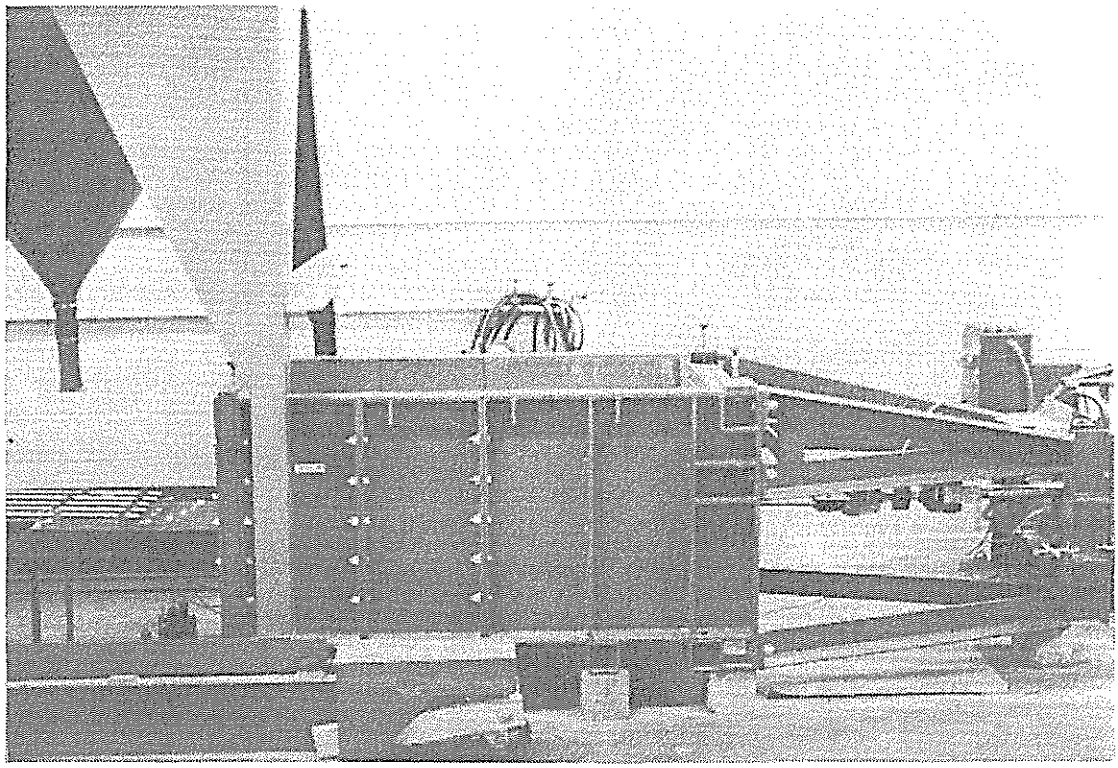

Figure 2.1 Side view of the pull-out box

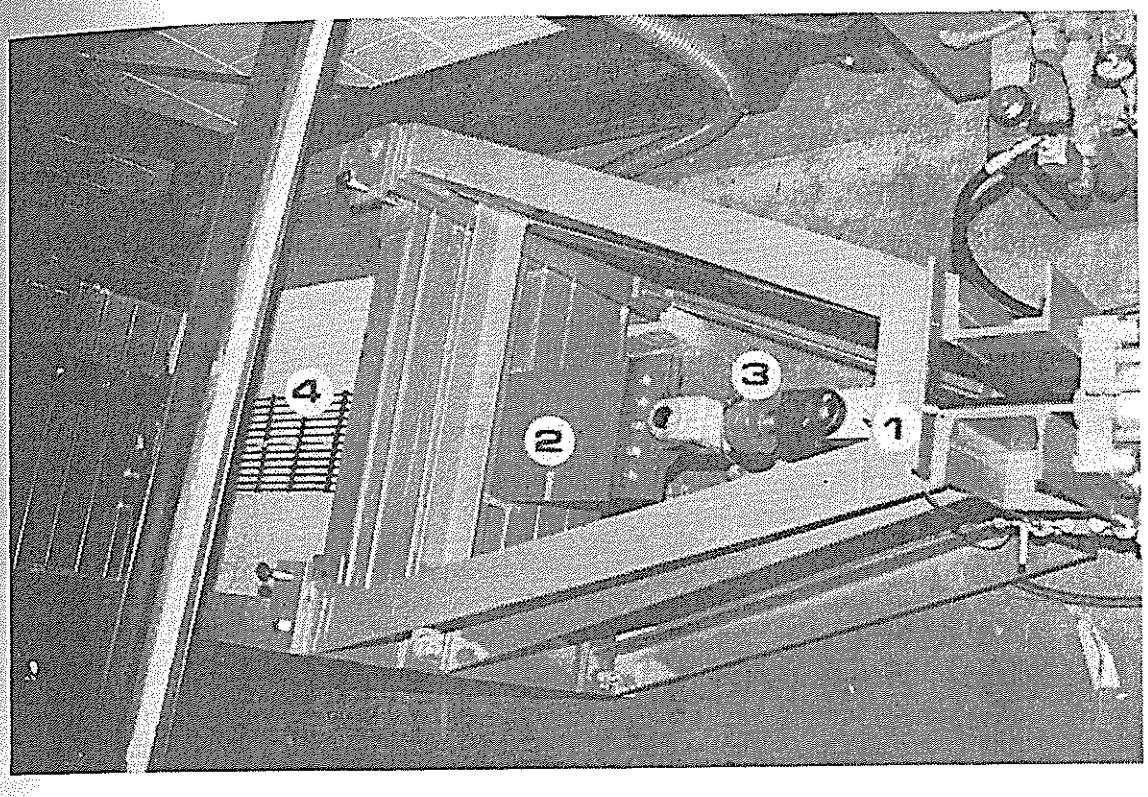

(1) Loading frame
(2) Clamping plates
(3) Load cell
(4) Geogrid

Figure 2.2 Top view of the pull-out box

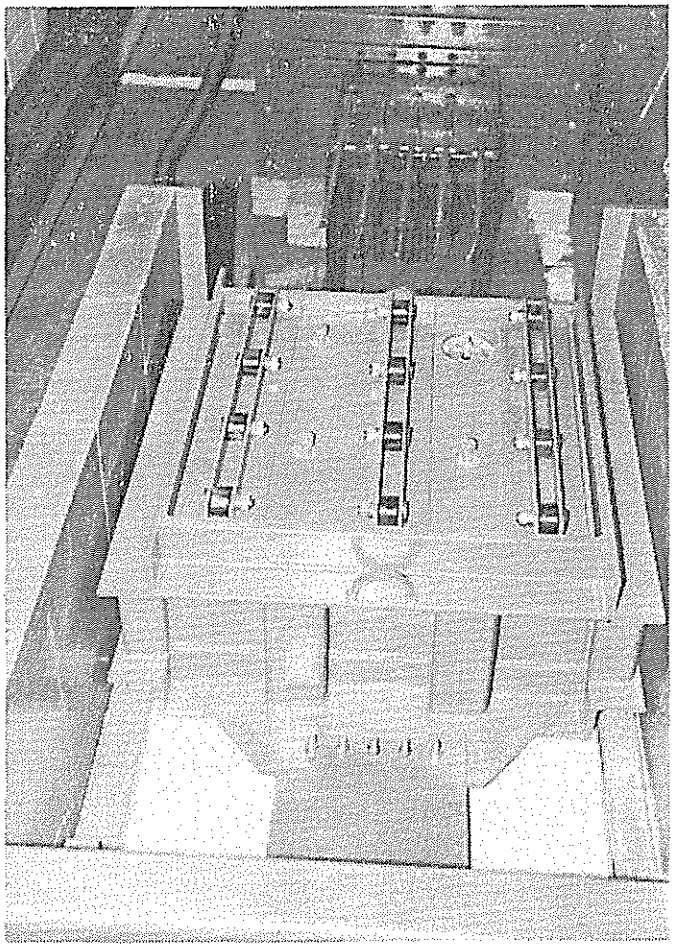

Figure 2.3 View of the large direct shear box

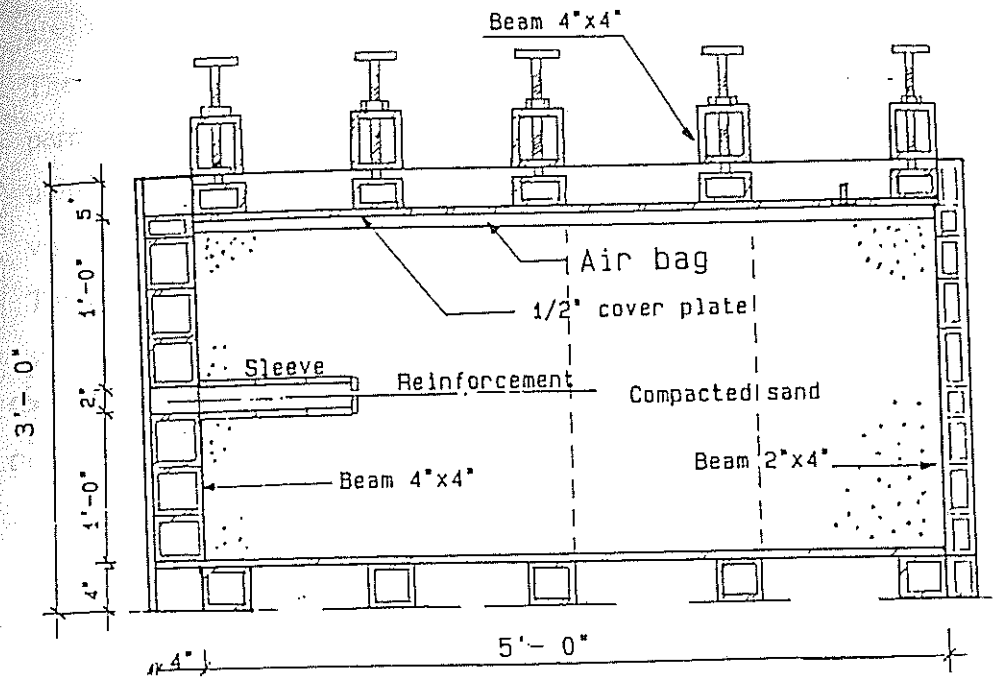

Figure 2.4-a Longitudinal Cross-Section of the Pull-out Box

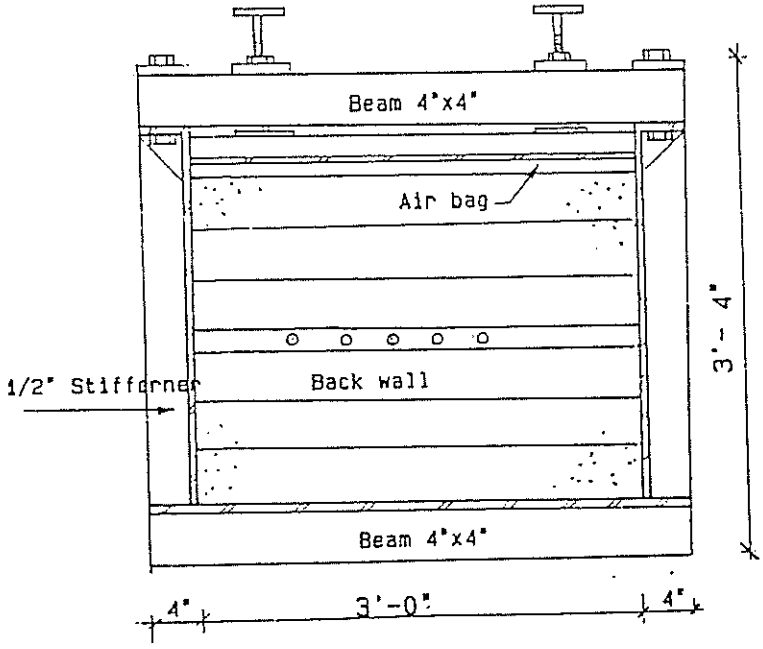

Figure 2.4-b Cross-section of the pull-out box

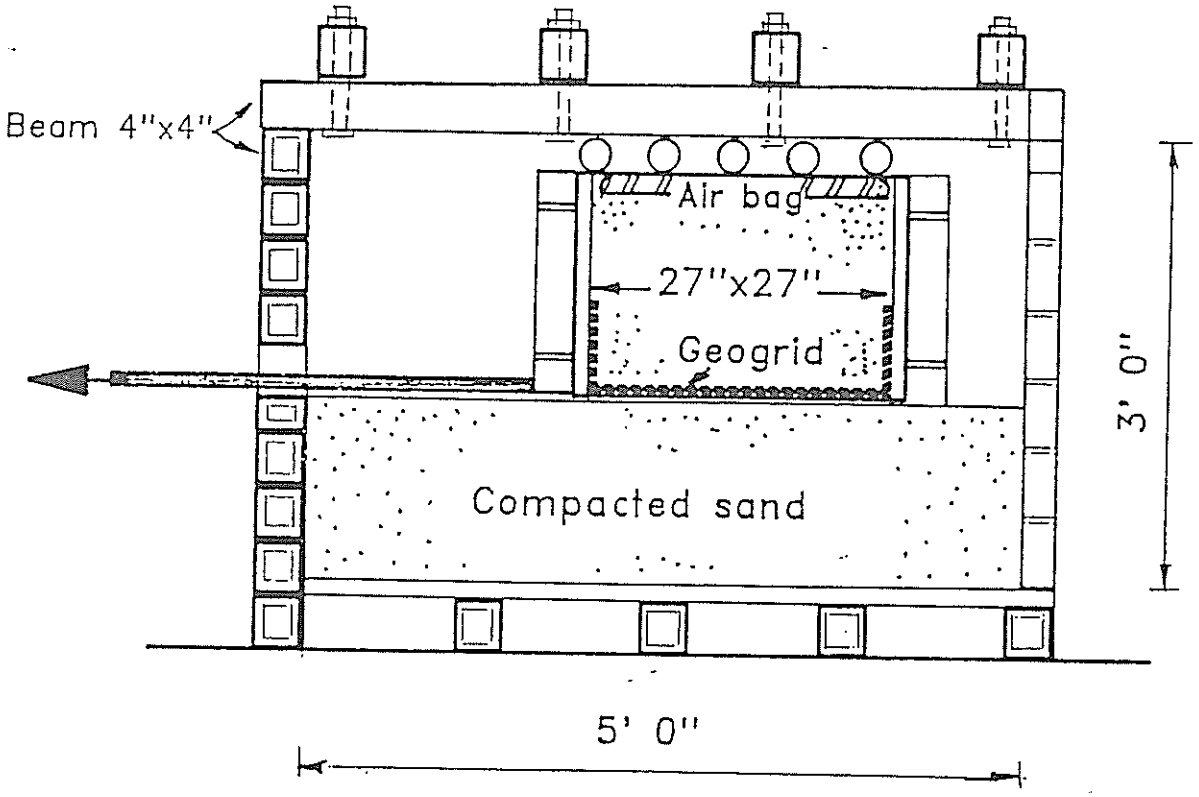

Figure 2.5 Longitudinal cross-section of the direct shear box

The level of the hydraulic ram can be adjusted at different heights. The upper plate is also adjustable to permit testing soil samples of various thicknesses.

2. The front wall consists of 4-inch by 4-inch rectangular beams. A 2-inch high slot permits pulling the clamping plates out of the box. In the pull-out box, the front modular units permit the evaluation of the effect of the rigid front boundary by using slots of variable opening sizes and facing types.

3. The rear wall consists of 2-inch by 4-inch rectangular beams. In the pull-out box, five slots are located in the rear wall to permit reinforcement instrumentation.

4. The inflated air bag, of 2 inches in thickness, is used to apply the vertical overburden pressure. The pressure system is able to apply a normal pressure up to 30 psi. A ¼-inch thick cover plate and 4 by 4 inch rectangular beams are used to confine the air bag above the soil.

5. The sleeve plates are composed of units of 4 inches in width. The plates are placed on the top and bottom of the slot in the front wall of the pull-out box. The sleeves minimize the lateral stress transfer to the rigid front wall during pull-out. The sleeves are designed in modular units to evaluate the minimum sleeve length required to eliminate the effect of the rigid front wall.

6. Two clamping plates of 1/8-inch in thickness. In the shear box, the clamping plates are bolted to the upper box; while in the pull-out box, they are bolted to the reinforcement inside the box.

2.2.B The Hydraulic Loading System

The pull-out load is applied by a hydraulic system. The system includes three basic units:

1. hydraulic ram model Miller H67B (Figure 2.6). The ram is mounted on the loading frame and applies the pull-out load through the clamping plates. The hydraulic piston of the ram is 5 inches in diameter and is able to apply an 18-inch maximum pull-out displacement.

2. Hydraulic power supply unit which consists of a Miller custom-built hydraulic pump of 5 HP and a 20 gallon fluid reservoir capacity and a cooling system. The details of the hydraulic unit are displayed in Figure 2.7.

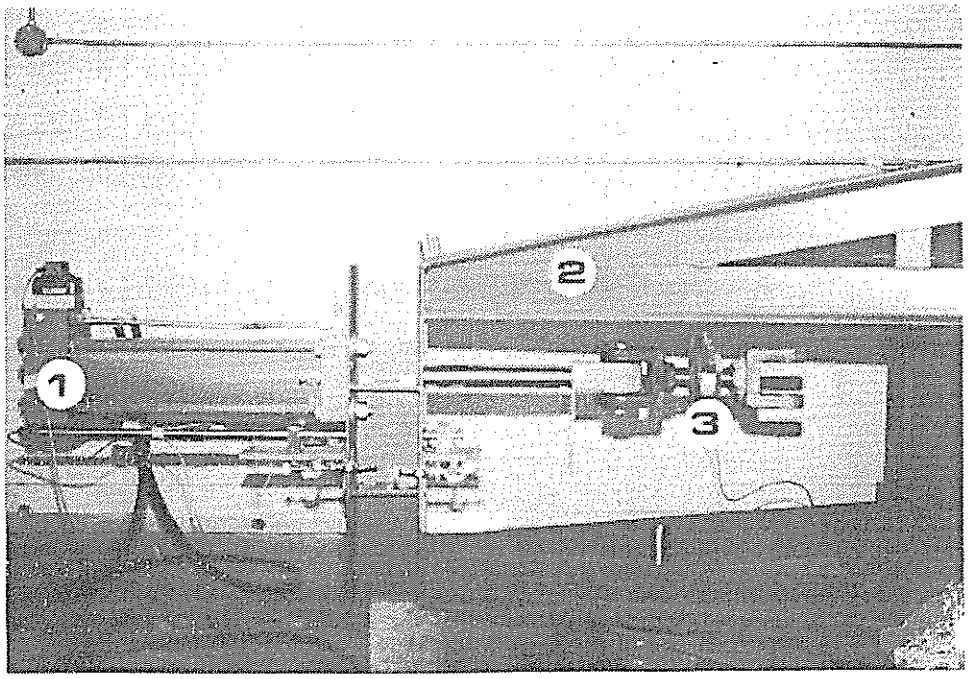

(1) Hydraulic ram
(2) Loading frame
(3) Load cell

Figure 2.6 View of the hydraulic ram and the loading frame

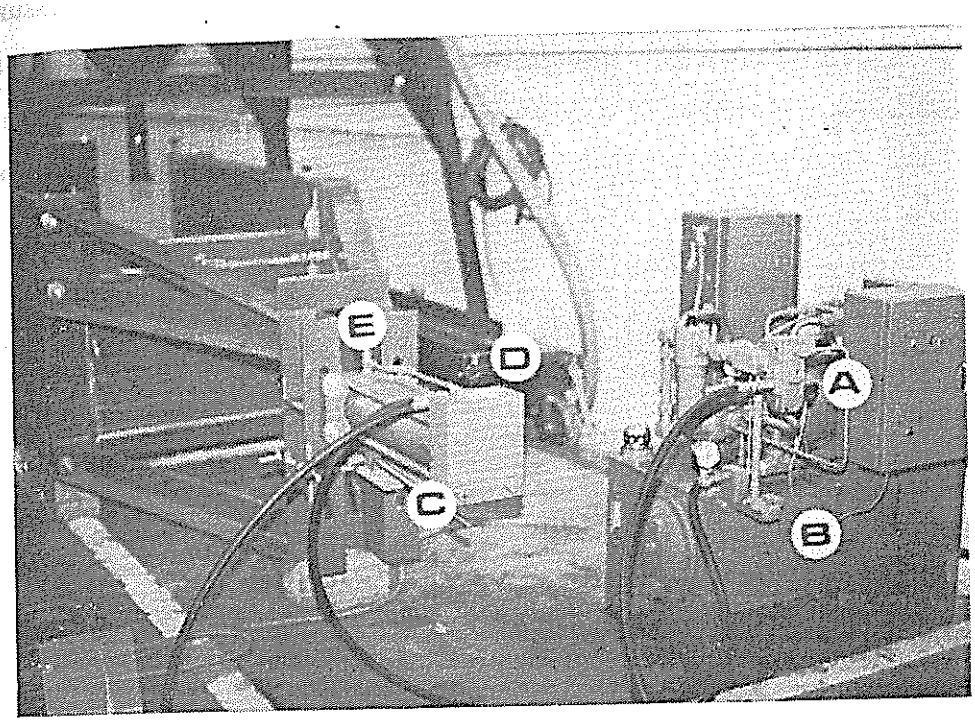

(A) Control box
(B) Fluid reservoir
(C) Hydraulic ram
(D) Servo valve
(E) Low pressure gauge

Figure 2.7 View of the hydraulic loading system

The pump is able to operate under two loading schemes, namely: (a) pressure-control scheme; where the pump fluid is controlled by a low pressure proportional control valve. The pressure is measured directly in the hydraulic ram by a test gauge; and (b) velocity-control scheme; where the pump operates under a constant pull-out velocity with variable pressures up to 3,000 psi (20 Mpa). The pump is controlled to operate under either of these schemes from the control box unit.

3. Control box unit (Figure 2.7). The commands to the hydraulic pump can be sent manually by the control keys in the board or through the computer when the control board is connected to the data acquisition system.

2.2.C The Sand Handling Facility:

The sand handling facility is custom-build equipment to minimize the operator's effort and control sand placement procedure. The facility is displayed in Figure 2.8 and it consists of:

1. a heavy duty movable sand vacuum model 'Invincible'. The sand is vacuumed from the box through a flexible hose, and it is filtered out to a dust container of 3 ft^3 capacity. The vacuum machine stores the sand in the elevated hopper.
2. An elevated sand hopper of 54 ft^3 storage capacity. The hopper supporting system is designed to permit its movement above the two boxes. The sand is loaded back to the box through the flexible hopper outlet.

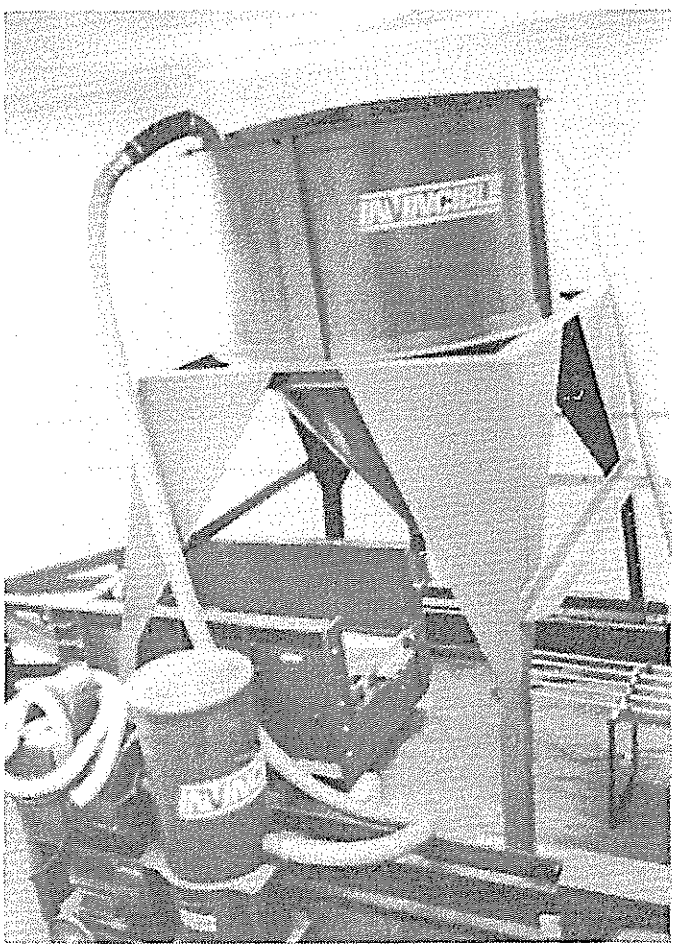

Figure 2.8 View of the sand handling facility

2.3 INSTRUMENTATION AND DATA ACQUISITION

The instruments used to measure the interaction response and the input testing parameters, for both of the pull-out and direct shear boxes, consist mainly of:

1. a load cell to measure the force applied from the hydraulic loading system,
2. a linear variable differential transformer (LVDT) to measure the displacement at the pull-out application point,
3. a velocity transducer to measure the applied displacement-rate at the front,
4. pressure cells to measure the soil earth pressure inside the box,
5. manometer gauge to measure the normal pressure applied from the air bag.

Moreover, in the pull-out box, LVDT's are placed at the back of the box to measure the displacements at different points along the reinforcement. The specifications of these instruments and the calibration procedures are presented in Appendix A.

2.3.A Load and Pressure Measurements

The pull-out force is measured by the load cell attached to the hydraulic piston and the clamping plates as shown in Figure 2.6. The load cell is model 'Lebow 3187' of 20 Kips (88 kN) capacity. A conditioner, shown in Figure 2.9, is connected to the cell in order to read and stabilize the output signal. Calibration tests are performed on the load cell by applying different predetermined loads and monitoring its response. A relationship between the applied load (in pounds) and the output response (in volts) is established.

The earth pressure on the front wall is measured by two earth pressure cells model 'GeoKon 3600' of 30 psi (200 kPa) capacity. The pressure cells are 2-inch (5 cm) in diameter and consist of two circular stainless steel plates welded together and spread apart by a narrow cavity. External pressure acting on the cell is balanced by an equal pressure induced in the internal fluid by an excitation voltage of 15 vdc. The excitation voltage is supplied from a stabilized power supply (Figure 2.9). Calibration tables to convert the output response (in mv) to the magnitude of the applied pressure (in psi) are established. The calibration tests are performed by applying both incremental hydrostatic air pressure and incremental dead weights on the cells. The results of calibration tests are presented in Appendix B.

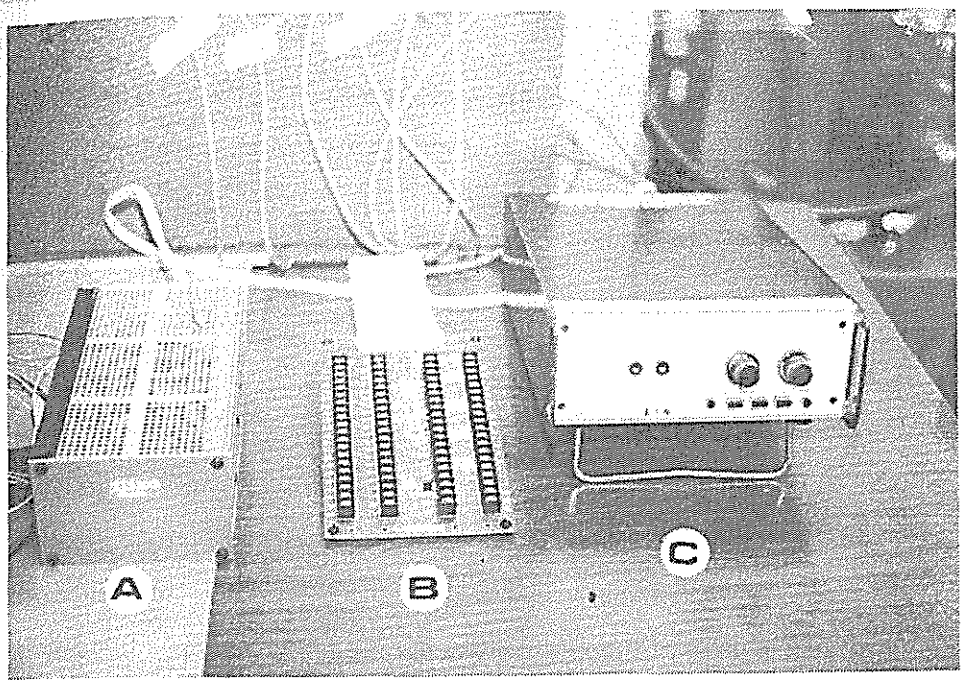

(A) Stabilized power supply
(B) Screw terminal board
(C) Load cell conditioner

Figure 2.9 Data acquisition supporting instruments

2.3.B Displacement Measurements

The front displacement of the geogrid in the pull-out box and the displacement of the upper box in the direct shear box are monitored by Linear Variable Differential Transformers (LVDT's). The LVDT's are mounted on the loading frame as shown in Figure 2.6. The LVDT's used are model 'Schaevitz' of stroke length ± 10 inch. An excitation voltage of 15 vdc is sent by a stabilized power supply. Displacement is monitored as the core rod moves inside the LVDT causing a voltage response equivalent to the displacement. The relationship between the core rod displacement and the output voltage is provided by the manufacturer.

Non-uniform shear stresses and displacements are developed along the extensible reinforcement. The displacements at different nodes along the reinforcement are monitored in order to determine the reinforcement length which is effectively mobilized under the specified level of pull-out load. In order to measure the displacements at different locations along the confined reinforcement, five LVDT's are connected to the transversal ribs of the geogrids. The LVDT's are mounted at the level of the reinforcement on a table in rear of the pull-out box. The displacement rods of the LVDT's are connected to the geogrid by 'tell-tale' inextensible wires through slots in the box's rear wall. The wires are kept stretched by counter weights through the rear table. A schematic diagram of the LVDT's connections at the rear table is depicted in Figure 2.10. A view of the displacement instrumentation of the geogrid at the rear table is shown in Figure 2.11.

2.3.C Displacement-rate Measurements

The velocity transducer is mounted on the loading frame to measure the displacement-rate at the front of the specimen. The velocity transducer measures the rate of the core rod displacement when it is moved inside the transducer shaft. An excitation voltage of 5 vdc is sent by the power supply. The output voltage is calibrated by applying several predetermined velocities, and the equivalent output voltages are monitored. The displacement-rate is measured to verify the command values sent by the computer when the test is conducted under a displacement-rate controlled mode.

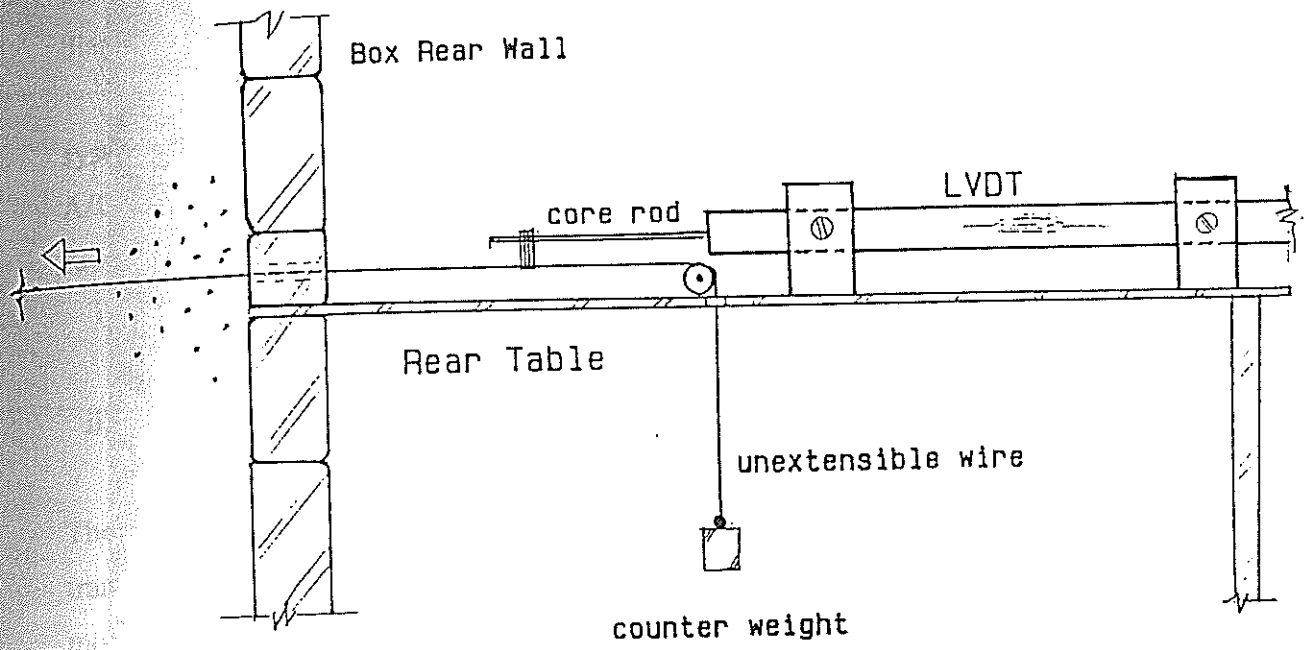

Figure 2.10 Detail of the LVDT connection at the rear table

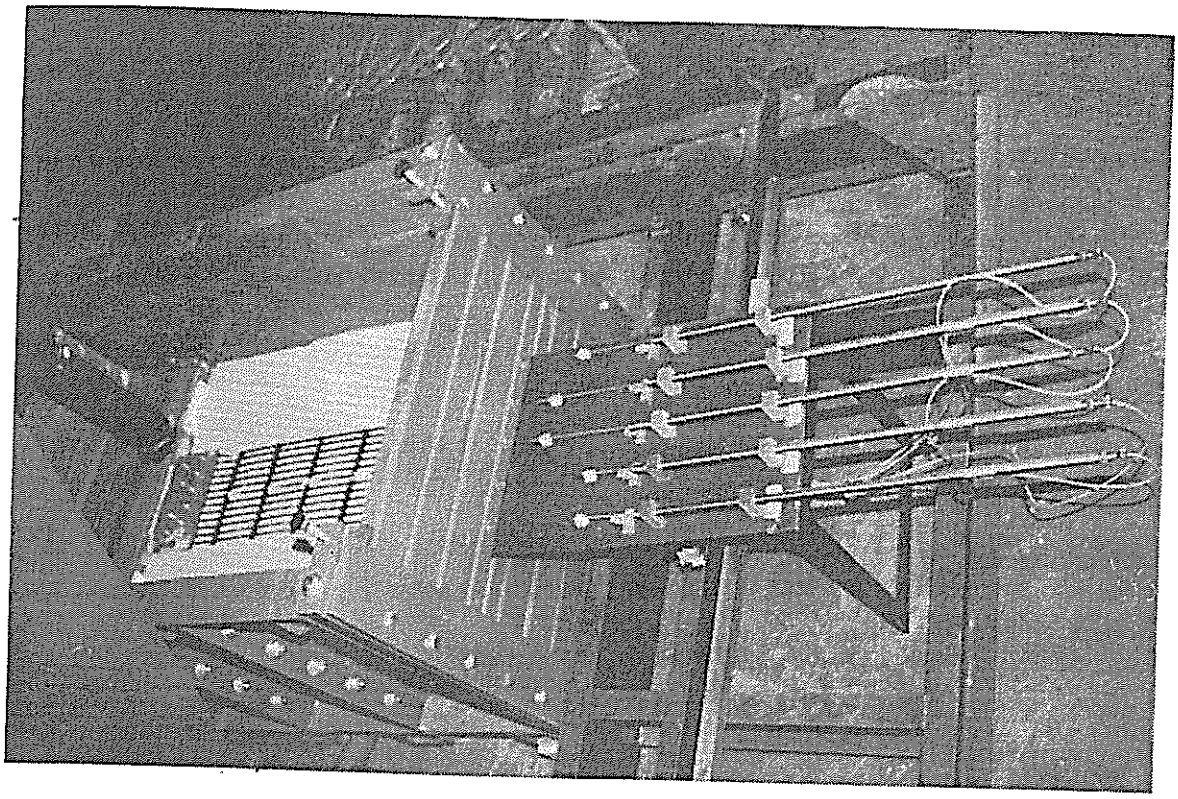

Figure 2.11 Displacement instrumentation of the geogrid

2.3.D Data Acquisition System

The output response parameters (i.e. displacement, velocity, load, and pressure) measured, respectively, by the LVDT's, velocity transducers, load cells, and pressure cells; are transmitted to an IBM-AT micro-computer through a data acquisition system. A schematic diagram of the instrumentation and the data acquisition system is displayed in Figure 2.12.

A data translation board model 'DT-2801 AD/DA' is plugged into one of the computer system extension slots. The data translation board includes eight differential (16 single-ended) A/D (Analogous to Digital) channels and two D/A (Digital to Analogous) channels. The dual function of the board is to:

i) translate the digital signals, sent by the operator, to analogous ones through the D/A channels,

ii) translate the analog output signals of the tests to digital form for display and storage through the A/D channels.

The data input and output are simultaneously monitored and stored in the computer. The data translation board is connected to the measuring instruments through a screw terminal board model DT707. The screw terminal board is shown in Figure 2.9. The connection scheme of the screw terminal board is:

i) each of the measuring instruments is connected to one of the A/D channels of the screw terminal,

ii) the A/D channels are connected to the control box in the hydraulic system. These channels translate the commands to operate the hydraulic loading system for either velocity control or pressure control.

The data acquisition board is programmed and controlled from the computer keyboard through the software "Labtech Notebook'. The software supports the data control management and organizes data display and storage. Figure 2.13 displays a view of the data acquisition control and monitoring system.

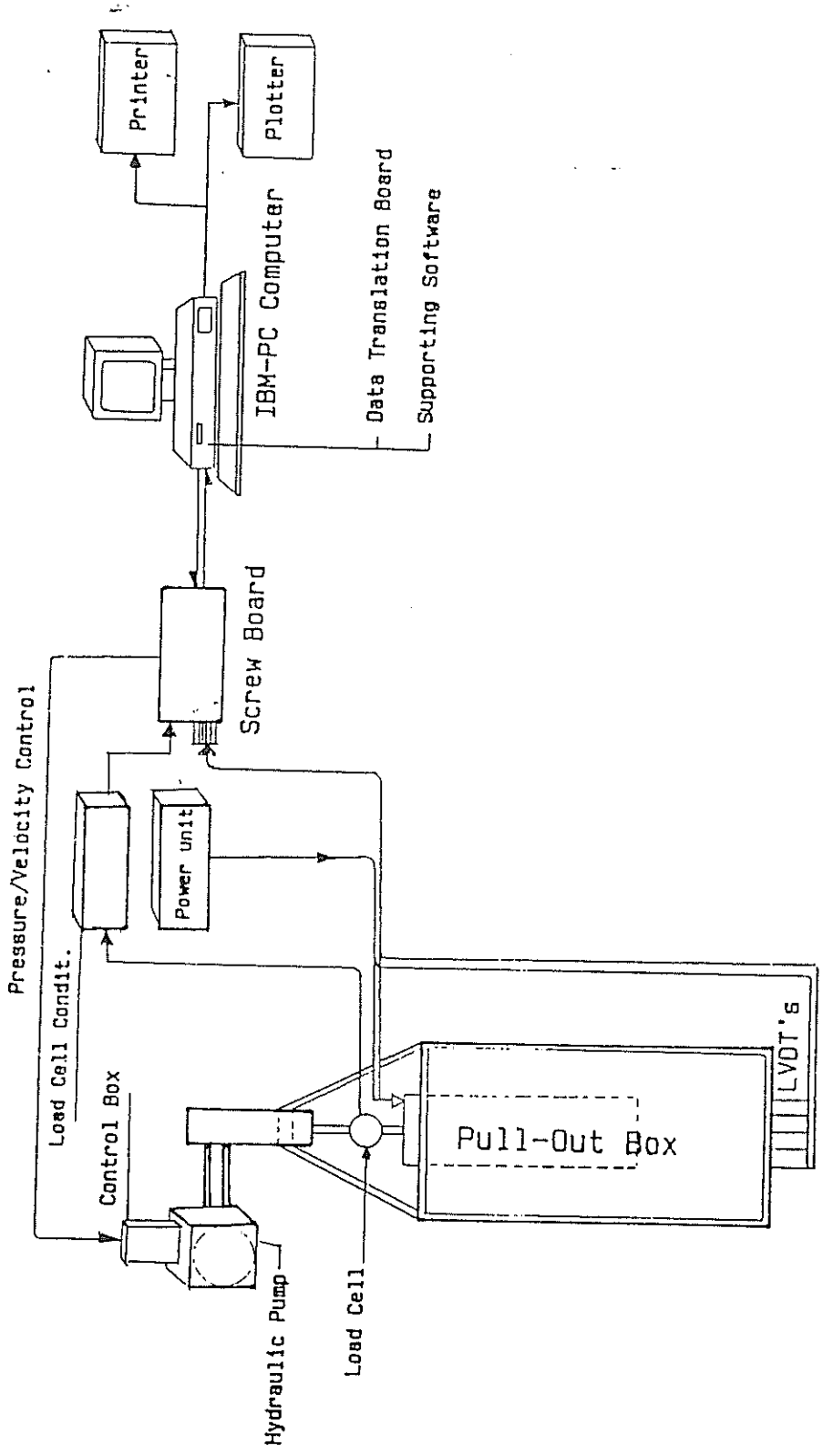

Figure 2.12 Schematic view of the data acquisition system

Figure 2.13 View of the data control system

CHAPTER 3
TESTING PROCEDURE AND DATA INTERPRETATION

3.1 INTRODUCTION

Pull-out and direct shear testing programs are conducted in order to evaluate the performance of the testing facility, the effect of testing parameters, and to provide the data base for the development of an analytical interpretation procedure. The testing program includes:

i) Unconfined extension tests: These tests are conducted on the geogrid specimens under constant extension-rates. Results are compared with the index test results provided by the manufacturers. The purpose of these tests is to evaluate the equipment performance, the accuracy of the control and monitoring system, and the material extension properties in the unconfined state.

ii) Pull-out tests: Constant displacement-rate pull-out tests are conducted under identical testing conditions in order to evaluate the equipment reproducibility and the pull-out performance of the geogrid. Tests are also conducted with variable testing parameters (e.g. confining pressure, soil density, and pull-out rate) and boundary conditions to evaluate their effect on the pull-out resistance.

iii) Direct shear tests: Tests are conducted on the sand-sand interface and geogrid-sand interface. The purpose of these tests is to evaluate the direct shear box. Results of these tests are also used in evaluating the results from the pull-out tests.

iv) Load-controlled pull-out tests: The purpose of these tests is to evaluate the performance of the pull-out facility under load-controlled modes. Unconfined extension tests and pull-out tests are conducted on the geogrid. In these tests, loads are applied incrementally and maintained constant during specific times. Long term (500 hour) pull-out creep test is also performed to evaluate the confined creep strain of the geogrid.

The methodology and interpretation of test results are discussed in this chapter. The procedures used in specimen preparation, soil compaction, and calibration of soil density are presented.

3.2 SOIL COMPACTION AND SPECIMEN PREPARATION

Soil compaction and relative density significantly affect pull-out and direct shear test results (11,19). In dense sand, as soil particles are displaced in the vicinity of the reinforcement, the soil tends to dilate. This dilation is restrained by the surrounding soil and results in a normal stress concentration at the interface and an increase in shearing resistance.

For a given relative density, soil placement and compaction can have a significant effect on test results. Uneven soil placement and compaction would result in a sample with a higher tendency for arching or non-uniform soil dilation (14,39). Poor compaction of soil layers and inadequate geogrid placement may result in differential settlement of the geogrid, which may lead to an incorrect measurement of the interface resistance. The compaction process should be adequately adopted for each type of soil in order to simulate, as closely as possible, the compaction process used in the field.

3.2.A Soil Placement

The sand used in this study is a uniform blasting sand. Its grain size distribution is shown in Figure 3.1. The shear stress-displacement relationship, under different confining pressures, is determined from the conventional direct shear test as shown in Figure 3.2. The results of these tests demonstrate a soil friction angle of 34°. Soil dry densities of 99 pcf (1.58 t/m^3) and 110.9 pcf (1.77 t/m^3) are obtained, respectively, from minimum and maximum soil density tests.

The sand is placed into the box by pouring it from the elevated hopper through a flexible outlet. The hopper is moved to the top of each of the two boxes to facilitate sand placement. Figure 3.3 shows a view of the elevated hopper and the two boxes. The hopper is moved during pouring to permit even distribution of the sand.

In the pull-out box, the sand is placed in four layers of 6-inch each, leveled and compacted to the desired relative density. The geogrid is placed on the top of the second layer, at mid-height of the box. Figure 3.4 depicts the sand placement scheme in the box. In the direct shear box, the sand in placed in two layers of 6-inch each in the lower part of the box. The geogrid is placed on the bottom of the upper box and two layers of sand, of 6-inch each are placed in the upper box. The sand compaction is applied manually using a vibrating electric hammer on each layer in a regular pattern.

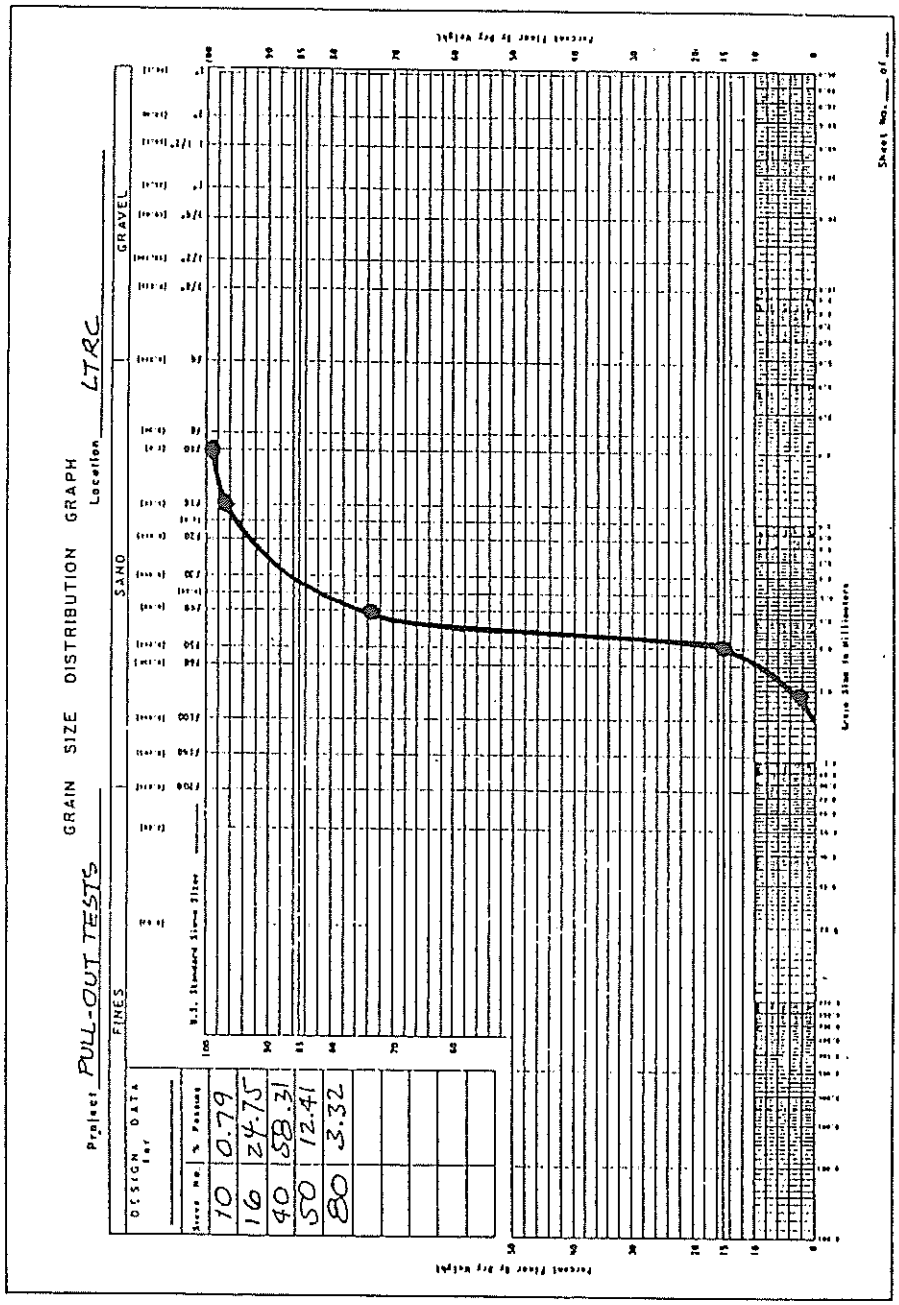

Figure 3.1 Grain size distribution of the blasting sand

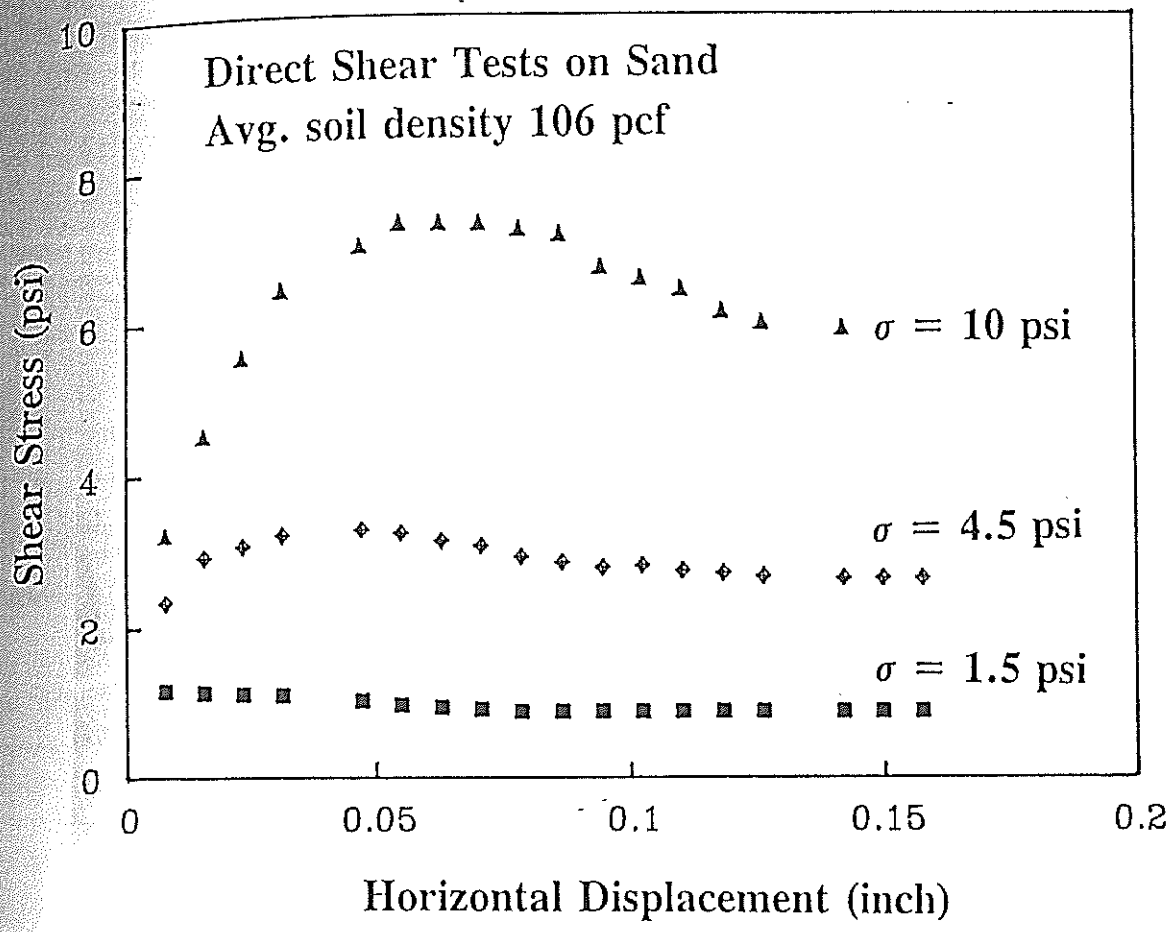

Figure 3.2 Results of direct shear tests on the sand

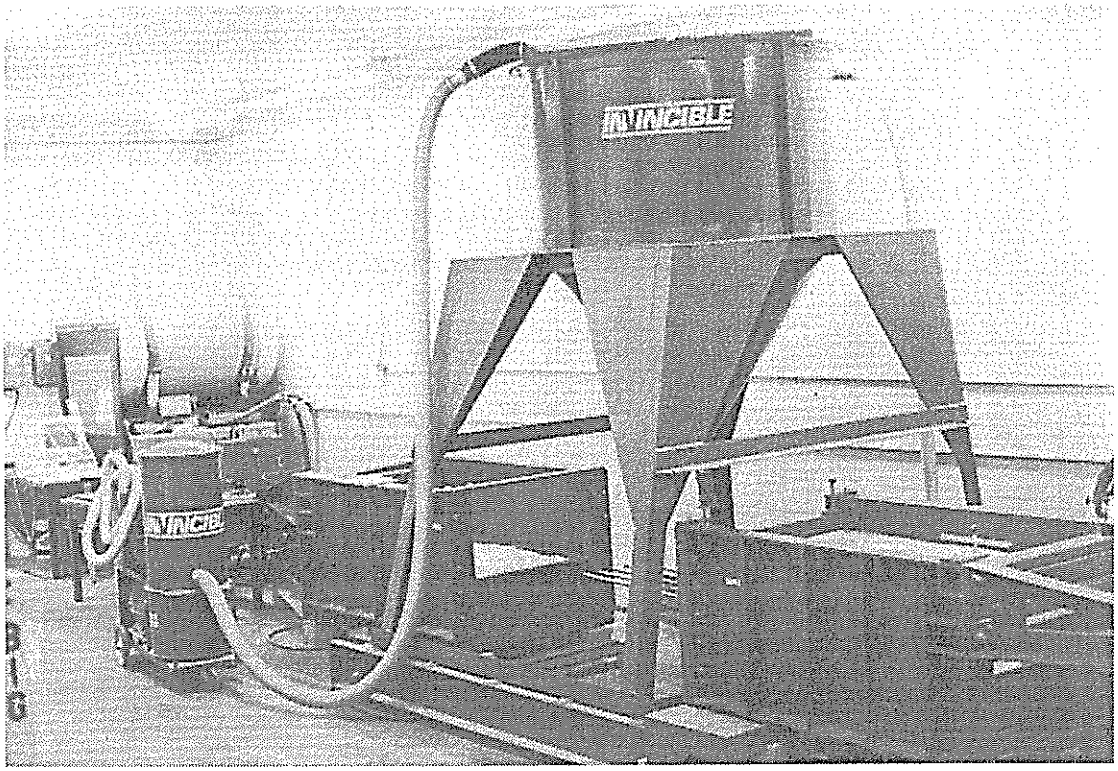

Figure 3.3 View of the elevated hopper and the two boxes

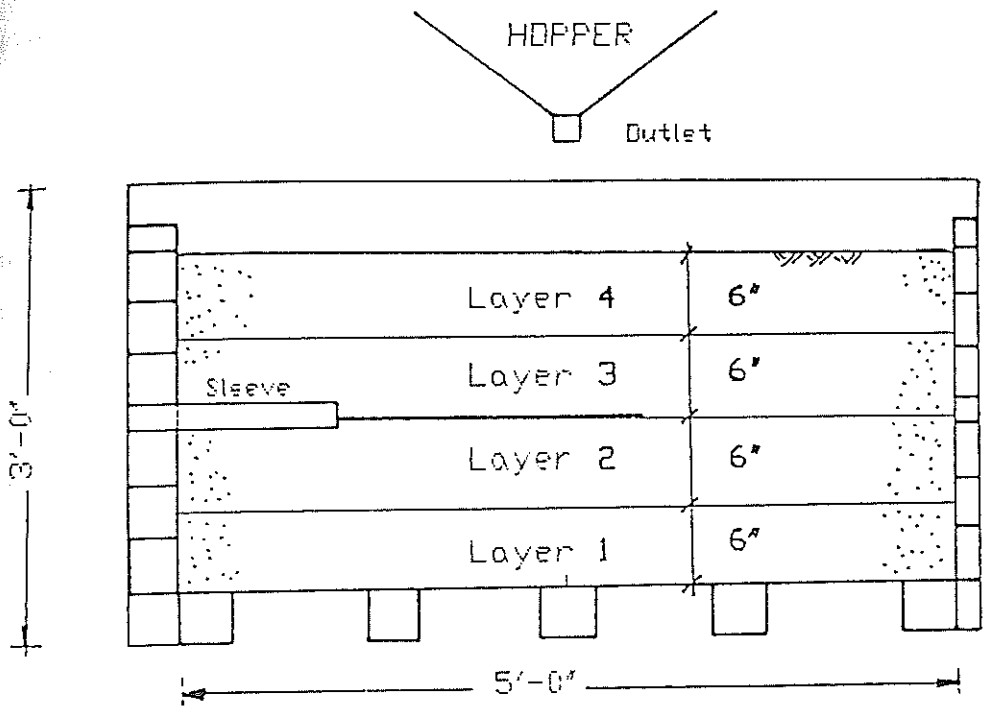

Figure 3.4 Sand placement scheme in the pull-out box

After compaction, the density is measured with a nuclear density gauge model 'TROXLER 3440'. Figure 3.5 displays the soil density measurement in the pull-out box. The gauge rod is embedded 8 to 12 inches into the soil. The density is measured at different locations to validate the uniform density distribution in the box. The locations of soil density measurements in the pull-out and direct shear boxes are shown in Figure 3.6.

3.2.B Compaction Control

In order to evaluate the effect of the compaction procedure on soil density, a compaction scheme which consists of coupling vibration and hammering effect is adopted. A vibrating electric hammer was modified allowing manual compaction of the soil layers.

Calibration tests are performed to establish the compaction effort and scheme necessary to achieve the required relative density. For the purpose of a performance evaluation study, calibration tests are performed with two different sand placement procedures, namely:

i) Variable falling height: In this procedure, the level of the outlet pipe in the hopper is fixed. This leads to different sand falling heights from the hopper outlet to each of the sand layers in the box.

ii) Constant falling height: In this procedure, the hopper outlet is connected to a flexible hose to keep the sand falling height constant from the outlet to each layer.

Under each of these two soil placement methods, different compaction efforts are applied to the sand layers; namely,

1. No compaction: the hopper outlet is moved above the box to permit uniform fill and soil layers are leveled with minimum disturbance in order to achieve minimum soil density.
2. 40 blows per layer: Soil was compacted by applying 40 blows uniformly at each layer.
3. 110 blows per layer.
4. 200 blows per layer.

Density is measured after compaction of each layer. The relationship between the applied number of blows and the resulting soil density, for the two cases of variable and constant sand falling heights, are shown in Figures 3.7-a and b, respectively. These curves can be used to estimate the number of blows per layer for a specific soil density. The results show that the constant falling height procedure (which maintains the falling distance constant above each layer)

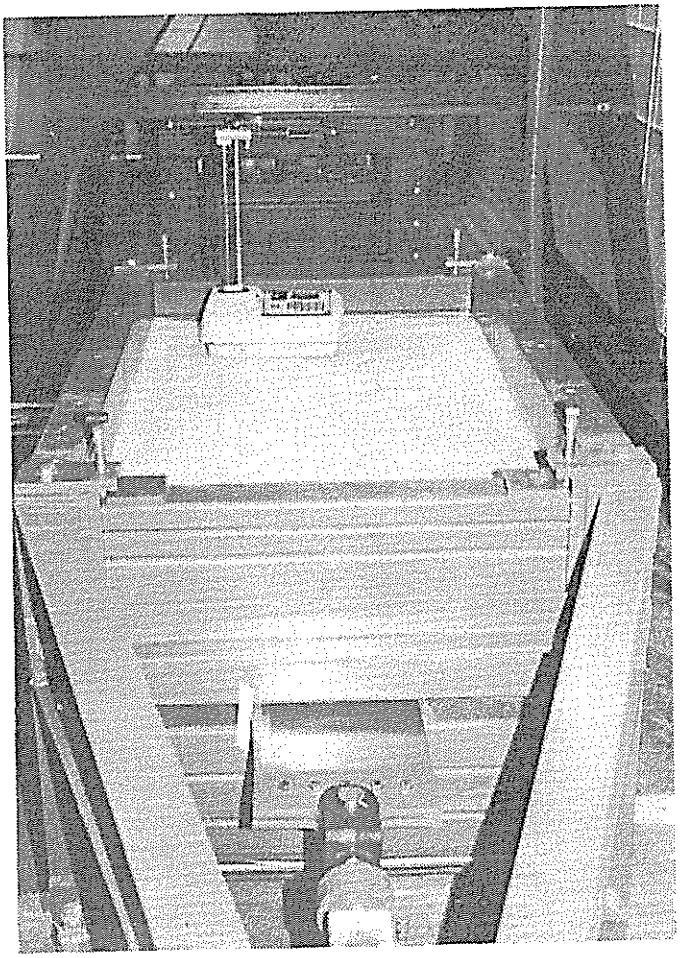

Figure 3.5 Soil density measurements in the pull-out box

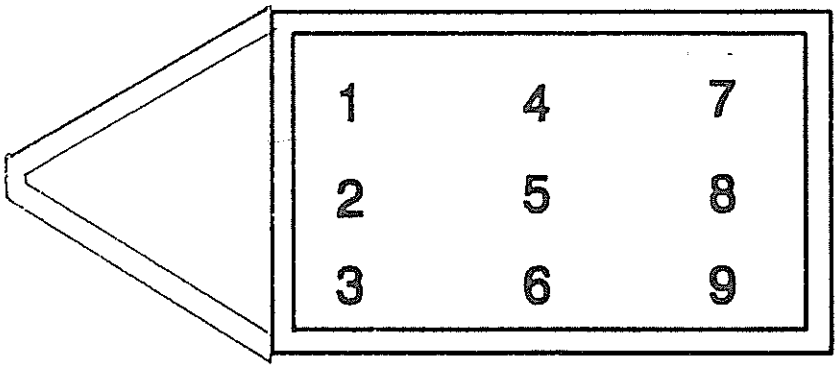

a) Points of density measurements in pull-out box

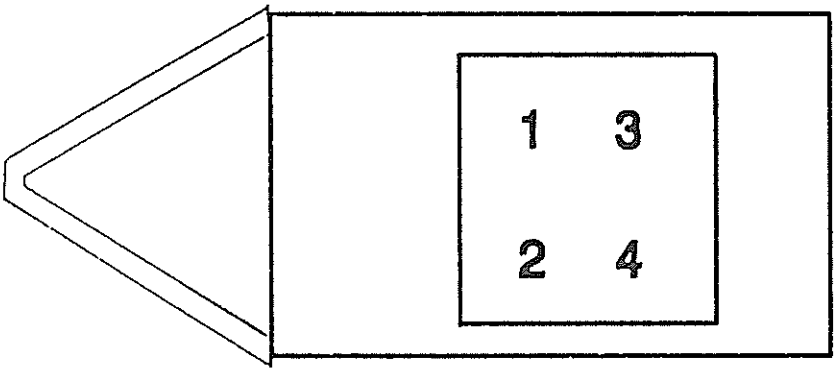

b) Points of density measurements in direct shear box

Figure 3.6 Locations of soil density measurements

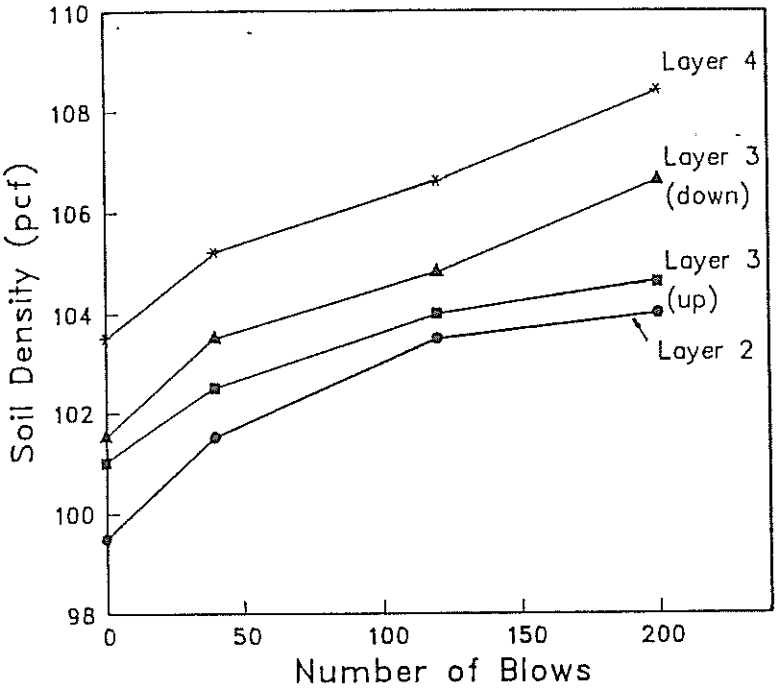

(a) Variable falling height procedure

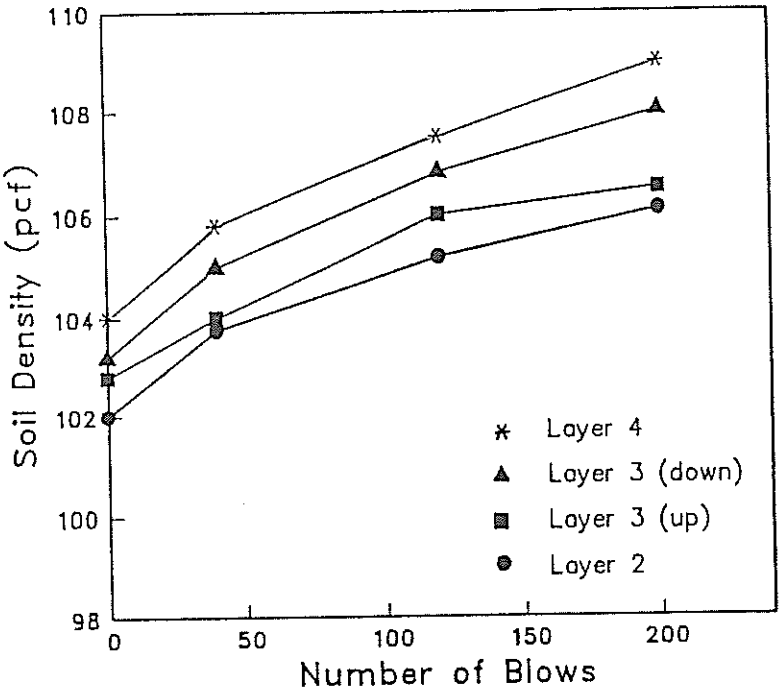

(b) Constant falling height procedure

Figure 3.7 Relationship between sand density and compaction

allows better control of compaction and results in soil densities independent of falling height. The results in the figure also indicate that placement and compaction of the upper sand layers results in an additional increase in sand density in the lower layers. A systematic and consistent sand placement, leveling and compaction techniques should be used in order to achieve a reproducible state of soil density.

3.2.C Reinforcement Preparation

The evaluation study of the pull-out and direct shear boxes is conducted using geogrid 'Tensar-SR2'. It is a uniaxial high density polyethylene (HDPE) geogrid commonly used in soil reinforcement. The geometrical configuration and specifications of the geogrid are presented in Figure 3.8. Specimens of various widths and lengths are tested in the pull-out box in order to evaluate the effect of specimen/box dimensions on the pull-out results. In the large shear box, the specimens have the same size as the upper box (i.e. 27-inch width by 27-inch length).

In the pull-out box, geogrid specimens are bolted to the clamping plates and placed over 1 ft of sand. Sleeves, of various lengths, are used around the clamping plates at the front wall. Figure 3.9 shows the placement of the geogrid in the pull-out box. In the direct shear box, the geogrid specimen is placed at the interface between the upper and lower parts of the box inside the upper box. Figure 3.10 displays the placement of the geogrid in the direct shear box.

The displacement distribution along the geogrid in the pull-out box is measured by five LVDT's connected to the transversal ribs of the geogrids. Figures 3.11 displays the locations of the displacement measurements along the geogrid. The LVDT's are placed on the rear table and connected to the geogrid through non-extensible wires. The wires extend through 1/2-inch plastic tubes embedded in the sand to prevent the frictional resistance of the sand to the movement of the wires. A sand layer of 1 ft thick is placed above the reinforcement, and the air bag is placed above the sand. The air bag is covered by the cover plate and the confining plates. Confining pressure is then applied from the regulated air supply.

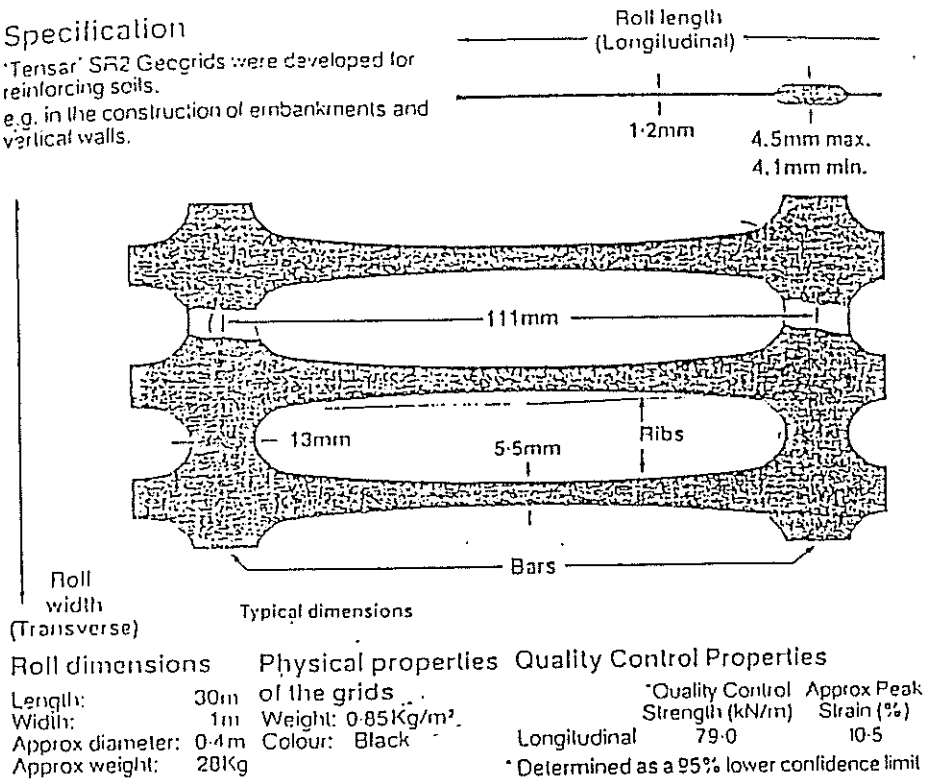

Figure 3.8 Geometric configuration and specifications of TENSAR-SR2

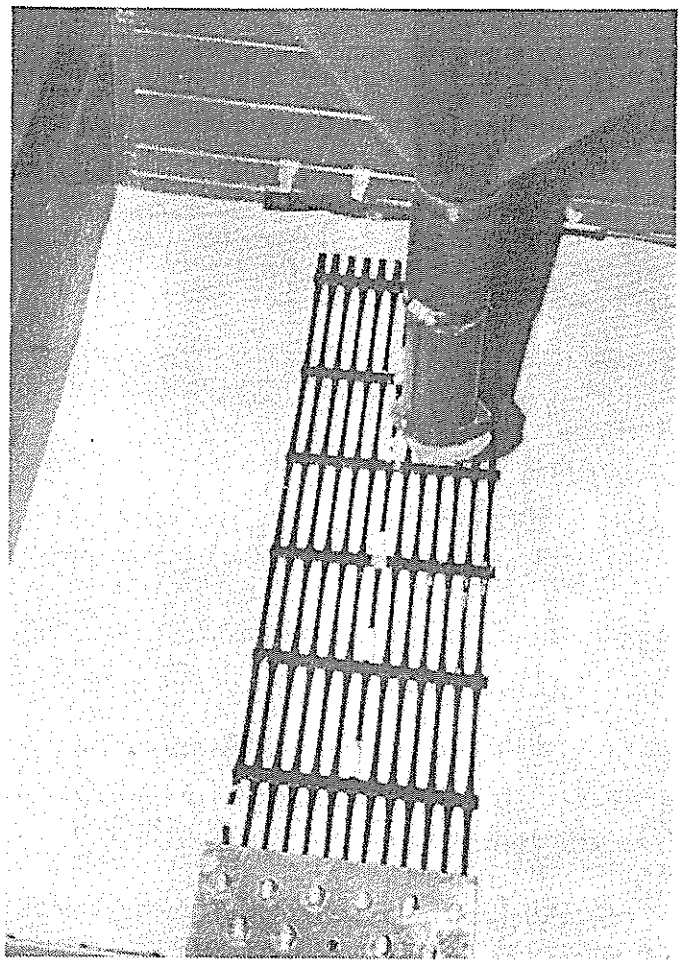

Figure 3.9 Placement of the geogrid in the pull-out box

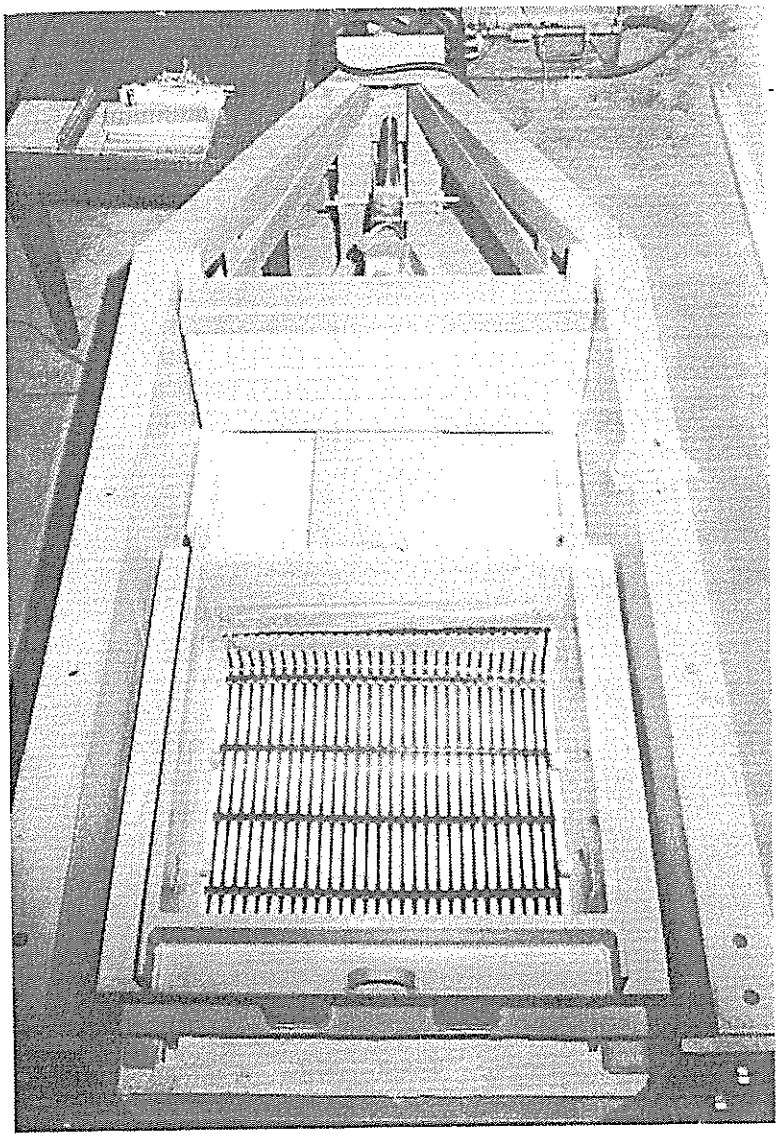

Figure 3.10 Placement of the geogrid in the large direct shear box

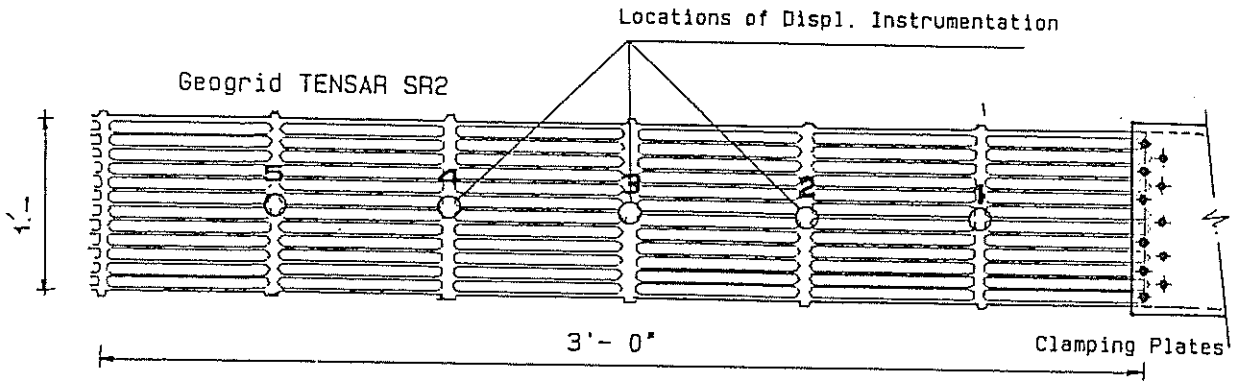

Figure 3.11 Locations of displacement measurement along the geogrid in pull-out box

3.3 DISPLACEMENT-RATE CONTROLLED TESTS

3.3.A Unconfined Extension Tests

Unconfined extension tests are performed on the geogrids in order to evaluate the material behavior in the unconfined state, the equipment performance, and its reproducibility under the displacement-rate controlled mode.

Geogrid specimens of 1-ft width and 3-ft length are tested in the unconfined state. The front end of the specimens are bolted to the clamping plates while the rear ends are clamped to the rear wall of the pull-out box. A computerized monitoring procedure is employed to operate the hydraulic pump to render a constant pull-out velocity of 0.15 inch/min (i.e. strain rate 0.4%/min). Table 3.1 displays the testing parameters in the unconfined extension tests. The front displacement, the pull-out velocity, and the load are monitored during the test. Figure 3.12 displays the unconfined load-strain relationship of the geogrid. The results in the figure demonstrate the reproducibility of test results.

Table 3.1
UNCONFINED EXTENSION TESTS ON GEOGRID

Test	Specimen Dimensions width (ft)	length (ft)	Strain rate (%/min)
TEST#1	1	3	0.40
TEST#2	1	3	0.42
TEST#3	1	3	0.44

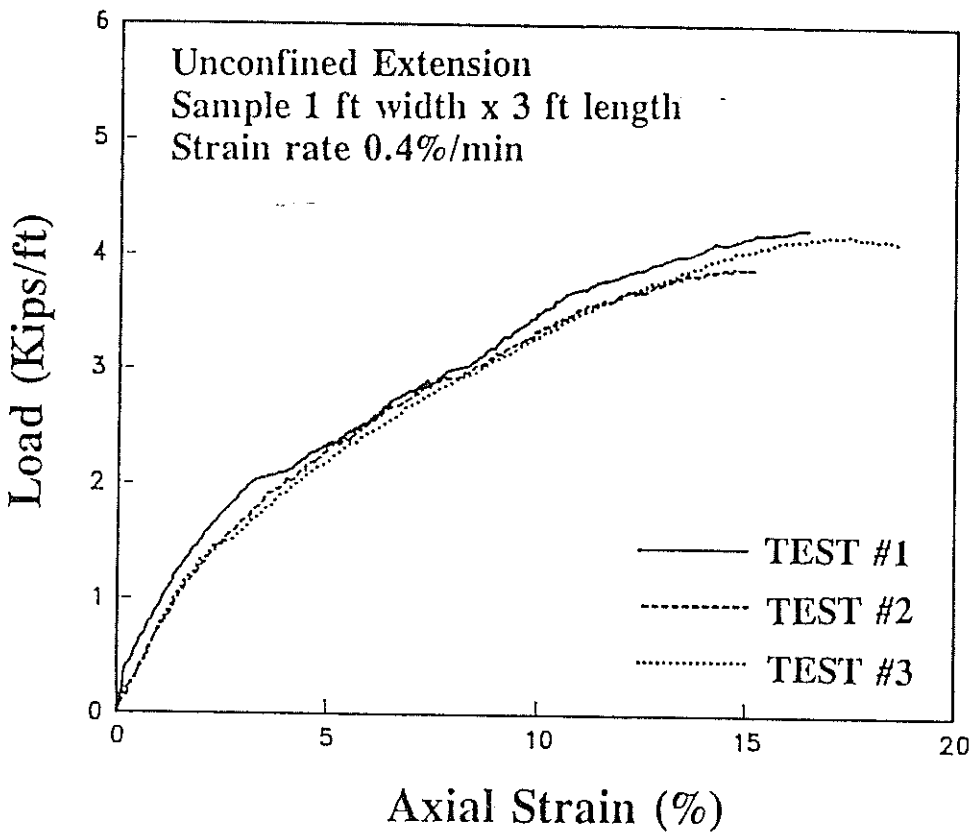

Figure 3.12 Unconfined extension test results on the geogrid

3.3.B Pull-out Tests

In order to evaluate the frictional resistance between the soil and the clamping plates, pull-out tests are performed on the clamping plates without the geogrids. Figure 3.13 displays pull-out test results on clamping plates of 1 ft and 2.5 ft widths under confining pressure of 7 psi (48 KN/m^2) and average soil density of 106 pcf (1.7 t/m^3). The results depict an interface friction angle of 20° between the soil and clamping plates. The frictional resistance of the clamping plates is subtracted from the results of pull-out tests on geogrids.

Pull-out tests are conducted on Tensar-SR2 geogrids in order to evaluate the equipment performance in pull-out testing and the interaction mechanism of geogrids in pull-out. Soil density of 104 pcf (1.67 t/m^3), confining pressure of 7 psi, and pull-out rate of 0.25 in/min are maintained for each test in order to evaluate the repeatability of pull-out test results. Six pull-out tests, under the identical set of testing parameters (Set No. 1), are performed. Table 3.2 presents the testing parameters in this set. Figures 3.14 and 3.15 display the load-displacement relationships of the geogrids in pull-out tests of set No. 1. The figures provide the peak pull-out resistance, front displacement at peak, and interface stiffness modulus. The results display similar values, and confirm the reproducibility of results and the precision of the testing equipment.

It should be noted that the large direct shear box can be modified to operate as a second pull-out box. In this case, the upper box is removed, the clamping plates are bolted to the geogrid, and 1 ft of soil is placed above the geogrid. Modifying the large direct shear box to run pull-out tests permits the accurate validation of the monitoring devices in both boxes. Moreover, the time required to run creep tests demands the use of the second box in creep tests while conducting displacement-rate controlled tests in the first one. For the purpose of evaluating pull-out test results when another pull-out box is utilized, some of the pull-out tests are conducted in the modified direct shear box (i.e second pull-out box). Test D-104A is one of the tests conducted in the second pull-out box. Pull-out test results in Figure 3.14 display similar values from both pull-out boxes under the identical testing conditions.

Table 3.2

TESTING PARAMETERS IN PULL-OUT TESTING SET NO. 1

Test	Geogrid Dimensions width (ft)	length (ft)	Pull-out rate (in/min)	Confining Pressure (psi)	Avg. Soil density (pcf)	Sleeve length (inch)	Soil thick. (ft)
Test-A3	1.0	3.0	0.25	7.0	103.6	12.	2.
Test-A4	1.0	3.0	0.25	7.0	104.0	12.	2.
Test-A5	1.0	3.0	0.26	7.0	104.5	12.	2.
Test-A7	1.0	3.0	0.27	7.0	104.2	12.	2.
Test-A8	1.0	3.0	0.26	7.0	104.1	12.	2.
D-104 A	1.0	3.0	0.25	7.0	104.2	12.	2.

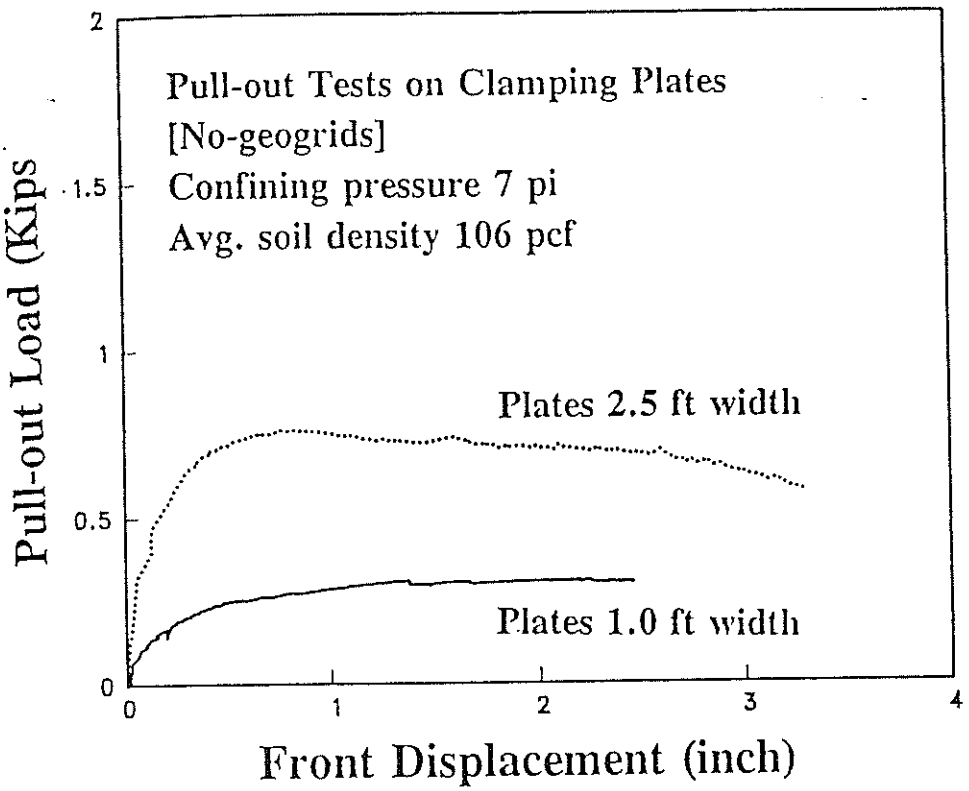

Figure 3.13 Frictional resistance of the clamping plates in the pull-out box

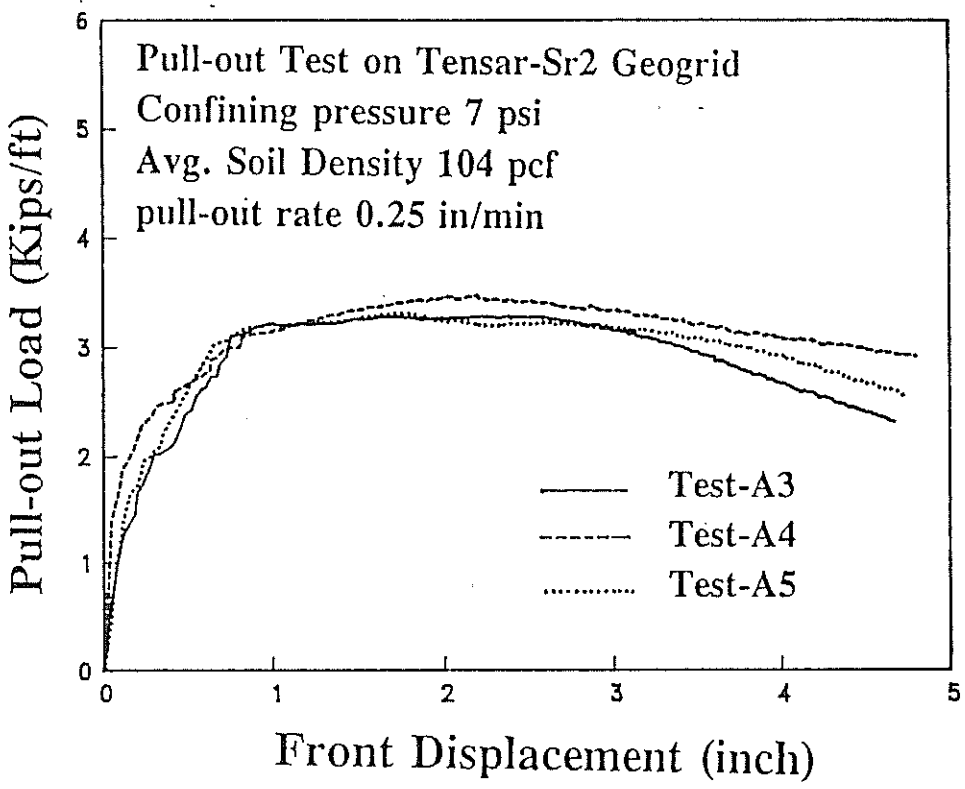

Figure 3.14 Pull-out test results on geogrids, Set No. 1

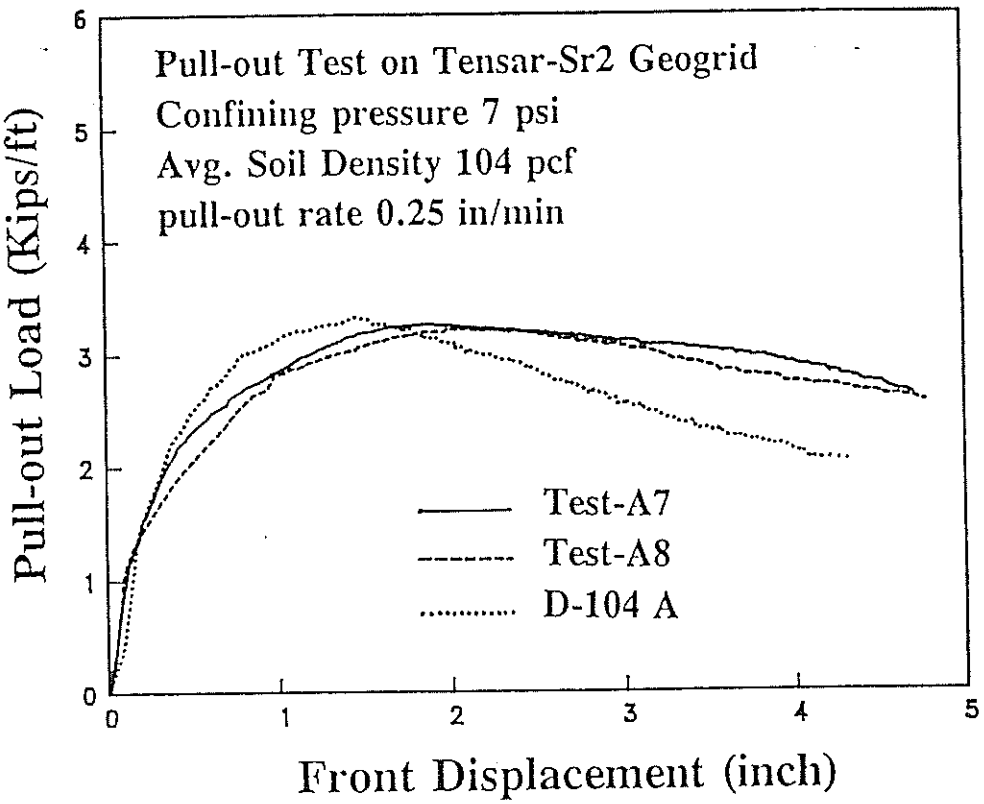

Figure 3.15 Pull-out test Results on geogrids, Set No. 1

Another set of pull-out tests are conducted on the geogrids with an average soil dry density of 106 pcf (1.7 t/m^3), confining pressure of 7 psi, and pull-out rate of 0.4 in/min. The testing parameters of this set (Set No. 2) are presented in Table 3.3. The load-displacement relationship of the geogrids is displayed in Figure 3.16. The comparison of test results of set No. 2 and set No. 1 demonstrates the effect of the change of testing parameters on the pull-out resistance of the geogrid. The effects of the variation of testing parameters (e.g. soil density, confining pressure, displacement-rate, sample dimensions and boundary conditions) on the pull-out response of the geogrids are discussed in detail in Chapter 4.

Table 3.3

TESTING PARAMETERS IN PULL-OUT TESTING SET NO. 2

Test	Geogrid Dimensions width (ft)	length (ft)	Pull-out rate (in/min)	Confining Pressure (psi)	Avg. Soil density (pcf)	Sleeve length (inch)	Soil thick. (ft)
Test-C2	1.0	3.0	0.41	7.0	105.5	12.	2.
Test-C3	1.0	3.0	0.40	7.0	106.0	12.	2.
Test-C4	1.0	3.0	0.38	7.0	N/M*	12.	2.

* Not measured

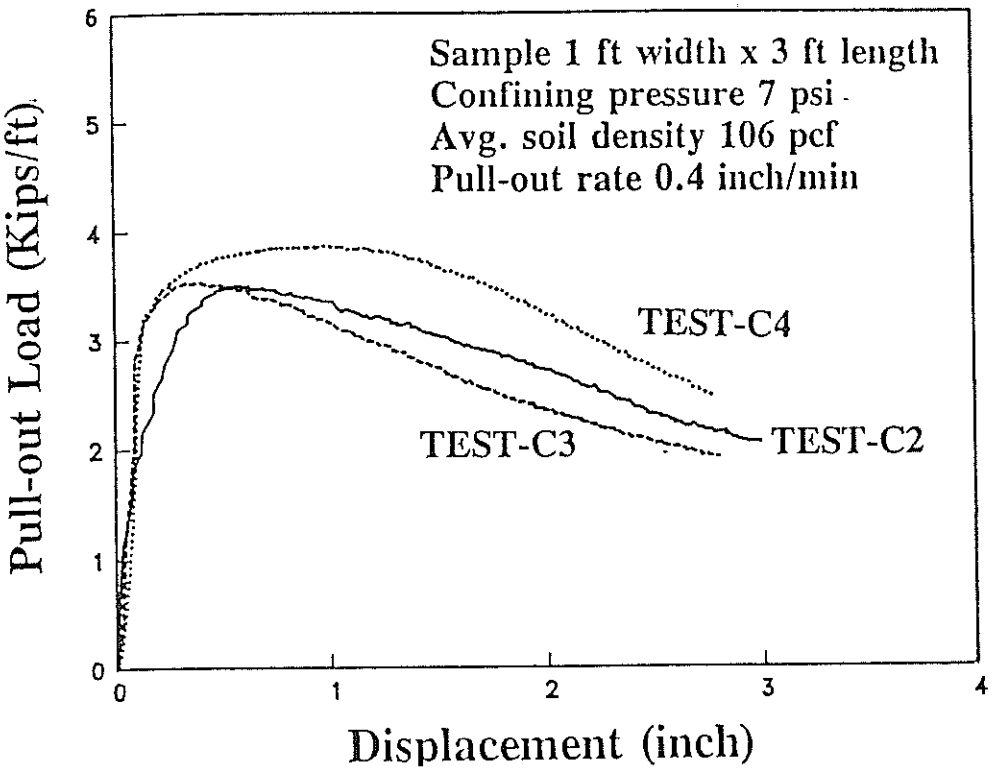

Figure 3.16 Pull-out test results on geogrids, Set No. 2

The displacements at different nodes along the geogrid are monitored by the LVDT's at the rear table. Figure 3.17 displays typical time-nodal displacement relationship of the geogrid in Set No. 1. The results in the figure demonstrate the progressive load transfer mechanism along the geogrid:

i) At the front node (i.e. at node 0), the slope of the front displacement verses time is practically constant and is equal to the controlled pull-out displacement rate.

ii) At the early stages of pull-out response, the differences in the slopes of nodal-displacement curves manifest the progressive load transfer along the geogrid. At this stage, most of the pull-out load is carried out by the front part of the geogrid. Consequently, higher strains are mobilized at the front part of the geogrid with practically no strain at the rear nodes.

iii) The slopes of time-nodal displacement curves become practically equal at the later stages of testing, indicating that the geogrid extension is fully mobilized along its length. At this stage, the geogrid moves as a rigid body without any further extension. The specific point on the displacement curve where the slopes become practically equal indicates the occurrence of the slippage failure of the reinforcement which is attained at the peak pull-out resistance.

Figure 3.18 displays the displacements at the front and rear nodes of the geogrid from different tests in Set No. 1. The repeatability of the displacement measurements and reproducibility of the monitoring system are demonstrated.

In order to illustrate the progressive load transfer mechanism along the geogrid in pull-out tests, the displacements at different loading levels are plotted along the length of the geogrid in Figure 3.19. The figure shows that, at an early stage of loading, the displacements of the front nodes are mobilized while practically no displacements are mobilized at the rear ones (nodes 4 and 5). At this early stage of pull-out loading, the front part of the geogrid experiences an extension response without slippage. The displaced length of the geogrid is its effective adherence length. At a later stage of pull-out loading, the geogrid reaches its peak strength, the rear node undergoes displacement, and the geogrid experiences a combined extension-displacement response.

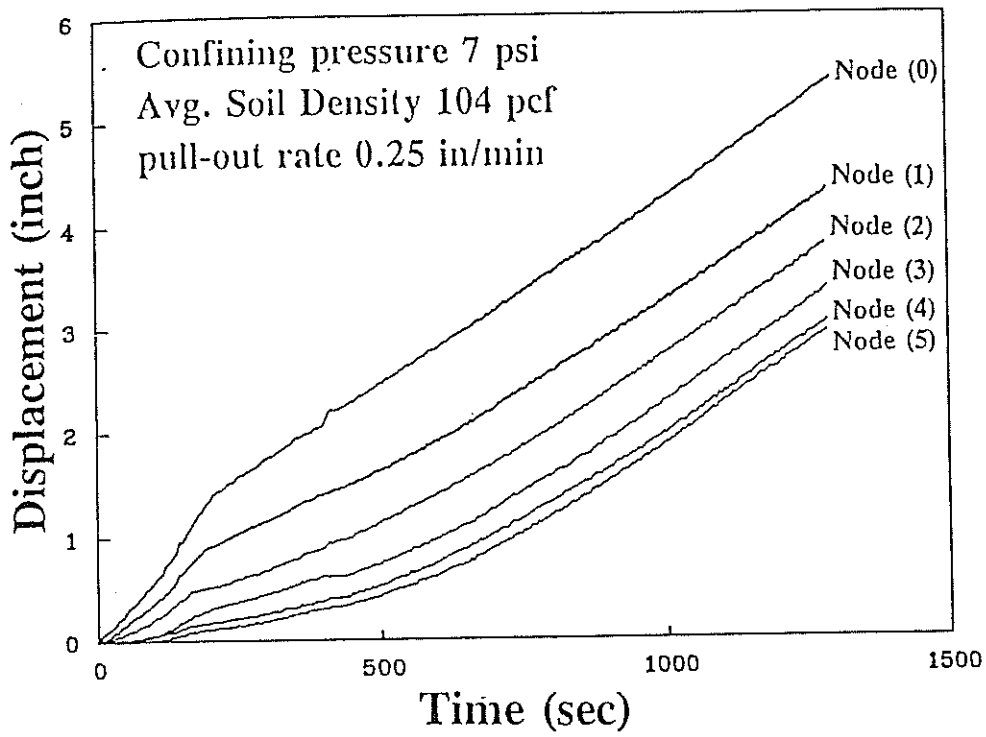

Figure 3.17 Typical time-nodal displacements measurements in Set No. 1 tests

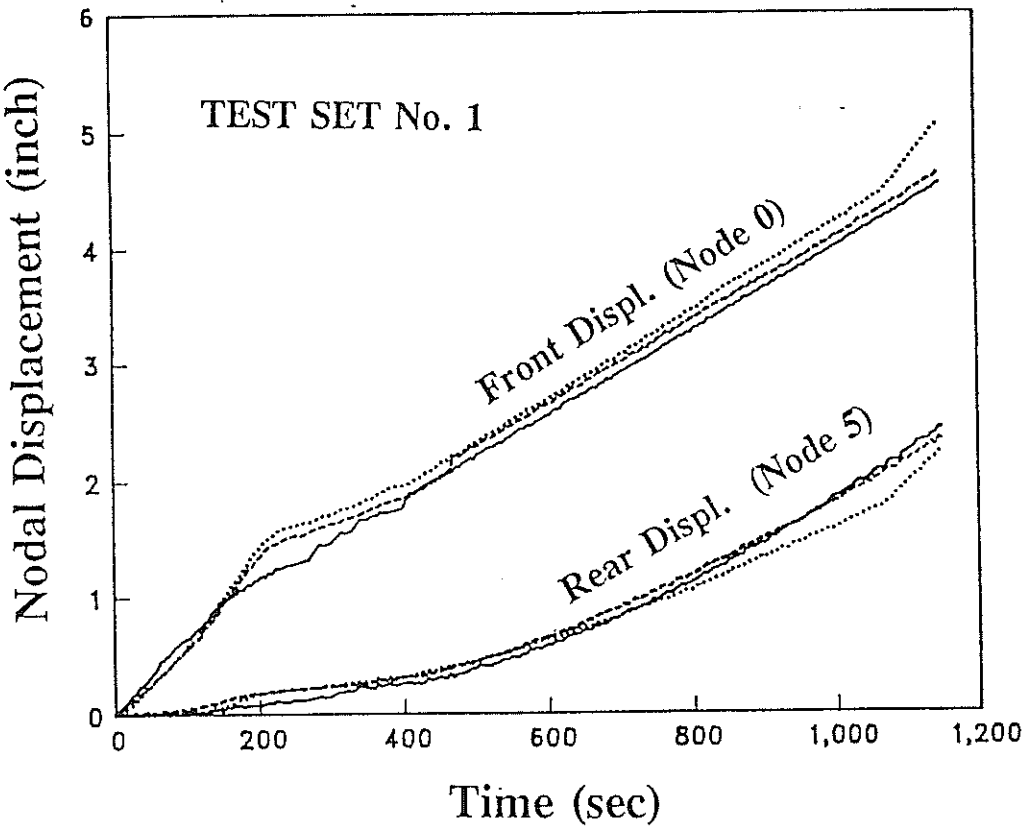

Figure 3.18 Time-nodal displacements measurements in Set No. 1 tests

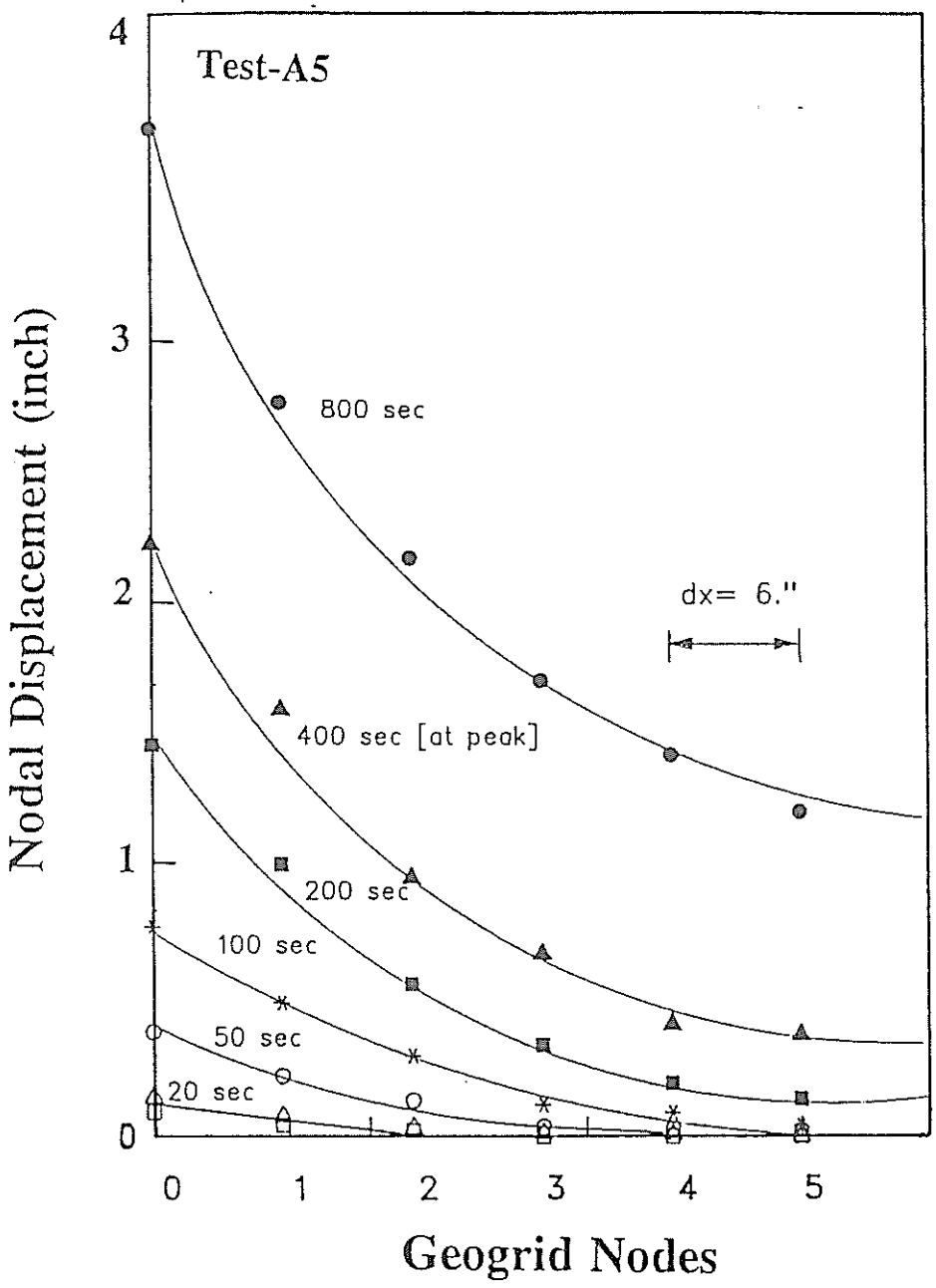

Figure 3.19 Displacements along the geogrid nodes in pull-out

The measured nodal displacements, from different tests in set 1, are normalized with respect to their front displacements in Figure 3.20. In this figure, displacement distributions along the geogrids are plotted at peak load and at 60 percent of peak load. The combined effect of geogrid elongation and interface shear resistance on pull-out resistance is displayed. Pull-out resistance reaches its peak at the displacement where the frictional resistance at the soil-geogrid interface is fully mobilized. Mobilization of shear strains require different magnitudes of displacements for different soils/reinforcement types, and depend on many factors that would affect the interaction performance. These factors are mainly related to the type, geometry and extensibility of the geogrid, the shear strength properties of the soil, and confining pressures.

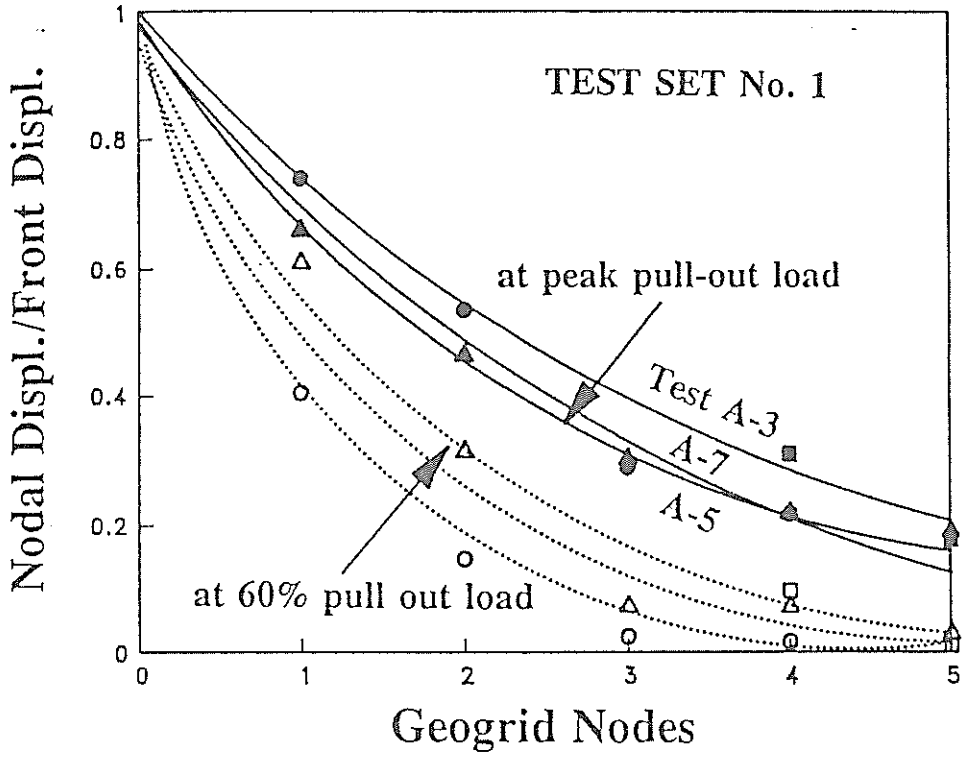

Figure 3.20 Normalized displacements along geogrids in Set No. 1 tests

3.3.C Direct Shear Tests

In the direct shear test, the clamping plates are bolted to the upper shear box which is permitted to move between the lower box and the confining beams on its top (see Figure 2.5). A direct shear testing program is conducted to evaluate the equipment performance. The testing parameters of the direct shear tests are reported in Table 3.4.

The frictional resistance induced between the upper box and the confining beams is measured in tests 'Shear-A' and 'Shear-B'. In these tests, confining pressure is applied without sand in the box in order to calibrate the frictional resistance of the shear box. Figure 3.21 displays the results of these tests. The frictional resistance is subtracted from the results of direct shear tests on sand-sand and sand-geogrid interface.

Direct shear tests are performed on the sand-sand interface, without the geogrid, in order to evaluate the shear stress-strain characteristics of the sand. Figure 3.22 displays the results of these tests. It should be noted that tests in the large direct shear box result in a soil internal friction angle (ϕ) of 27°. Nevertheless, a soil friction angle of 34° is obtained from the conventional direct shear tests results for similar soil relative density. The results demonstrate the influence of shear box dimensions, and the associated boundary conditions, on the shear resistance of sand. However, the evaluation of the effect of the box size on direct shear test results is not in the scope of this research.

Direct shear tests are performed with the geogrid samples at the interface. Geogrid specimens of 27 inches by 27 inches are placed on the bottom of the upper shear box. Figure 3.23 displays the results of these tests. A soil-geogrid interface friction angle (δ) of 28 degrees is obtained. Figure 3.24 depicts the shear stress-displacement relationship at the soil-soil and soil-geogrid interface. An efficiency factor ($\tan \phi / \tan \delta$) practically equaling 1, is obtained from these tests. The results conform with other reported efficiency factors for geogrids (2,11).

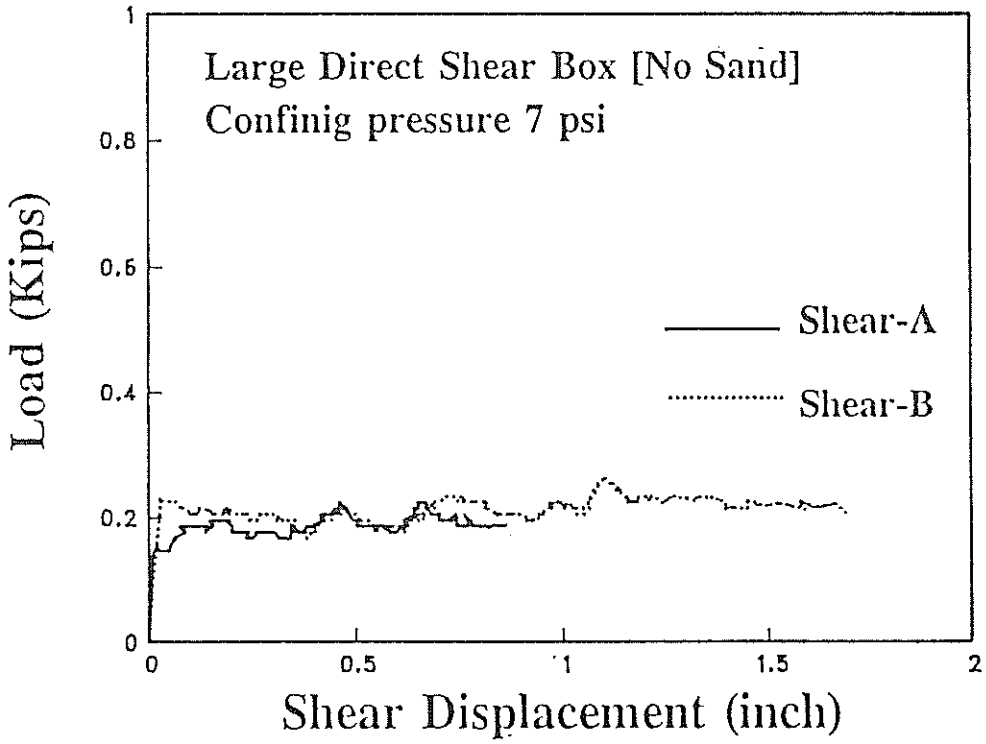

Figure 3.21 Frictional resistance of upper box in direct shear test

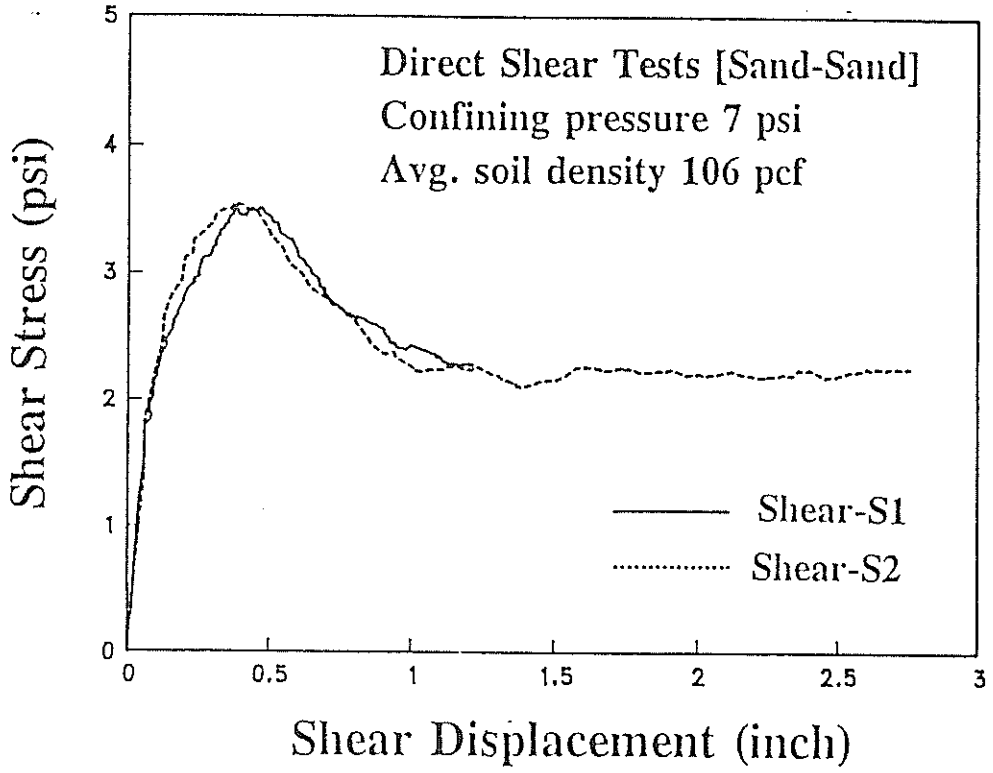

Figure 3.22 Results of direct shear tests on sand-sand interface

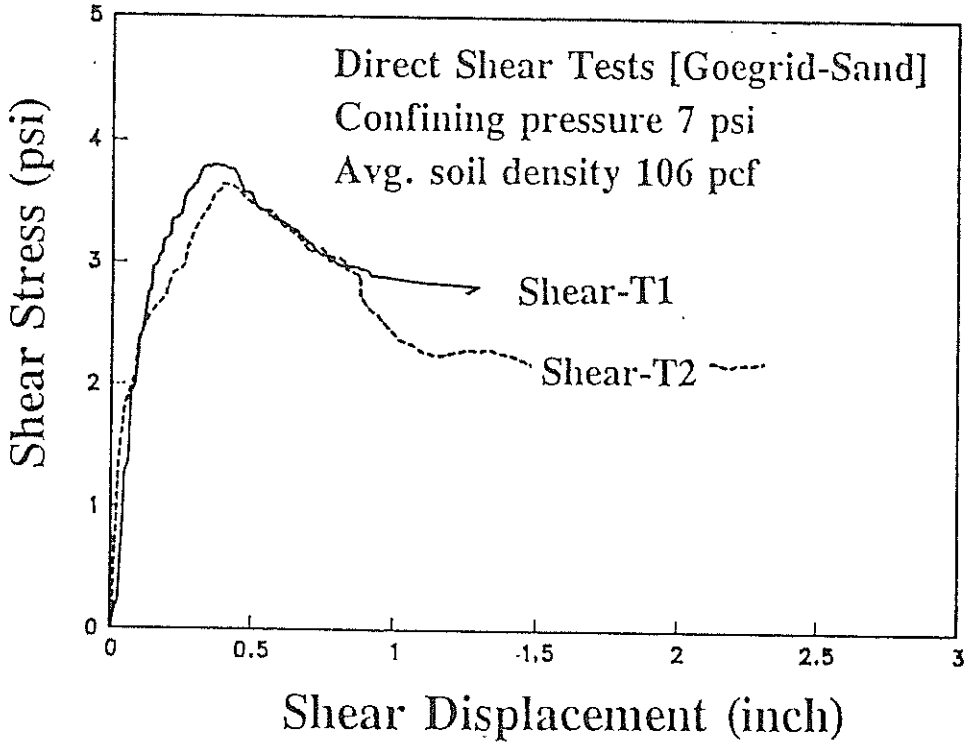

Figure 3.23 Results of direct shear tests on geogrid-sand interface

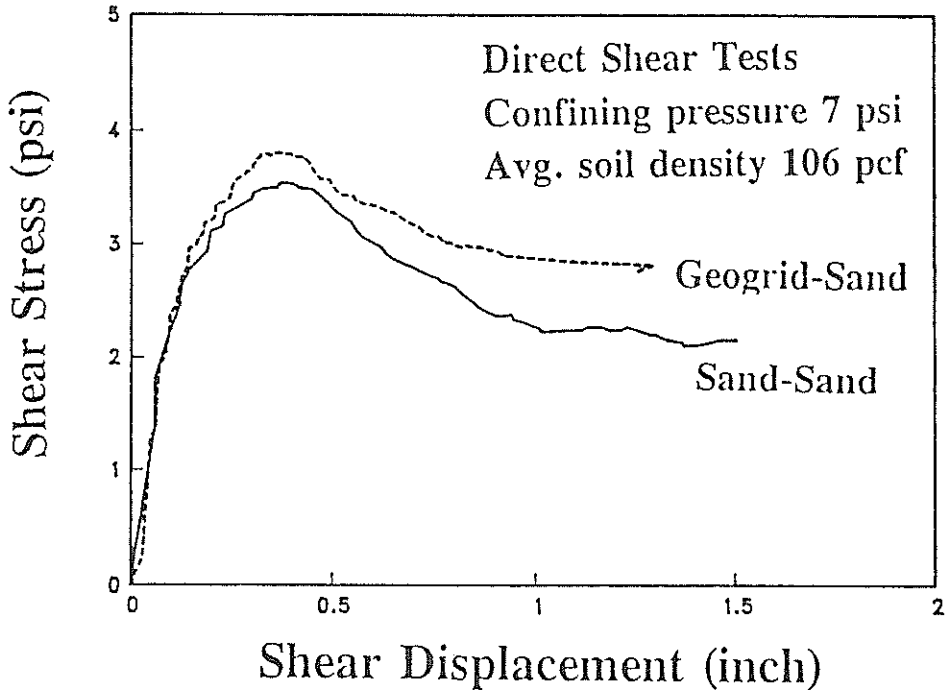

Figure 3.24 Effect of reinforcement on the frictional resistance in direct shear test

3.4 LOAD-CONTROLLED TESTS

When geosynthetic reinforced samples are subjected to sustained loading conditions, the strain response consists of an elastic strain followed by a time-dependant creep strain (Figure 3.25). The main design concerns for the long term stability of the reinforced earth structures are:

i) to predict the long term creep displacement under a constant pull-out load,

ii) to evaluate the critical creep load (or creep strain) below which creep rupture is unlikely to occur.

The critical creep pull-out load can be determined by subjecting the specimen to a stepwise increasing load over a time interval. This interval can be determined at each load level when the deformation is stabilized. The critical creep load can be established following a procedure similar to that used for ground anchors (41), which is illustrated in Figure 3.26. In this procedure, the measured front displacement for each load is plotted against Log time (T). An upward concavity of the creep curve indicates an accelerated creep failure. The slope of the displacement versus Log (T) is plotted against the applied pull-out load to determine the critical creep load Tc.

A limited number of load-controlled tests on 'Tensar-SR2' geogrids are performed in the pull-out box. The conditions of these tests are described in Table 3.5. The purpose of these tests is to evaluate the performance of the testing facility under time-dependent stepped loading conditions. The loads are incrementally applied to the inclusion and maintained constant during a specified period. The induced loads, displacements and displacement-rate at the front are recorded during the tests.

Load-controlled extension tests are performed on the geogrid in the unconfined state. In these tests, geogrid samples of 1 ft wide and 3 ft long are tested. Increasing loads are applied to the samples starting from 10 percent of the maximum strength of the unconfined geogrid. The loads are increased to 40 percent and 70 percent of the maximum strength. Each load increment is kept for 120 minute in order to evaluate the load-displacement monitoring system (Figure 3.27). The axial strains versus the time relationship from these tests are displayed in Figure 3.28. In this figure, creep strains induced by a specific loading are determined as the sum of the strains produced by the previous load increments (42). This concept of strain superposition is illustrated in Figure 3.29.

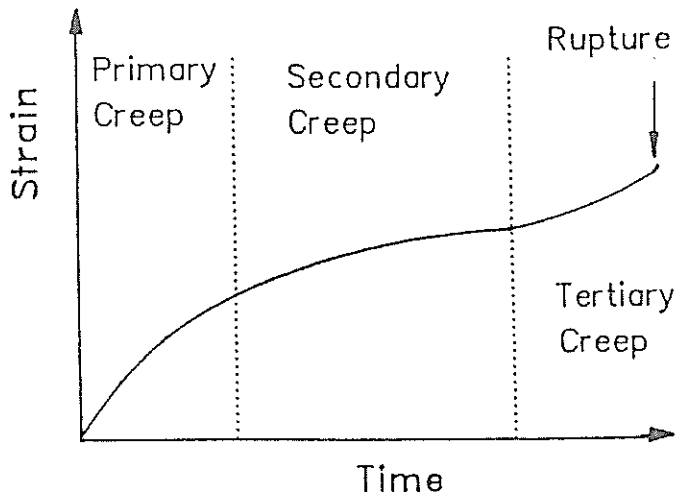

Figure 3.25 Illustration of creep concept

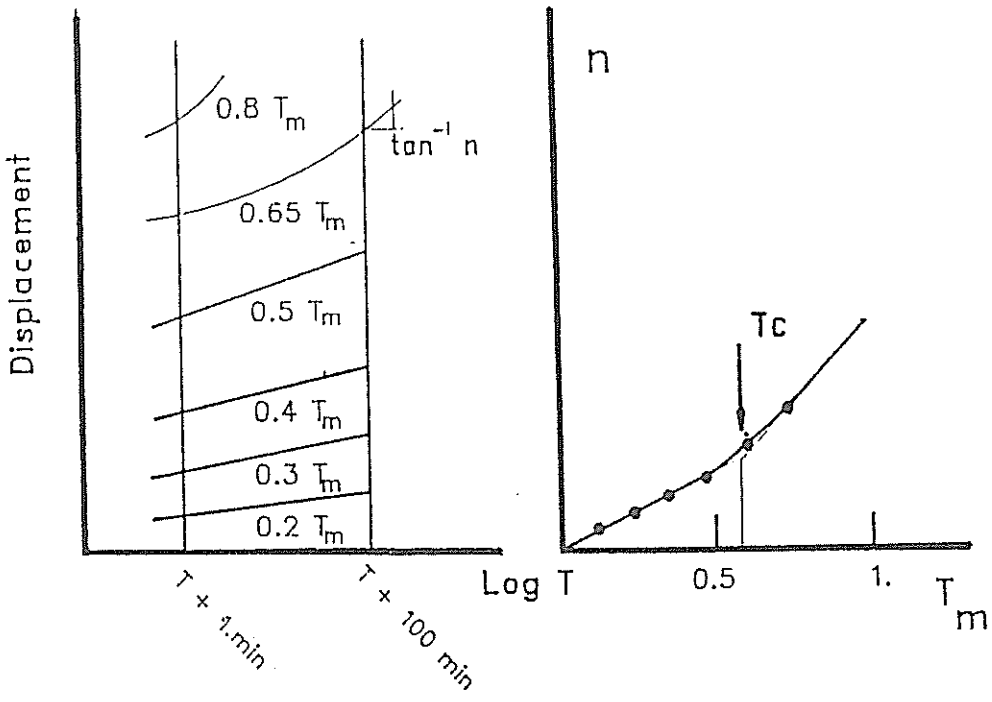

Figure 3.26 Determination of the critical creep load (41)

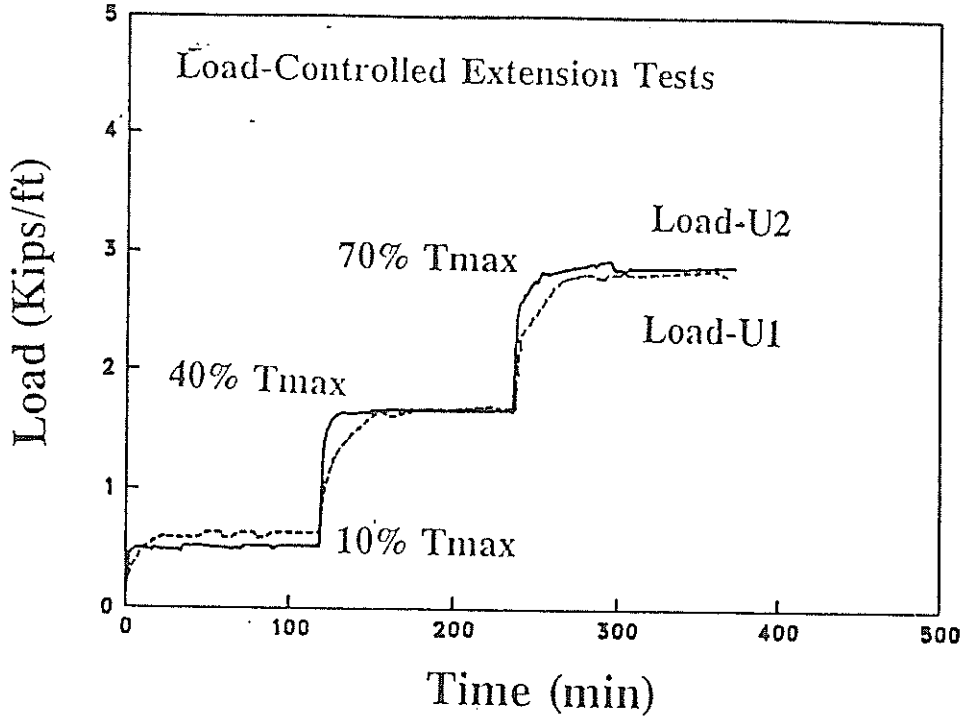

Figure 3.27 Loading scheme in load-controlled extension tests

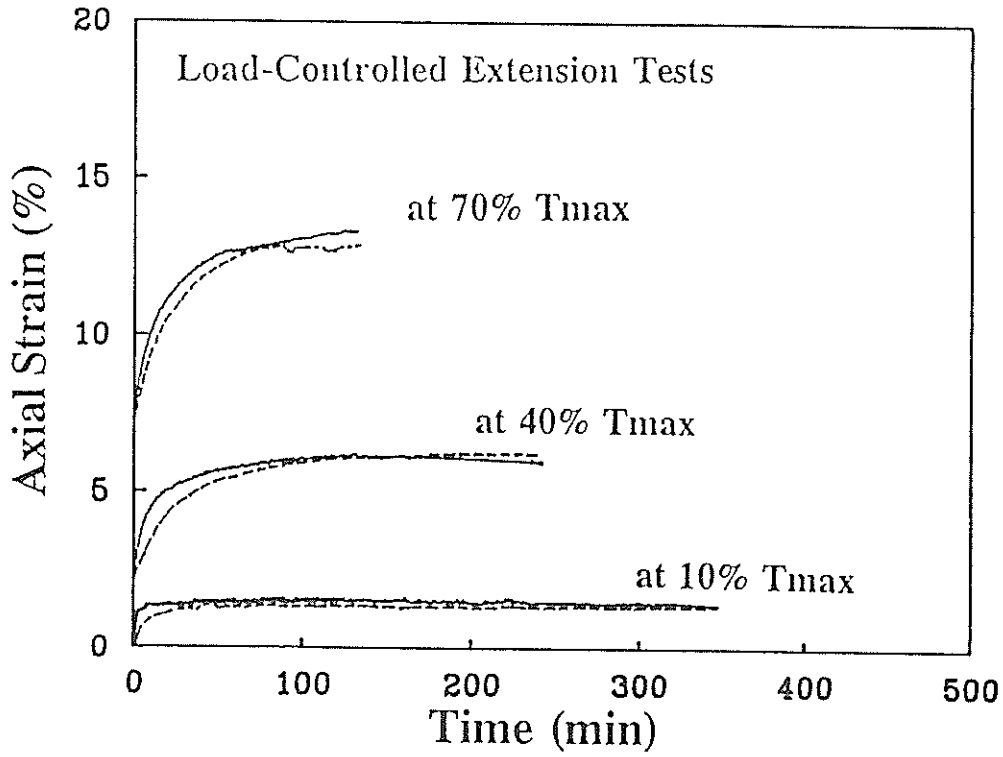

Figure 3.28 Axial strains versus time in unconfined load-controlled tests

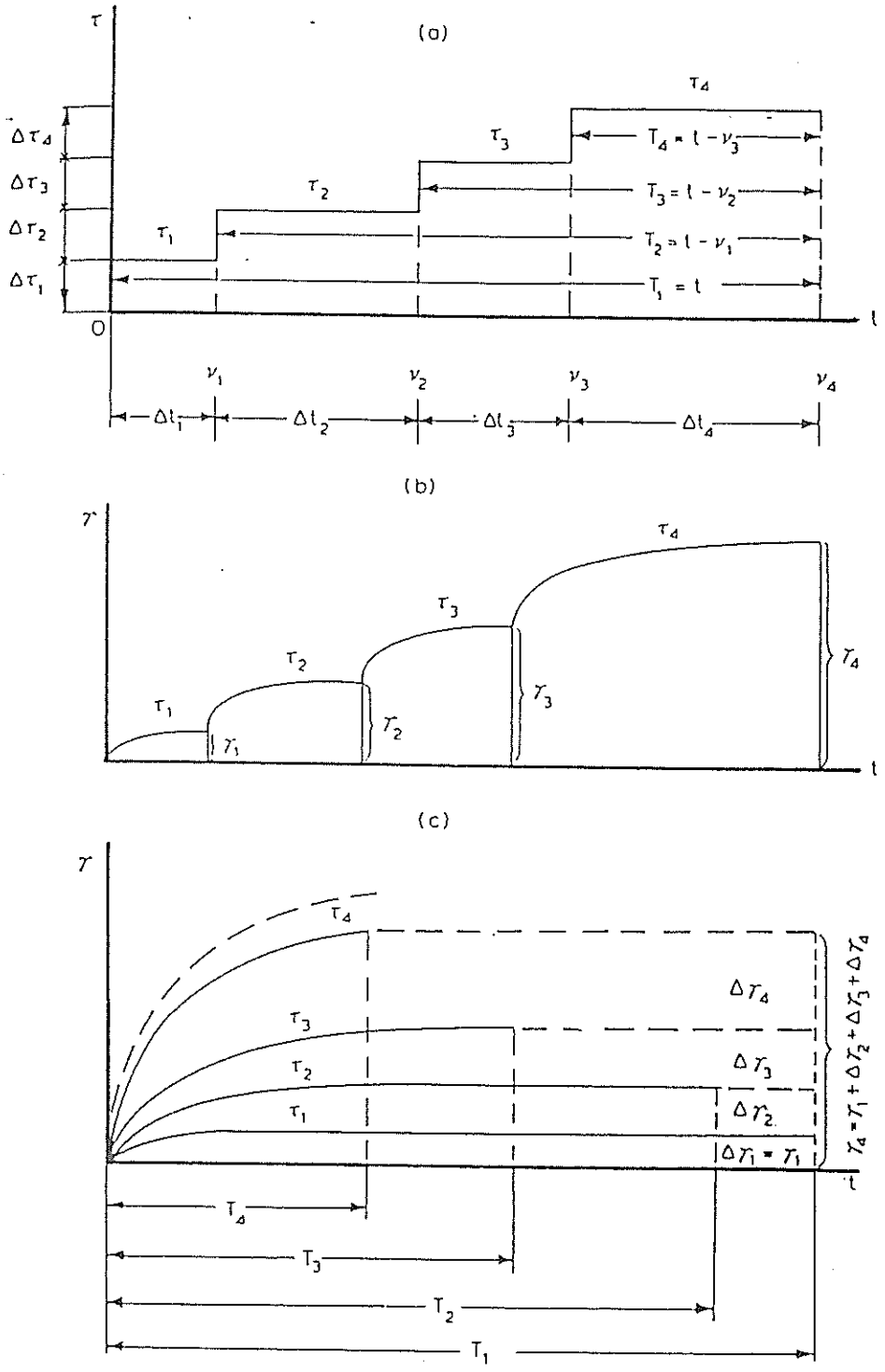

Figure 3.29 Concept of strain superposition in stepped loading tests (42)

Stepped load-controlled pull-out tests are performed on the geogrid. In these tests, the specimens are subjected to different loading levels defined as percentages of the maximum pull-out resistance (Tmax) obtained from displacement-rate controlled tests. Figure 3.30 displays the loading scheme. Geogrid specimens of 1 ft wide and 3 ft long are tested under confining pressure of 7 psi and soil density of 106 pcf. The front displacements, at each loading increment, are displayed versus time in Figure 3.31. The displacement-rates appear stabilized with time during the testing period. However, geogrid specimen may exhibit unstabilized creep displacements if tested for longer periods of time. The evaluation of confined creep characteristics of specific geogrids in pull-out is not within the scope of this research.

Table 3.5

STEPPED LOAD-CONTROLLED TESTS

Test	Test type	Stepped loads (% of Tmax)	Confining pressure (psi)	Soil density (pcf)
Load-U1	unconfined	10% - 40% - 70%	---	---
Load-U2	unconfined	10% - 40% - 70%	---	---
Load-1	pull-out	5%-8%-30%-50%-70%	7.0	106.0
Load-2	pull-out	30%-50%-70%	7.0	N/M

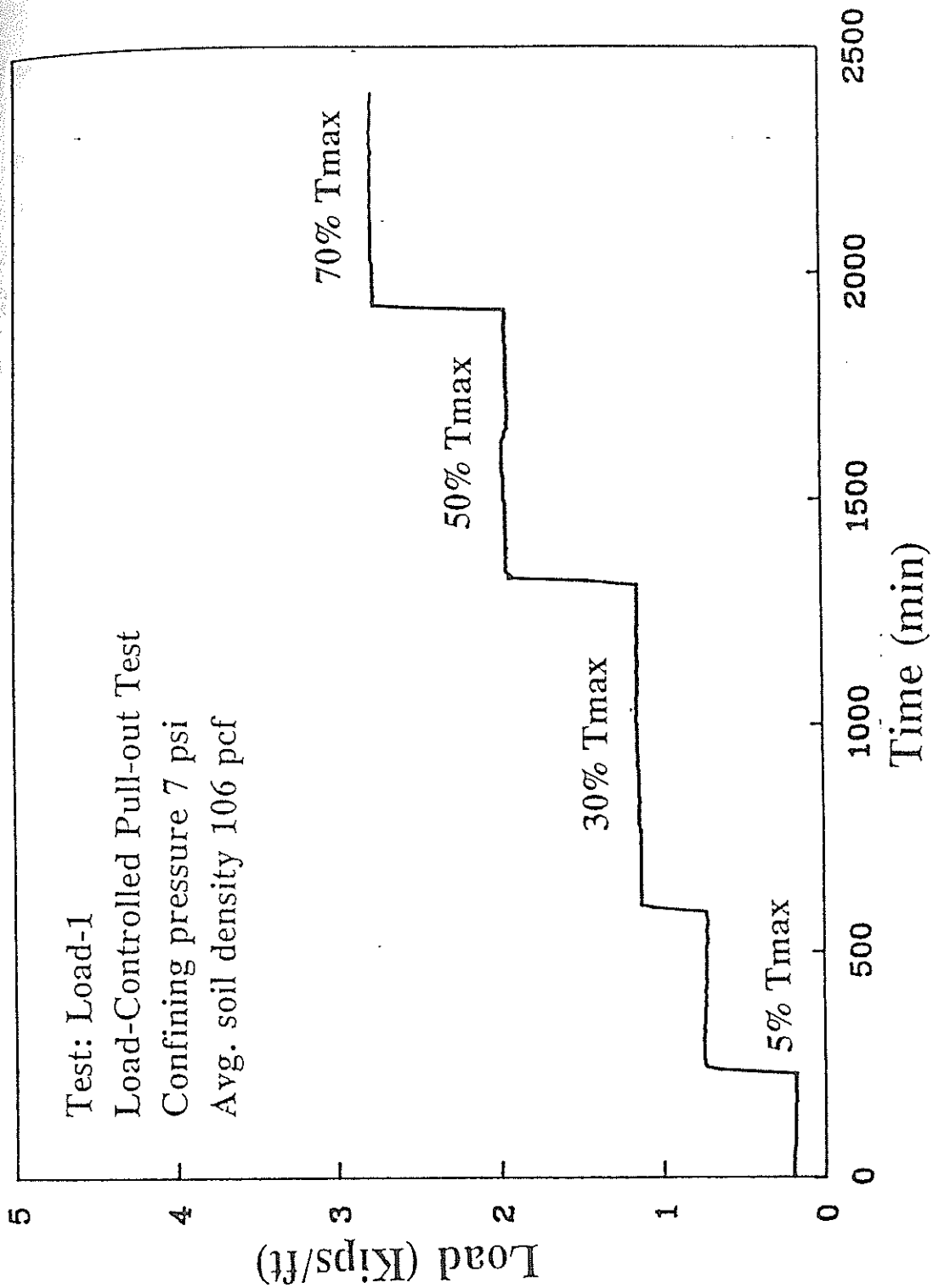

Figure 3.30 Loading scheme in stepped load-controlled pull-out test

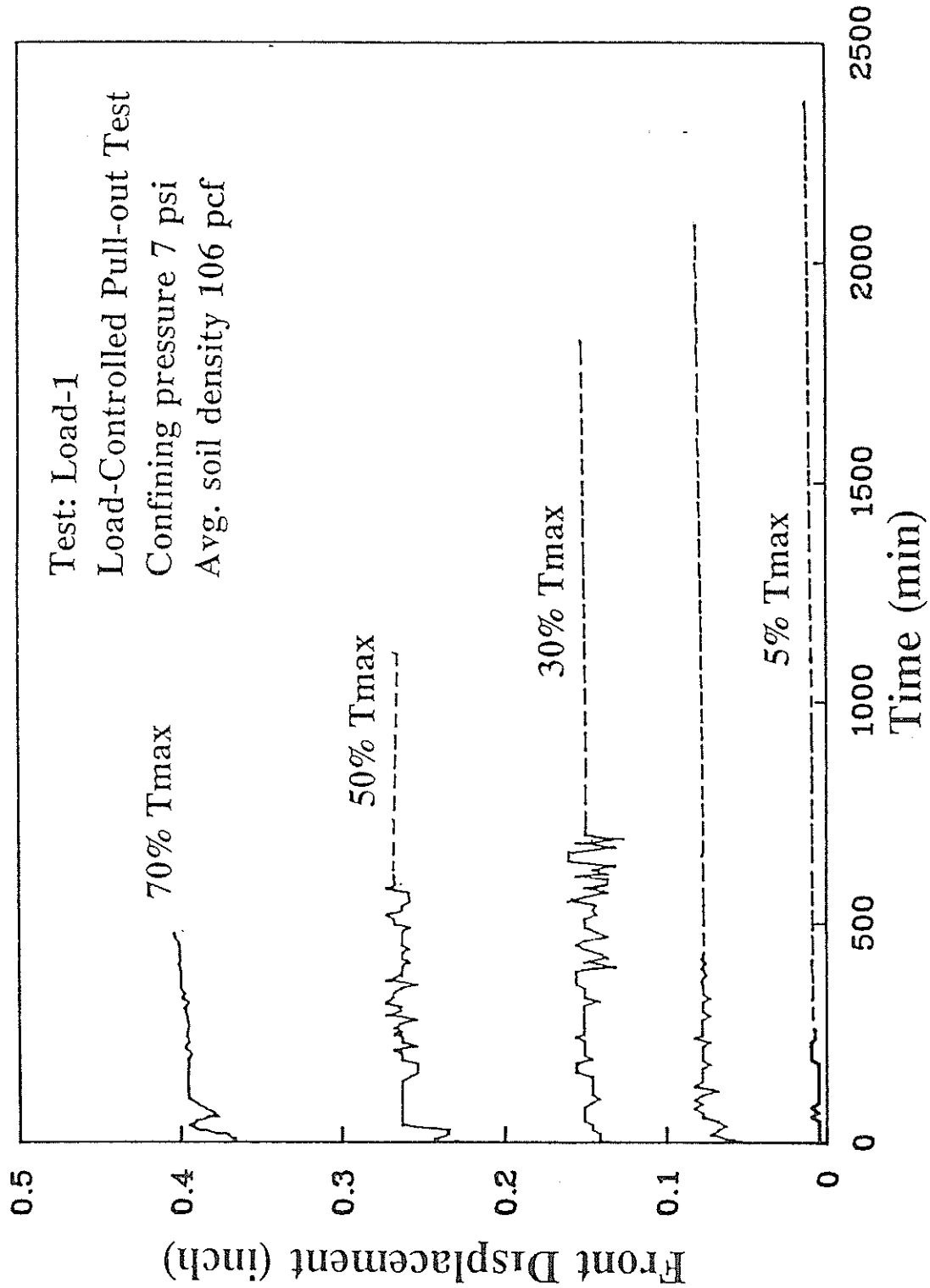

Figure 3.31 Front displacement versus time in stepped load-controlled pull-out test

CHAPTER 4

EFFECT OF TESTING PARAMETERS ON THE INTERACTION MECHANISM

4.1 INTRODUCTION

The soil-reinforcement interaction involves three basic load-transfer mechanisms:

i) lateral friction on the soil-reinforcement interface as in geotextiles, strips and bars,

ii) passive earth pressure on the transversal elements of geogrids, welded wire meshes and bar mats, and

ii) particle interlocking as in the geotextiles and geogrids.

Load transfer in most of the geosynthetic materials is a combination of these mechanisms. Figure 4.1 displays the load transfer mechanism between the soil and geogrids. Mobilization of these mechanisms requires different magnitudes of displacements that would substantially affect the interaction performance. The relative contribution of each mechanism to the total pull-out resistance depends on many factors such as:

i) material properties (e.g. its type, geometry, extensibility and creep properties),

ii) soil characteristics (e.g. its relative density, shear strength and grain size distribution),

iii) loading conditions (e.g. overburden pressure, displacement-rate and testing boundary conditions).

Figure 4.2 illustrates the relative contribution of each load transfer mechanism in different types of geosynthetics.

The major objectives of the performance evaluation study are:

i) to assess the sensitivity of test results to the changes in the testing parameters and the precision of the measurements under different testing conditions,

ii) to evaluate the effect of boundary conditions and other testing parameters on the interaction mechanism of geogrids, and

iii) to establish a data base for the development of a reliable interpretation procedure for pull-out tests.

For this purpose, a parametric study is conducted and the effects of the main testing parameters (i.e. geogrid specimen size, rigid box boundaries, displacement-rate, soil compaction and relative density, and confining pressure) on the pull-out interaction response are investigated.

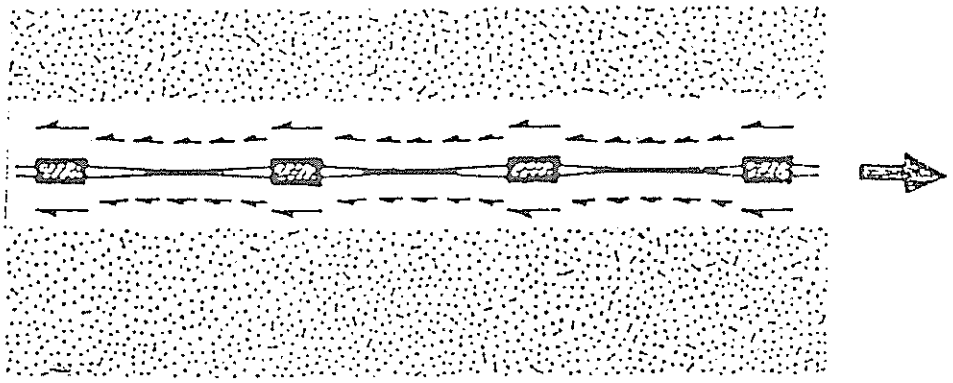

a) Friction Between Soil & Surface

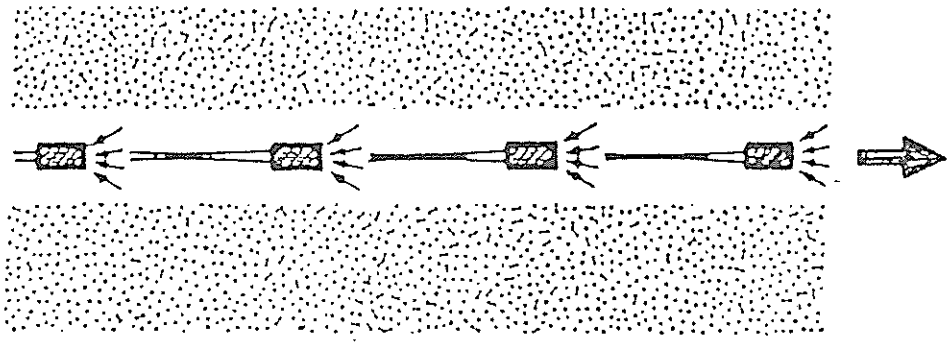

b) Soil Passive Resistance

Figure 4.1 Load transfer mechanism between soil and Geogrids

Figure 4.2 Soil-reinforcement interaction mechanism for geosynthetics

4.2 EFFECT OF TESTING PARAMETERS ON PULL-OUT RESPONSE

The pull-out facility is designed to permit evaluation of the effect of the different parameters on the pull-out response. The main parameters considered in the performance evaluation study are:

a) dimensions of geogrid specimen,

b) sleeve length,

c) soil thickness above and under the geogrid,

d) pull-out displacement rate,

e) soil relative density,

f) applied confining stress.

4.2.A Effect of Reinforcement Dimensions

The development of soil-wall friction along the box walls can influence test results. The applied confining pressures can be partially carried by the friction along the side walls (37). Consequently, the confining pressure near the side walls can be reduced. The effect of side wall friction on the confining pressure is investigated by measuring the normal pressures at different locations in the box. Two pressure cells are placed horizontally at the level of the geogrid specimen. The cells are located near the box center and near the box walls. Figure 4.3 displays a schematic diagram of the locations of the pressure cells in the box. Different confining pressures are applied and the magnitudes of normal pressures are measured before pull-out loading. The measured pressures at the two cells are displayed in Figure 4.4. The results display a reduction in the applied pressures near the box walls.

The effect of the side walls can be reduced by selecting the width of the geogrid specimen to keep the geogrid under uniform normal pressure and away from the side walls. In order to rationally evaluate the geogrid width, which is sufficient to minimize the effect of side walls, geogrid specimens of 0.5 ft to 2.5 ft width are tested in the pull-out box. Pull-out tests are conducted on the geogrids in confining pressure of 7 psi (48 KN/m^2) and average soil density of 106 pcf (1.7 t/m^3). Table 4.1 displays the testing parameters used in these tests. Figure 4.5 displays the placement of the 2.5 ft wide geogrid specimen in the box. The results of the pull-out tests are depicted in Figure 4.6.

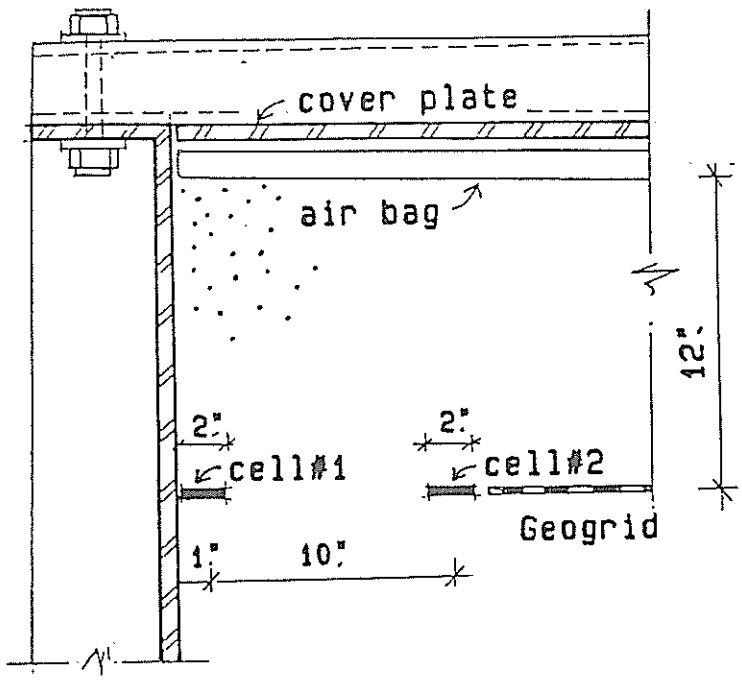

Figure 4.3 Locations of the pressure cells in the pull-out box

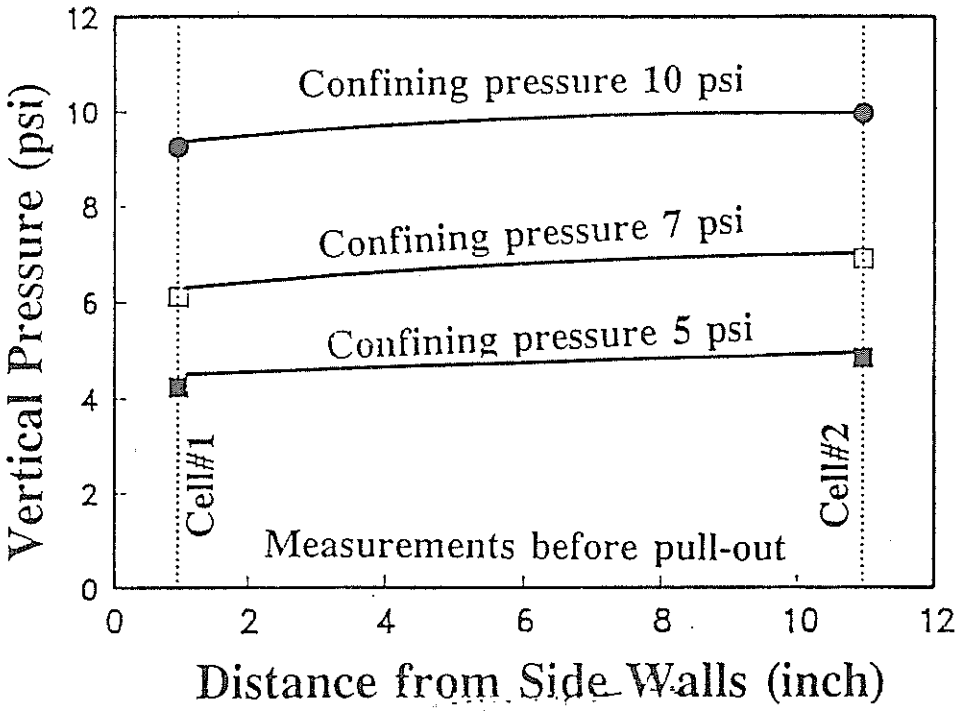

Figure 4.4 Effect of side-wall friction on confining pressure

Table 4.1

PULL-OUT TESTING PARAMETERS FOR EVALUATION OF GEOGRID DIMENSIONS

Test	Geogrid Dimensions length x width (ft)	Sleeve Length (inch)	Soil Thick. (inch)	Pull-out Rate (in/min)	Soil Dry Density (pcf)	Confining Pressure (psi)
W-0.5 B	3.0 x 0.5	12	24	0.14	105.9	7
W-0.5 C	3.0 x 0.5	12	24	0.14	106.0	7
W-1.0 A	3.0 x 1.0	12	24	0.15	105.7	7
W-1.0 B	3.0 x 1.0	12	24	0.15	105.8	7
W-1.5 A	3.0 x 1.5	12	24	0.13	105.8	7
W-1.5 B	3.0 x 1.5	12	24	0.14	105.7	7
W-2.0 B	3.0 x 2.0	12	24	0.12	105.5	7
W-2.0 D	3.0 x 2.0	12	24	0.12	105.8	7
W-2.5 A	3.0 x 2.5	12	24	0.12	105.4	7
W-2.5 B	3.0 x 2.5	12	24	0.12	105.8	7
L-1.5 A	1.5 x 1.0	12	24	0.15	105.6	7

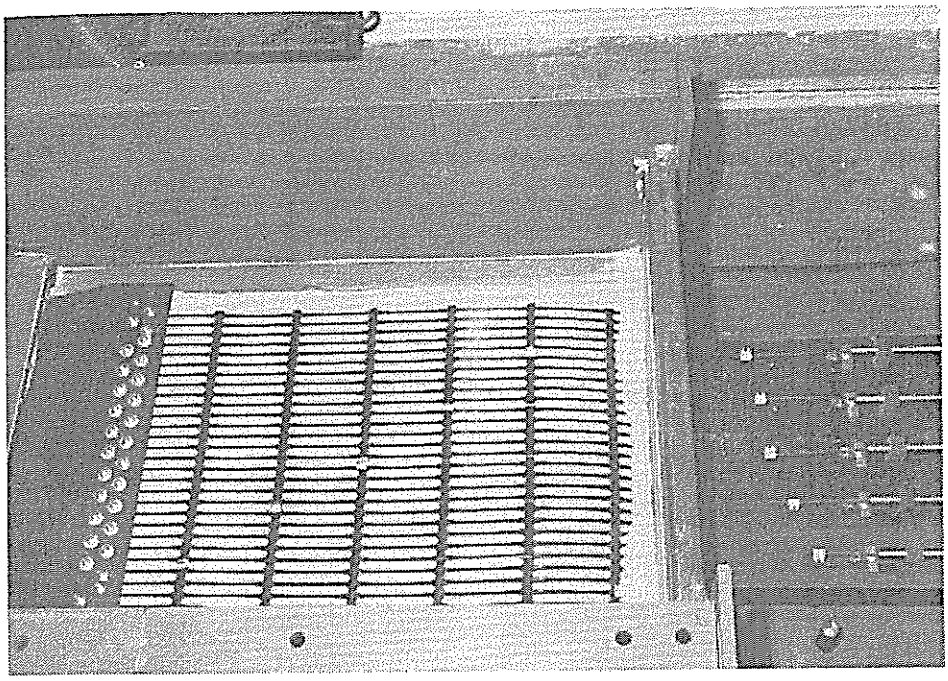

Figure 4.5 Placement of 2.5 ft-wide geogrid specimen in the box

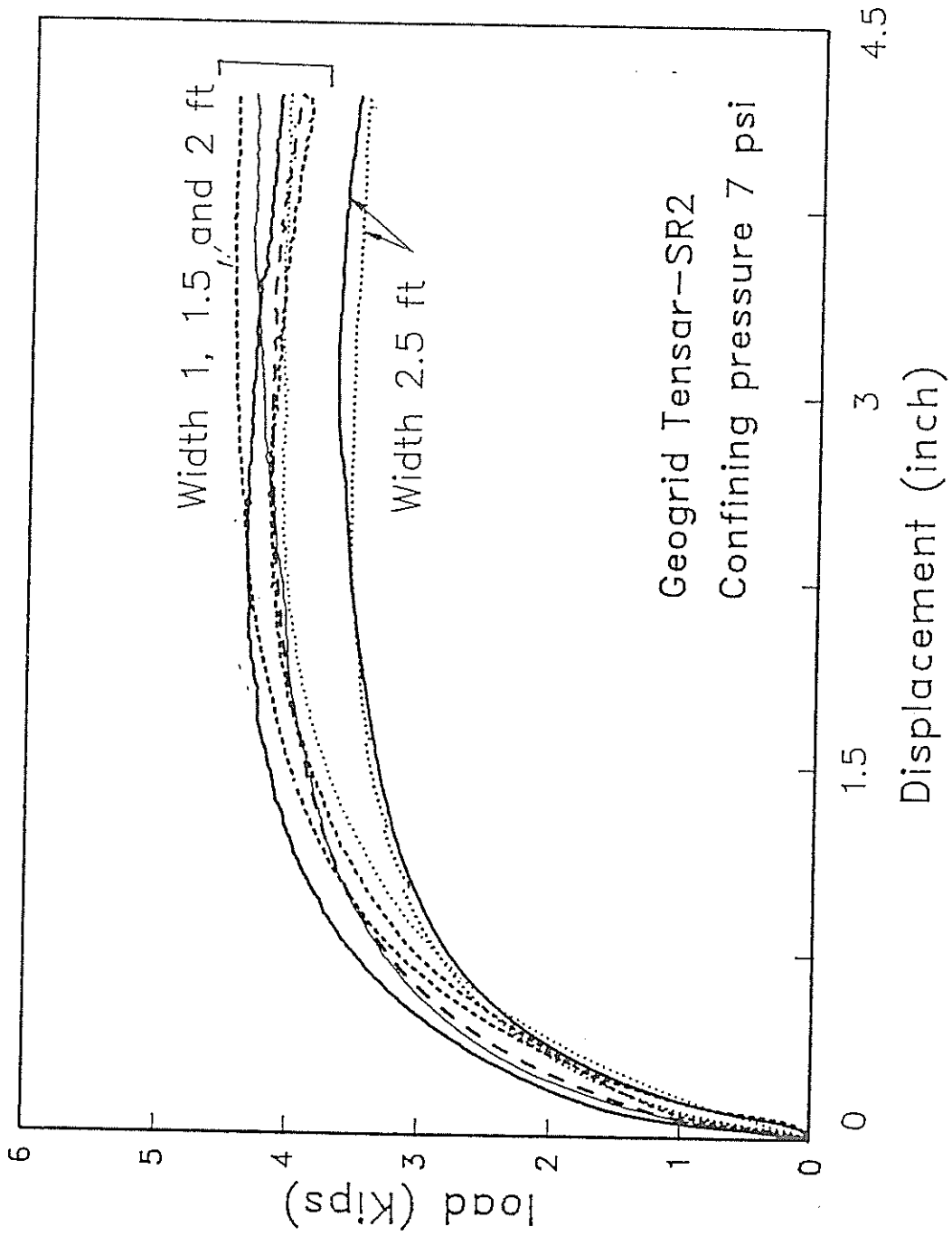

Figure 4.6 Pull-out test results on geogrids of different widths

The results in Figure 4.6 show that the pull-out resistance/unit width of the geogrid are practically equal when specimens of 0.5 to 2 ft width are tested in the box. A reduction in the peak pull-out resistance is displayed when geogrid specimens of 2.5 ft are tested. The results suggest a minimum distance of 0.5 ft between the geogrid and the box walls in order to eliminate the effect of side wall friction.

The displacement distribution along the length of the geogrid is not uniform (see figure 3.19). Consequently, pull-out resistance of the geogrid is a function of the length of the geogrid. Results of pull-out tests on geogrid specimens of 1.5 ft and 3 ft lengths are displayed in Figure 4.7. The results show that the increase in pull-out resistance is non-linearly related to the increase in the geogrid length. An analytical procedure, incorporating the effect of the geogrid's length on the pull-out resistance, is required in order to interpret pull-out resistance for geogrids of different lengths. An analytical procedure to evaluate the effective length of geogrid specimens under different pull-out loads is presented in Chapter 5.

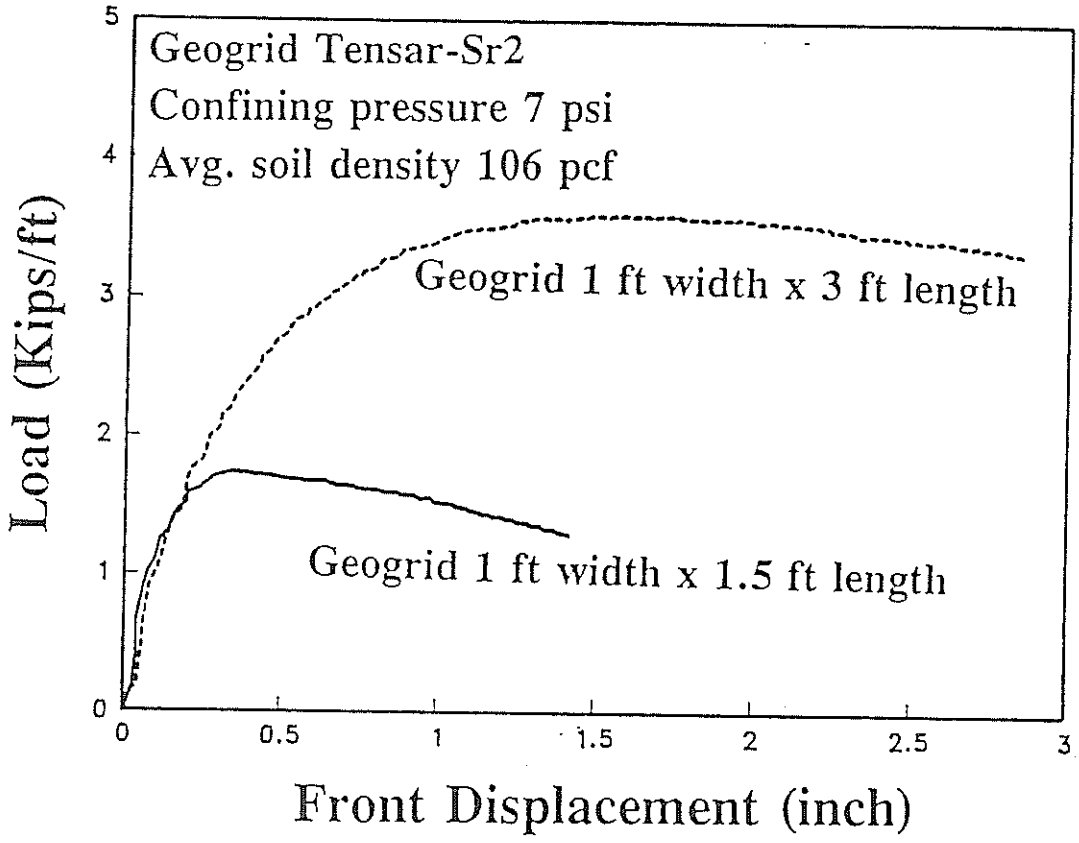

Figure 4.7 Pull-out test results on geogrids of different lengths

4.2.B Effect of Sleeve Length

The interaction between the soil-inclusion system and the rigid front wall of the pull-out box can affect the measured pull-out resistance. As the reinforcement is pulled-out of the box, lateral pressure develops against the rigid front face and results in an apparent increase in the geogrid pull-out resistance. Results of tests to investigate the effect of front wall roughness on the pull-out resistance (37) are shown in Figure 4.8. An apparent increase in the shear resistance at the soil-inclusion interface with the increase in the soil-front wall friction angle.

The effect of the rigidity of the front wall can be reduced by incorporating sleeves around the slot in the front wall. The sleeves transfer the pull-out application point inside the soil mass far beyond the rigid front wall. In order to evaluate the effect of sleeve length in reducing the rigid front wall effect, pull-out tests are conducted with different sleeve lengths, namely:

i) no sleeves,

ii) 4 inch sleeve length,

iii) 8 inch sleeve length, and

iv) 12 inch sleeve length.

Two different sets of tests are performed on geogrids to investigate the effect of sleeve length. The first set is performed on geogrids under an average soil density of 104 psi (1.67 t/m^3) and a pull-out rate of 0.8 in/minute (20 mm/minute). The second set is performed under a soil density of 106 psi (1.7 t/m^3) and pull-out rate of 0.4 in/minute (10 mm/minute). The testing parameters of these sets are displayed in Table 4.2.

Figures 4.9 and 4.10 display the pull-out test results of the first and second sets, respectively. The results demonstrate a significant increase of the pull-out resistance when no sleeves are incorporated. The pull-out resistance of the geogrid decreases as the sleeve length increases. Such decrease in pull-out resistance is mainly due to a reduction in the lateral soil pressure at the front wall.

The lateral soil pressure, developed at the front wall, is measured in Set No. 1 using two earth pressure cells fixed on the box rigid front wall at 3 and 8 inches above the sleeve. Figure 4.11 depicts a schematic diagram of the locations of the pressure cells on the front wall. The lateral earth pressure on the front wall for different sleeve lengths is monitored during pull-out.

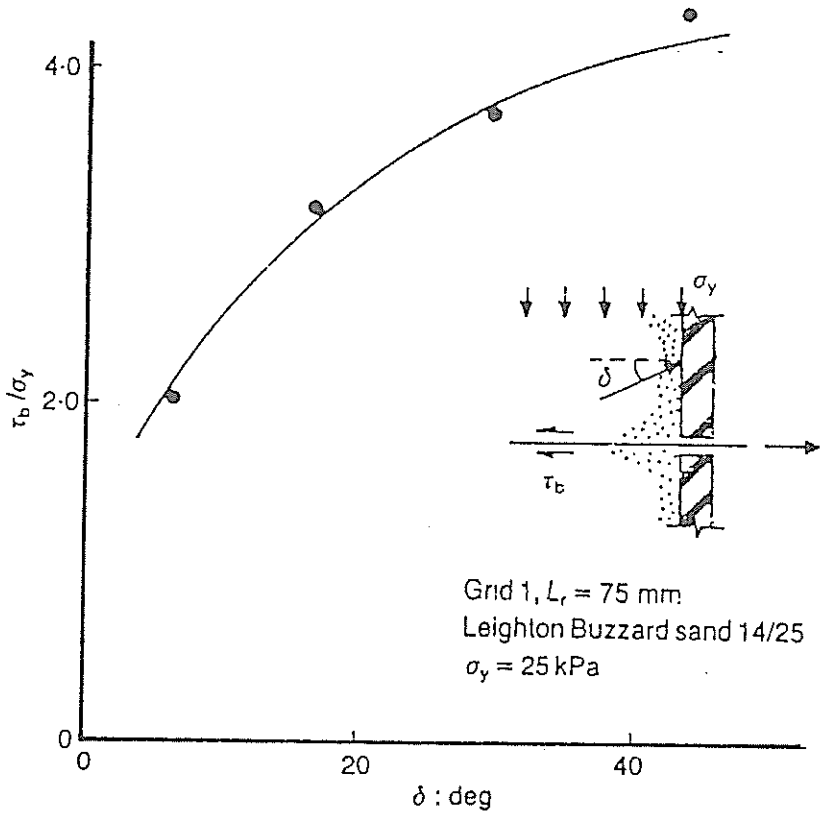

Figure 4.8 Effect of wall roughness on pull-out test results (37)

Table 4.2

PULL-OUT TESTING PARAMETERS FOR EVALUATION OF SLEEVE LENGTH

Test	Geogrid Dimensions length x width (ft)	Sleeve Length (inch)	Soil Thick. (inch)	Pull-out Rate (in/min)	Soil Dry Density (pcf)	Confining Pressure (psi)
Set # 1:						
Test-P1	3.0 x 1.0	0	24	0.80	104.0	7
Test-P2	3.0 x 1.0	8	24	0.81	104.4	7
Test-P3	3.0 x 1.0	12	24	0.80	N/M *	7
Set # 2:						
S-0 A	3.0 x 1.0	0	24	0.40	105.7	7
S-0 B	3.0 x 1.0	0	24	0.39	106.3	7
S-4 A	3.0 x 1.0	4	24	0.42	105.9	7
S-8 A	3.0 x 1.0	8	24	0.40	106.4	7
S-8 B	3.0 x 1.0	8	24	0.40	106.0	7
Test-C2	3.0 x 1.0	12	24	0.41	105.5	7
Test-C3	3.0 x 1.0	12	24	0.40	106.0	7

* N/M = Not measured

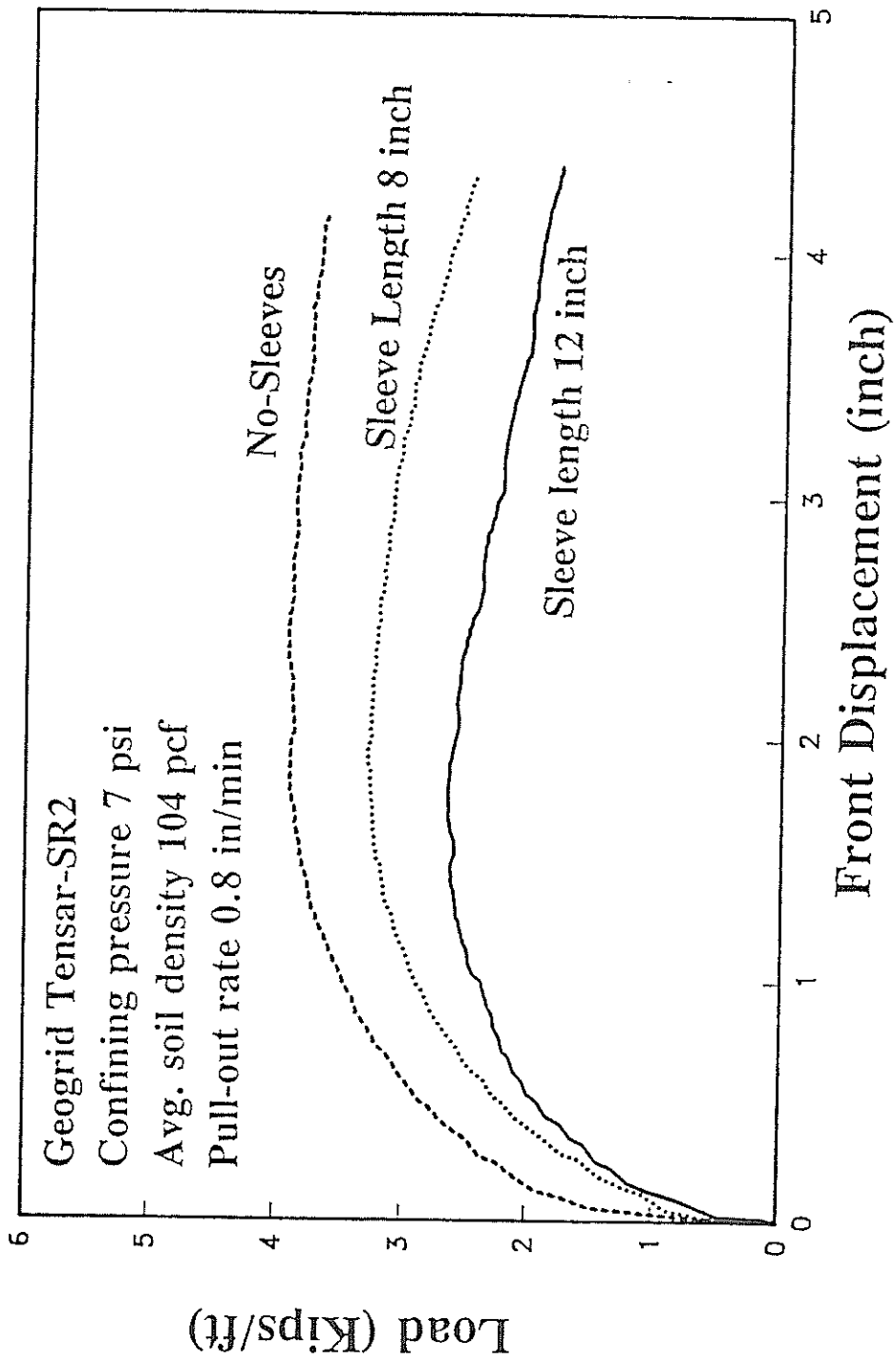

Figure 4.9 Effect of sleeve length on the pull-out resistance of geogrid

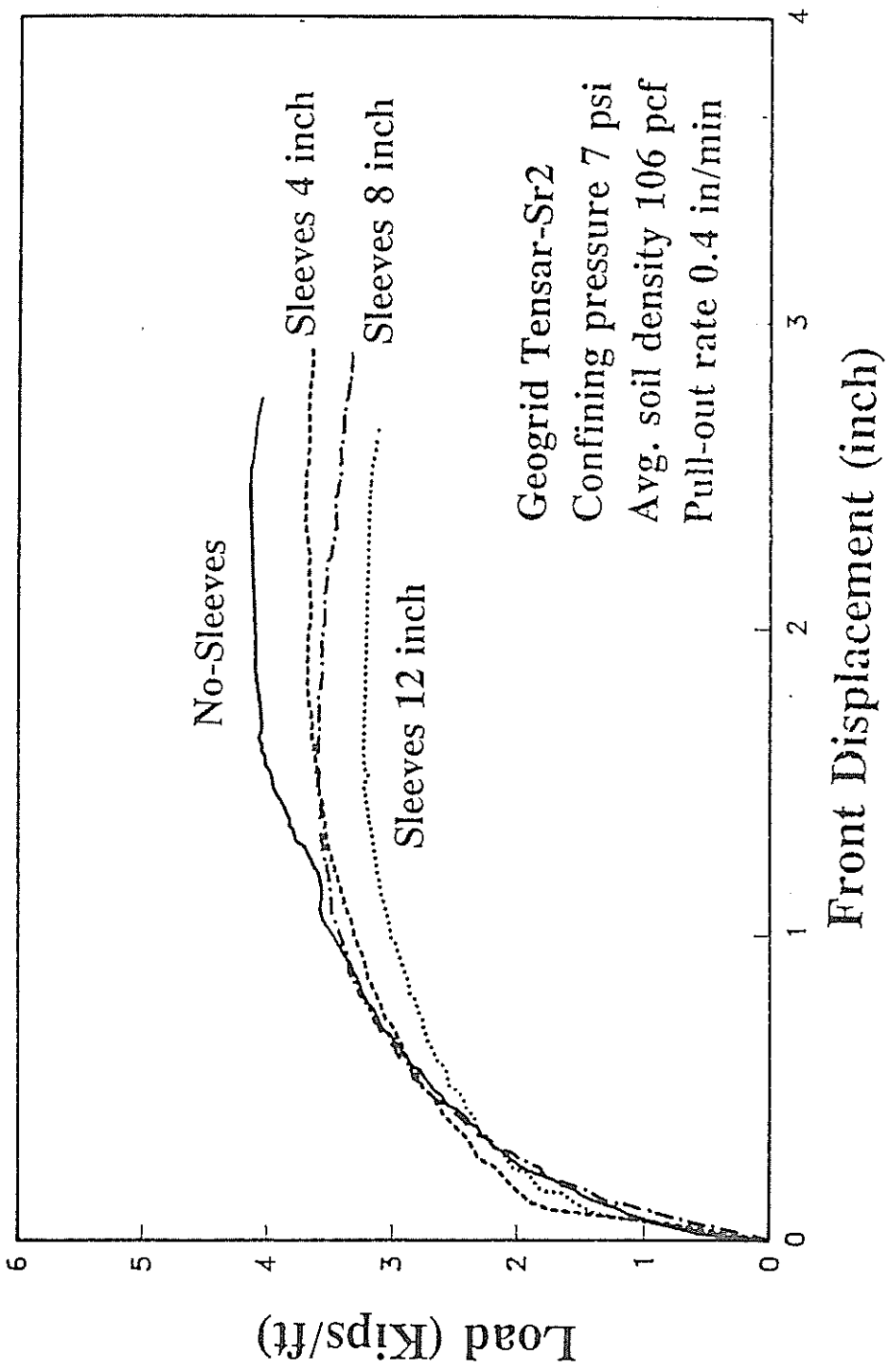

Figure 4.10 Effect of sleeve length on the pull-out resistance of geogrid

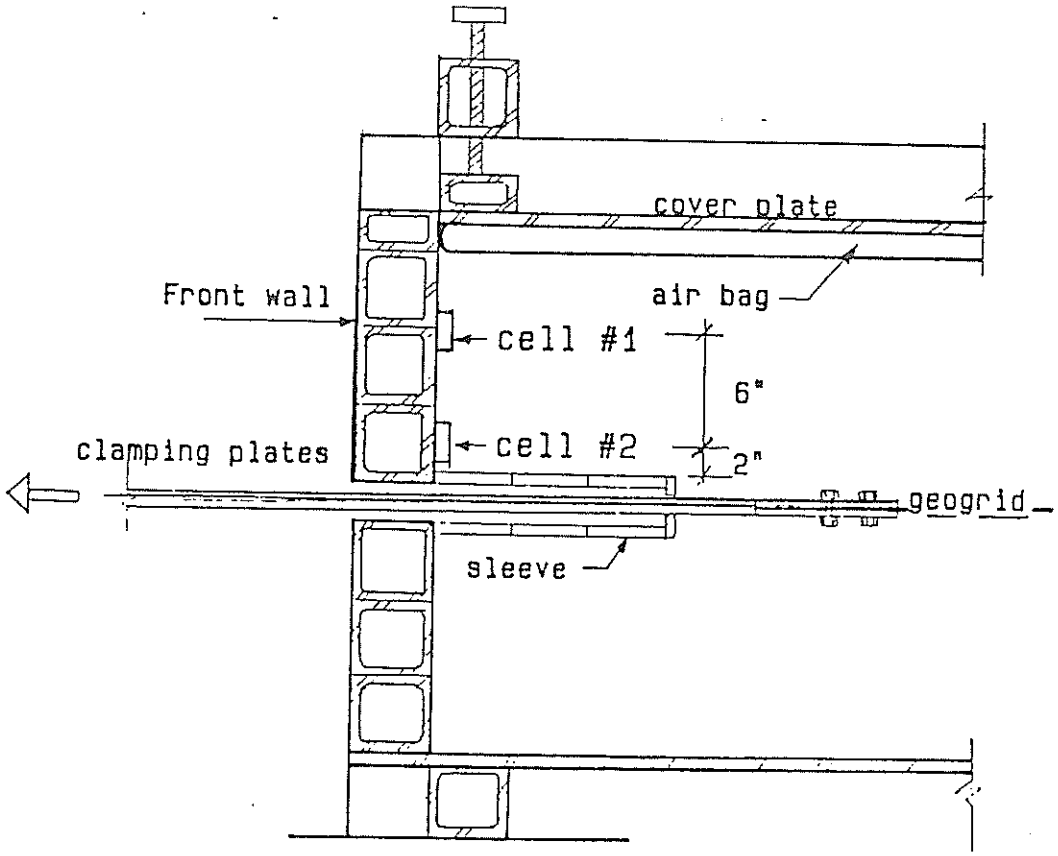

Figure 4.11 Schematic diagram of the locations of earth pressure cells

The measurements of the lateral pressure are displayed in Figures 4.12-a,b and c for tests with no sleeves, an 8-inch sleeve length, and a 12-inch sleeve length, respectively. The initial lateral pressures recorded in both cells are approximately equal at the beginning of the tests. Figure 4.12-a shows that the lateral earth pressure in the upper cell (cell No. 2) substantially increased during the tests when no sleeves are incorporated. When sleeves of 8 and 12 inches are incorporated. Figures 4.12-b and c show a slight increase of earth pressure at the upper cell, while earth pressure at the lower cell remains practically constant.

The results demonstrate the significant affect of the sleeve length on the development of earth pressure at the front wall. The use of 8-inch sleeve length results in a substantial reduction of the earth pressure on the front wall. The increase of the sleeve length from 8 to 12 inches has practically no effect on the development of lateral earth pressure. The relationship between sleeve length and lateral pressures on the front wall is shown in Figure 4.13. The effect of sleeve length on the displacement distribution along the geogrid is shown in Figure 4.14. The figures show that the increase in the lateral earth pressure during pull-out is negligible when a sleeve length of 12 inches is used.

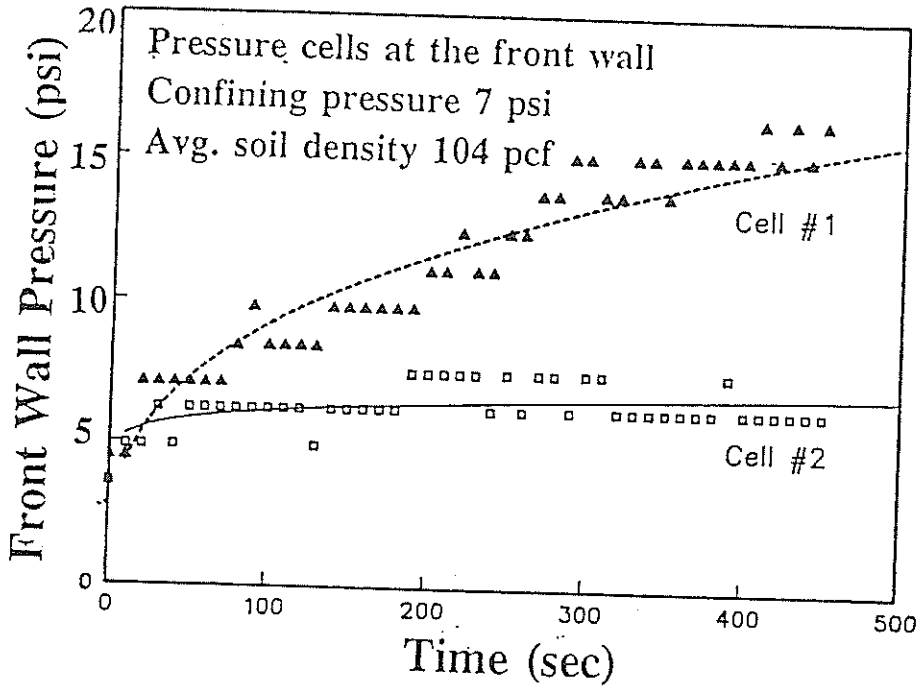

Figure 4.12-a Earth pressure on the front wall [no-sleeves]

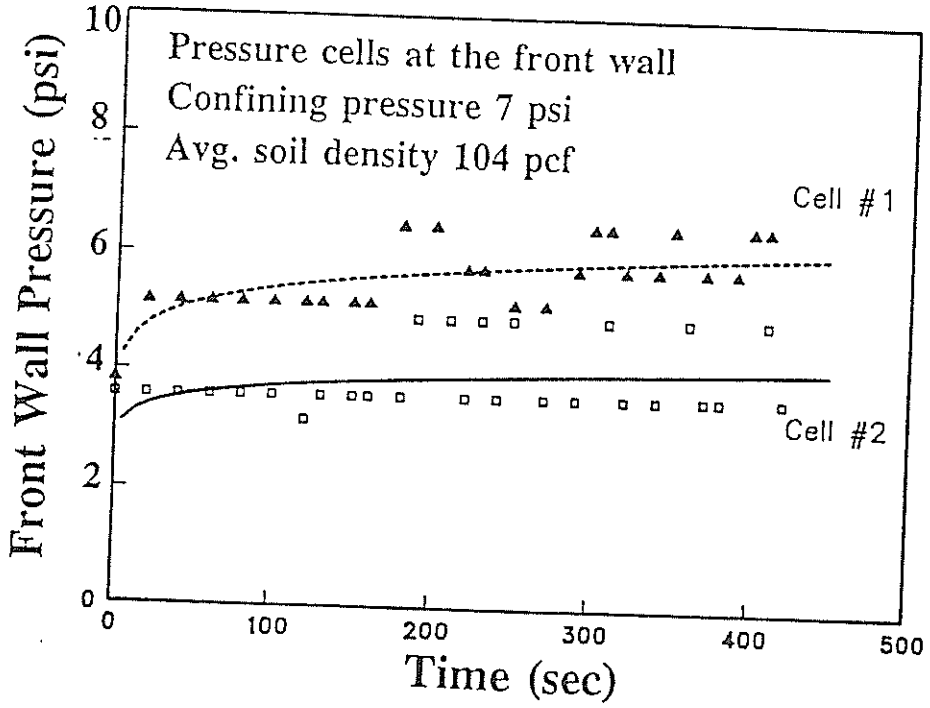

Figure 4.12-b Earth pressure on the front wall [sleeve length 8-inches]

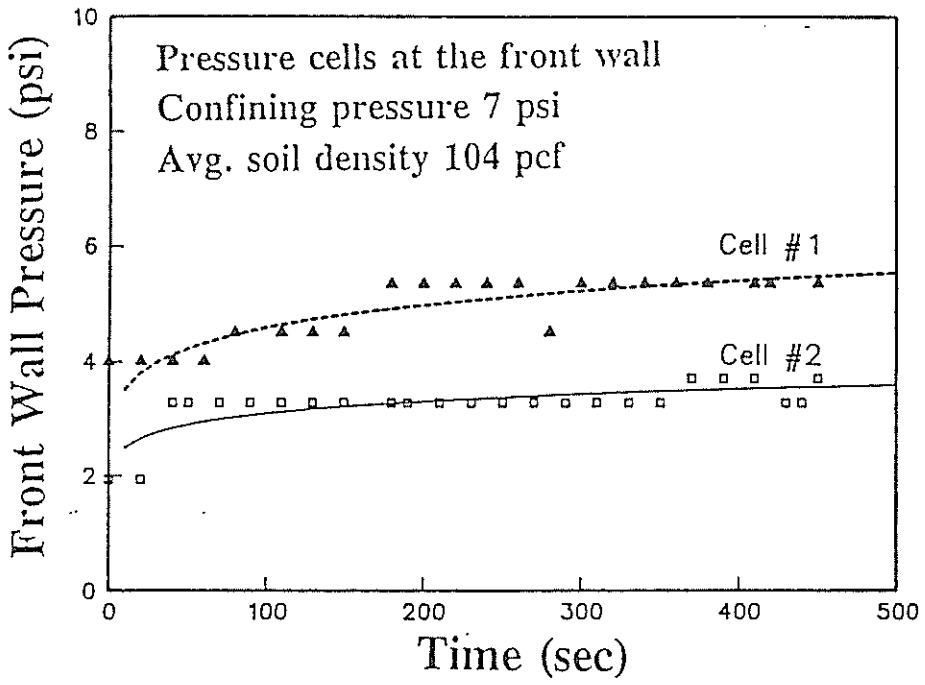

Figure 4.12-c Earth pressure on the front wall [sleeve Length 12-inches]

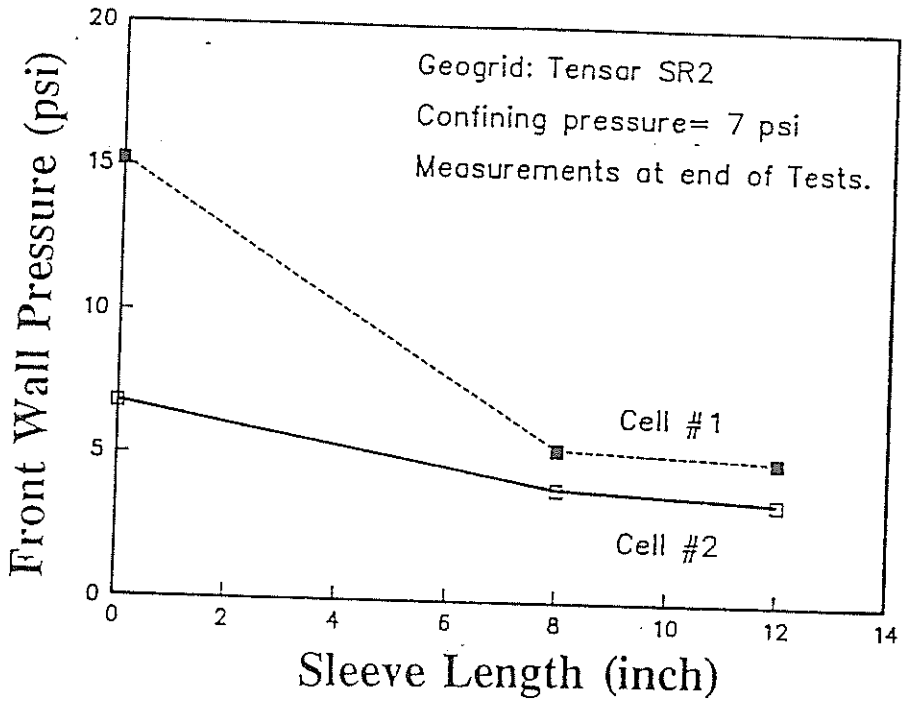

Figure 4.13 Effect of sleeve length on lateral earth pressure

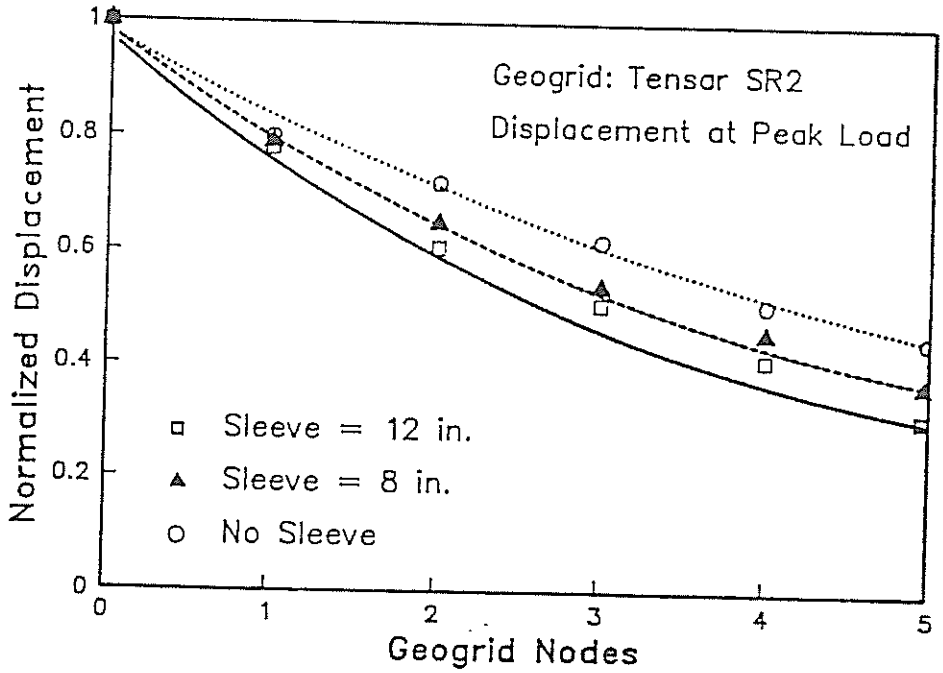

Figure 4.14 Effect of sleeve length on normalized displacement along the geogrid

C. Effect of Soil Thickness

The interaction between the soil, the geogrid, and the rigid boundaries above and below reinforcement can affect the pull-out test results. These rigid boundaries can cause an crease in the normal stresses in the vicinity of the geogrid surface if the soil thickness is small ough to restrain the soil dilatancy. Moreover, friction can develop between the bottom rigid undary and the soil, and consequently, increases the mobilized shear stresses at the interface.

In order to investigate the effect of the thickness of the soil on the pull-out response, pull-t tests are performed in soil samples of different thicknesses; namely:

i) soil thickness of 4-inches above and 4-inches under the geogrid,

ii) soil thickness of 4-inches above and 12-inches under the geogrid,

iii) soil thickness of 12-inches above and 12-inches under the geogrid,

iv) soil thickness of 16-inches above and 12-inches under the geogrid.

The above tests are performed on geogrids under a confining stress of 7 psi (48 KN/m^2) and a soil dry density of 104 pcf (1.67 t/m^3). The parameters of these tests are displayed in Table 4.3. The effect of soil thickness on the pull-out response of the geogrid is shown in Figure 4.15. The figure demonstrates:

i) The decrease in soil thickness results in an apparent increase in the pull-out resistance of the geogrid.

ii) The increase in the soil thickness from 12-inches to 16-inches above the geogrid does not seem to have more effect on the pull-out resistance of the geogrid.

The displacements along the geogrid nodes at peak pull-out resistance are normalized with respect to the front displacement in Figure 4.16. The displacements distributions for different soil thicknesses show that a decrease in soil thickness results in an increases shear resistance at the interface. Consequently, it affects the distribution of mobilized shear stresses along the geogrid and reduces the effective adherence length. The results lead to the conclusion that a soil thickness of 1 ft above and under the geogrid reinforcement (a total of 2 ft soil thickness) is sufficient to eliminate the effect of the upper and the lower boundaries on the pull-out response.

Table 4.3

PULL-OUT TESTING PARAMETERS FOR EVALUATION OF SOIL THICKNESS

Test	Geogrid Dimensions length x width (ft)	Sleeve Length (inch)	Soil Thick. (inch)	Pull-out Rate (in/min)	Soil Dry Density (pcf)	Confining Pressure (psi)
Test-B1	3.0 x 1.0	12	16	0.25	103.3	7
Test-B2	3.0 x 1.0	12	16	0.25	103.6	7
Test-B3	3.0 x 1.0	12	28	0.25	103.8	7
Test-A3	3.0 x 1.0	12	24	0.25	103.6	7
Test-A4	3.0 x 1.0	12	24	0.25	104.0	7
Test-B4	3.0 x 1.0	12	8	0.25	N/M *	7

* N/M = Not measured

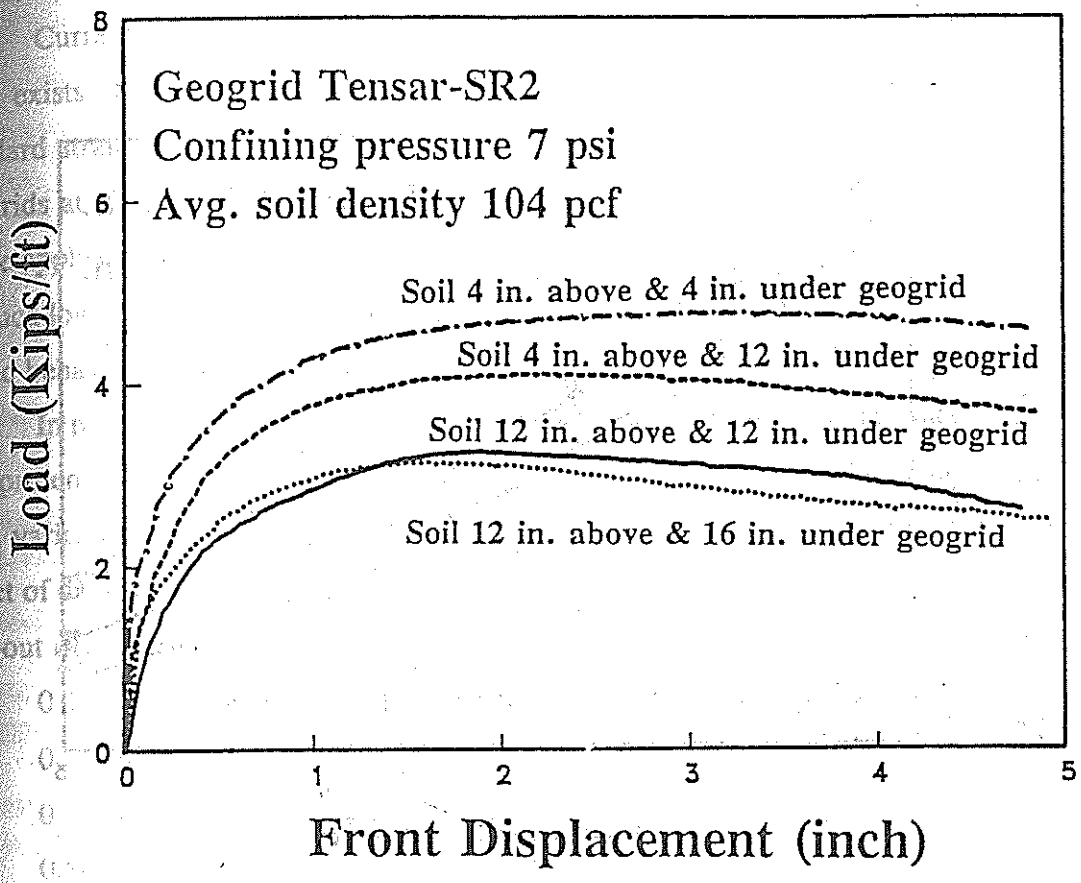

Figure 4.15 Effect of Soil thickness on pull-out resistance

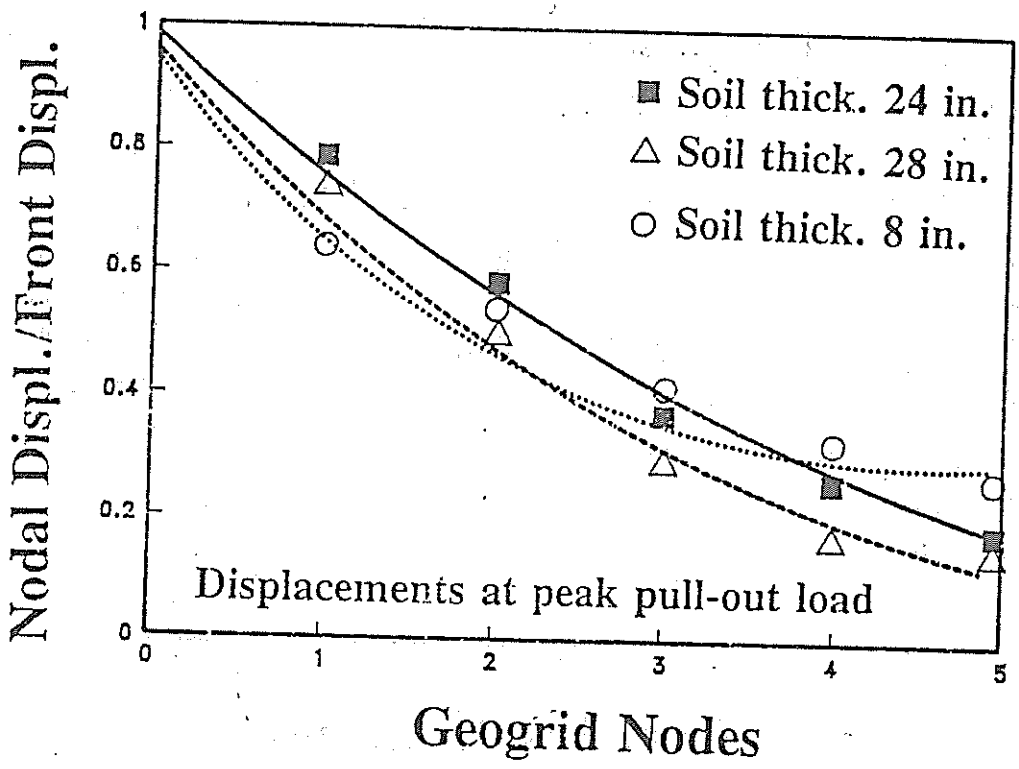

Figure 4.16 Effect of soil thickness on the normalized displacement along the geogrid

D. Effect of Displacement-Rate

Currently, no standard testing procedure that specifies the displacement-rate for pull-out ... exists. For unconfined extension tests, ASTM Designation D4595-86 recommends a ...ndard strain-rate of 10 ±3% per minute for the wide strip method test. Wide strip tests on ...grids at different strain rates (6) showed that the geogrid tension strength varies according ... the applied rate of strain. However, in pull-out tests, reinforcement reaches its peak strength ... much lower strain levels which suggests selecting lower displacement-rates in order to monitor ...bric behavior at these strain levels.

In pull-out tests, previous studies are conducted under different displacement-rates. Table ...4 presents values of pull-out displacement-rates used by different investigators. Displacement-...ates varied from 0.004 to 0.6 inch/minute (0.1 to 15 mm/minute). In order to investigate the ...ffect of displacement-rate on pull-out response, tests are performed on geogrids under different ...ull-out displacement-rates, namely:

i) 0.15 in/minute (4 mm/minute),
ii) 0.25 in/minute (6 mm/minute),
iii) 0.40 in/minute (10 mm/minute),
iv) 0.80 in/minute (20 mm/minute).

In these tests, an applied normal stress of 7 psi (48 KN/m^2), and different sets of soil densities are identically maintained. The parameters of these tests are displayed in Table 4.5. Figure 4.17 displays the pull-out response of geogrids under a confining pressure of 7 psi (48 KN/m^2), a soil dry density of 106 pcf (1.7 t/m^3) and displacement rates of 0.15 in/minute and 0.4 in/minute. The results of pull-out tests on geogrids tested in a soil density of 104 pcf (1.67 t/m^3) are displayed in Figure 4.18. The results in both figures show that as the pull-out rate increases, the peak pull-out resistance decreases. A more post-peak softening of the pull-out load is also shown with the increase of the pull-out rate. From the results in the figures, it is difficult to determine the effect of the pull-out rate on the interface stiffness modulus.

The effect of the displacement-rate on the geogrid pull-out resistance is displayed in Figure 4.19. The displacements along the geogrid nodal points are normalized with respect to the front displacement (i.e at node 0) and are plotted along the geogrid in Figure 4.20.

The figure demonstrates a mobilization of shear displacement at the rear nodes when geogrids are tested at higher displacement-rates.

The results in Figures 4.19 and 4.20 show that the peak pull-out resistance appears to be less sensitive to the changes of displacement-rates under 0.25 in/minute. These results suggest the use of low displacement-rates (in the range of 0.25 in/minute) in pull-out tests.

Table 4.4

COMPARISON BETWEEN DISPLACEMENT-RATES IN DIFFERENT PULL-OUT BOXES (19)

Box	Testing Method	Displacement-rate
- Caltrans Box, (39) [54"x36"x20"]	Displacement-rate pull-out on geogrids	2%/minute (0.17 in/minute)
- V. Elias Box (40) [36"x36"x18"]	Displacement-rate pull-out on metal strips	0.1 in/minute
- STS Box (18) [48"x30"x18"]	Displacement-rate pull-out on geogrids	0.004 in/minute
- Utah State Univ. Box (35)	displacement-rate pull-out on wire mesh	0.04 in/minute
- Drexel Univ. Box (18)	Displacement-rate pull-out	0.01-0.6 in/minute
- Univ. of Grenoble (43)	Displacement-rate pull-out on geotextiles	0.25 in/minute

4.5

-OUT TESTING PARAMETERS FOR EVALUATION OF DISPLACEMENT-RATE

est	Geogrid Dimensions length x width (ft)	Sleeve Length (inch)	Soil Thick. (inch)	Pull-out Rate (in/min)	Soil Dry Density (pcf)	Confining Pressure (psi)
et # 1:						
Test-C2	3.0 x 1.0	12	24	0.40	105.5	7
Test-C3	3.0 x 1.0	12	24	0.40	106.0	7
W-1.0 A	3.0 x 1.0	12	24	0.15	105.7	7
W-1.0 B	3.0 x 1.0	12	24	0.15	105.8	7
Set # 2:						
Test-A5	3.0 x 1.0	12	24	0.25	104.5	7
Test-A7	3.0 x 1.0	12	24	0.25	104.2	7
Test-A9	3.0 x 1.0	12	24	0.40	103.6	7
Test-A10	3.0 x 1.0	12	24	0.40	103.4	7
Test-P3	3.0 x 1.0	12	24	0.80	N/M *	7

* N/M = Not measured

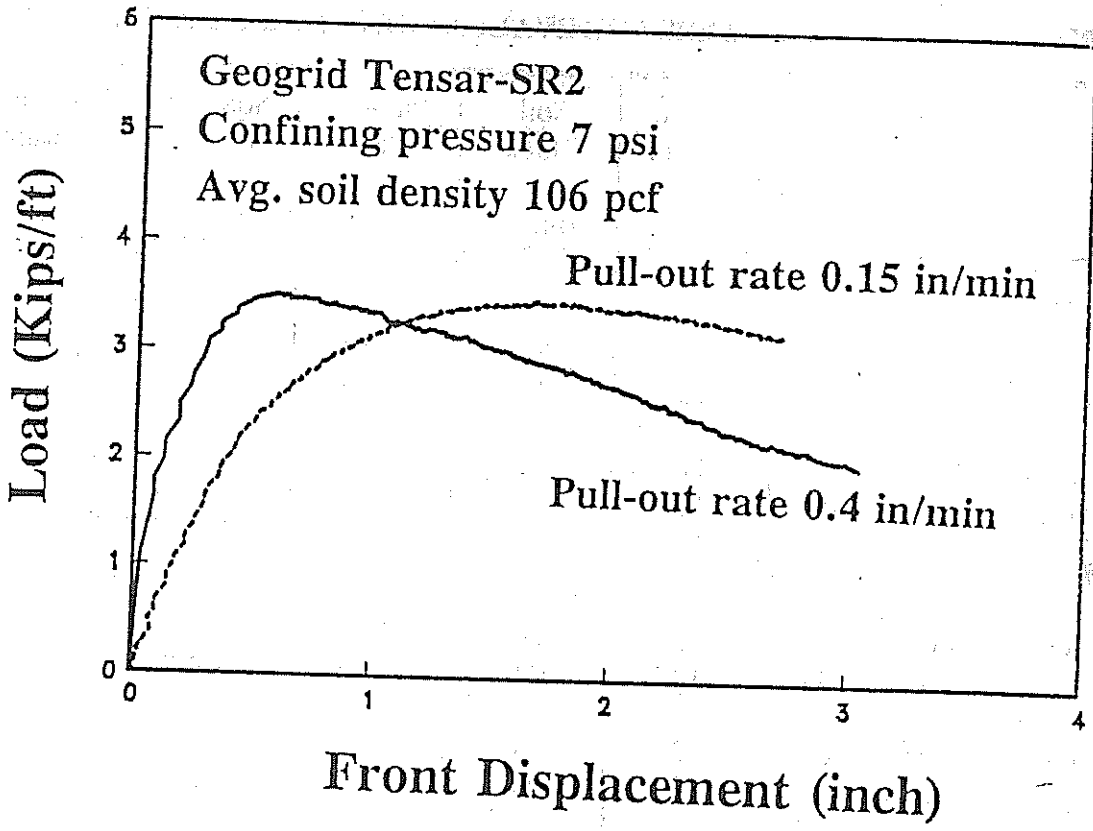

Figure 4.17 Effect of displacement-rate on pull-out response

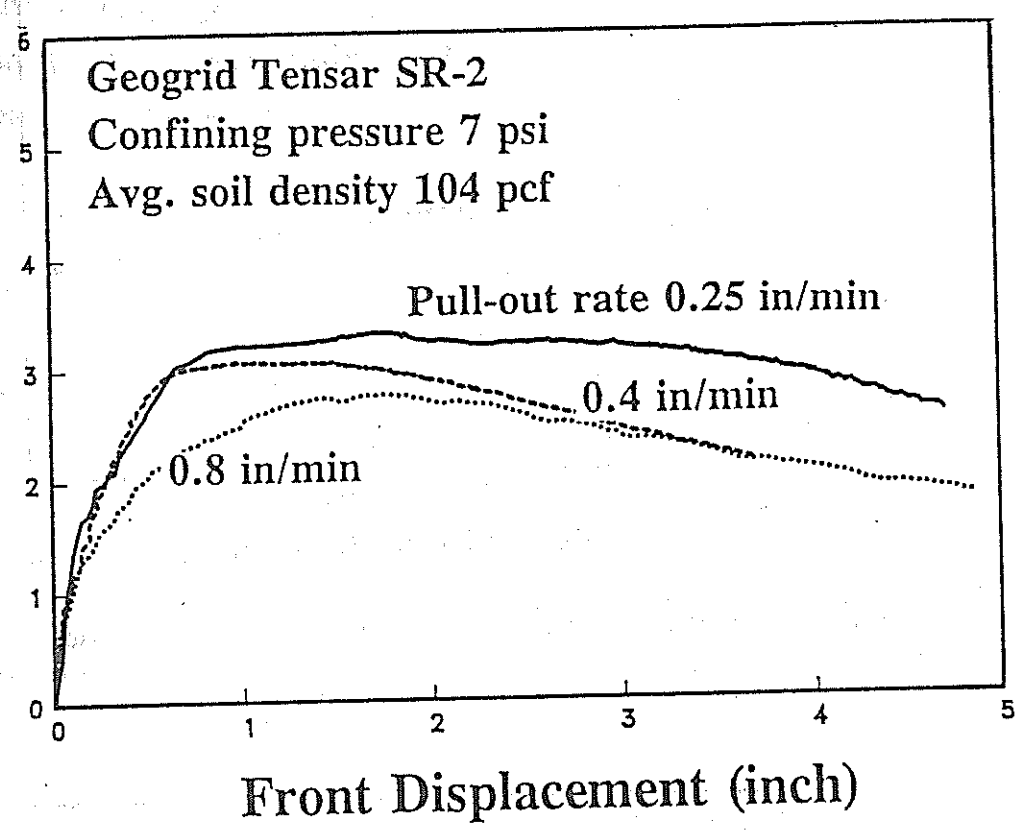

Figure 4.18 Effect of displacement-rate on pull-out response

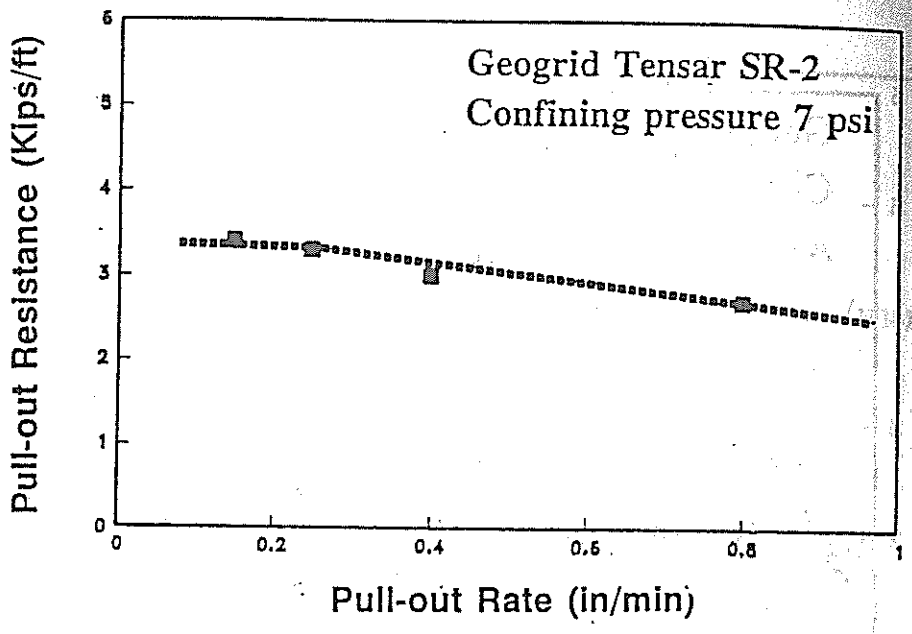

Figure 4.19 Effect of displacement-rate on pull-out resistance

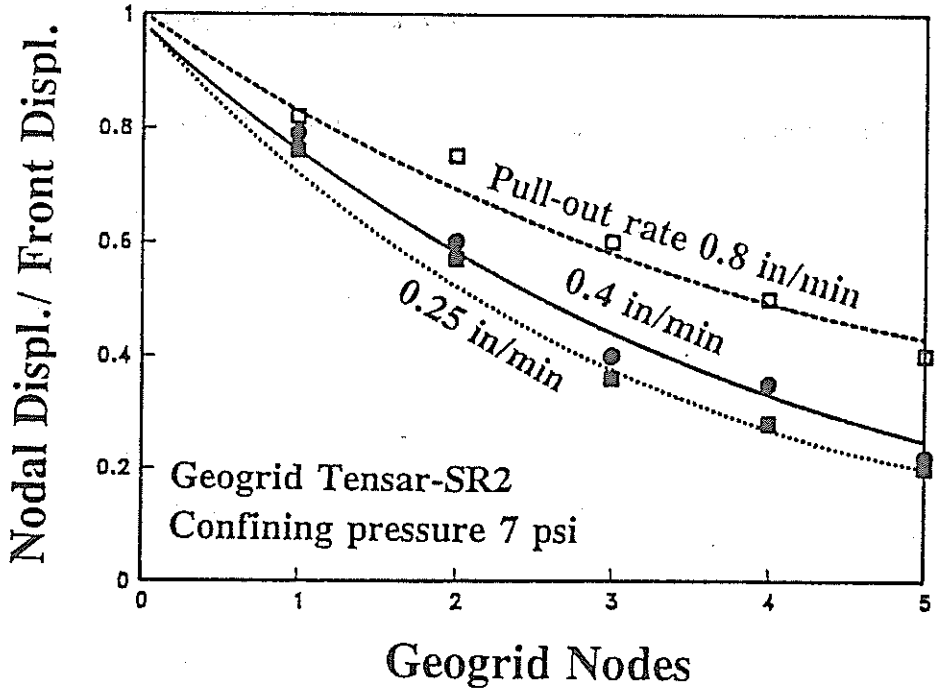

Figure 4.20 Effect of displacement-rate on normalized displacement along the geogrid

Effect of Soil Density

The frictional resistance between the soil and the reinforcement is highly influenced by l relative density (11,19). Dense soils tend to dilate when shear stresses are mobilized he reinforcement interface. As the dilatancy is restrained by the surrounding soil, normal es increase at the reinforcement level and, consequently, increasing the shear resistance at nterface.

In order to evaluate the effect of relative soil density on the pull-out response, tests are ormed in soils compacted to different dry densities; namely:

i) average soil density of 102 pcf (1.62 t/m^3) (soil relative density 30%),

ii) average soil density of 104 pcf (1.67 t/m^3) (soil relative density 50%),

iii) average soil density of 106 pcf (1.7 t/m^3) (soil relative density 70%),

iv) average soil density of 108 pcf (1.73 t/m^3) (soil relative density 85%).

he geogrids are tested under a confining pressure of 7 psi (48 KN/m^2) and different sets of splacement-rates. The parameters of these tests are displayed in Table 4.6. The results of hose tests are displayed in Figures 4.21 and 4.22. The figures demonstrate an increase in the eak pull-out resistance and interface stiffness modulus of the geogrid as soil density increases.

In pull-out tests, sand is placed in four layers in the box, leveled, and compacted to the esired relative density. Manual compaction is applied on each layer. After compaction, density is measured by a nuclear density gauge, and an average density is calculated from nine different measurements along the box. The average soil density is considered acceptable within ± 0.5 pcf of the desired soil density. The compaction and density control procedures permits the evaluation of the pull-out resistance due to changes in the soil density in the range of ± 1.0 pcf. Results of pull-out tests with different soil densities are compiled in Figure 4.23. The figure displays the precision of pull-out measurements and demonstrates the effect of soil density on pull-out resistance.

Soil compaction increases the lateral earth pressure on the geogrid transversal elements and the mobilized frictional resistance at the interface. Consequently, shear displacement and elongation of the geogrid are restrained under high soil densities. The effect of soil density on the mobilized shear displacement is demonstrated in Figure 4.24..

In Figure 4.24, the nodal-displacements along the geogrid, at peak pull-out load, a... normalized with respect to the front displacement. The higher soil density results in a highe... shear stress concentration at the vicinity of the point of application and, consequently, a much... shorter effective adherence length. Low soil density leads to a more uniform distribution of the... interface shear stresses along the reinforcement.

Table 4.6

PULL-OUT TESTING PARAMETERS FOR EVALUATION OF SOIL DENSITY

Test	Geogrid Dimensions length x width (ft)	Sleeve Length (inch)	Soil Thick. (inch)	Pull-out Rate (in/min)	Soil Dry Density (pcf)	Confining Pressure (psi)
Set # 1:						
D-101 A	3.0 x 1.0	12	24	0.22	101.1	7
D-102 A	3.0 x 1.0	12	24	0.22	102.1	7
Test-A8	3.0 x 1.0	12	24	0.25	104.1	7
D-104 A	3.0 x 1.0	12	24	0.24	104.2	7
Set # 2:						
W-1.0 A	3.0 x 1.0	12	24	0.15	105.7	7
W-1.0 B	3.0 x 1.0	12	24	0.15	105.8	7
D-108 A	3.0 x 1.0	12	24	0.25	107.7	7
D-108 B	3.0 x 1.0	12	24	0.24	107.5	7

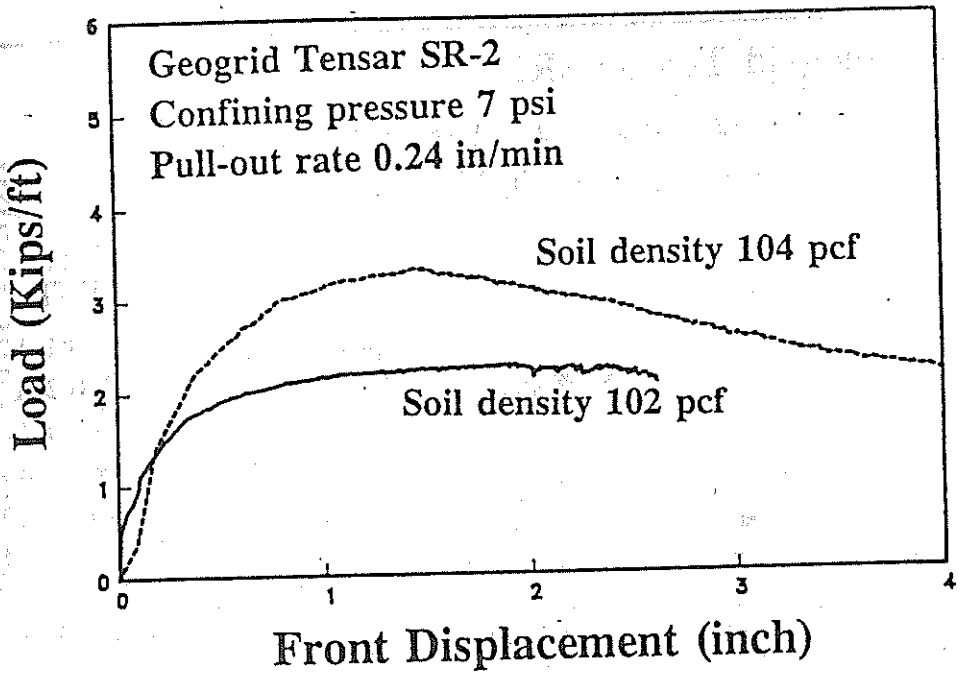

Figure 4.21 Effect of soil density on pull-out response of geogrid

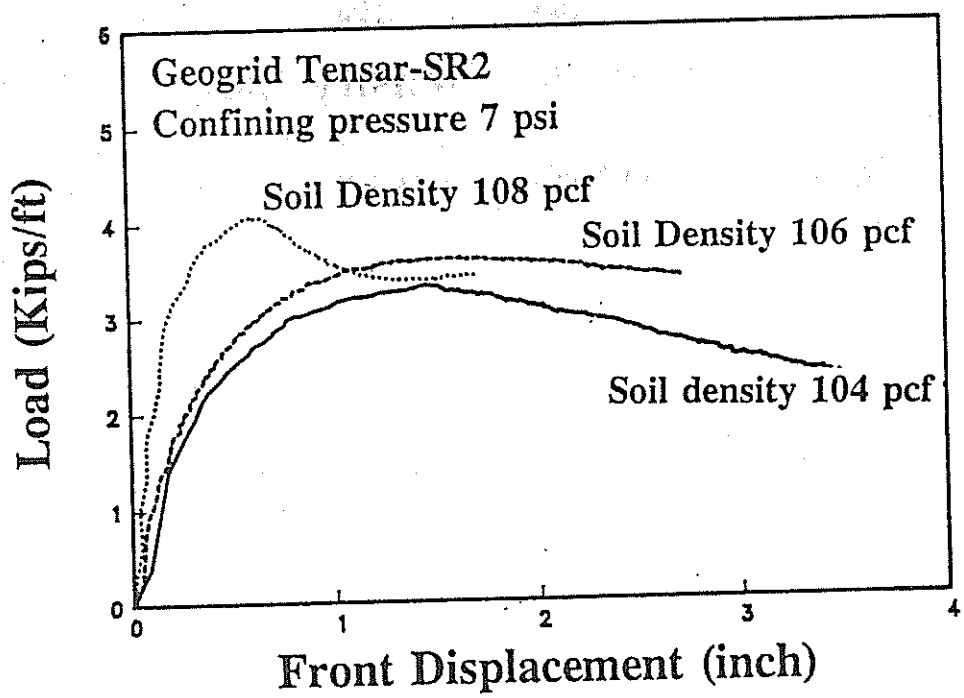

Figure 4.22 Effect of soil density on pull-out response of geogrid

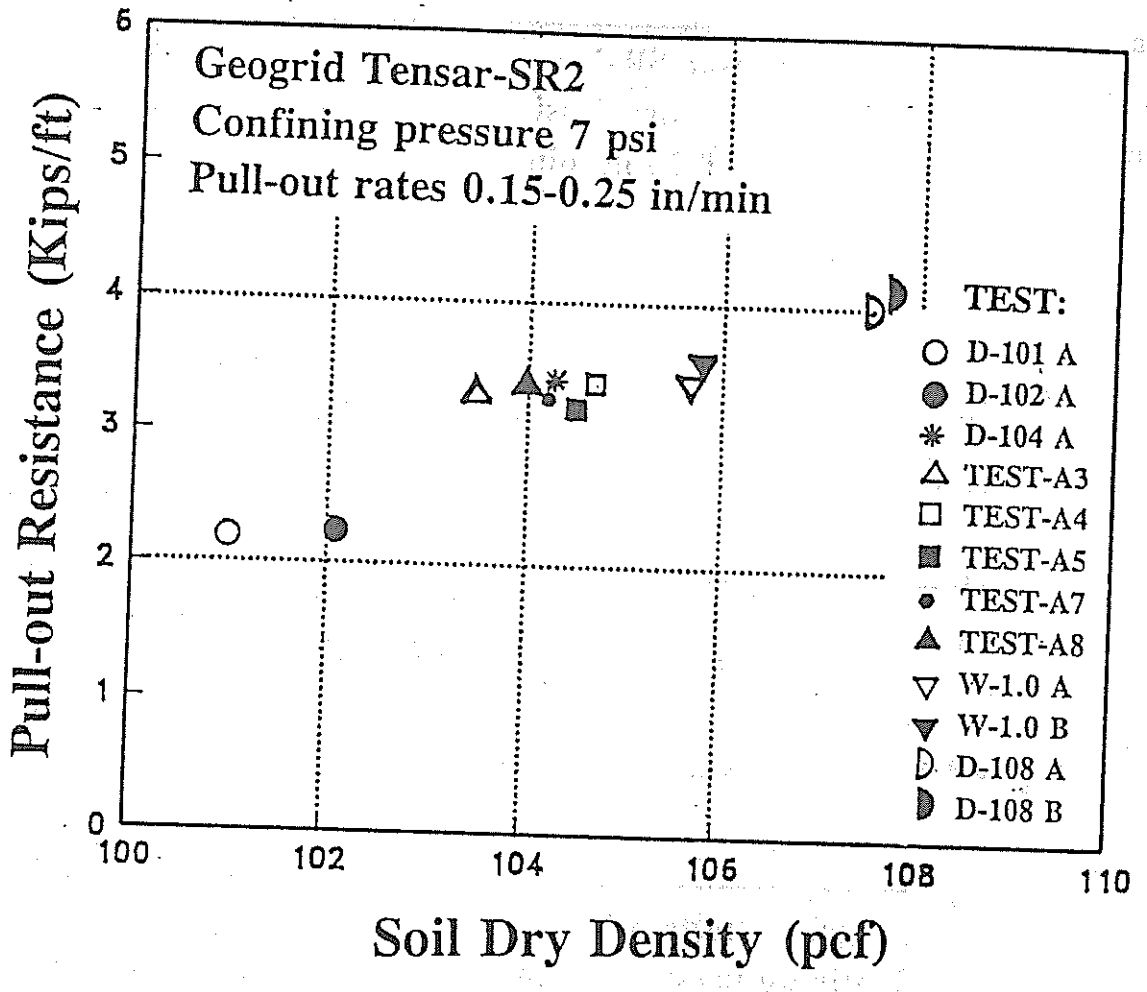

Figure 4.23 Variation of pull-out response with soil density

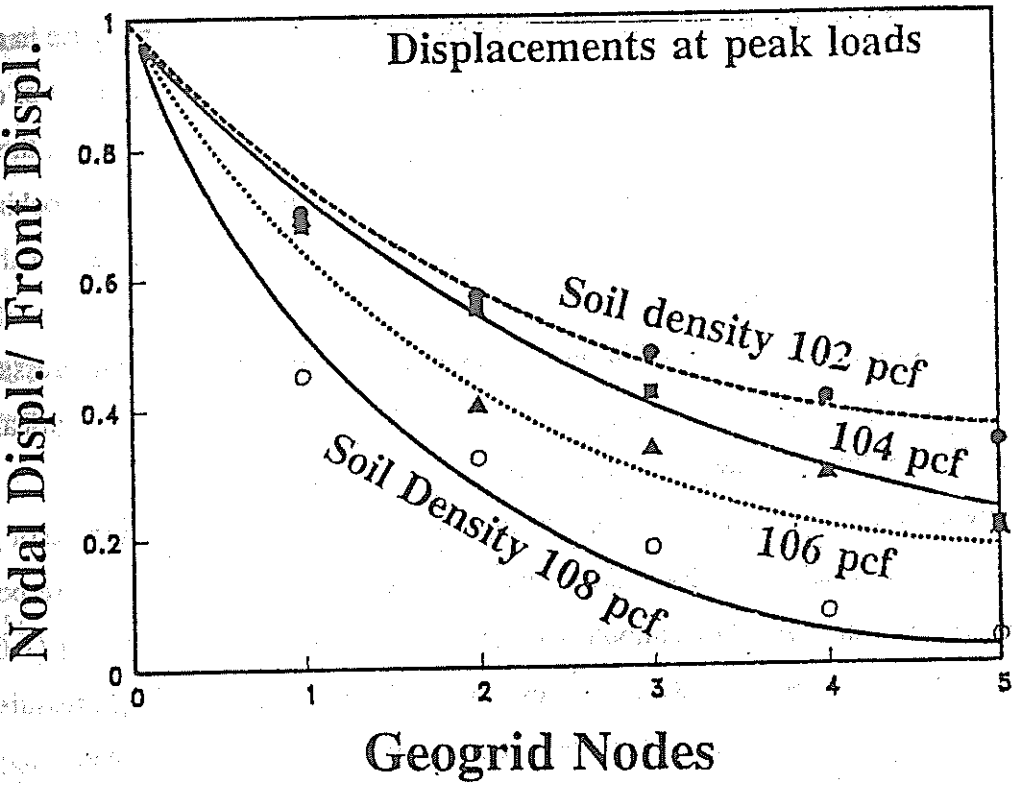

Figure 4.24 Effect of soil density on displacement distribution along the geogrid

4.2.F Confining Pressure

The effect of confining pressure on the frictional resistance of the reinforcement has be demonstrated by several investigators (10,12). Figure 4.25 displays the effect of the increa of confining pressure on the confined extension properties of geogrids. The increase in confini pressure results in an increase in the shear resistance along the interface. The effect of confini pressure on the shear resistance of geogrids is displayed in Figure 4.26. Moreover, the increas in confining pressure increases the passive resistance of the soil and particles interlocking within the transversal elements. The restrained elongation results in an apparent increase of the tensile strength and the stiffness modulus.

Two sets of tests are conducted in order to evaluate the effect of confining pressure. Each set of testing is conducted under specific soil density while maintaining identical testing parameters. The testing parameters of these sets are displayed in Table 4.7.

Figure 4.27 displays the effect of confining pressure on the pull-out response of geogrids under confining pressures 5 psi (34 KN/m^2) and 7 psi (48 KN/m^2). These tests are performed with a displacement-rate of 0.25 in/minute and an average soil density of 104 pcf (1.67 t/m^3). Figure 4.28 displays the results of pull-out tests on geogrids under confining pressures 7 psi (48 KN/m^2) and 10 psi (68 Kn/m^2). These tests are performed with a displacement-rate of 0.15 in/minute and average soil density of 106 pcf (1.7 t/m^3). The results in both figures demonstrate an increase in the pull-out resistance of the geogrid and in its interface stiffness modulus with the increase in confining pressure.

The results suggest that the design criteria for geogrid reinforced soil structures should take into account the in-soil confined extension properties derived from pull-out tests rather than the material properties obtained from unconfined extension tests. Although a lower (and consequently more conservative) peak strength is usually obtained from unconfined tests; the unconfined behavior of the geogrid is substantially more ductile and its strain level at peak is higher than that obtained under confined conditions. This may results in non-conservative design values for the admissible geogrid extension and the related structure displacements.

The normalized displacement distributions along the geogrids, at the peak pull-out loads, are shown in Figure 4.29 for different confining pressures. The figure illustrates the effect of the confining pressure on the mobilized load transfer along the reinforcement. The shear stress

oil-geogrid interface is more uniformly mobilized along the geogrid under low confining
es. The increase in the confining pressure restrains the geogrid displacement and results
her mobilization of shear strains near the pull-out application point, lower shear strains at
ar, and consequently a shorter effective adherence length.

ble 4.7

LL-OUT TESTING PARAMETERS FOR EVALUATION OF CONFINING PRESSURE

Test	Geogrid Dimensions length x width (ft)	Sleeve Length (inch)	Soil Thick. (inch)	Pull-out Rate (in/min)	Soil Dry Density (pcf)	Confining Pressure (psi)
Set # 1:						
Test-A6	3.0 x 1.0	12	24	0.28	104.7	7
Test-A5	3.0 x 1.0	12	24	0.25	104.5	7
Test-A8	3.0 x 1.0	12	24	0.25	104.1	7
Set # 2:						
W-1.0 A	3.0 x 1.0	12	24	0.15	105.7	7
W-1.0 B	3.0 x 1.0	12	24	0.15	105.8	7
Sig-10 A	3.0 x 1.0	12	24	0.16	105.8	7
Sig-10 B	3.0 x 1.0	12	24	0.17	106.1	7
Sig-10 C	3.0 x 1.0	12	24	0.16	106.4	7

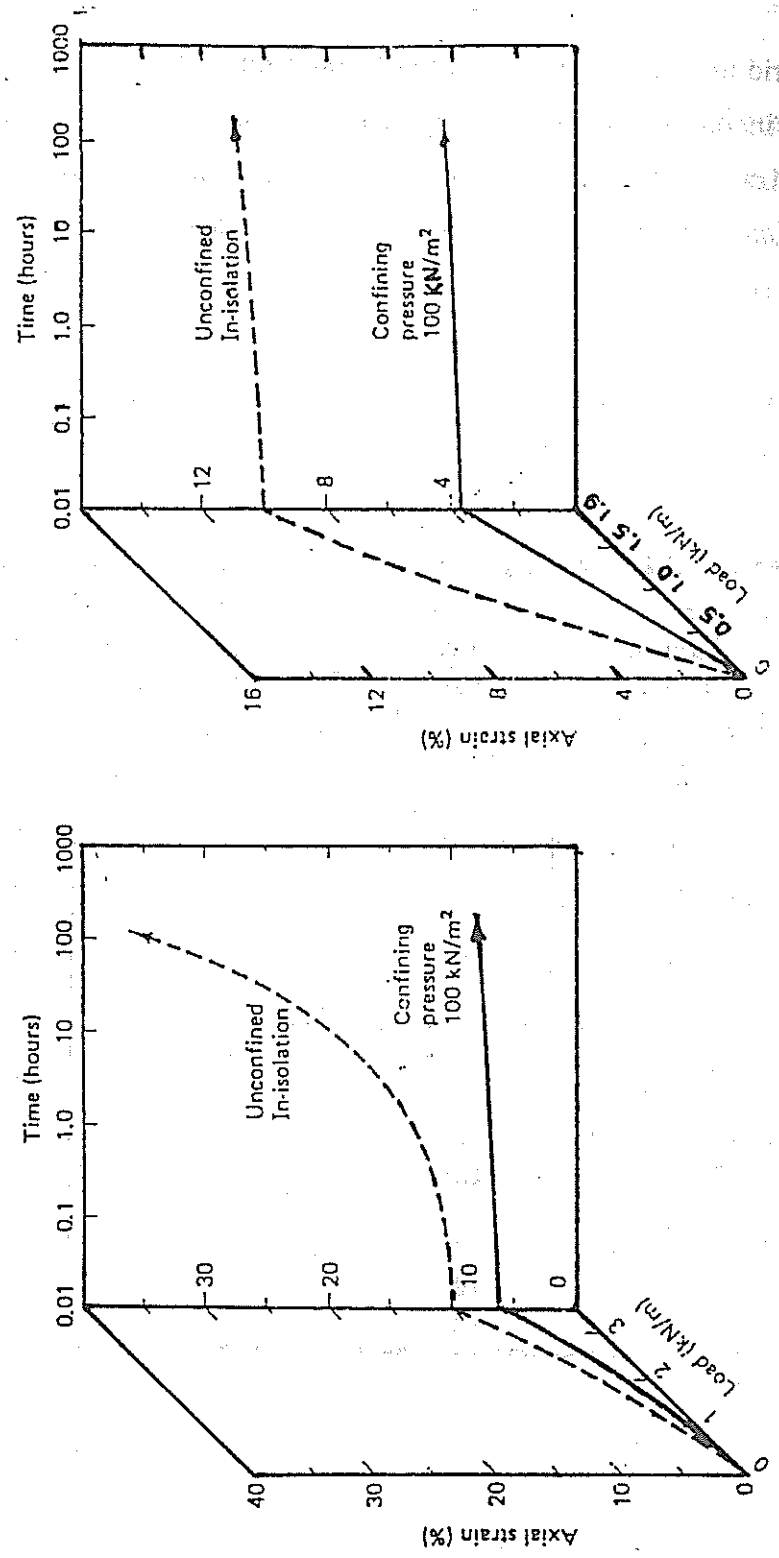

Figure 4.25 Effect of confining pressure on the extension properties of geogrids (10)

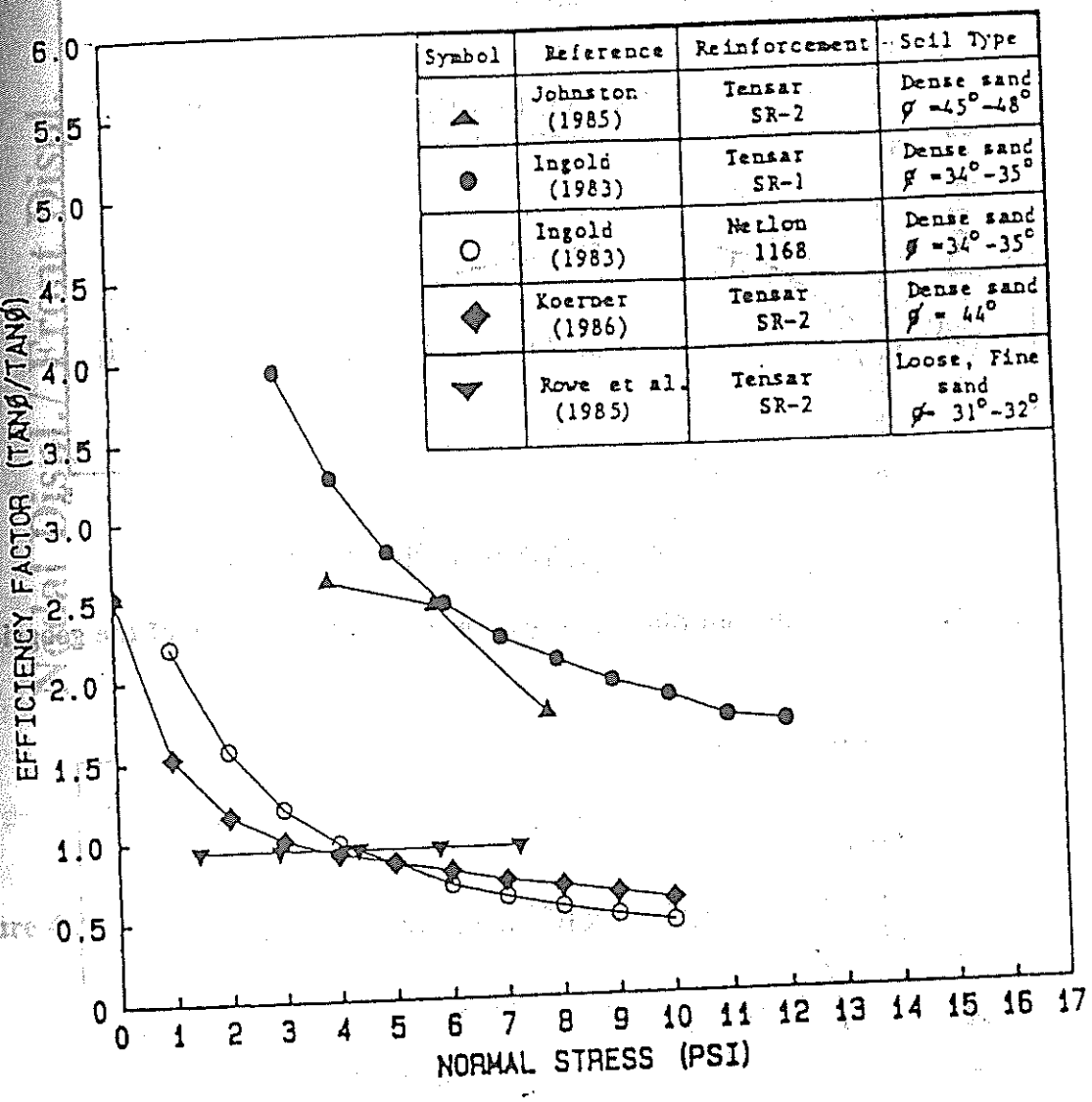

Figure 4.26 Relationship between the efficiency factor and confining pressure for various geogrids (11)

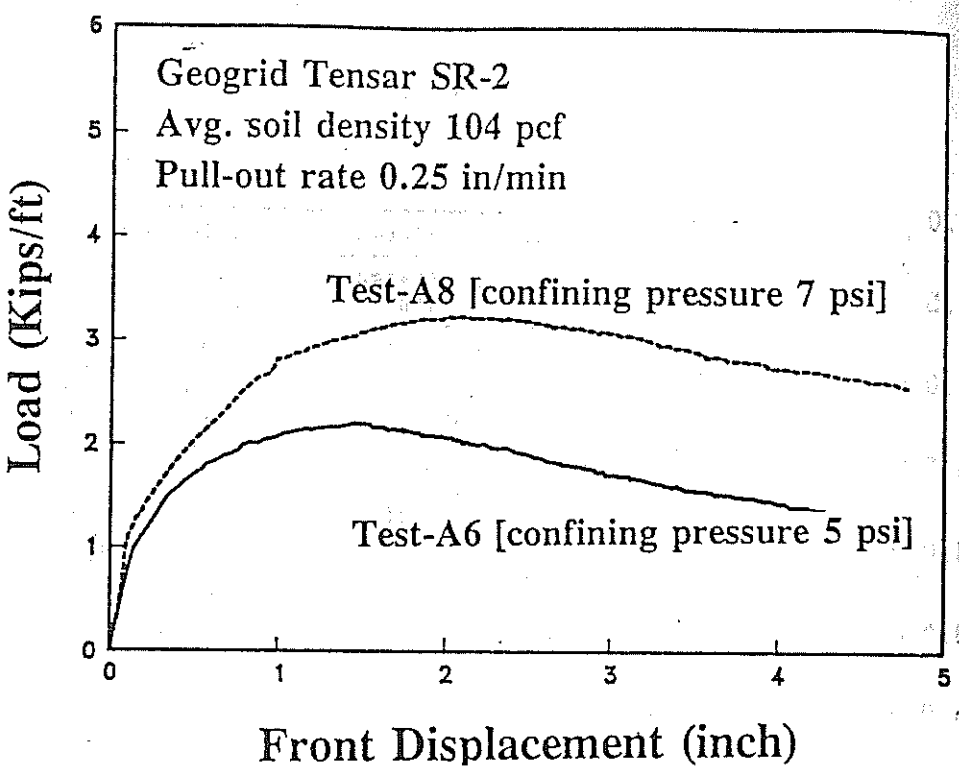

Figure 4.27 Effect of confining pressures on pull-out resistance of the geogrid

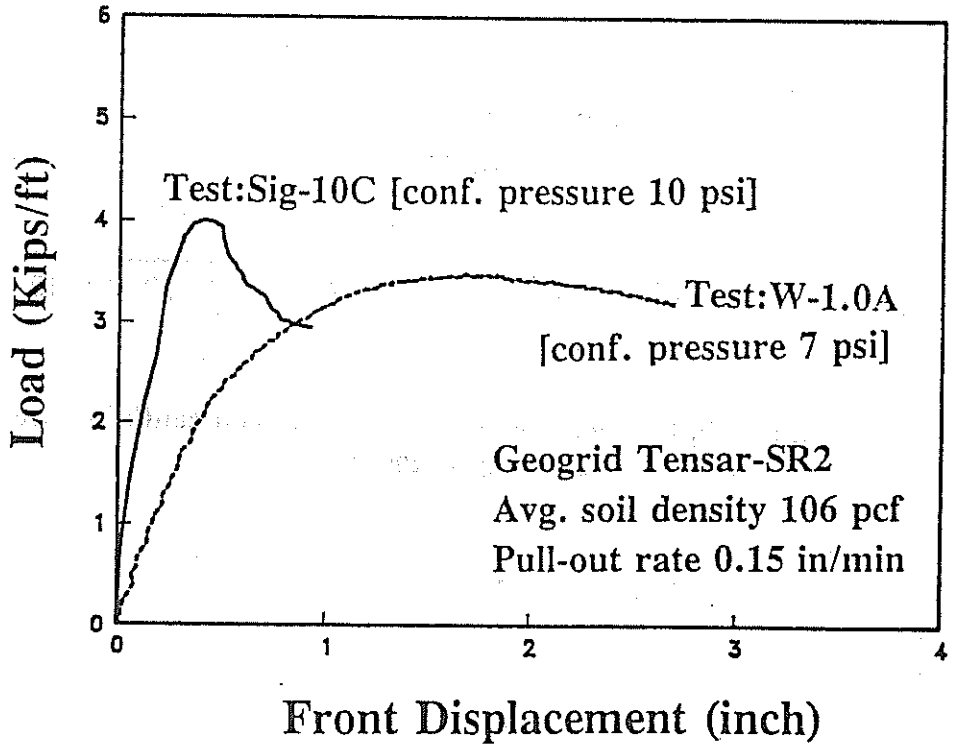

Figure 4.28 Effect of confining pressure on the pull-out resistance of the geogrid

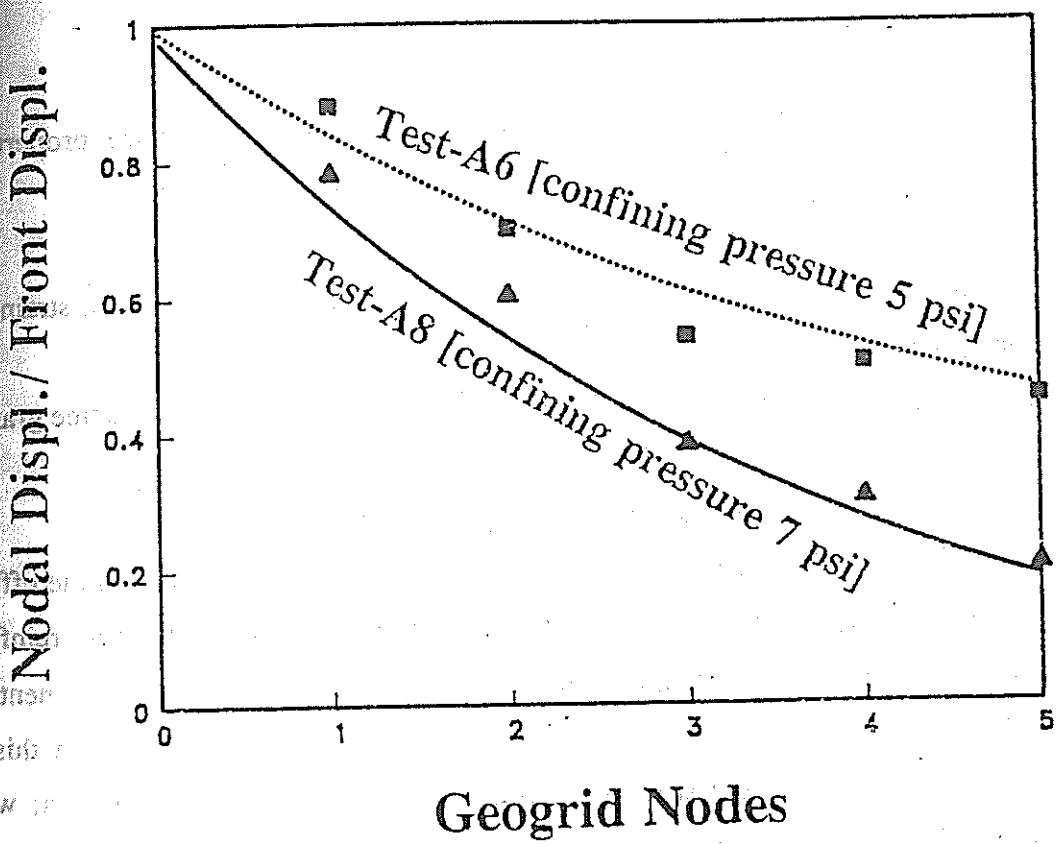

Figure 4.29 Effect of confining pressure on the displacement distribution along geogrid

CHAPTER 5
ANALYSIS OF PULL-OUT TEST RESULTS

5.1 INTRODUCTION

The large number of factors that affect the soil-geogrid interface properties raise difficulties in developing an interpretation procedure from pull-out test results. These factors are mainly related to:

i) testing: such as apparatus and sample dimensions, boundary conditions, strain rate, and the applied confining pressure,

ii) soil characteristics: such as its relative density, dilation properties, and fine grain portion of the soil,

iii) reinforcement: its type, geometry, and extensibility.

The major concern in the interpretation of the pull-out tests results pertains to the effect of the reinforcement extensibility on the interaction pull-out parameters. Inextensible reinforcement (such as metallic strips) moves as rigid members in the soil, and the soil displacement required to mobilize the interface lateral friction is in the order of mm. (44,45,46). In this type of reinforcement, a constant shear stress distribution is developed along the length; while, for extensible reinforcement, its non-uniform extensibility results in a decreasing shear displacement distribution along its length. Therefore, the interface shear stress is not uniformly mobilized along the total reinforcement length. As the reinforcement extensibility depends upon its length, pull-out interface parameters become a function of the specimen length in pull-out tests. The effect of geogrid specimen length has to be evaluated in order to extrapolate pull-out test results to the reinforcement length in the field. The displacement measurements along the length of the geogrid becomes necessary in order to interpret this effect. Several investigators (13,34) measured the displacement distributions at several points along the geogrid during pull-out (Figures 5.1-a and b). Typical displacement measurements along the geogrids during pull-out tests of this study are shown in Figures 5.2.

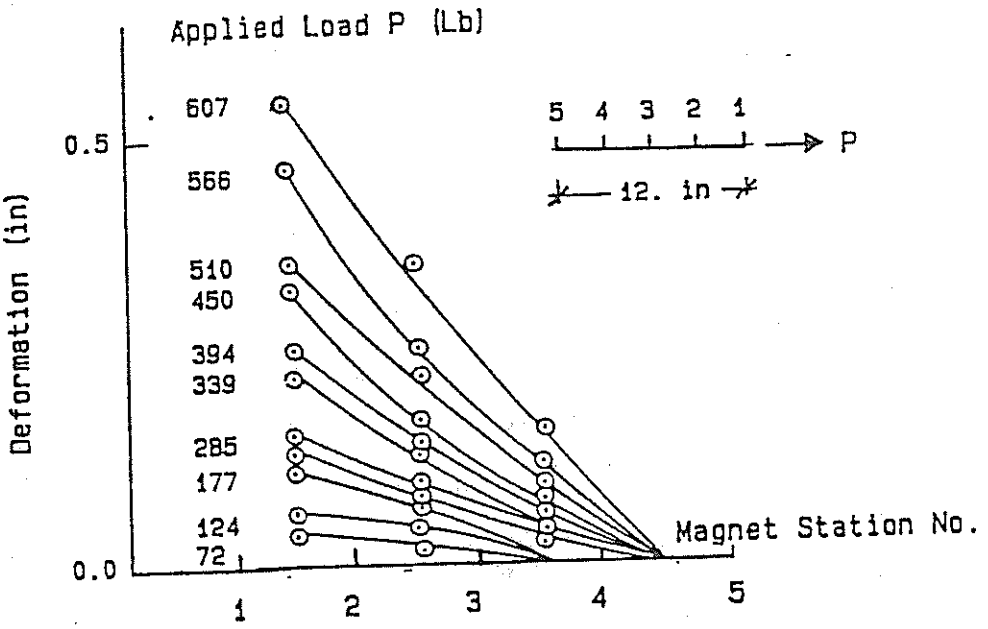

(a) after 34,

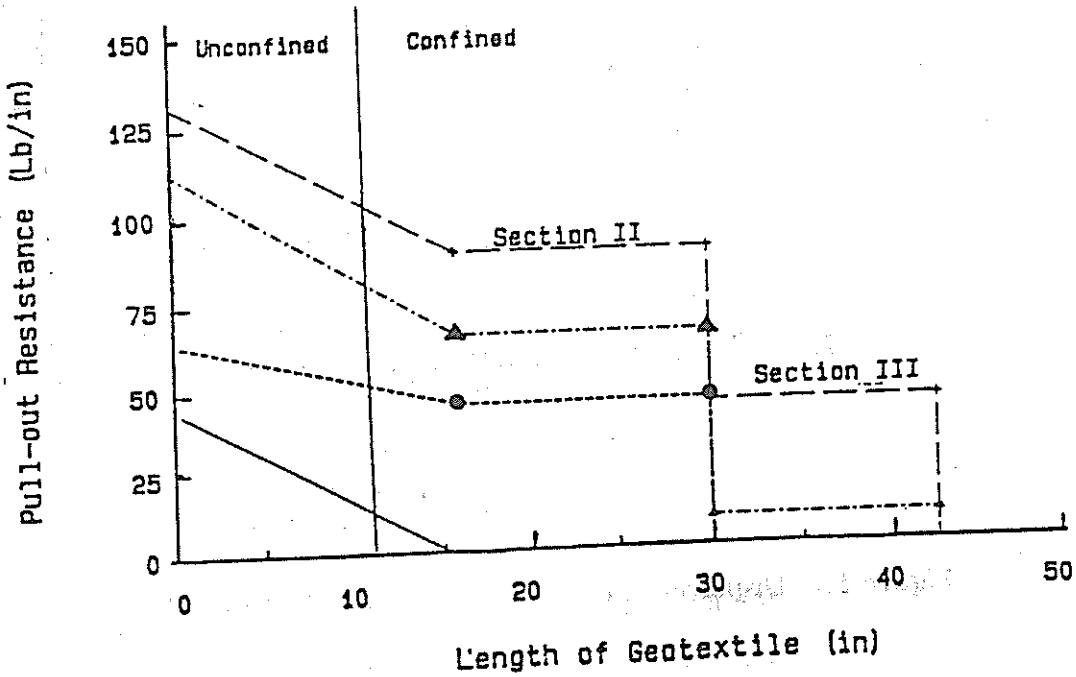

(b) after 13

Figure 5.1 Displacement measurements along the geogrid in pull-out

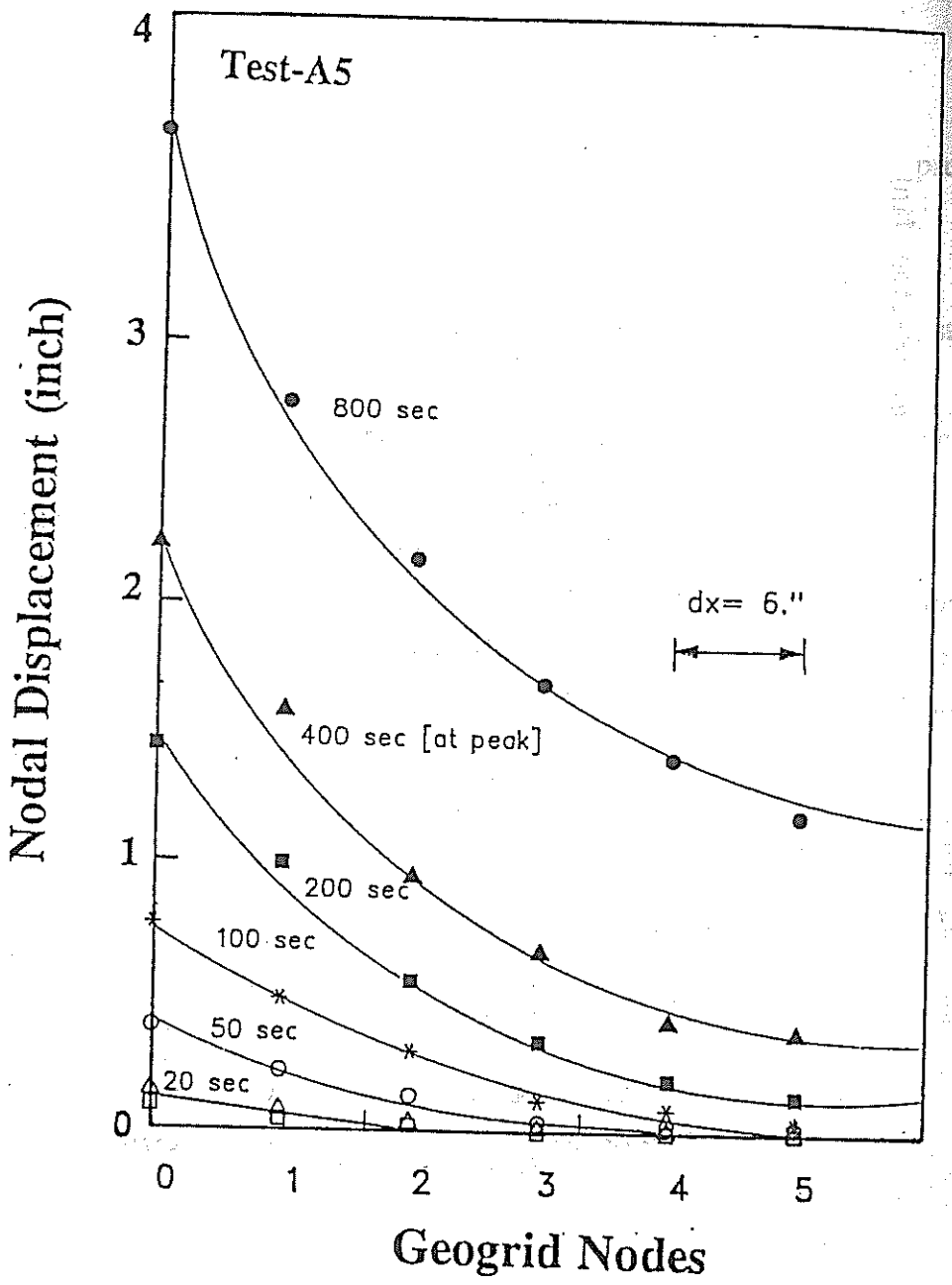

Figure 5.2 Displacement Distribution along the geogrid nodes

The shear strength at the soil-reinforcement interface is commonly calculated from pull-out test results from the relationship (47,48):

$$\tau = \sigma_v \tan \delta \qquad \ldots\ldots\ldots\ldots\ldots \quad (5.1)$$

where, τ = shear stress at the interface,

σ_v = normal stress at the reinforcement level,

δ = soil-reinforcement interface friction angle.

The pull-out resistance can, accordingly, be calculated from the relationship:

$$P_r = 2 \cdot \gamma \cdot d \cdot \tan \delta \cdot L_e \qquad \ldots\ldots\ldots\ldots\ldots \quad (5.2)$$

where, P_r = pull-out resistance in force per unit width of the reinforcement,

γ = unit weight of soil,

d = thickness of soil above reinforcement,

L_e = length of reinforcement resisting pull-out force.

The disadvantage of this method is that it ignores the non-uniform shear stress distribution along the extensible reinforcement. It assumes an even distribution over the length and defines δ as the slope of the pull-out stress versus normal stress.

The previous approach can be modified by distributing the mobilized shear stress over the actual portion of the elongated sample (13). The pull-out load per unit area can then be calculated as:

$$\text{Pull-out stress} = \frac{\text{mobilized load}}{\text{actual strained section} \times 2} \qquad \ldots\ldots\ldots \quad (5.3)$$

A modified form of Equation (5.2) is recommended (41), to include the effect of extensibility, in determining the pull-out resistance:

$$P_r = F^* \cdot \alpha \cdot \sigma_v \cdot L_e \cdot c \qquad \ldots\ldots\ldots \quad (5.4)$$

where,

F^* is a pull-out resistance factor obtained from pull-out tests,

c is the reinforced unit perimeter [$c=2$ for grids and sheets],

α is a scale effect correction factor.

The scale effect correction factor represents the nonlinearity of the P_r-L_e relationship due extensibility. For inextensible reinforcement, α is approximately 1. For extensible reinforce α can be determined from the equation:

$$\alpha = \tau_{avg}/\tau_p \qquad \ldots\ldots\ldots\ldots\ldots\ldots \quad (5.5)$$

where τ_{avg} and τ_p are the average and ultimate interface lateral shear stresses mobilized along the reinforcement, respectively. The disadvantage of this empirical formula is that α depends primarily upon the interface shear strain softening and not, explicitly, upon the extensibility of the reinforcement.

The coefficient of friction between the soil and geogrid (tan δ) is also obtained (49) by using the slope of the pull-out curve along the mobilized length of the reinforcement (K_r) in the relationship:

$$K_r / 2b = \sigma_v \cdot \tan \delta \qquad \ldots\ldots\ldots\ldots \quad (5.6)$$

where b is the reinforcement width, and σ_v is the normal stress in the level of the geogrid.

Several analytical approaches are implemented in order to interpolate the displacement distribution for any reinforcement length. An analytical solution, relating the pull-out displacement to pull-out load and reinforcement stiffness and length, was presented in the form (50):

$$u = \frac{P \cosh (\alpha x)}{\sqrt{2 K_a K_s} \sinh (\alpha L)} \qquad \ldots\ldots\ldots\ldots\ldots \quad (5.7)$$

where P = the applied pull-out load,

x = the longitudinal coordinate along the reinforcement,

$\alpha = \sqrt{2K_s / K_a}$

K_a = reinforcement stiffness,

K_s = interface shear stiffness from pull-out tests,

L = reinforcement length.

ure 5.3 displays the computed pull-out displacements along a six feet reinforcement utilizing analytical model.

A theoretical load transfer model, derived from the (t-z) method commonly used in sign of friction piles, was also proposed (12). Figure 5.4 presents the numerical simulation the pull-out resistance using this model along with the experimental results.

The review of the previous approaches demonstrates that the concept of a uniformly obilized interface shear stress, which can be used for inextensible reinforcement, can not be dequately used for the interpretation of pull-out tests in extensible reinforcement. In order to velop an appropriate load transfer mechanism, an instrumentation scheme should be mplemented in pull-out tests to measure the interface shear strain at different points along the reinforcement.

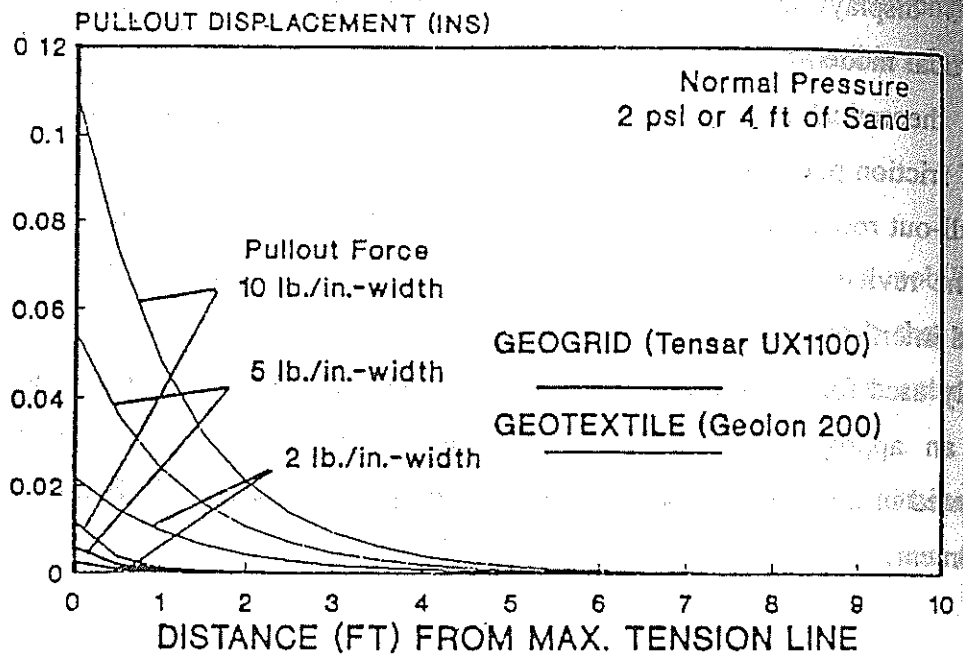

Figure 5.3 Computed pull-out displacements along the reinforcements (40)

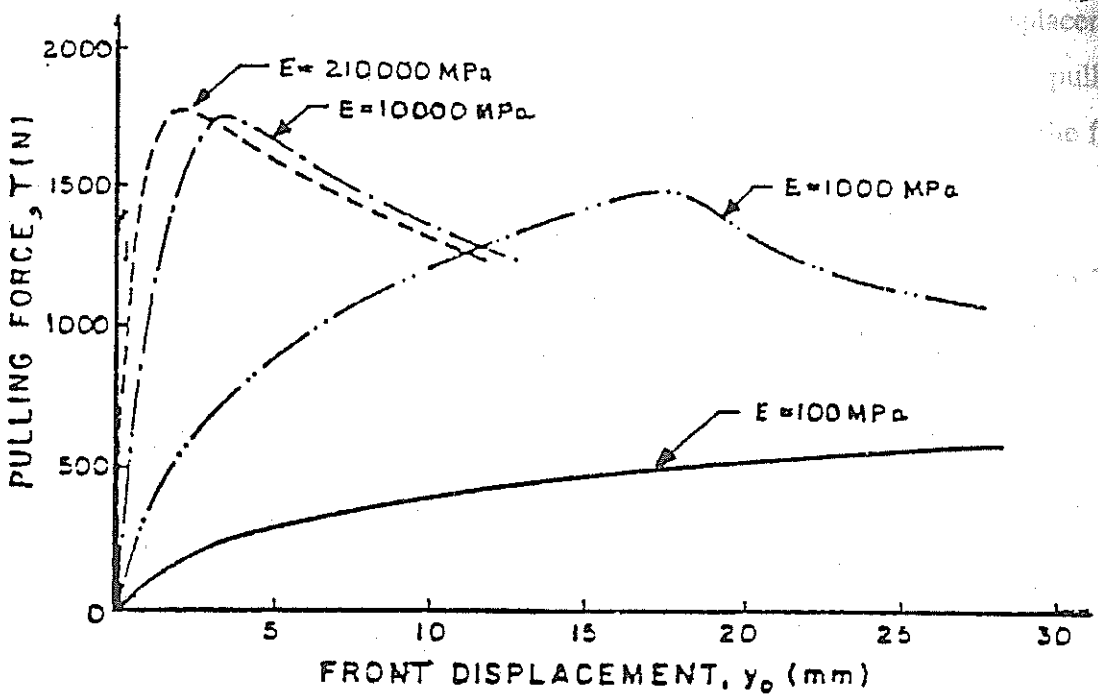

Figure 5.4 Numerical simulation of pull-out tests on woven strips (12)

MODELING LOAD TRANSFER IN PULL-OUT TESTS

The displacement measurements at different points along the specimens in the pull-out ts along with the appropriate interaction laws (relating the shear strain at any point along the nforcement to the mobilized shear stress at the interface) are used to develop a load transfer odel. In this model; the interpretation procedure permits the determination of:

i) the in-soil confined material properties,

) the shear stress-strain relationship at the interface,

ii) the displacement distribution along the geogrid length under the specified pull-out load.

This procedure is evaluated through comparison of the interface properties derived from the pull-out tests with those obtained directly from the direct shear tests.

The proposed data analysis procedure is illustrated through the interpretation of the displacement-rate controlled pull-out tests results presented in the previous chapters. This procedure consists of the following steps:

1. From the Time-Nodal displacements relationship (see Figure 3.17), the displacements distributions along the reinforcement can be plotted for different pull-out loads. Figures 5.2 and 5.5 display the displacement distribution along the specimen length obtained from Tests under confining pressure of 7 psi. From the discretized elements along the geogrid reinforcement (Figure 5.6), it can be seen that the displacement of each element i results from the elongation of the element (i.e. $\delta_{i-1} - \delta_i$) and its shear displacement δ_i.

2. The strain ϵ_i of each element i can be calculated from the relationship:

$$\epsilon_i = [\ \delta_{i-1} - \delta_i\ ] / \Delta x \qquad \ldots\ldots\ldots\ldots\ldots \qquad (5.8)$$

where δ_{i-1} and δ_i are the displacements at nodes i-1 and i, respectively; and Δx is the length of element i.

3. The in-soil geogrid stress (force/unit width) versus strain can now be plotted for the front element of the geogrid. Figure 5.7 depicts the confined stress-strain relationship for the geogrid.

4. The confined stress-strain properties (e.g. stiffness modulus E.t) are assumed to be unique for each confining pressure. The E.t values can be determined from the slope of the stress-strain curve at each loading level.

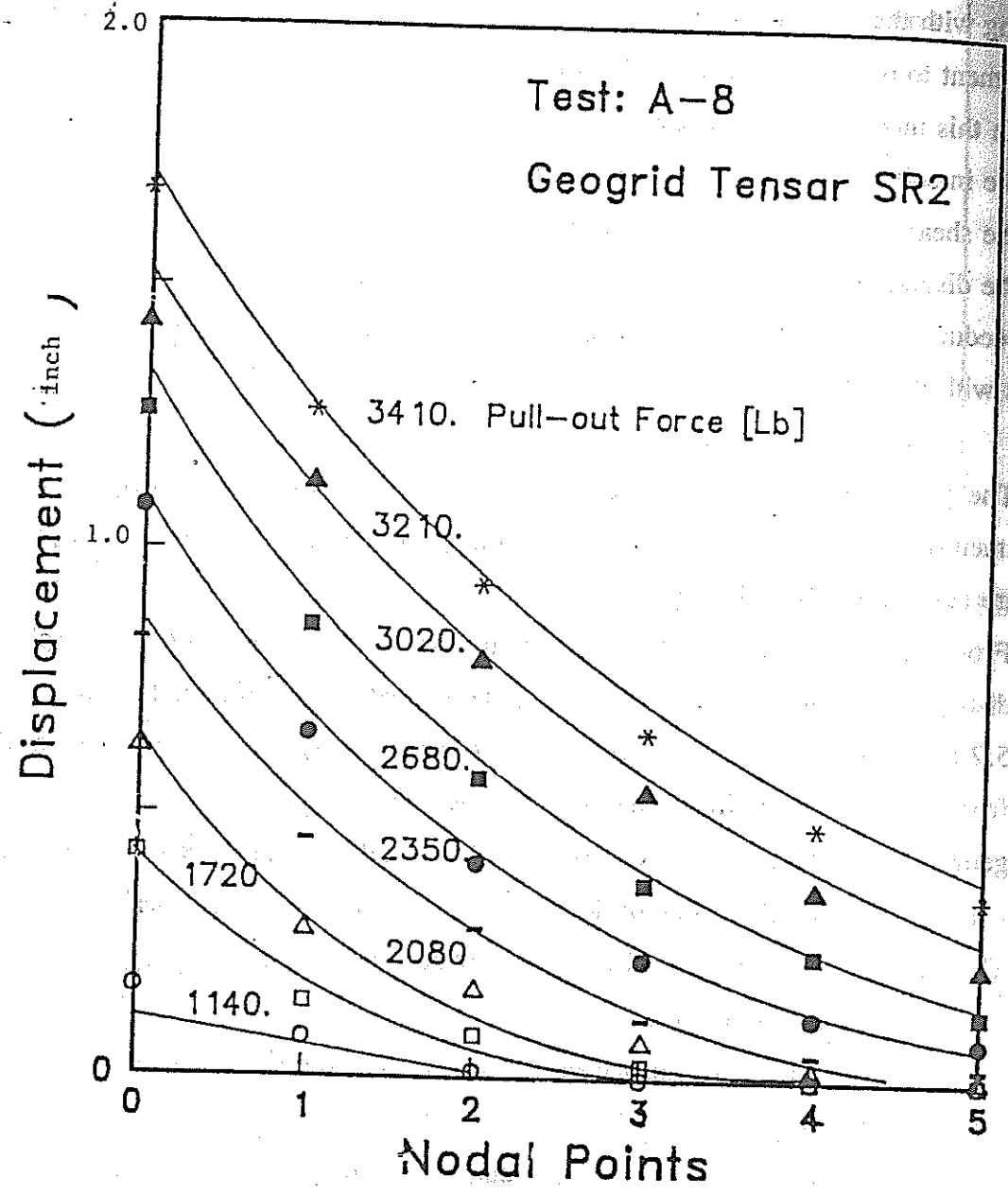

Figure 5.5 Displacement distribution along the geogrid Nodes

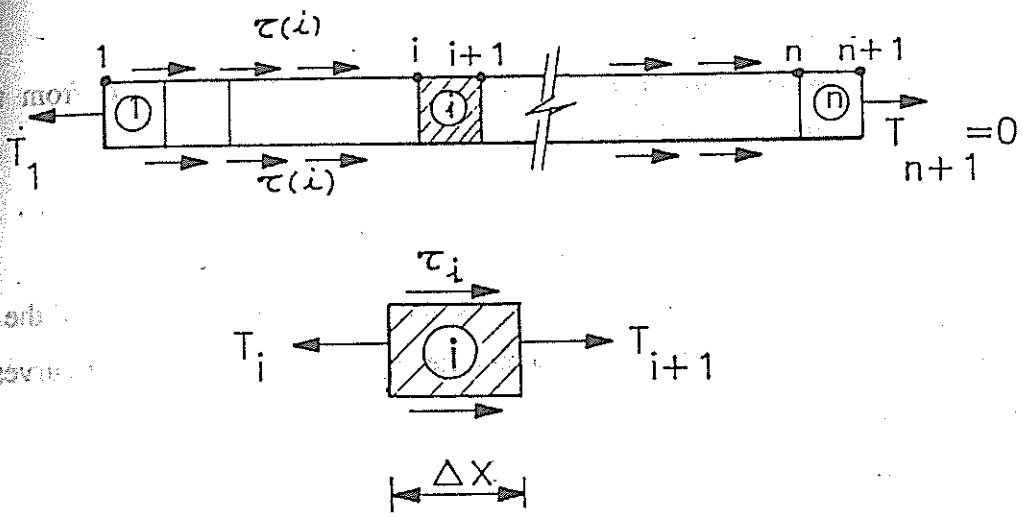

Figure 5.6 Schematic diagram of the discretized geogrid

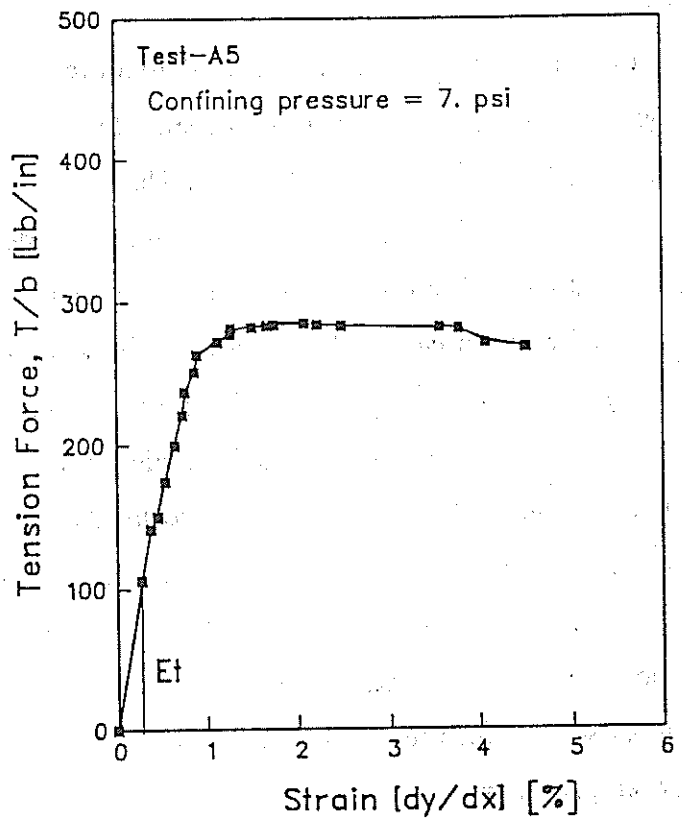

Figure 5.7 Confined stress-strain relationship of the geogrid

5. The tension force T_i at each node i can be calculated from the relationship:

$$[T_{i-1} - T_i] / b = E.t. [\delta_{i-1} - \delta_i] / \Delta x \quad \ldots\ldots\ldots\ldots \quad (5.9)$$

6. The shear stress distribution along the specimen can be calculated from the static equilibrium equation of each element i:

$$[T_{i-1} - T_i] = \tau_i \, . \, P \, . \, \Delta x \quad \ldots\ldots\ldots\ldots \quad (5.10)$$

where P is the geogrid perimeter [= 2b].

7. The shear stress-strain relationship at the interface can then be plotted for all the elements of the geogrid. Figures 5.8 and 5.9 depict the shear stress-displacement curves derived from different pull-out tests.

The results of pull-out tests on geogrids are implemented into the numerical procedure. The calculated shear stress-displacement curves are compared with those obtained directly from tests performed in the large direct shear box under the same confining pressure. The results are presented in Figure 5.10.

The analysis of pull-out test results on the geogrid reinforcement illustrates the non-uniformity of the displacement distribution along the geogrid length. The peak shear stress mobilized at the interface is a function of the sample length. Therefore, the extrapolation of the pull-out test results to reinforcements of different lengths should be considered when pull-out test results are implemented into design. The established interface properties and confined stress-strain relationships of the reinforcement can be implemented to back-calculate the displacement distribution along the geogrid of any length under the same testing conditions. Thereby, laboratory pull-out test results could be extrapolated to full scale reinforcement length. along

The analytical procedure is used to predict the displacements and the pull-out forces at the nodes of geogrid reinforcements of lengths 1.5 ft, 3 ft, and 6 ft. The calculated displacements and pull-out loads are displayed in Figure 5.11 and 5.12, respectively. The figures also display the measured displacements and pull-out loads for reinforcements of lengths 1.5 ft and 3 ft. The comparison between the analytical and experimental results illustrates the applicability of the proposed procedure.

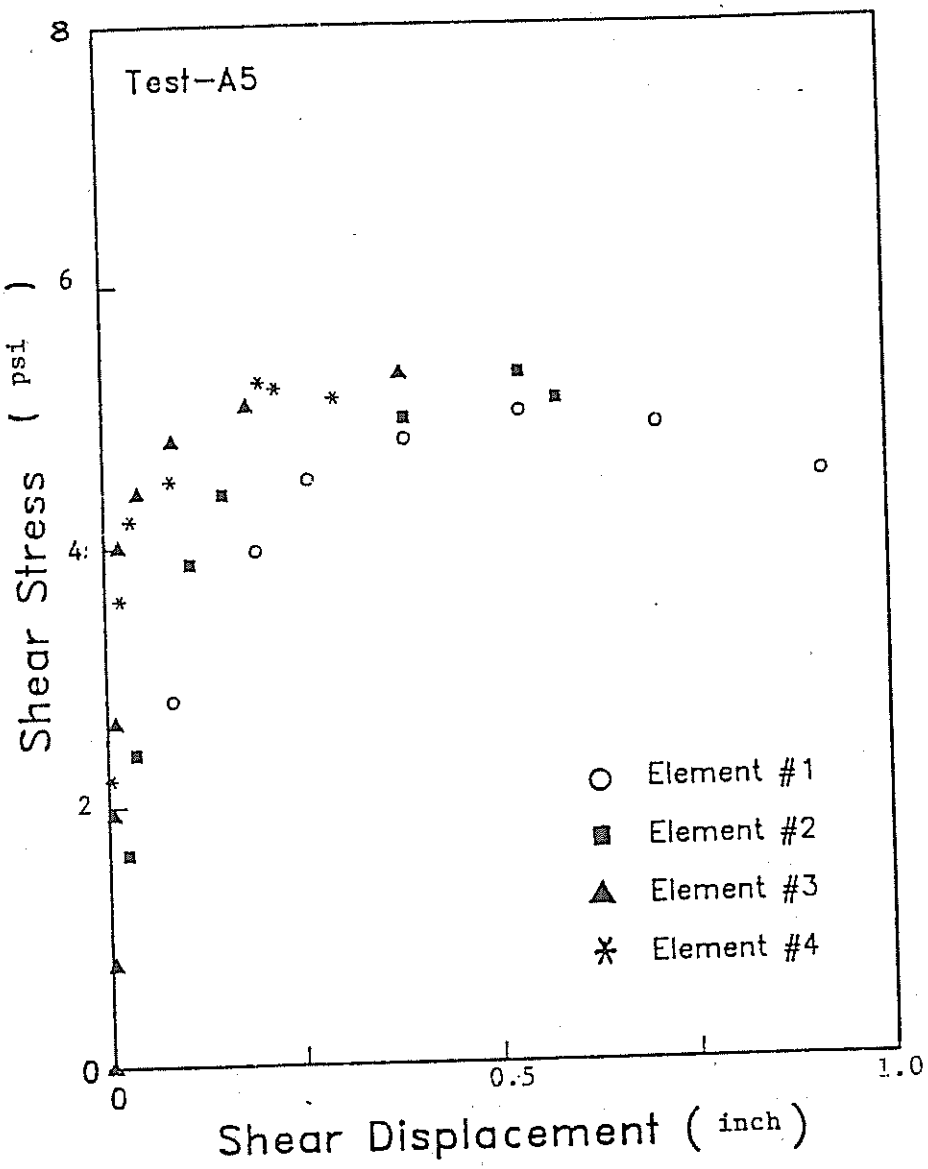

Figure 5.8 Interface shear stress-displacement relationship for the geogrid

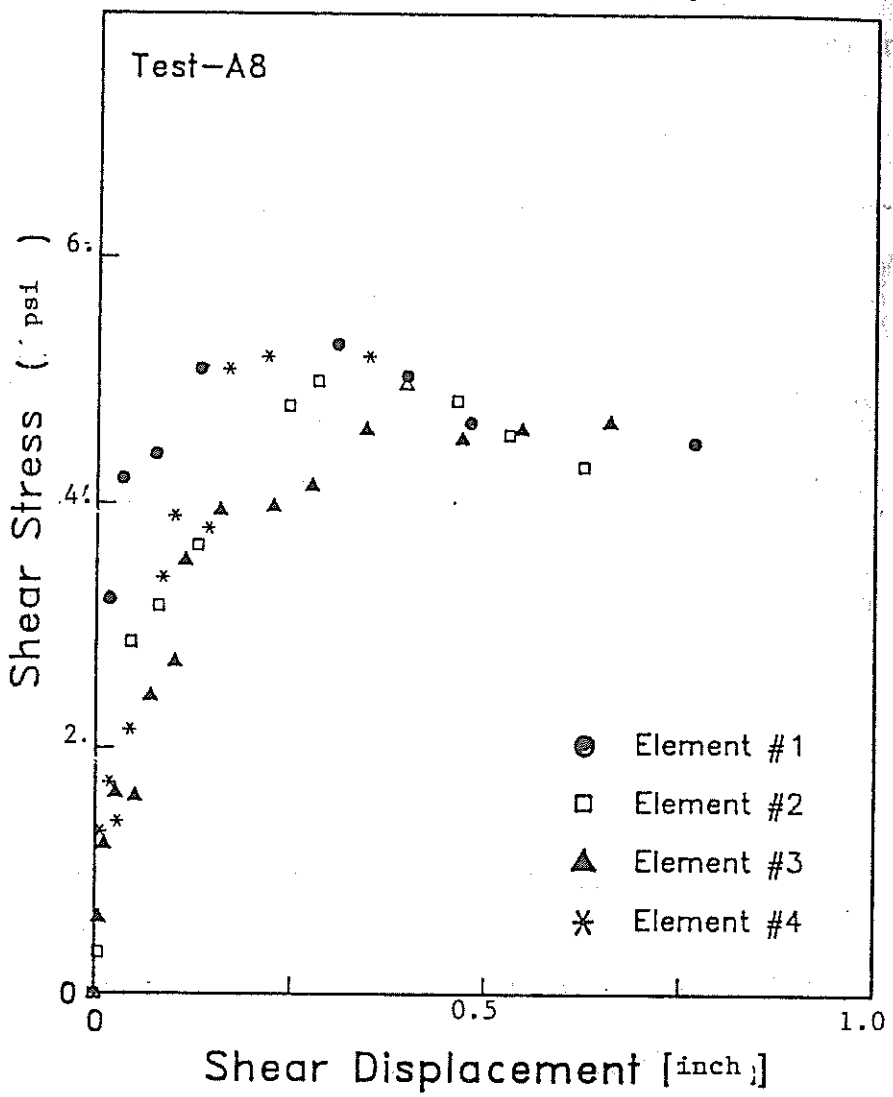

Figure 5.9 Interface shear stress-displacement relationship for the geogrid

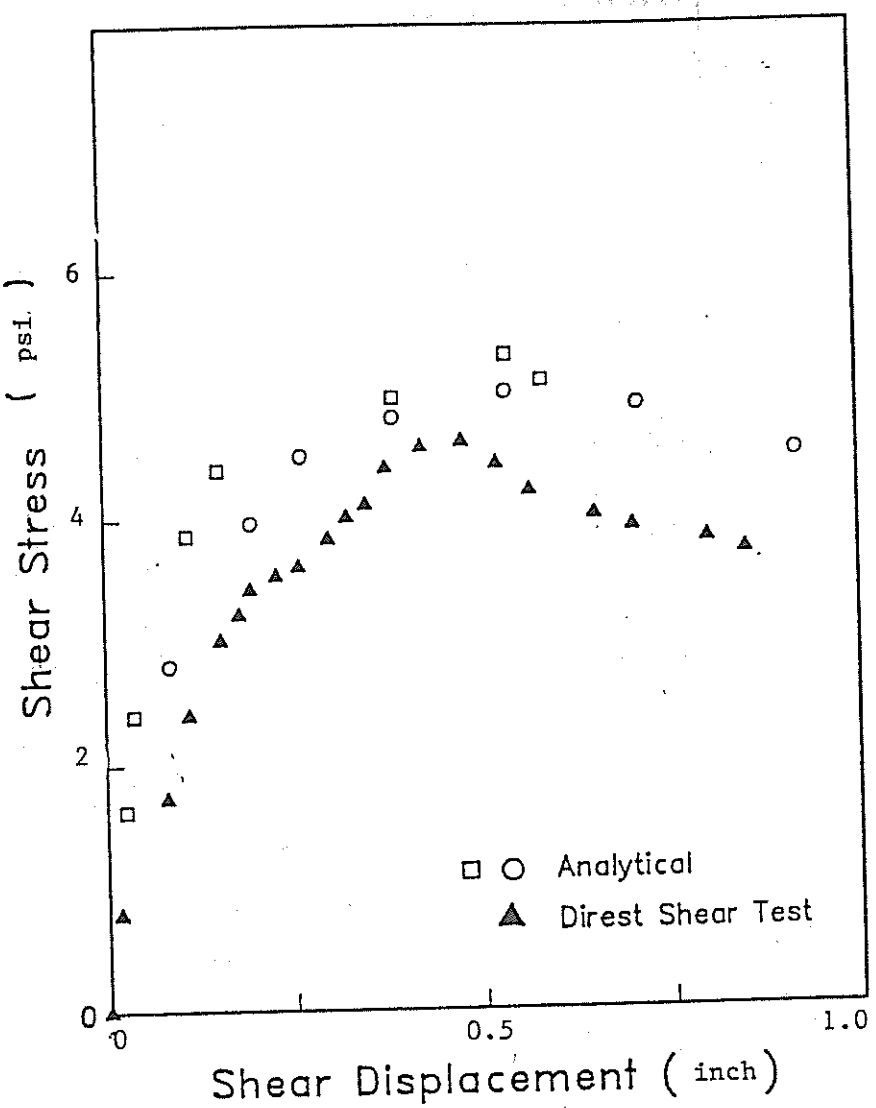

Figure 5.10 Analytical and experimental shear stress-displacement relationship

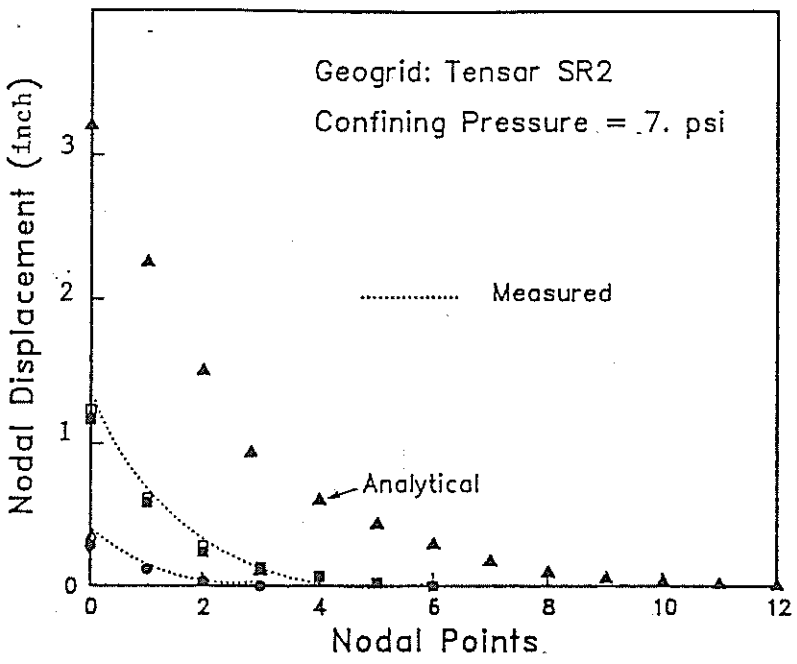

Figure 5.11 Analytical and experimental displacement distribution along the geogrid

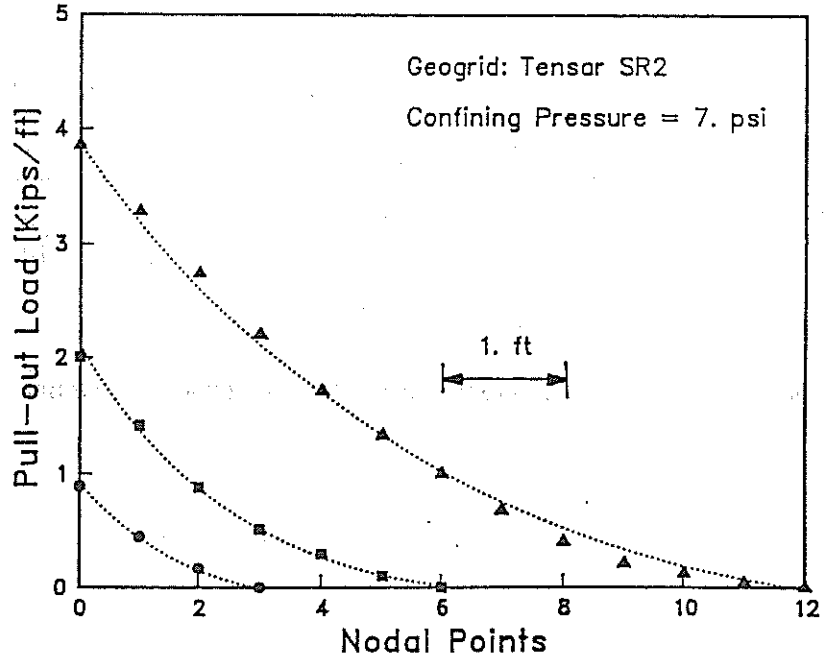

Figure 5.12 Analytical pull-out load distribution along the geogrid

CHAPTER 6
CONCLUSIONS AND RECOMMENDATIONS

6.1 CONCLUSIONS

The pull-out box and the large direct shear box are constructed in order to evaluate the short- term and long-term interface parameters and confined stress-strain properties of the geogrids. Displacement-rate controlled tests are conducted to provide the parameters related to short-term performance of the geogrids; namely, pull-out resistance, front displacement at peak, and interface stiffness modulus. The instrumentation of the pull-out box permits the measurement of the nodal displacements along the confined geogrid. These measurements are utilized in a load-transfer model in order to determine the stress-strain properties of the geogrids. Load-controlled pull-out tests are conducted to evaluate the performance of the pull-out testing facility in creep tests on confined geogrids. Shear tests are also performed on the geogrids in the large direct shear box in order to provide the shear stress-strain properties at the soil-geogrid interface.

The results of the pull-out tests on the geogrids in granular soils illustrate the importance of soil density and the applied confining pressures on the pull-out behavior. The high soil density and confining pressure increase the geogrid frictional resistance at the interface and increase the lateral earth resistance on the transversal elements. Consequently, they restrain the deformation of the geogrid along its length and decrease its effective adherence length.

Pull-out testing program is conducted in order to evaluate the performance of the facility and to assess the effect of different testing parameters (i.e. geogrid dimensions, box boundary conditions, pull-out rate, soil density, and confining pressure) on the interface properties. The parametric study led to the following conclusions:

1. The friction between the soil and the side walls can reduce the amount of normal pressure on the geogrid specimen. This effect can be reduced by either lubricating the box side walls or by selecting the width of the geogrid specimen so that uniform confining pressure is maintained along the specimen width. A minimum distance of 6 inches between the geogrid and the side walls is sufficient to eliminate the effect of side

2. The lateral earth pressure developed at the facing increases the soil-geogrid resistance to pull-out. The use of sleeves around the pull-out slot transfers the soil-geogrid interface resistance far behind the rigid front wall, which imposes a practical solution to reduce the front rigid wall effect. Pull-out tests with different sleeve lengths led to the conclusion that a sleeve length of 1 ft is sufficient to eliminate this boundary effect.
3. Another boundary parameter that influences pull-out test results is the upper and lower box boundaries. When soil thickness is small, the rigid bottom plate increases soil friction at the soil-geogrid interface. Moreover, the top and bottom boundaries may restrain soil dilatancy and, consequently, may lead to an increase in the confining pressure at the interface. Pull-out tests on geogrids in different soil thicknesses demonstrate that a minimum soil thickness of 1 ft above and 1 ft under the geogrid are sufficient to eliminate the effect of these boundaries on test results.
4. The pull-out resistance of geogrid is also influenced by the displacement-rate. Results of pull-out tests demonstrate that pull-out resistance is less sensitive to changes in displacement-rates under 0.25 in/minute. Displacement-rates less than 0.25 in/minute (6 mm/minute) are recommended for pull-out tests on the geogrids with similar specimen lengths and testing parameters to those in this study. Lower displacement-rates may be required to monitor the pre-peak response of geogrid specimens of much smaller lengths and in lower soil densities and confining pressures.
5. Pull-out test results on the geogrids in different soil densities demonstrate the influential effect of soil density and compaction procedure. A compaction procedure is developed in order to obtain uniform soil density along the geogrid. For geogrids tested in fine grained soils, different soil placement techniques and compaction procedures need to be developed and evaluated.
6. Test results on the geogrids under different confining pressures demonstrate that pull-out resistance is mobilized at strain levels much lower than those in unconfined extension tests. This conclusion suggests that the design criteria of reinforced-structures should be based on the strain levels obtained from pull-out test results rather than from the unconfined extension test results.

Modeling load transfer in soils reinforced with geogrids is complex and involves several interaction mechanisms. However, a simplified load-transfer model for extensible reinforcement is developed in order to rationally extrapolate laboratory pull-out test results to full-scale reinforcement lengths. Development of this model required the appropriate instrumentations to measure the displacements at different locations along the geogrid. The data analysis permitted the derivation of the soil-geogrid interaction parameters and the in-soil stress-strain relationship of the reinforcement from pull-out tests.

6.2 RECOMMENDATIONS FOR A STANDARD TESTING METHOD FOR GEOGRID PULL-OUT IN GRANULAR SOILS

6.2.A Scope

The following recommendations pertain to providing the guidelines for a standard procedure for pull-out tests. The scope of the test method is to determine the pull-out resistance of geogrids embedded in granular soils. However, the practice is applicable to other types of geosynthetics such as geotextiles and geomembranes.

1. Different compositional and environmental testing parameters will affect the pull-out response of geosynthetics in coarse and fine grained soils.
2. The pull-out tests provide the pull-out resistance of the specific geogrid under the specified testing parameters. The pull-out resistance depends on many factors such as soil relative density, confining pressure and pull-out rate. All testing parameters should be reported with the test results.
3. As the pull-out test results depend on the soil properties such as grain size distribution, relative density and moisture content; tests should be conducted using soils with similar characteristics with those used in-situ.
4. For standard practice of testing of geosynthetics, refer to the related publications:
   - ASTM standard D-2905: Statement of Number of Specimens Required to Determine

the Average Quality of Textiles.

- ASTM standard D-4354: Practice for Sampling of Geotextiles for Testing.
- GRI Test Method GG5 (51): Standard Test Method for Geogrid Pull-out.

6.2.B Definitions

1. Pull-out load: Force per unit width measured at a specific displacement level.
2. Pull-out Resistance: the peak pull-out load of the geogrid measured during pull-out test.
3. For definitions on other terms related to geosynthetics, refer to the following publications:
   - ASTM standard D-123: Definitions of terms related to textiles
   - ASTM standard D-653: Terms and Symbols related to Soil and Rock Mechanics

6.2.C Summary of Method

1. The geogrid is bolted to the clamping plates and embedded within two layers of soil. The clamping plates extend from inside the soil to the pull-out machine.
2. Confining pressure is applied on the top soil layer by means of a confined air bag.
3. A horizontal pull-out load is applied to the clamping plates and, consequently, the geogrid under constant displacement-rate or constant load.
4. The pull-out load and the front displacement of the geogrid are monitored during the test. A plot of the pull-out load versus the front displacement is obtained for different confining pressures. The pull-out resistance is obtained by dividing the peak pull-out load by the specimen width.
5. Inextensible wires can be attached to the embedded geogrids at different nodes along its length and connected to extensometers (LVDT's) in order to monitor the geogrid deformation along its length. Plots of pull-out loads at nodal points along the geogrid can then be obtained. These plots can be employed in evaluating the pull-out resistance at different effective lengths of the geogrid.
6. The data obtained from pull-out tests (i.e pull-out resistance and the displacement curves along the geogrid length) can be used in evaluating the pull-out response of geogrids in reinforced-soil structures. The results can also provide, through the appropriate load transfer model, the confined stress-strain properties of the geogrids.

6.2.D Apparatus

1. The details of the pull-out box and soil handling facility are described in Chapter 2 of this report.
2. The length of the pull-out box permits testing geogrid specimens of 3 ft in length. The minimum length of the pull-out box should be selected so as to permit testing representative specimen lengths of the specified geogrid. A representative specimen length is the length with a number of transversal ribs sufficient to establish displacement curves along its length. Analysis of pull-out test results indicates that measurement at five transversal ribs are sufficient to establish the displacement curves.
3. The width of the pull-out box permits testing geogrid specimens of 2 ft maximum width with a distance of 6 inches between the geogrid and the side walls. However, pull-out tests on geogrids specimens of 0.5-ft wide shows that the results are identical to those on 2 ft wide specimens. The width of the pull-out box should allow for a minimum distance of 0.5 ft between the geogrid and each side of the box. Otherwise, some other methods should be employed to minimize side friction.
4. The dimensions of the box should be increased, if necessary, so that the minimum box length and width are greater than 20 times the D_{85} of the soil (51).
5. The height of the box should allow for a minimum depth of 1 ft of soil above and under the geogrid.
6. Sleeves should be incorporated around the slot at the front wall of the box. The sleeves consist of two thin metal plates extending the full width of the box. The sleeves should provide sufficient stiffness to withstand the confining pressure without deformation. The sleeves should have a minimum length of 8 inches.
7. Two clamping plates, of the same width as the geogrid specimen, connect the specimen to the pull-out machine. The geogrid specimen is clamped by bolts between its longitudinal ribs. Different clamping mechanisms may be required based on the geogrid type and its geometry. The clamps must allow the specimen to remain horizontal with uniform load distribution along its width. Calibration tests should determine the friction between the clamping plates and the soil for each soil type and density prior to testing.

8. A flexible pneumatic bladder (an air bag), of the same size as the pull-out box, should be used to apply confining pressure on the soil. The air bag should be designed to withstand the anticipated pressures. The air pressure should be constant for the duration of the test.

6.2.E Loading Mechanism

The loading machine should apply horizontal pull-out at the level of the geogrid. The pull-out force may be applied by one of the following loading mechanisms:

1. Constant displacement-rate controlled Test: The pull-out force is applied at a constant displacement-rate during the test. This testing procedure (which is most commonly used) provides the interface parameters related to the short term pull-out performance of the geogrids. The displacement rate should not exceed 0.25 in/min (6 mm/min).
2. Stepped load-controlled test: The pull-out loads are applied incrementally to the geogrid and maintained constant during a specific period. This testing procedure is applied to determine either the short-term or long-term pull-out resistance of the geogrid, according to the loading period.
3. Creep Test: A constant pull-out load is applied on the geogrid for a specific period to determine the time dependent pull-out resistance and the corresponding creep strains of the geogrid. The loading level is usually a percentage of the short term pull-out resistance and testing duration may vary from 500 to 10,000 hours.

6.2.F Geogrid Sampling

1. Geogrid specimens should be representative samples according to ASTM standard D-4354: Practice for Sampling of Geotextiles for Testing.
2. The pull-out resistance varies, for most geogrids, according to the direction of the specimen. Pull-out tests are usually performed on specimens with the same direction used to resist pull-out forces in the structure.

6.2.G Instrumentation

1. The front displacement is monitored by an LVDT mounted on the loading frame.
2. The displacements at different nodes along the geogrids are monitored by 5 LVDT's mounted at the rear table. The LVDT's are connected to the geogrid transversal ribs by inextensible 'Tell-tale' wires. The wires are kept stretched by means of counter weights at the rear table. It is recommended to protect the wires in ½-inch plastic tubes in order to eliminate soil resistance to their movement.
3. A velocity transducer may be mounted on the loading frame in order to monitor the displacement-rate of the clamping plates.
4. The pull-out load is measured by a load cell mounted on the hydraulic ram.
5. The confining pressure is supplied through a regulated air source and monitored by a pressure gauge.
6. Continuous readouts from the monitoring instruments are translated through a data acquisition system for display and storage. The data acquisition system also controls the pull-out loading device to operate under the specific testing mode.

6.2.H Procedure

1. An elevated hopper is used to place the soil in the pull-out box. The soil is placed in four lifts of 6 inches each.
2. The geogrid specimen is bolted to the clamping plates and placed on the top of the second soil layer. The clamping plates extend a sufficient distance in the box to insure that the geogrid remains confined throughout the test. The LVDT's are connected to the geogrid along its length.
3. Each soil layer is compacted to the desired relative density. A predetermined compaction procedure should be employed to obtain uniform soil density throughout the box.
4. After compaction, soil density is measured by a nuclear density gauge at different locations in the box. The average soil density should be equal to the required density within an acceptable deviation of $\pm$ 0.5 pcf.
5. The air bag is placed on the top soil layer and confined by the cover plate. Confining pressure is applied to the air bag.

6. Pull-out load is applied to run the tests under the specified testing mode. Continuous readings of the measuring devices are recorded by the data acquisition system. Loading is continued till pull-out slippage occurs.

6.2.I Results

1. For displacement-controlled pull-out tests, the pull-out load is plotted versus front displacement as in Figure (3.13). The relationship yields the peak pull-out load (pull-out resistance) and the stiffness modulus at the soil-geogrid interface.
2. The nodal displacements are plotted along the geogrid length for different loading levels. The relationships yield the effective geogrid length at different pull-out loads.
3. Pull-out load and displacement measurements, for different confining pressures, are implemented in one of the analytical procedures discussed in Chapter 5 in order to obtain the friction coefficient at the interface and to calculate the pull-out resistance of the geogrid in the site.

REFERENCES

1. Bonaparte, R., Holtz, R.D., and Giroud, J.P., "Soil Reinforcement Design Using Geotextiles and Geogrids," Geotextile Testing and the Design Engineer, ASTM STP 952, 1987, pp. 69-116.

2. Koerner, R.M., Designing with Geosynthetics, 2nd edition, Printice-Hall, Englewood Cliffs, NJ., 1990.

3. Juran, I., Ider, H., Acar, Y., and Guermazi, A., "A Comparative Study of Soil Improvement/Reinforcment Techniques for Highway Embankments," FHWA/LA-89/225, 1989.

4. Andrawes, K.Z., McGown, A., and Murray, R.T., "The Load-Strain-Time-Temperature Behavior of Geotextiles and Geogrids," 3rd International Conference on Geotextiles, Vienna, 1986, Vol. 3, pp. 707-712.

5. Myles, B., "A Review of Existing Tension Testing Methods," Geotextiles Testing and the Design Engineer, ASTM STP 952, 1987, pp. 57-68.

6. Rowe, R.K., and Ho, S.K., "Determination of Geotextile Stress-Strain Characteristics using a Wide Strip Tests", 3rd International Conference on Geotextiles, Vienna, 1986, Vol. 3, pp. 885-890.

7. Shrestha, S.C., and Bell, J.R., "A Wide Strip Tensile Test of Geotextiles," 2nd International Conference on Geotextiles, Las Vegas, 1982, Vol. 3, pp. 739-744.

8. Shrestha, S.C., and Bell, J.R., "Creep Behavior of Geotextile Under Sustained Loads," 2nd International Conference on Geotextiles, Las Vegas, 1982, Vol. 3, pp. 769-774.

9. American Society of Testing and Matrials, Standard Test Method for Tensile Properties of Geotextiles by the Wide-Width Strips Method, ASTM Standard D-4595-86, Vol. 04.08, 1990.

10. McGown, A., Andrawes, K.Z., and Kabir, M.H., "Load-Extension Testing of Geotextiles Confined In-Soil," 2nd International Conference on Geotextiles, Las Vegas, 1982, Vol. 3, pp. 793-798.

11. Juran, I., Knochenmus, G., Acar, Y.B., and Arman, A., "Pull-out Response of Geotextiles and Geogrids (Synthesis of Available Experimental Data)," Proc. of Symp. on Geotextiles for Soil Improvement, ASCE, GSP No. 18, 1988, pp. 92-111.

12. Juran, I. and Chen, C.L., "Soil-Geotextile Pull-out Interaction Properties, Testing and Interpretation," TRB, 67th Annual Meeting, Washington D.C., 1988.

13. Bonczkiewicz, C., Christopher, B.R., and Atmatzidis, D.K., "Evaluation of Soil-Reinforcement Interaction by Large Scale Pullout Box" TRB, 67th Annual Meeting, Washington D.C., 1987.

14. Rowe, R.K., Ho, S.K., and Fisher, D., "Determination of Soil-Geotextile Interface Strength Properties," 2nd Canadian Symposium on Geotextiles, 1985, pp. 25-34.

15. Ingold, T.S., "Laboratory Pull-out Testing of Grid Reinforcement in Sand," Geotech. Testing Journal, ASTM, 1983, 6(3), pp. 101-111.

16. Myles, B., "Assessment of Soil Fabric Friction by Means of Shear," 2nd International Conference on Geotextiles, Las Vegas, 1982, Vol. 3, pp. 787-791.

17. Palmeira, E., and Milligan, G., "Large Scale Direct Shear Tests on Reinforced Soil," Soils and Foundations, Japanese Society of Soil Mech. and Found. Eng., 1989, Vol. 29, No. 1, pp. 18-30.

18. Koerner, R.M., Direct Shear/Pull-out Tests on Geogrids, Report No. 1, Deptartment of Civil Engineering, Drexel Univ., Philadelphia, PA., 1986.

19. Knochenmus, G., Review of the Available Pull-out Testing Facility, Louisiana Transportation Research Center, Research Project 87-1G7, 1987.

20. Farrag, Kh., Interaction Properties of Geogrids in Reinforced-Soil Walls, Testing and Analysis, Ph.D. Dissertation, Louisiana State University, 1990.

21. Siel, B.D., Tzong, W.H., and Chou, N.N., "In-Soil Stress-Strain Behavior of Geotextile," Geosynthetics Conference, New Orleans, 1987, Vol.1, pp. 260-265.

22. Leshchinsky, D., and Field, D.A., "In-Soil Load Elongation, Tensile Strength and Interface Friction of Non-Woven Geotextiles," Geosynthetics Conference, New Orleans, 1987, Vol. 1, pp. 238-249.

23. Knochenmus, G., "Stress-Strain Behavior of Non-woven Geotextiles under Confined Conditions," M.Sc. Thesis, Louisiana State University, 1989.

24. Christopher, B.R., Holtz, R.D., and Bell, W.D., "New Tests for Determining the In-Soil Stress-Strain Properties of Geotextiles" 3rd International Conference on Geotextiles, Vienna, 1986, Vol. 3, pp. 683-688.

25. Broms, B.B., "Triaxial Tests with Fabric-Reinforced Soil," International Conference on the Use of Fabrics in Geotechnics, Paris, 1977, Vol. 3, pp. 129-133.

26. Holtz, R.D., Tobin, W., and Burke, W.W., "Creep Characteristics and Stress-Strain Behavior of a Geotextile-Reinforced Sand," 2nd International Conference on Geotextiles, Las Vegas, 1982, Vol. 3, pp. 805-809.

27. Richards, E.A., and Scott, J.D., "Soil Geotextile Friction Properties," 2nd Canadian Symposium on Geotextile & Geomembrane, 1985, pp. 13-24.

28. Martin, J.P., Koerner, R.M., and Whitty, J.E., "Experimental Friction Evaluation of Slippage Between Geomembranes, Geotextiles and Soils," Proceedings International Conference on Geomembranes, Denver, 1984, pp. 191-196.

29. Saxena, S.K., and Budiman, J.S., "Interface Response of Geotextiles," Proceedings of the 11th International Conference on Soil Mechanics and Foundation Engineering, San Francisco, 1985, Vol. 3, pp. 1801-1804.

30. Degoutte, G., and Mathieu, G., "Experimental Research of Friction Between Soil and Geomembranes or Geotextiles Using 30 x 30 cm_2 Shearbox," 3rd International Conference on Geotextiles, Vienna, 1986, Vol. 4, pp. 1251-1255.

31. Williams, N.D., and Houlihan, M.F., "Evaluation of Interface Friction Properties Between Geosynthetics and Soils," Geosynthetics Conference, New Orleans, 1987, Vol. 2, pp. 616-627.

32. Miyamori, T., Iwai, S., Makiuchi, K., "Frictional Characteristics of Non-Woven Fabrics," 3rd International Conference on Geotextiles, Vienna, 1986, Vol. 3, pp. 701-705.

33. Juran, I., and Christopher, B., "Laboratory Model Study of Geosynthetic Reinforced Soil Retaining Walls," Journal of Geotechnical Engineering, ASCE, 1989, Vol. 115, No. 7, pp. 905- 926.

34. Tzong, W.H., and Cheng-Kuang, S., "Soil-Geotextile Interaction Mechanism in Pullout Test," Geosynthetics Conference, New Orleans, 1987, Vol. 1, pp. 250-259.

35. Anderson, L.R., and Nielsen, M.R., "Pull-Out Resistance of Wire Mats Embedded in Soil," Report for the Hilfiker Company, Eureka, CA., 1984.

36. Jewell, R.A., "Some Effects of Reinforcement on the Mechanical Behavior of Soils," Ph.D. Thesis, Cambridge University, Cambridge, England, 1980.

37. Palmeira E.M. and Milligan, G.W., "Scale and Other Factors Affecting the Results of Pull-out Tests of Grids Buried in Sand", Geotechnique 39, No. 3, 1989, pp. 511-524.

38. Brand, S.R., and Duffy, D.M., "Strength and Pullout Testing of Geogrids," Geosynthetics Conference, New Orleans, 1987, Vol. 1, pp.226-236.

39. Johnston, R.S., "Pull-out Testing of Tensar Geogrids," M.Sc. Thesis, University of California at Davis, 1985.

40. Elias, V., "Friction in Reinforced Earth Utilizing Fine Grained Backfills," International Conference of Soil Reinforcement, Paris, 1979, pp.435-438.

41. Christopher, B.R., Safder, A.G., Giroud, J.P., Juran, I., Mitchell, J.K., Schlosser, F., and Dunnicliff, J., "Reinforced Soil Structures, Design and Construction Guide," FHWA Report No. RD-89-043, 1989.

42. Vyalov, S.S., Rheological Fundamentals of Soil Mechanics, Developments in Geotechnical Engineering 36, Elsevier, 1986.

43. Gourc, J.P., Delmas, P., and Giroud, J.P., "Experiments on Soil Reinforcement with Geotextiles," ASCE Convention, Portland, Oregon, 1980.

44. Schlosser, F., and Elias, V., "Friction in Reinforced Earth," ASCE National Convention, Pittsburgh, PA., (1978) pp. 735-764.

45. Schlosser, F., and Guilloux, A., "Friction Between Soil and Strips in Reinforced Earth Structures," International Conference of the Reinforcement of Soils, Paris, France, (1979), Vol. 1.

46. Schlosser, F., Jacobsen, H.M., and Juran, I., "Soil Reinforcement," 8th. European Conference on Soil Mechanics and Foundation Engineering, Helsinki, 1983.

47. Jewell, R.A., Milligan, G., Sarsby, R.W., and Dubois, D., "Interaction between Soil and Geogrids ", Proceedings, Polymer Grid Reinforcement, London, 1984, pp. 18-30.

48. Steward, J.E., Williamson, R., and Mohney, J., " Guidelines for use of Fabrics in Construction and Maintenance of Low-Volume Roads", FHWA Report No. TS-78-205, 1977.

49. Solomone, W.G., Boutrup, E., Holtz, R.D., Kovacs, W.D., and Sulton, C.D., "Fabric Reinforcement Designed Against Pull-out," The Use of Geotextiles for Soil Improvement, ASCE, Portland, Oregon, 1980, pp. 80-177.

50. Yuan, Z. and Chua, K.M., "An Analytical Model for Pull-out of Soil Reinforcement," TRB, 70th Annual Meeting, Washington D.C., 1991.

51. Geosynthetic Research Institute, Standard Test Method for Geogrid Pull-out, GG5, Drexel University, Philadelphia, PA, 1991.

APPENDIX A

EQUIPMENT DETAILS

LIST OF FIGURES OF APPENDIX A

Figure		Page
A-1	Top view of the pull-out box	154
A-2	Longitudinal view of the pull-out box	155
A-3	Cross section A-A of the pull-out box	156
A-4	Cross section B-B of the pull-out box	157
A-5	Cross section C-C of the pull-out box	158
A-6	Longitudinal view of the loading frame	159
A-7	Top view of the loading frame	160
A-8	Detail of the loading system	161
A-9	Detail of the elevated hopper	162

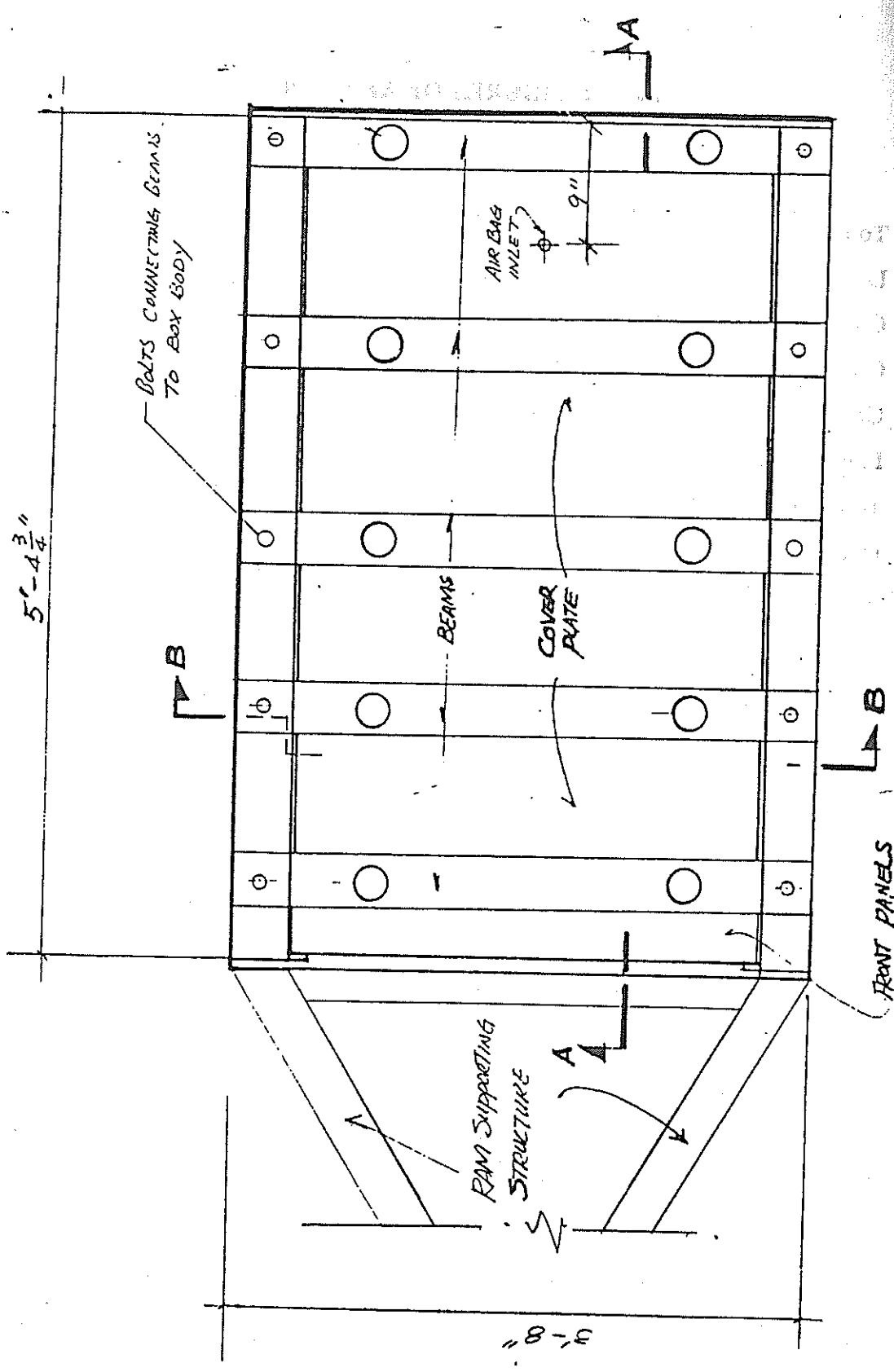

Figure A-1 Top view of the pull-out box

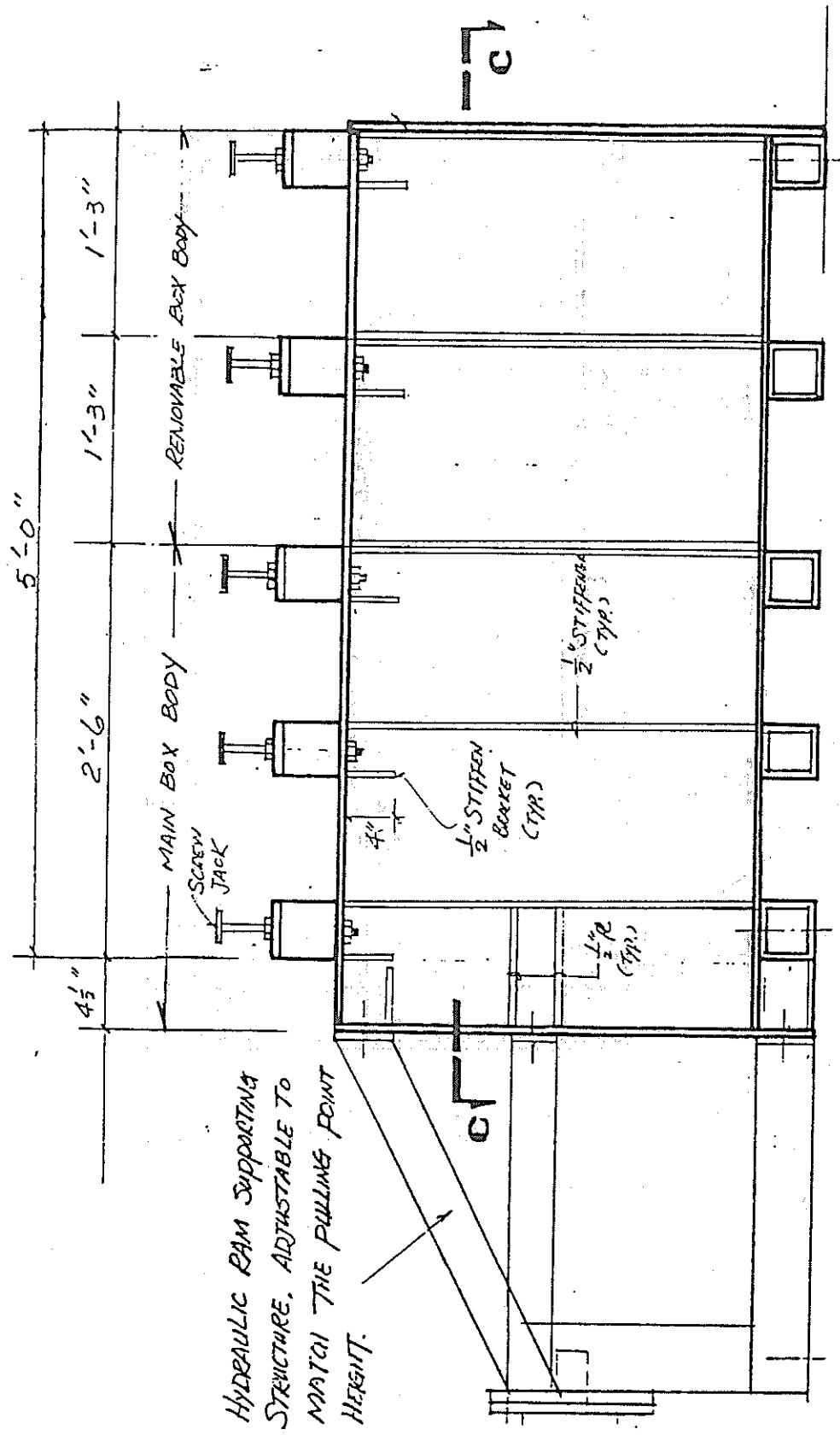

Figure A-2 Longitudinal view of the pull-out box

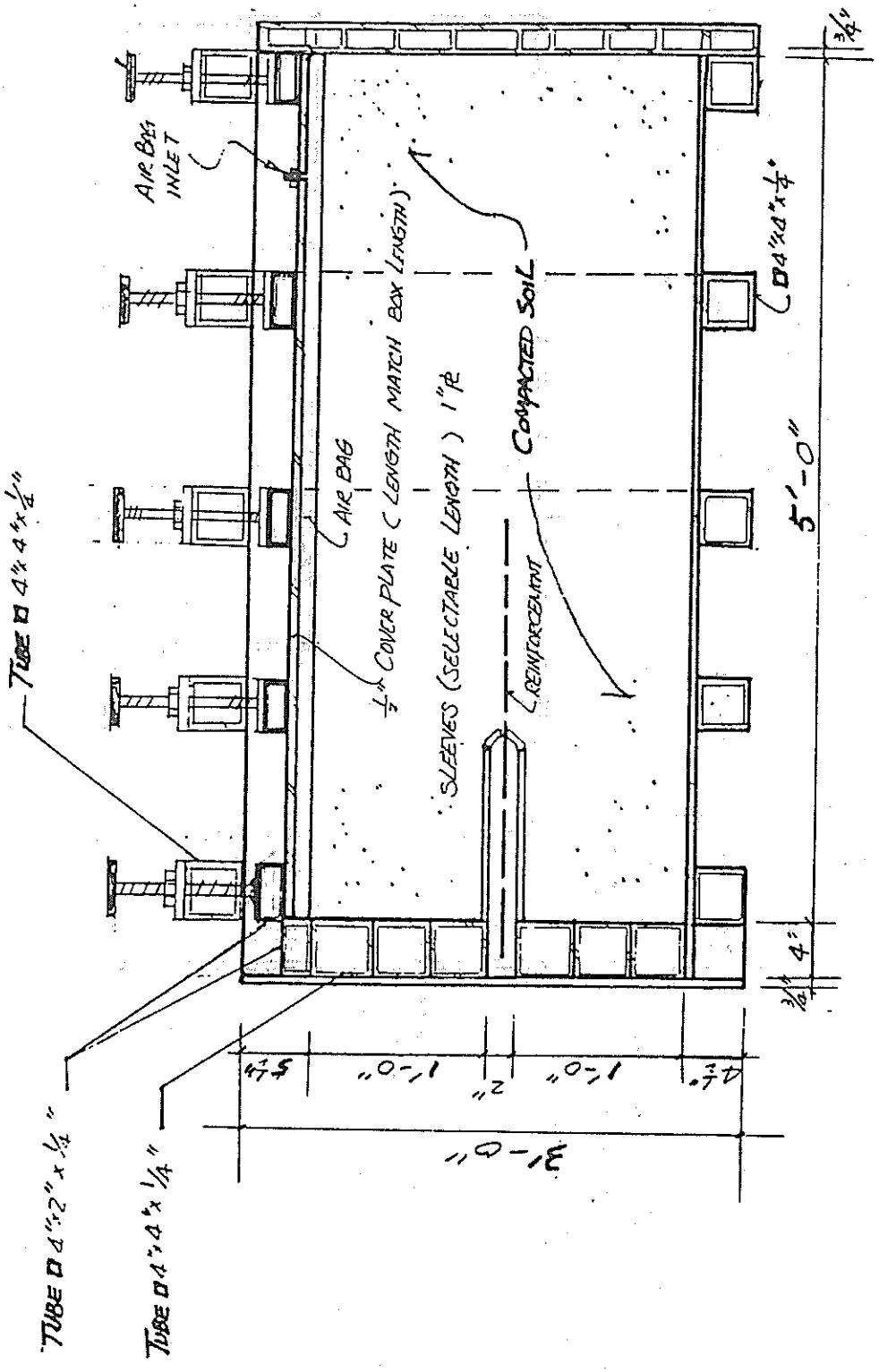

Figure A-3 Cross-section A-A of the pull-out box

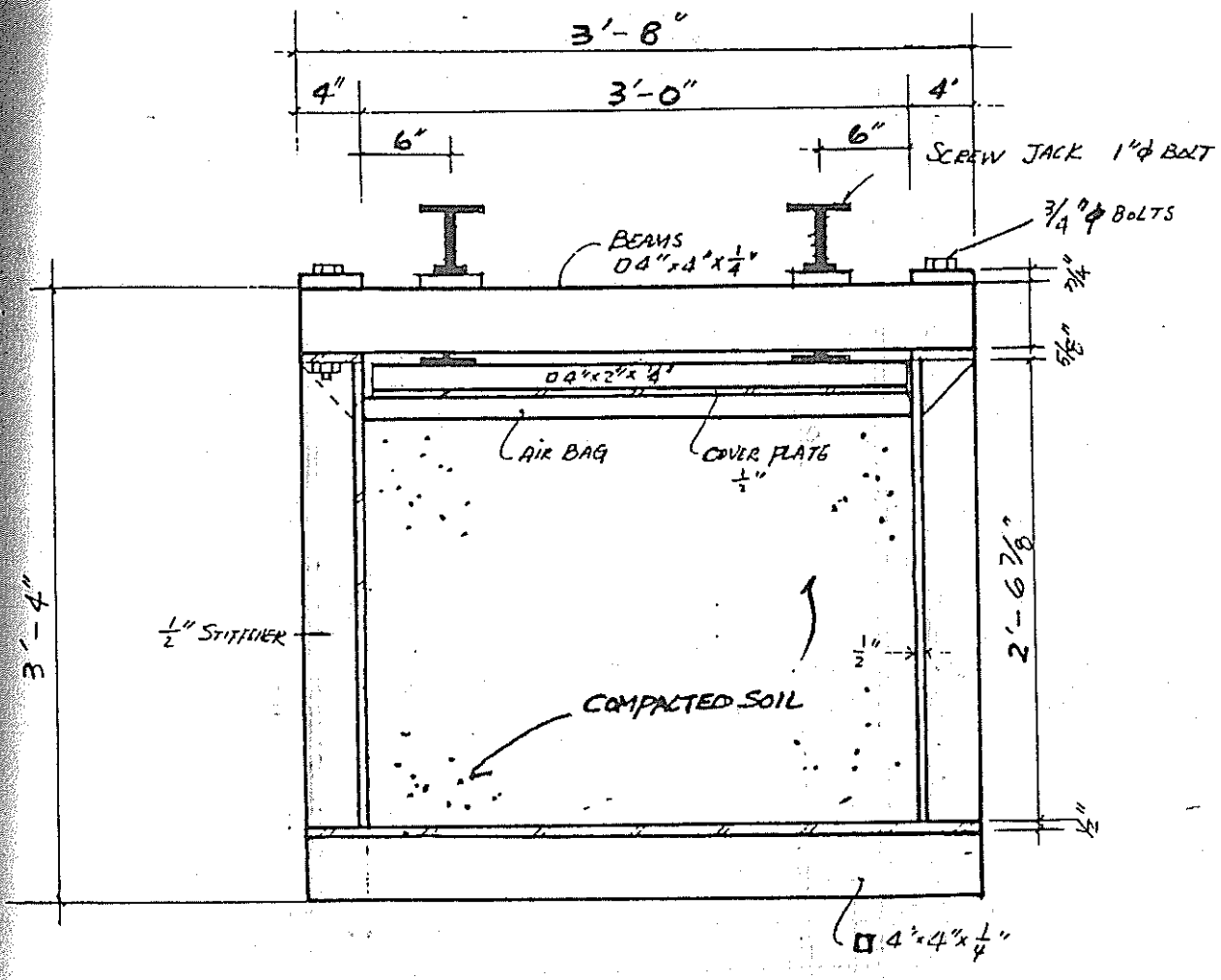

Figure A-4 Cross-section B-B of the pull-out box

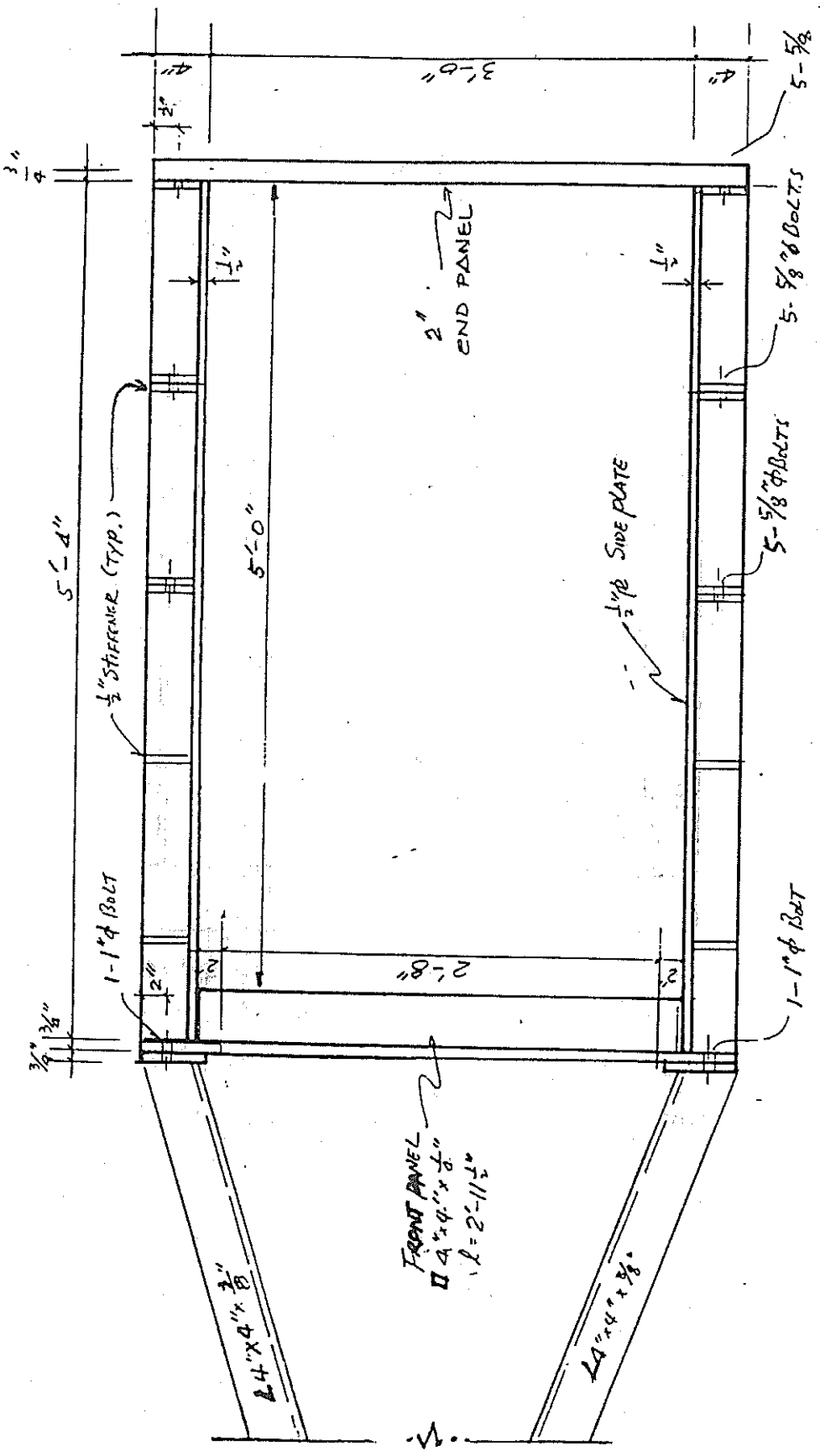

Figure A-5 Cross-section C-C of the pull-out box

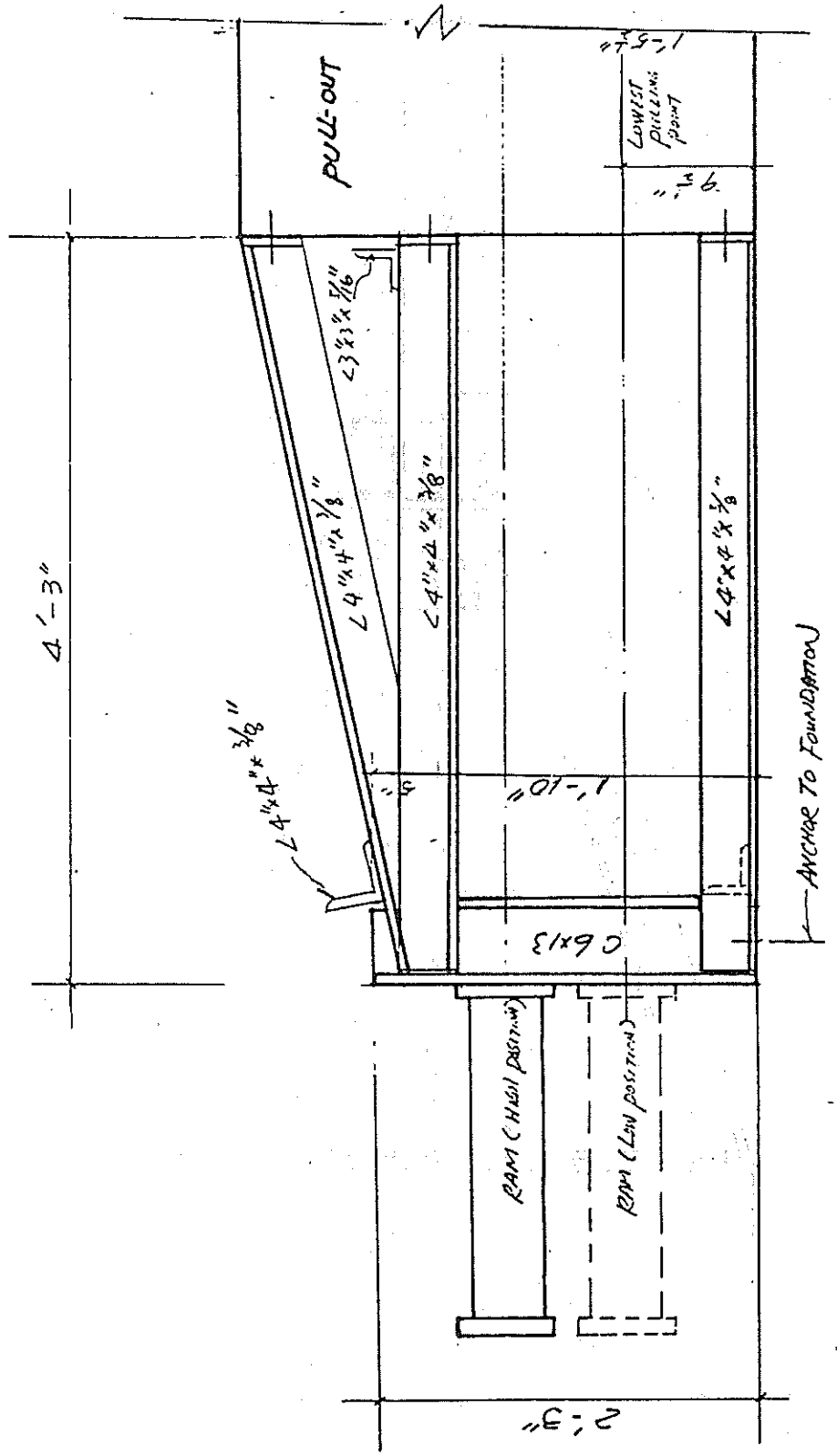

Figure A-6 Longitudinal view of the loading frame

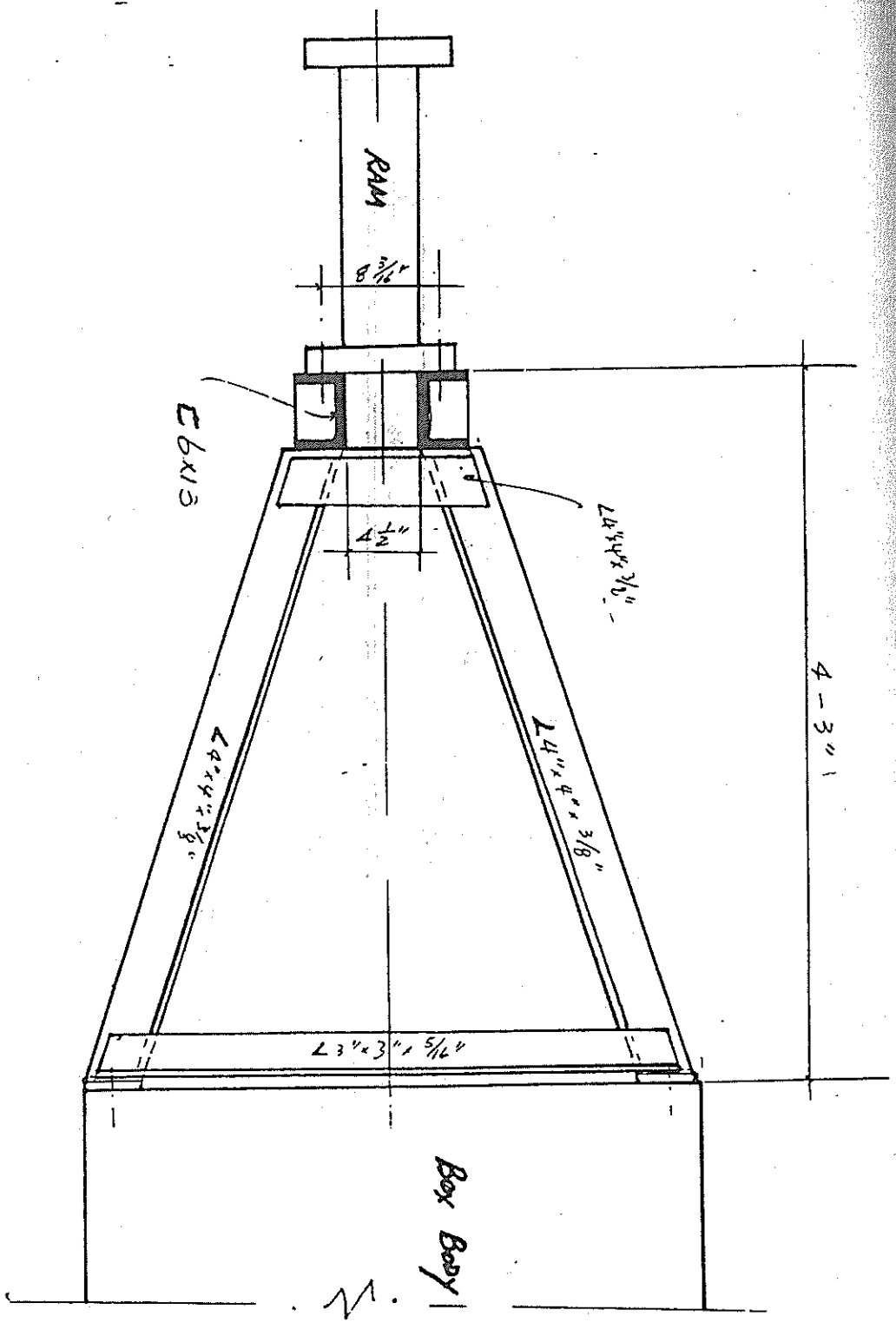

Figure A-7 Top view of the loading frame

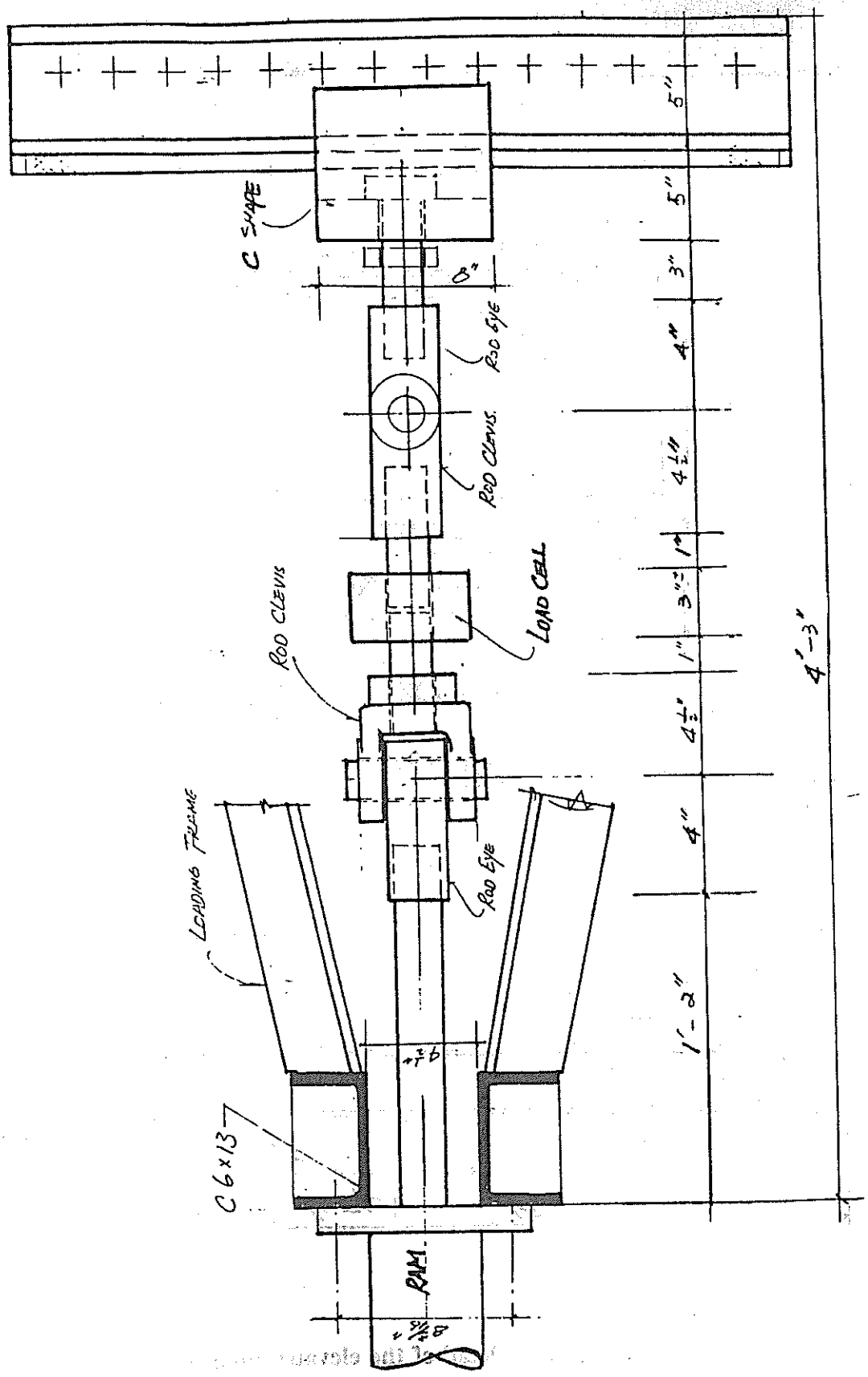

Figure A-8 Detail of the loading system

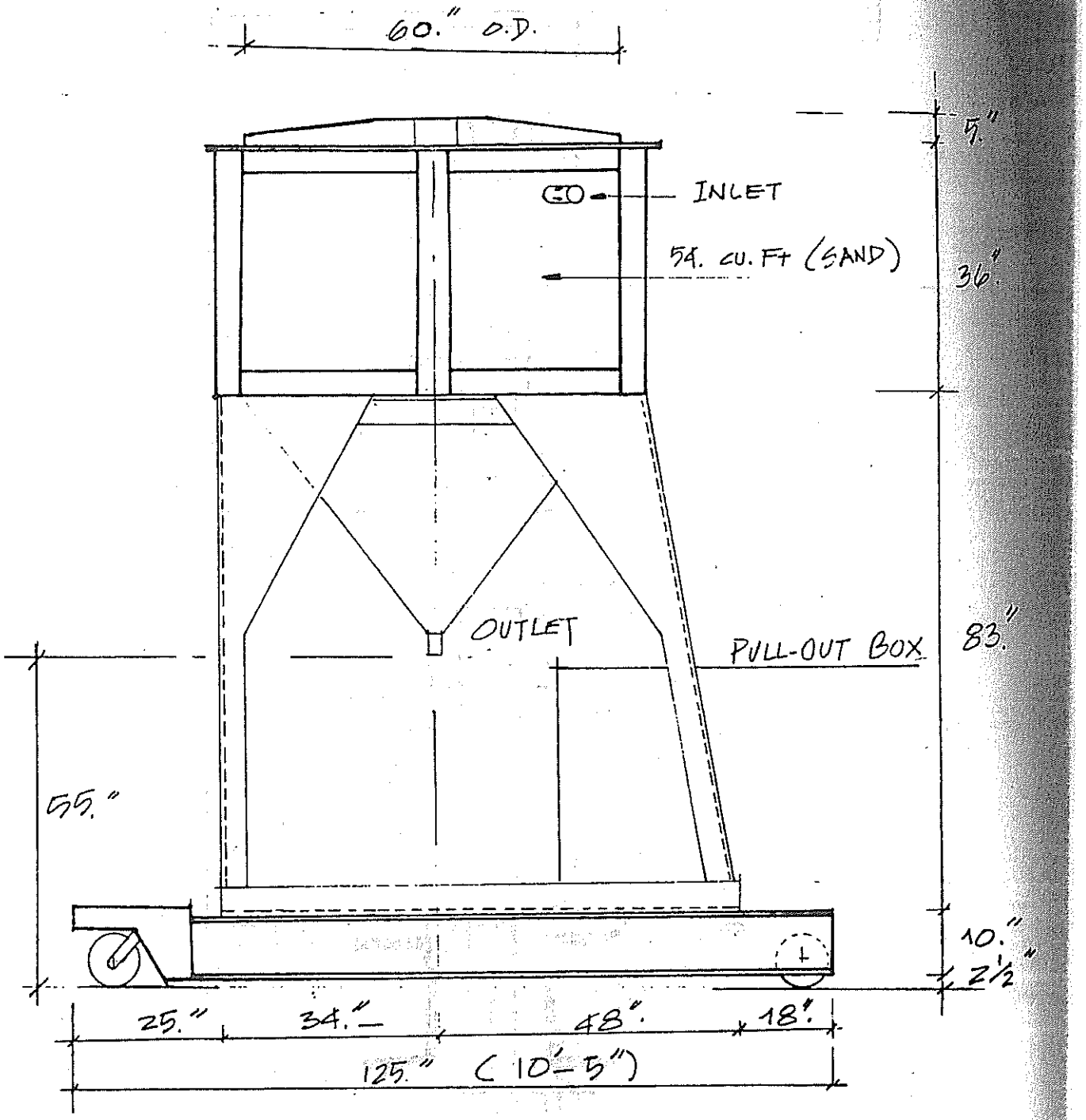

Figure A-9 Detail of the elevated hopper

APPENDIX B

INSTRUMENTS SPECIFICATIONS

LIST OF FIGURES OF APPENDIX B

Figure		Page
B-1	Schematic diagram of the hydraulic pump	166
B-2	Electrical scheme of the computer-pump interface	167
B-3	Specifications of the LVDT	168
B-4	Specifications of the load cell	169
B-5	Specifications of the pressure cells	170
B-6	Calibration charts of the pressure cells	171
B-7	Schematic diagram of the data acquisition interface	172
B-8	View of computer data moitoring during pull-out test	173

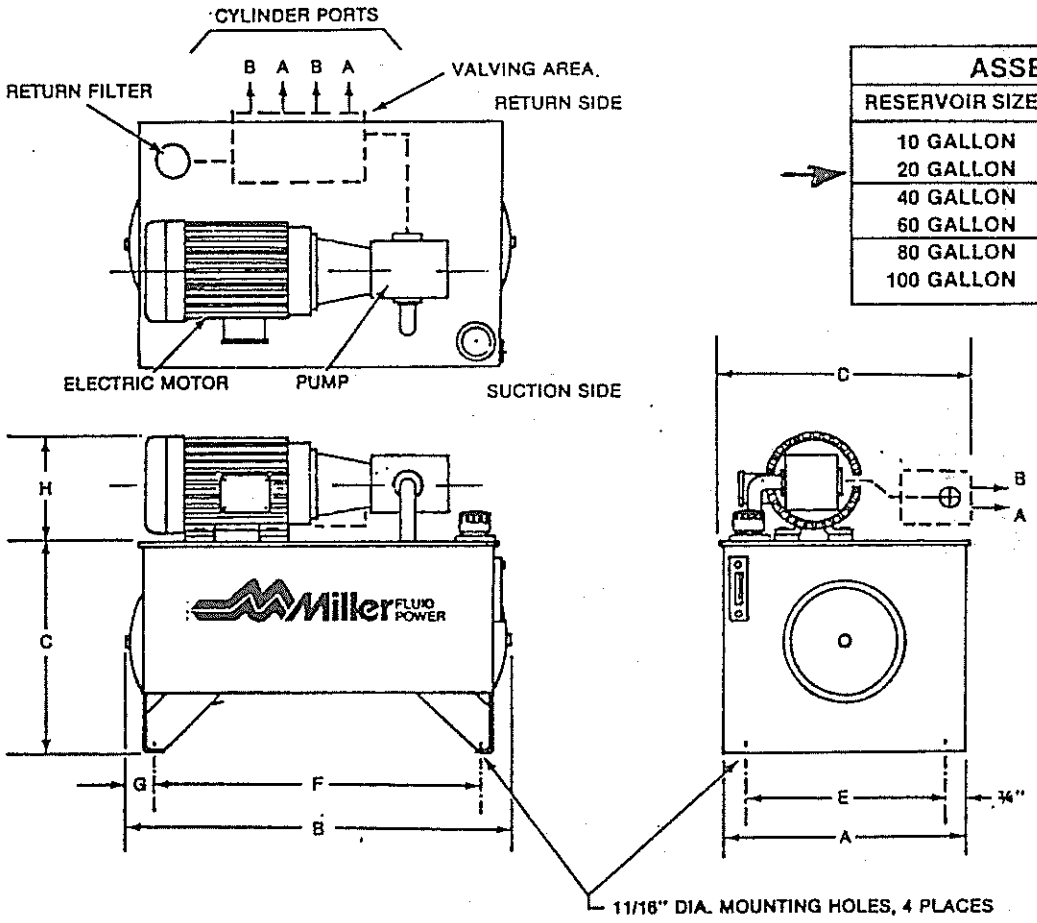

ASSEMBLY DIMENSIONS (INCHES)							
RESERVOIR SIZE	A	B	C	D	E	F	G
10 GALLON	16	26¼	18	23	14½	20¼	3
20 GALLON	21	34¼	18	28	19½	28¼	3
40 GALLON	24	38¼	21	31	22½	32¼	3
60 GALLON	25	40¾	25	32	23½	34¼	3¼
80 GALLON	30	49¾	27	35	28½	43¼	3¼
100 GALLON	30	49¾	29	35	28½	43¼	3¼

MOTOR DIMENSION (INCHES)	
FRAME SIZE	H
143TC/145TC	8½
182TC/184TC	11
213TC/215TC	14
254TC/256TC	15
284TC/286TC	17½
324TC/326TC	18½

DIMENSIONS MAY VARY DEPENDING ON INDIVIDUAL CIRCUIT DESIGN AND LAYOUT.

Figure B-1 Schematic Diagram of the Hydraulic Pump

COMPUTER INTERFACE GEOTECHNICAL DUAL TEST SYSTEM

1. A 0 to +5 VDC Command to OP–AMP 1 will vary the pressure at the Remote Proportional Pressure Control (Item #11) from 500 PSI (0 volts) to 3000 PSI (+5 volts) when the pump is set to deliver 2.5 GPM and from 500 to 2000 PSI when delivering 3.75 GPM.
2. A 0 to – 5 VDC Command to OP–AMP 2 will RETRACT the cylinder and a 0 to +5 VDC Command will EXTEND the cylinder. Speed will be proportional to the command voltage.

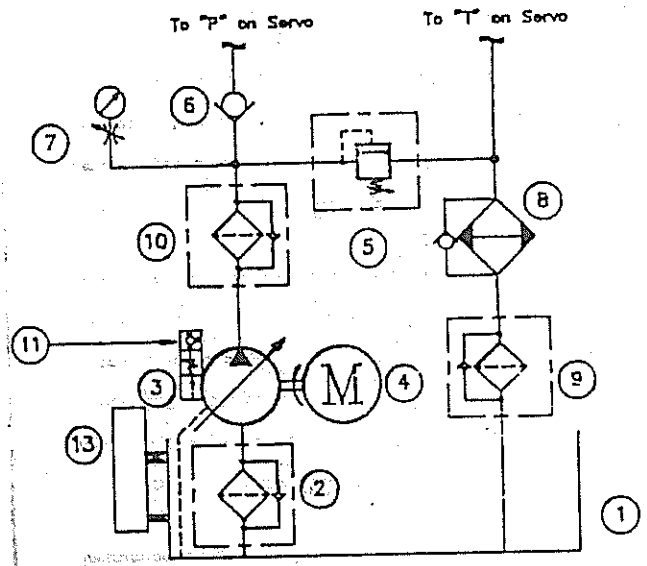

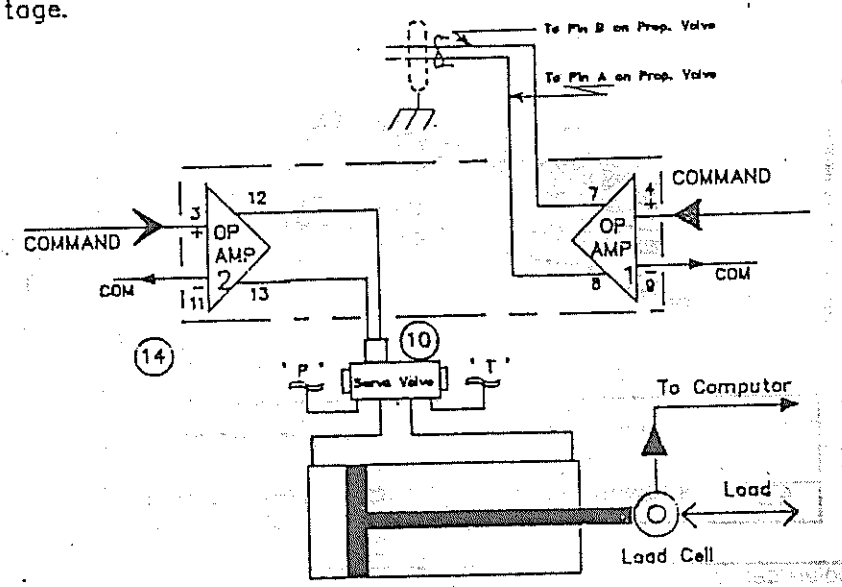

Figure B-2 Electical Scheme of the Computer-Pump Interface

Figure B-3 Specifications of the LVDT

The following information applies to the DC-LVDT with which these instructions are packed:

CALIBRATION TEST DATA

Input for this unit is ±15 VDC

Range: ± 10. " Sensitivity: _____ V/inch

Output Load: .5MEG ohms

Linearity: ± _____ percent of full range

AC Ripple: <25 mv (max.)

CORE DATA

Length: 12.00 inches Diameter: .188 inch

Thread: 1-72 _____ 6-40 _____

4-40 ✓ Special _____

Tested by: ST 52 Date: MY 6 '83

CAUTION

The following cautions should be observed at all times:

Do not machine, grind, or tap any part of an LVDT core.

Do not interchange cores: cores and coils are precisely matched on assembly.

When clamping the LVDT, do not exert more force than is necessary to hold it firmly. Physical stress may affect its operation.

Schaevitz Engineering
U.S. Route 130 & Union Avenue
Pennsauken, NJ 08110
Tel: (609) 662-8000
TLX: (710) 892-0714

DS1012 Printed in U.S.A. 5M12/86PIP

schaevitz

The Name in Transducer Technology

OPERATING INSTRUCTIONS

DC-OPERATED LVDT
Series DC-D, HCD, HPD, HR-DC

MODEL NUMBER 10,000 HCD SERIAL NUMBER 453

Approved by Quality Control ST 52 Date MY 6 '83

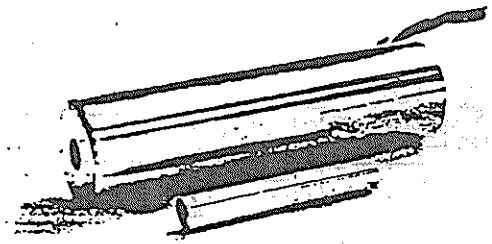

The information contained in this leaflet applies to any Schaevitz DC-operated LVDT (Linear Variable Differential Transformer) of the series listed above; specific data for this model has been incorporated on the last page.

The DC-LVDT maintains all the desired characteristics of the AC LVDT, but with the simplicity of DC operation. It consists of two integral parts: the AC-operated LVDT and a carrier-signal-conditioning module. Use of thick-film hybrid circuitry permits high-density packaging of all necessary electronics, the LVDT, and core in one housing. The unit can operate from a single source such as a battery, while virtually any DC meter can be used for readout.

Before proceeding, check the information on the back page.

STRAIN GAGE LOAD CELL

MODEL 3187 - 20K S/N 751 CALIBRATION DATE 3/19/90

SPECIFICATIONS:

RATED CAPACITY-TENSION & COMPRESSION... 20,000 Lbs.
MAX. LOAD (without zero shift).....50% overload (150% of rated capacity
SIGNAL SENSOR.....4 arm bonded strain gage bridge
BRIDGE RESISTANCE.....350 ohms nominal
MAX. BRIDGE EXCITATION.....20 volts DC or AC RMS
COMPENSATED TEMP. RANGE.....70° F. to 170° F.
USEABLE TEMP. RANGE.....-65° F. to +200° F.
*EFFECT OF TEMP. ON ZERO.....±0.002% of rated capacity/°F.
*EFFECT OF TEMP. ON OUTPUT.....±0.002% of reading/°F.
NONLINEARITY.....±0.___% of rated capacity
OUTPUT.....COMP. -2.998 mV/V at rated cap.
TENS. +3.003 mV/V at rated cap.

*Within compensated temperature range

ELECTRICAL CONNECTIONS:

RECEPTACLE: PT02E-10-6P or MS-3102 A-14S-5P PIG
MATING CONNECTOR: PT06W-10-6S or MS-3106 E-14S-5S TAILS

PINS	FUNCTION	RESISTANCE
RED A (+) and (-) D BLK	Excitation	358.3 ohms
GRN B (+) and (-) C WHT	Signal	350.7 ohms

CALIBRATION:

A precision wire wound resistor, when shunted across one leg of the strain gage bridge, produces an electrical signal equivalent to an applied load. This shunt calibration is valid only when used with high input impedance indicators. The equivalent values below were determined by factory calibration.

LOAD VALUE	ACROSS PINS	RESISTOR VALUE
14,539 Lbs. compression	GRN B and D BLK	40 K ohms
14,526 Lbs. tension	GRN B and A RED	40 K ohms

Figure B-4 Specifications of the Load Cell

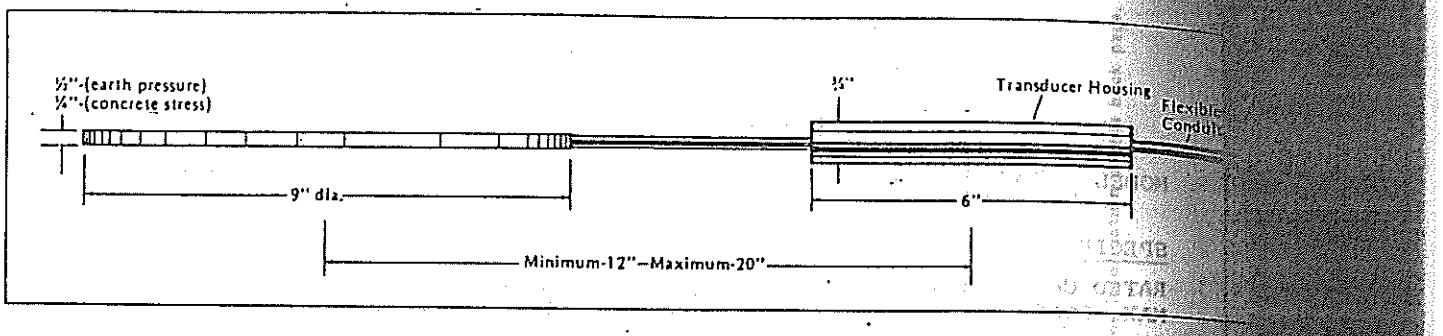

Geokon offers the following four basic types of transducers:

Pneumatic (Models 2510 and 2520). This transducer is a Petur Model P-100 and is connected to the readout location via twin pneumatic tubes (Model T-102). It is read out using the Petur Model C-102 Readout Box.

Semiconductor Strain Gage – Conventional style pressure transducer compatible with many existing dataloggers where 5 volt DC or AC excitation is provided. The signal output is large enough to be scanned directly without further amplification. They may also be read remotely using the Geokon Model RB-101 Readout Box.

Resistance Strain Gage – These transducers are compatible other resistance strain gage systems such as load cells, bore deformation gages etc. They may be read out using conven al strain indicator or readout boxes (Vishay P350A, Vishay P etc.).

Vibrating Wire (Model 4500H). This transducer is compati with the rest of the Geokon line of vibrating wire instrum and is recommended for use with the Model GK-4 Datalo or GK-401 Readout Box. It incorporates all of the advanta es of the vibrating wire system of measurements.

SPECIFICATIONS

Model Number		EP Cell 2510 / CS Cell 2520	3500 / 3600	3650 / 3660	4800E / 4800C
Transducer type	–	Pneumatic	Semiconductor strain gage	Resistance strain gage	Vibrating wire
Typical ranges available	psi	15 to 3000*	25,100,500 1000,3000,5000	25,100,500 1000,3000,5000	50,100,500 1000,3000,5000
Over-range capacity	% F.S.	3000 psi max.	200	200	150
Accuracy	% F.S.	0.4*	1	0.5	0.25
Resolution	% F.S.	0.4*	infinite	infinite	0.1
Thermal effect on zero	% F.S./°F	zero	<0.05	<0.02	<0.05
Excitation voltage	V	–	max.6v (DC or AC)	max.10v (DC or AC)	5v sq.wave
Signal output	mv/v	–	20	3	1200-2000Hz frequency
Bridge resistance	ohms	–	150in 115out	350	coil 150
Transducer housing dia.	in.	1.5	1.625	2.25	1
Transducer housing length	in.	6	6	6	6
Weight (less cable	lbs.	5 7	5 7	5 7	5 7
Connecting leads	–	Polyethylene twin tubes	4-cond. shielded	4-cond. shielded	2-cond. shielded
Readout box	–	Petur C-102	Geokon RB-101	Vishay P350A	Geokon GK-401

*Depends on pressure gage in readout box.

Figure B-5 Specifications of the Pressure Cells

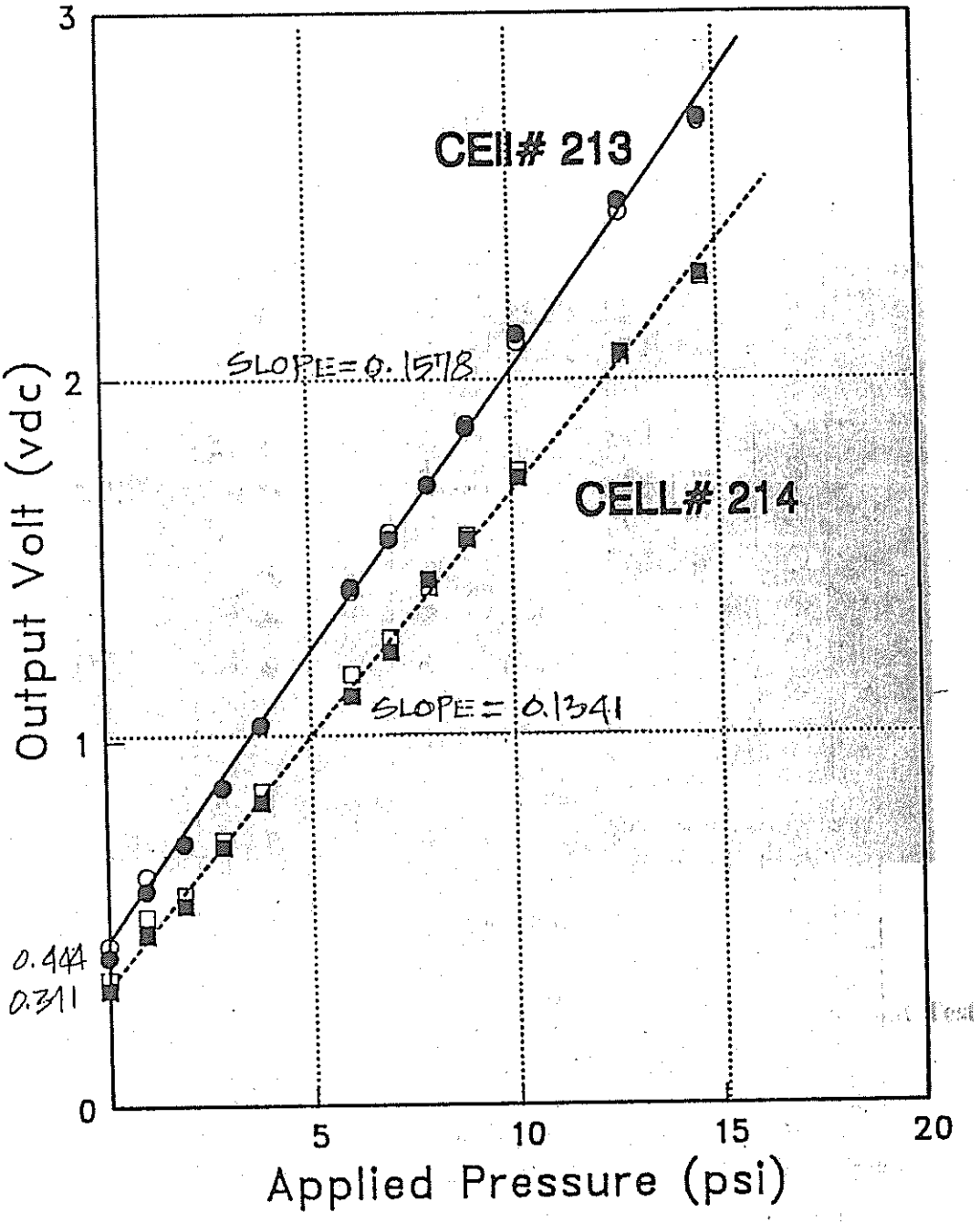

Figure B-6 Calibration Chart for the Pressure Cells

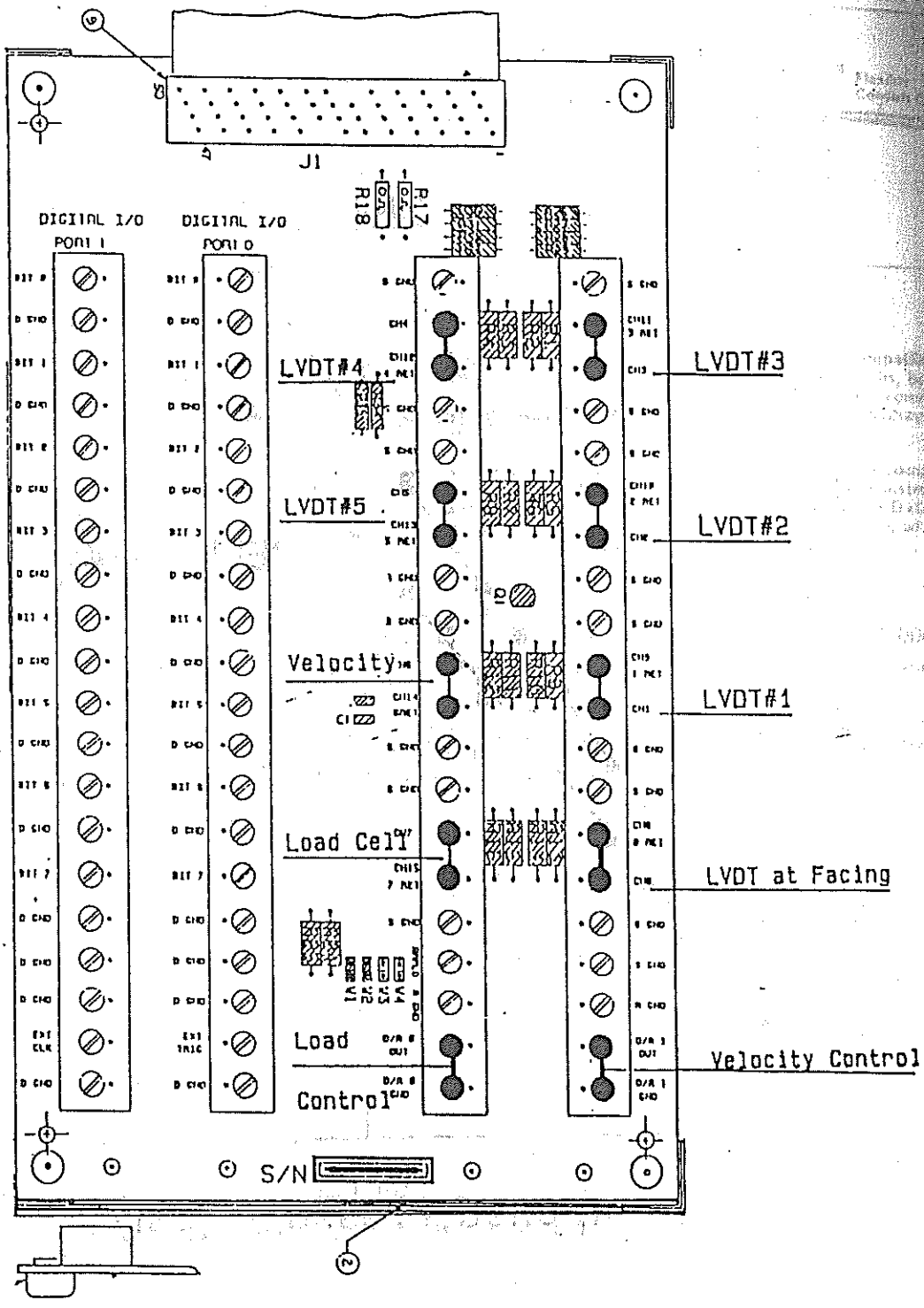

Figure B-7 Schematic Diagram of the Data Acquisition Interface

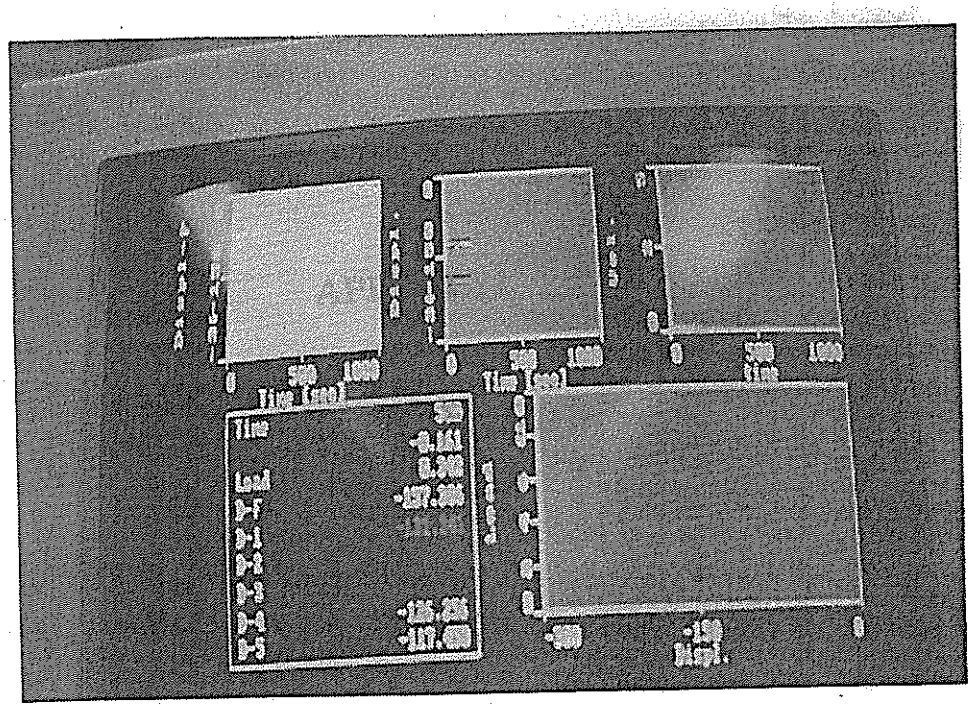

Figure B-8 View of the Computer Data Monitoring During Pull-out Test

APPENDIX C

TEST RESULTS

LIST OF PULL-OUT TESR RESULTS IN APPENDIX C

Test	Page
Test #1	179
Test #2	180
Test #3	181
Test-A3	182
Test-A4	183
Test-A5	184
Test-A6	185
Test-A7	186
Test-A8	187
Test-A9	188
Test-A10	188
Test-C2	189
Test-C3	190
Test-C4	191
Test-B1	192
Test-B2	193
Test-B3	194
Test-B4	195
Test-P1	196
Test-P2	197
Test-P3	198
Test: W0-0	199
Test: W0-5.B	200
Test: W0-5.C	201
Test: W1-0.A	202
Test: W1-0.B	203
Test: W1-5.A	204

Test	Page
Test: W1-5.B	205
Test: W2-0.B	206
Test: W2-0.D	207
Test: W2-5.A	208
Test: W2-5.B	209
Test: L1-5.A	210
Test: S-0.A	211
Test: S-0.B	212
Test: S-4.A	213
Test: S-8.A	214
Test: S-8.B	215
Test: D-101.A	216
Test: D-102.A	217
Test: D-104.A	218
Test: D-108.A	219
Test: D-108.B	220
Test: Sig-10.A	221
Test: Sig-10.B	222
Test: Sig-10.C	223
Test: Load-U1	224
Test: Load-U2	224
Test: Load-1	225

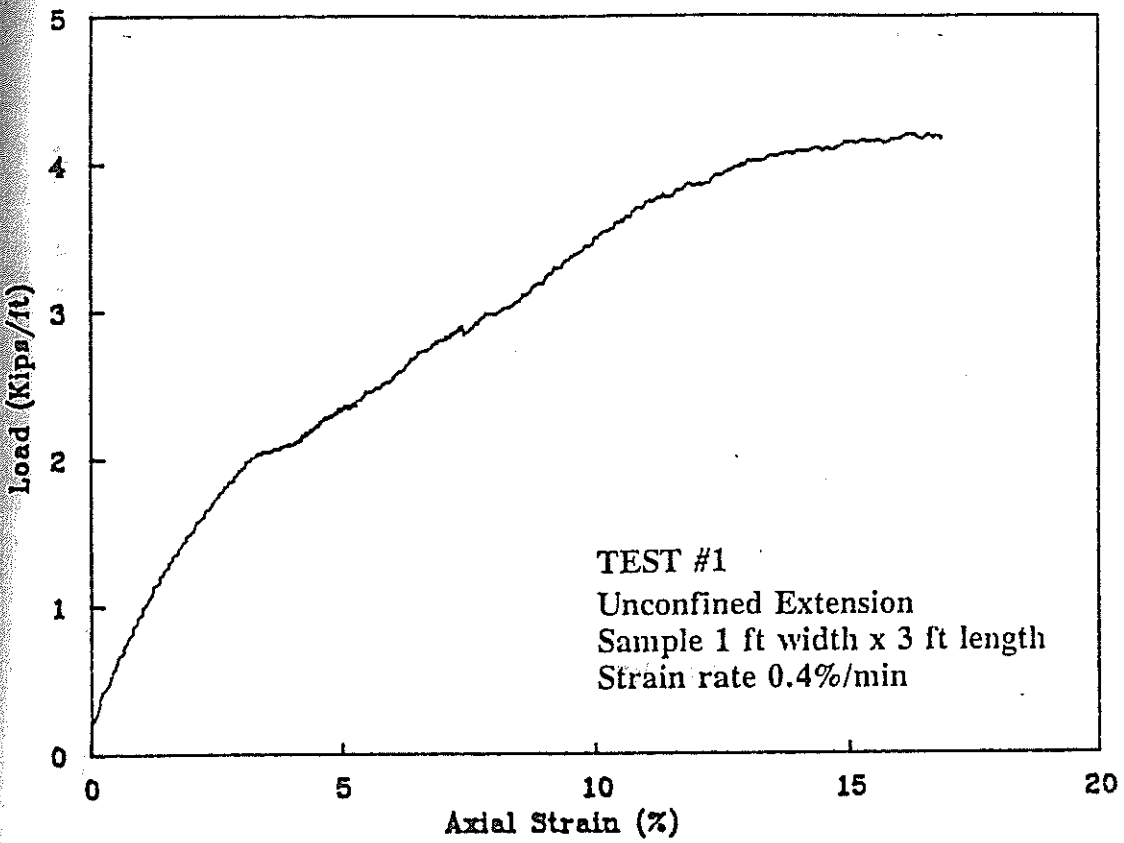
Load (Kips/ft)
0
1
2
3
4
5
0
5
10
15
20
Axial Strain (%)
TEST #1
Unconfined Extension
Sample 1 ft width x 3 ft length
Strain rate 0.4%/min

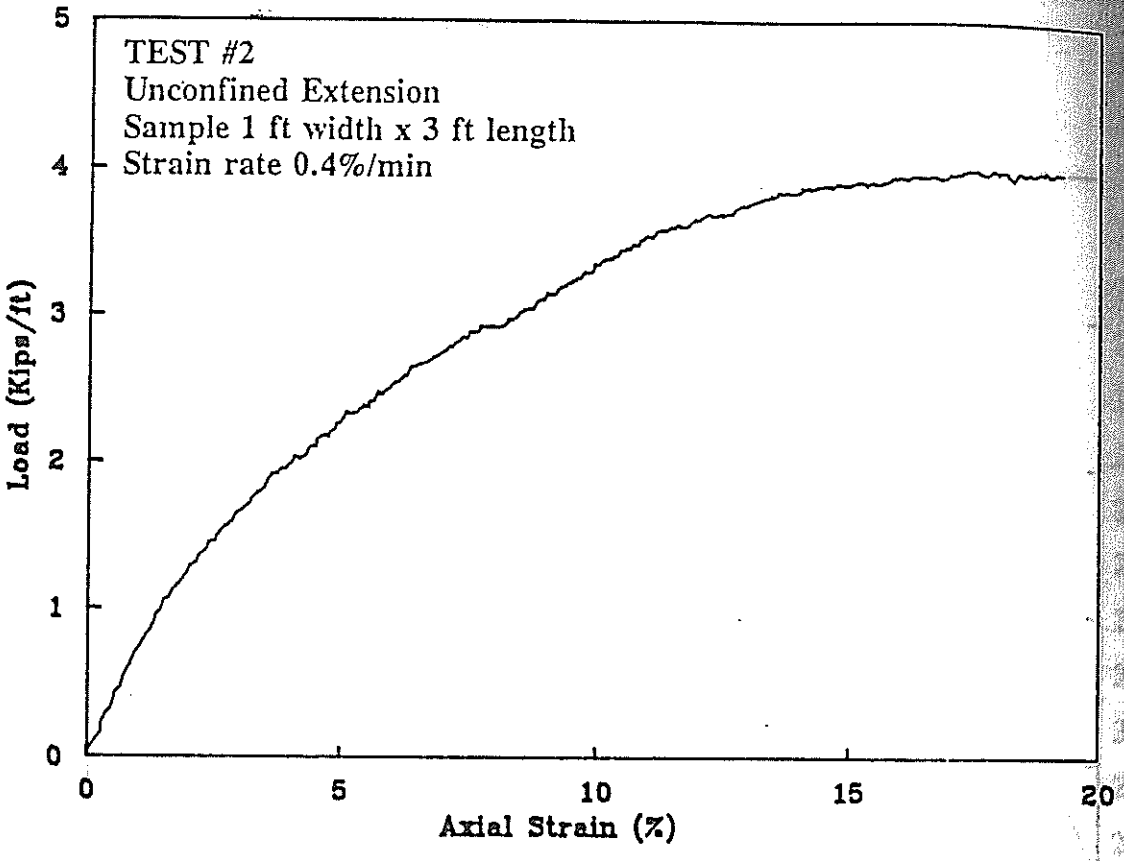
TEST #2
Unconfined Extension
Sample 1 ft width x 3 ft length
Strain rate 0.4%/min
Load (Kips/ft)
0
1
2
3
4
5
0
5
10
15
20
Axial Strain (%)

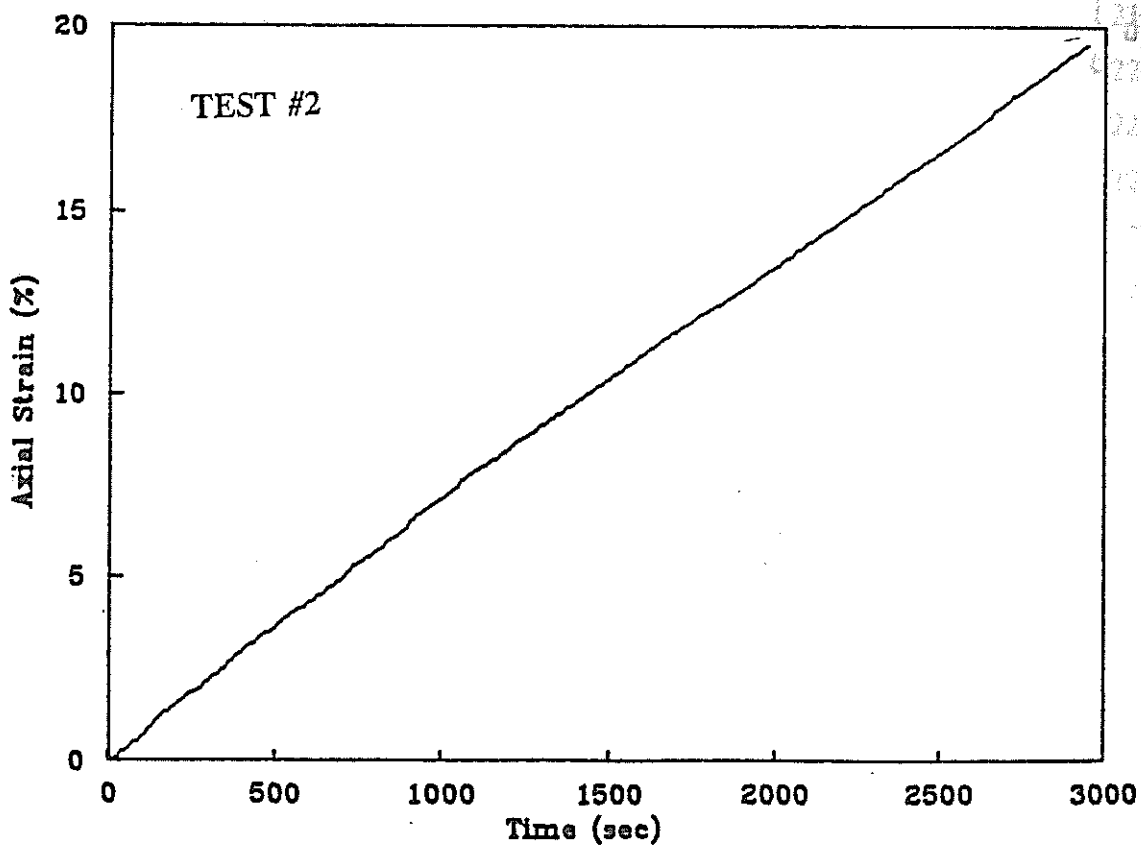
TEST #2
Axial Strain (%)
0
5
10
15
20
0
500
1000
1500
2000
2500
3000
Time (sec)

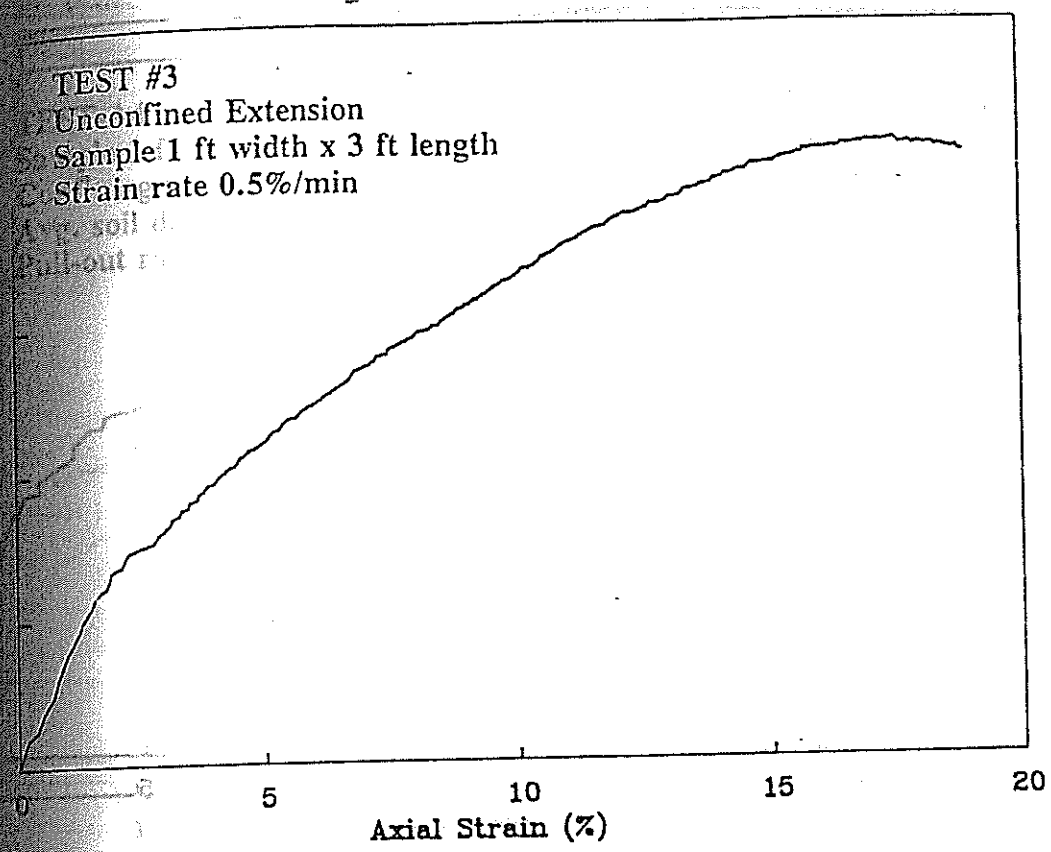
TEST #3
Unconfined Extension
Sample 1 ft width x 3 ft length
Strain rate 0.5%/min
0
5
10
15
20
Axial Strain (%)

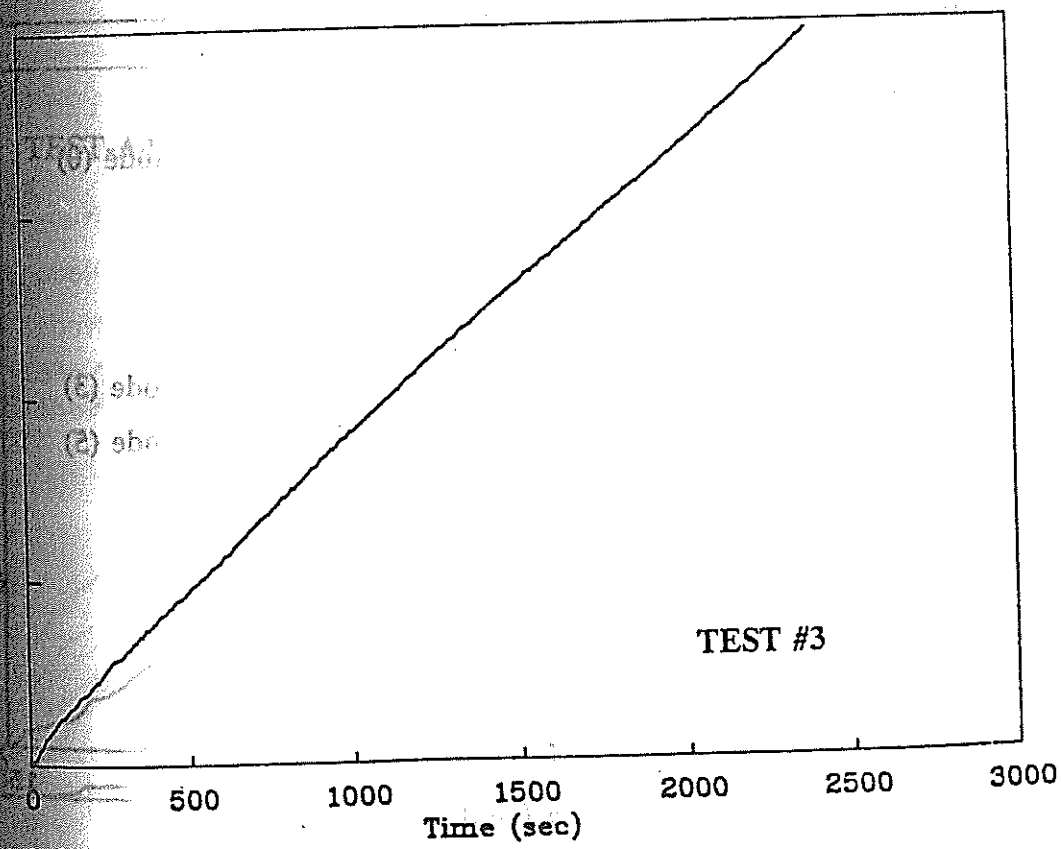
TEST #3
0
500
1000
1500
2000
2500
3000
Time (sec)

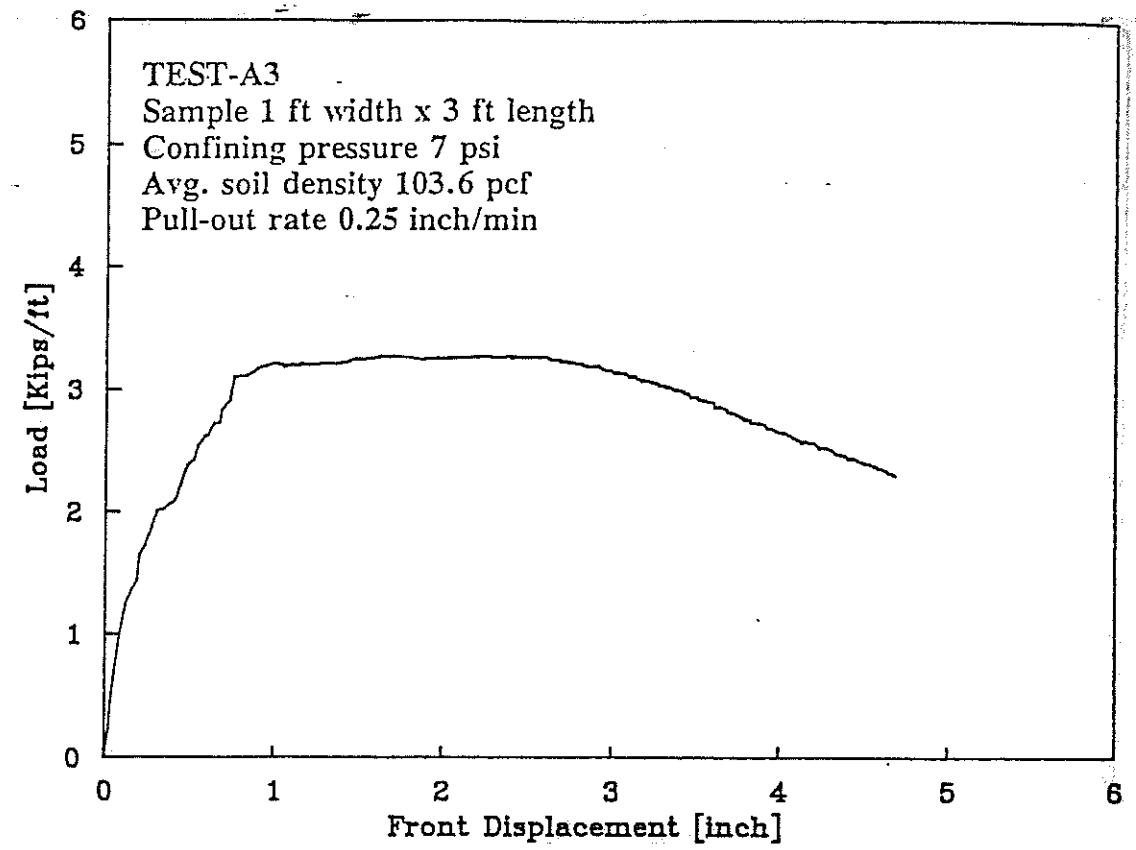
TEST-A3
Sample 1 ft width x 3 ft length
Confining pressure 7 psi
Avg. soil density 103.6 pcf
Pull-out rate 0.25 inch/min
Load [Kips/ft]
Front Displacement [inch]
0
1
2
3
4
5
6

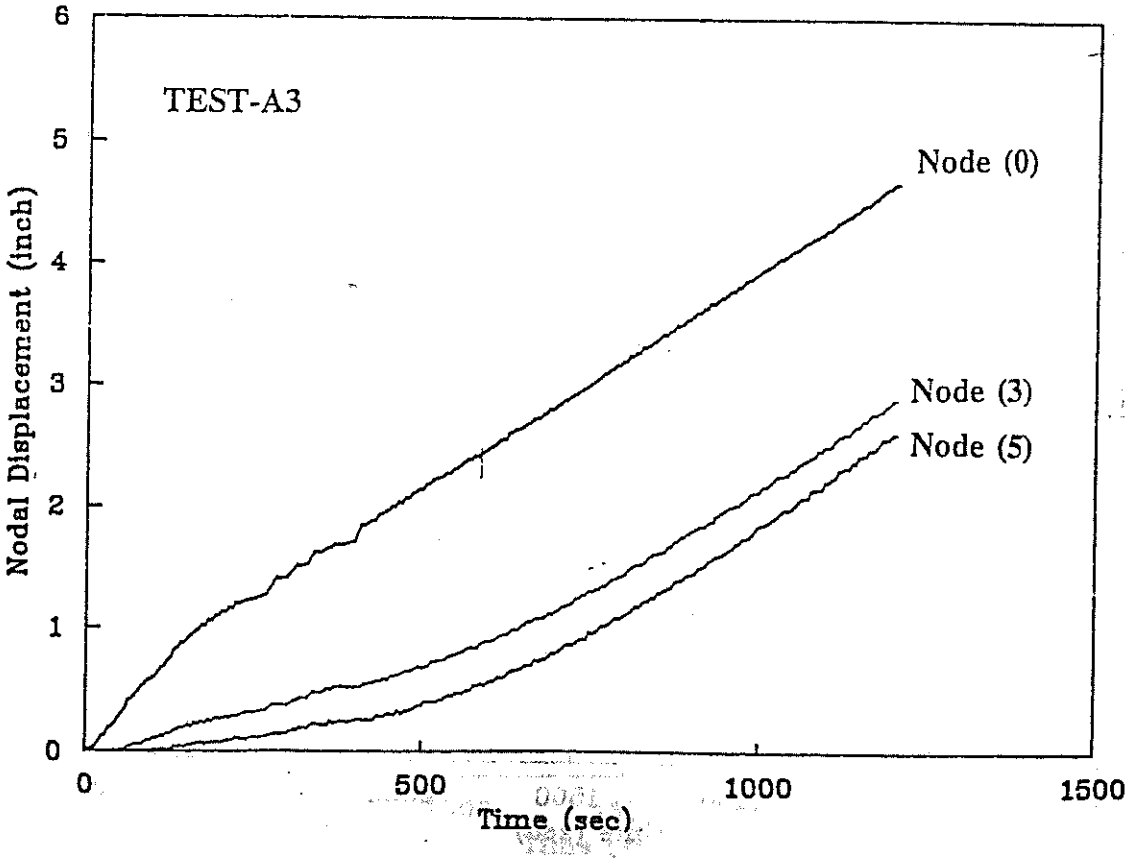
TEST-A3
Node (0)
Node (3)
Node (5)
Nodal Displacement (inch)
Time (sec)
0
500
1000
1500

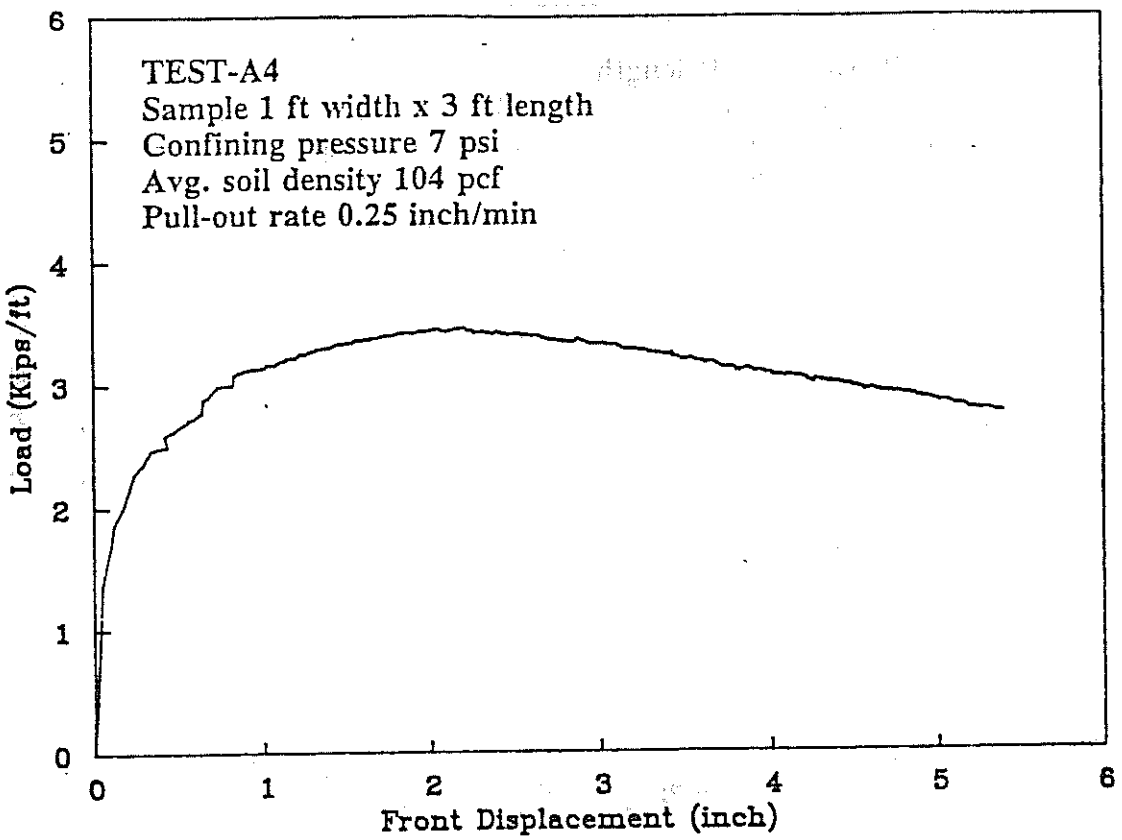
TEST-A4
Sample 1 ft width x 3 ft length
Confining pressure 7 psi
Avg. soil density 104 pcf
Pull-out rate 0.25 inch/min
Load (Kips/ft)
Front Displacement (inch)
0
1
2
3
4
5
6

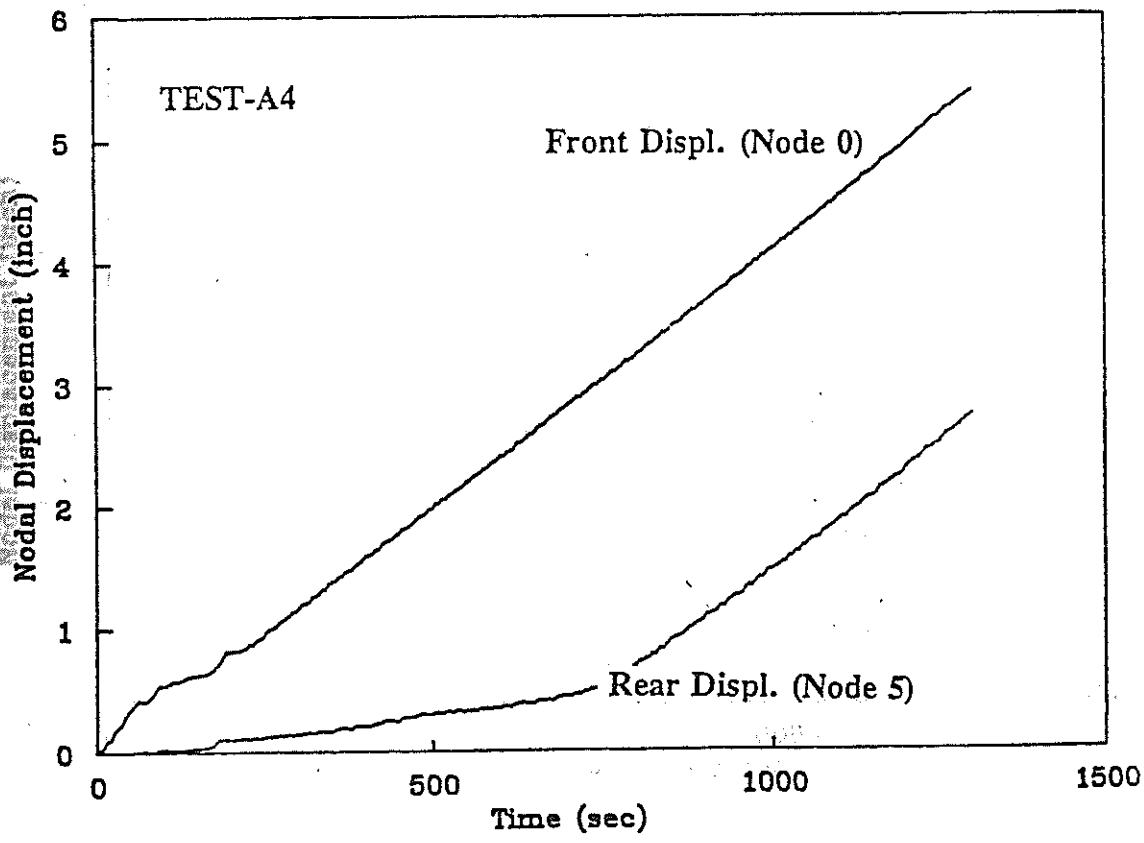
TEST-A4
Front Displ. (Node 0)
Rear Displ. (Node 5)
Nodal Displacement (inch)
Time (sec)
0
500
1000
1500

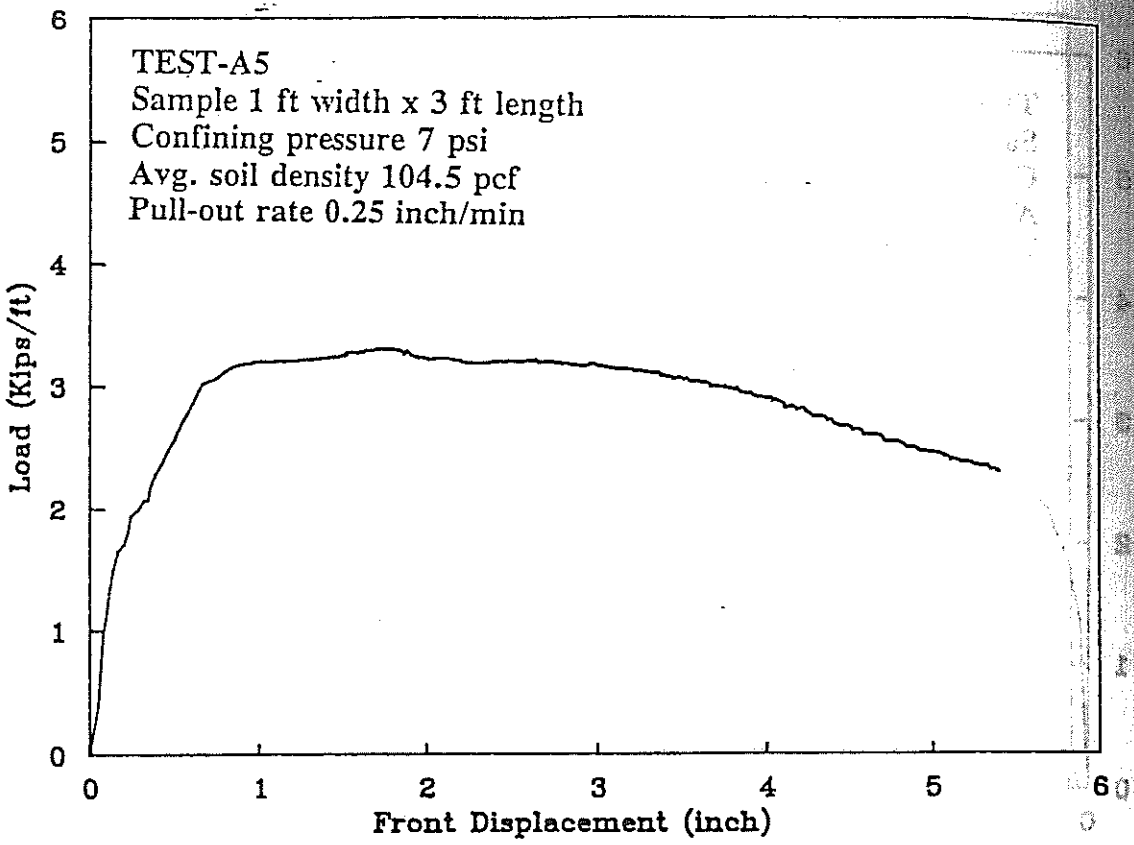
TEST-A5
Sample 1 ft width x 3 ft length
Confining pressure 7 psi
Avg. soil density 104.5 pcf
Pull-out rate 0.25 inch/min
Load (Kips/ft)
Front Displacement (inch)
0
1
2
3
4
5
6

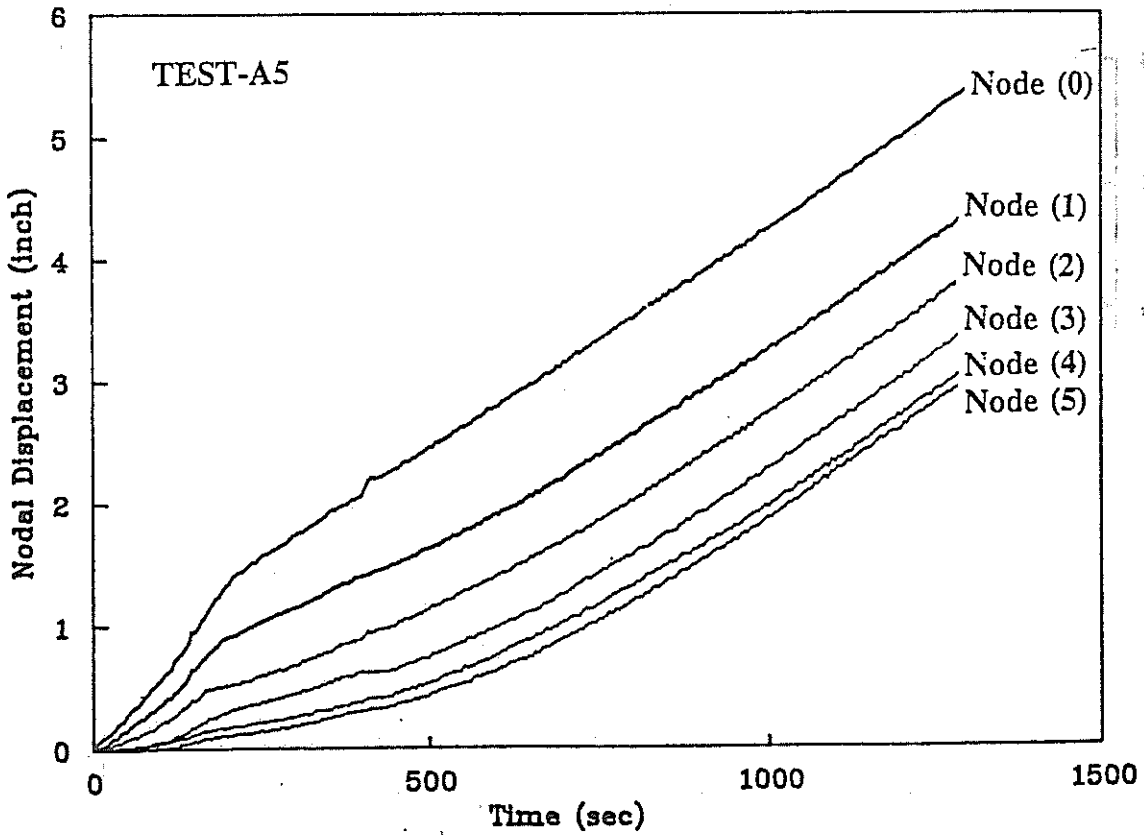
TEST-A5
Node (0)
Node (1)
Node (2)
Node (3)
Node (4)
Node (5)
Nodal Displacement (inch)
Time (sec)
0
500
1000
1500
1
2
3
4
5
6

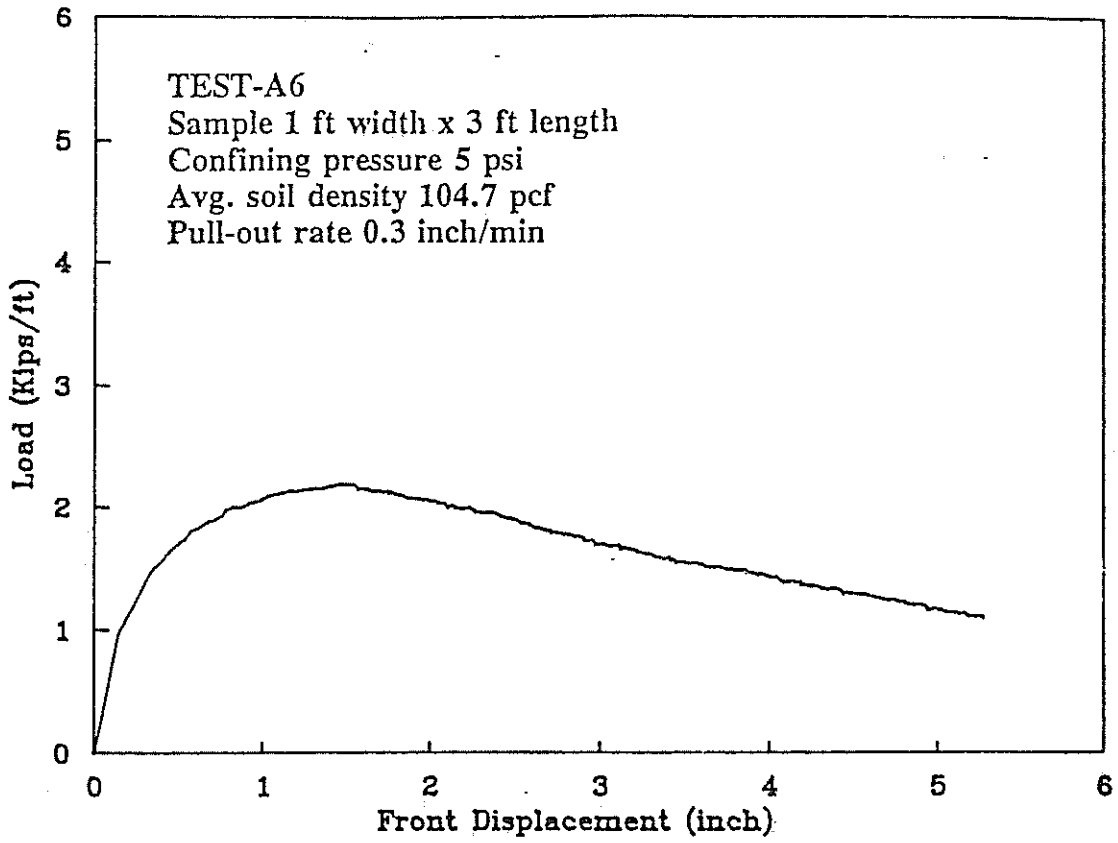
TEST-A6
Sample 1 ft width x 3 ft length
Confining pressure 5 psi
Avg. soil density 104.7 pcf
Pull-out rate 0.3 inch/min
Load (Kips/ft)
Front Displacement (inch)
0
1
2
3
4
5
6

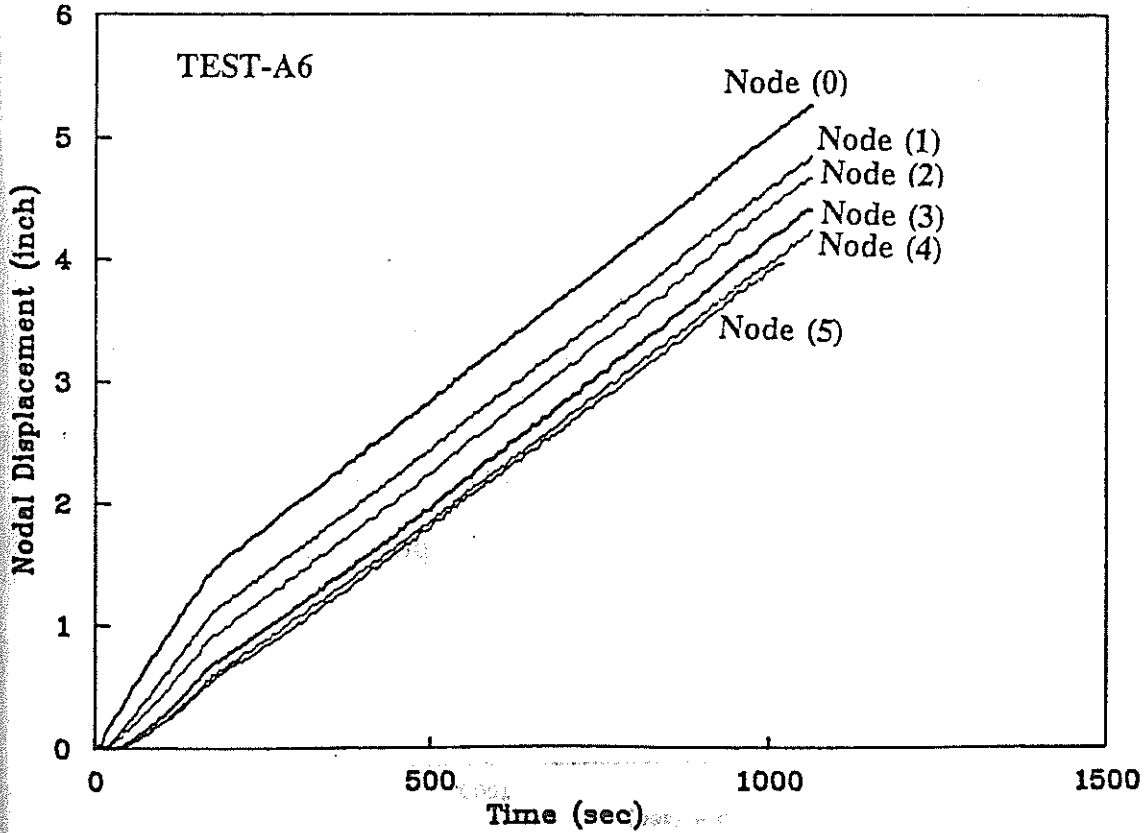
TEST-A6
Node (0)
Node (1)
Node (2)
Node (3)
Node (4)
Node (5)
Nodal Displacement (inch)
Time (sec)
0
500
1000
1500

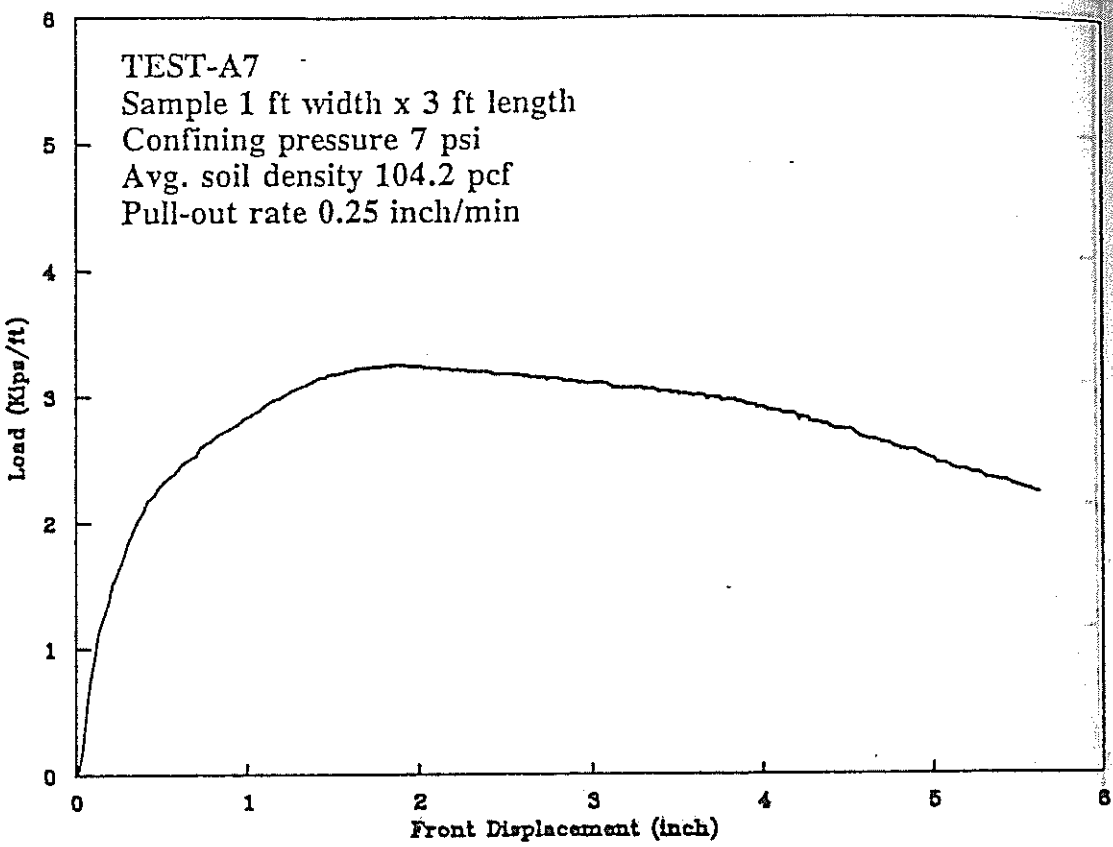
TEST-A7
Sample 1 ft width x 3 ft length
Confining pressure 7 psi
Avg. soil density 104.2 pcf
Pull-out rate 0.25 inch/min
Load (Kips/ft)
Front Displacement (inch)
0
1
2
3
4
5
6

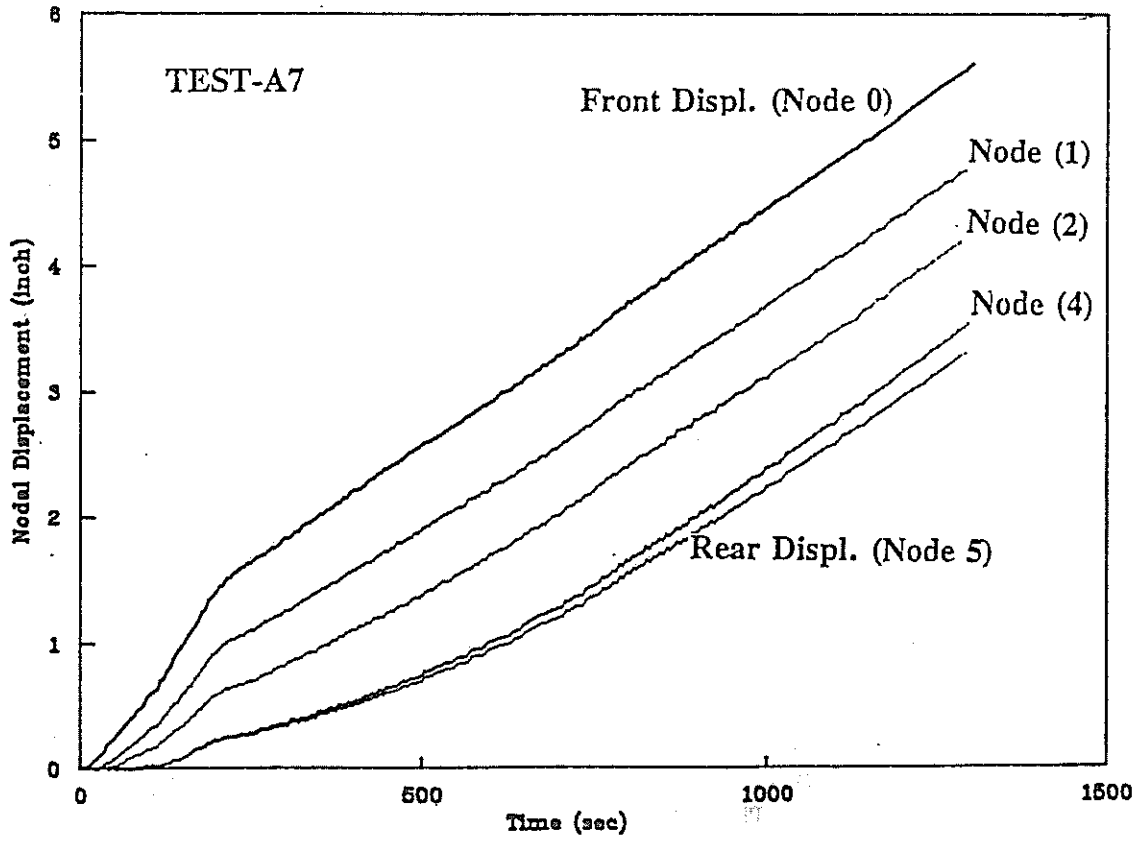
TEST-A7
Front Displ. (Node 0)
Node (1)
Node (2)
Node (4)
Rear Displ. (Node 5)
Nodal Displacement (inch)
Time (sec)
0
500
1000
1500

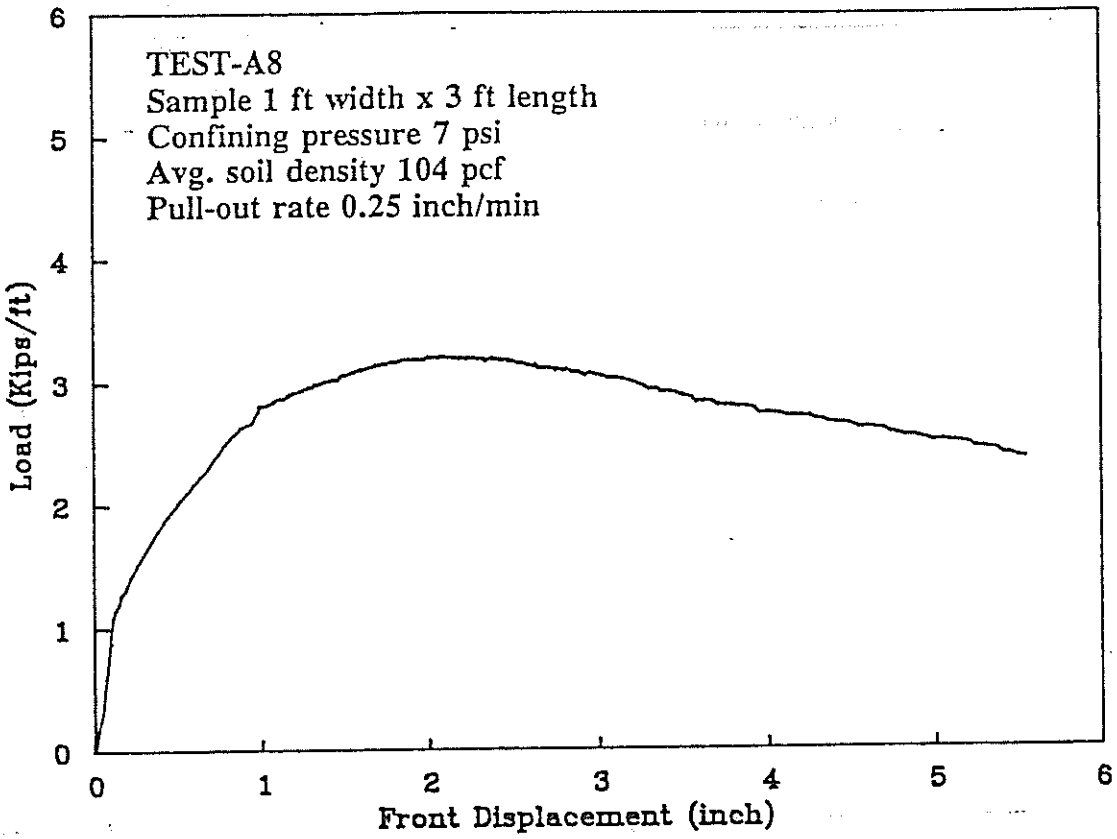
TEST-A8
Sample 1 ft width x 3 ft length
Confining pressure 7 psi
Avg. soil density 104 pcf
Pull-out rate 0.25 inch/min
Load (Kips/ft)
Front Displacement (inch)
0
1
2
3
4
5
6

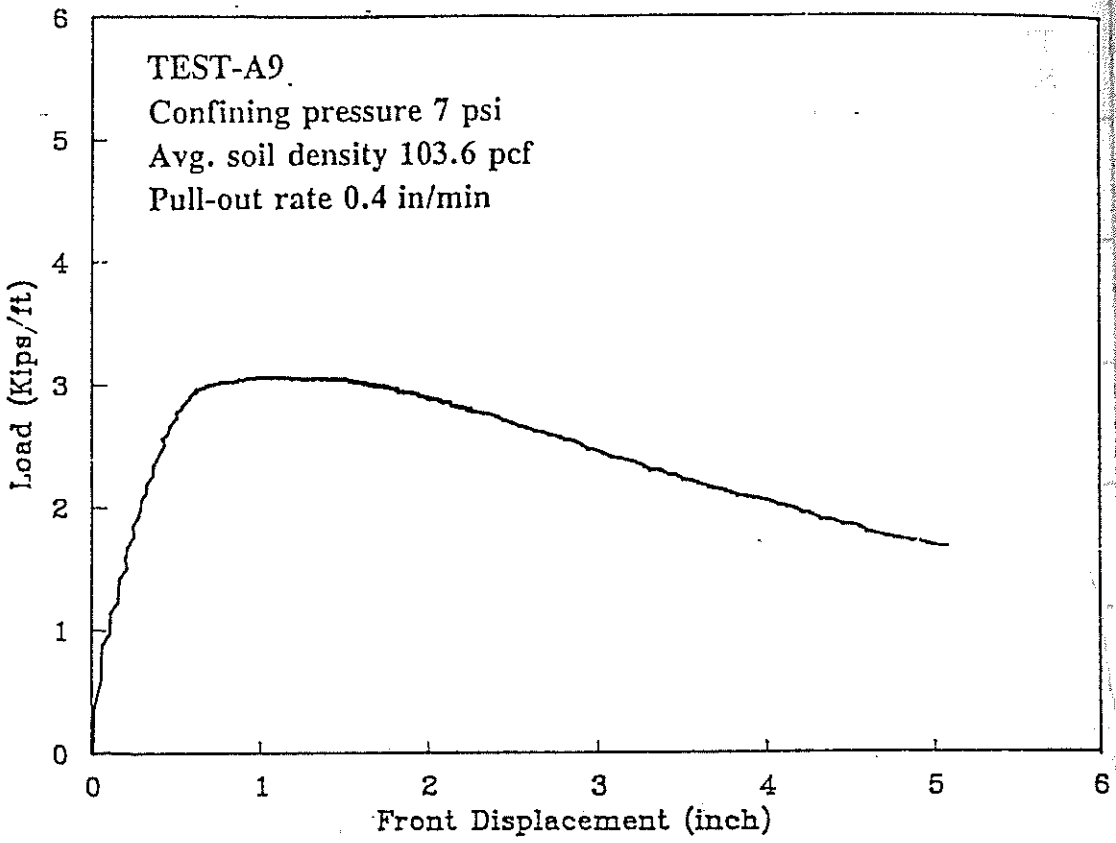
TEST-A9
Confining pressure 7 psi
Avg. soil density 103.6 pcf
Pull-out rate 0.4 in/min
Load (Kips/ft)
Front Displacement (inch)
0
1
2
3
4
5
6

TEST-A10

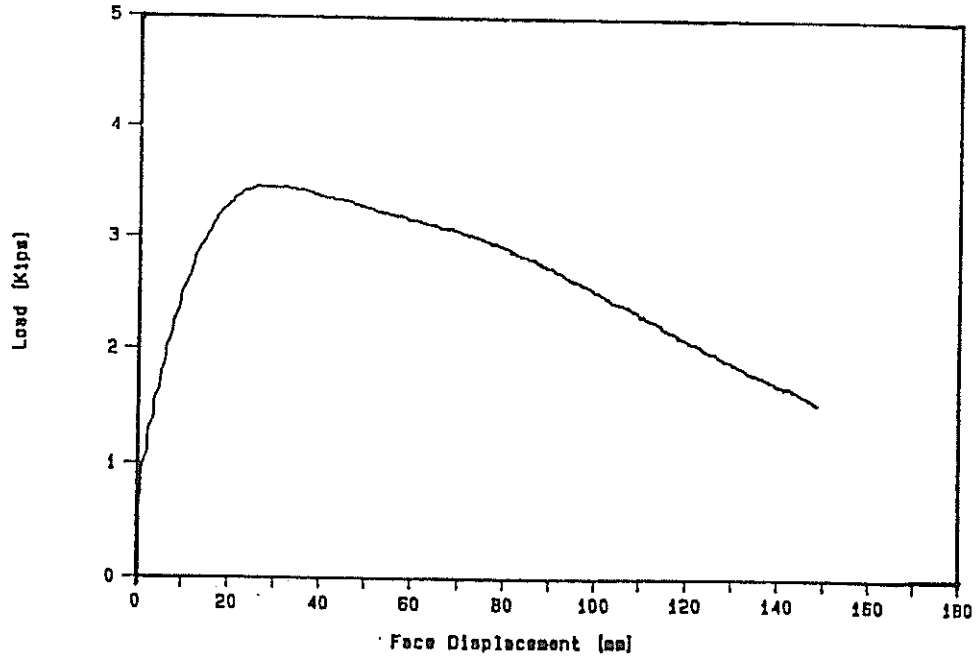
Load [Kips]
Face Displacement [mm]
0
1
2
3
4
5
0
20
40
60
80
100
120
140
160
180

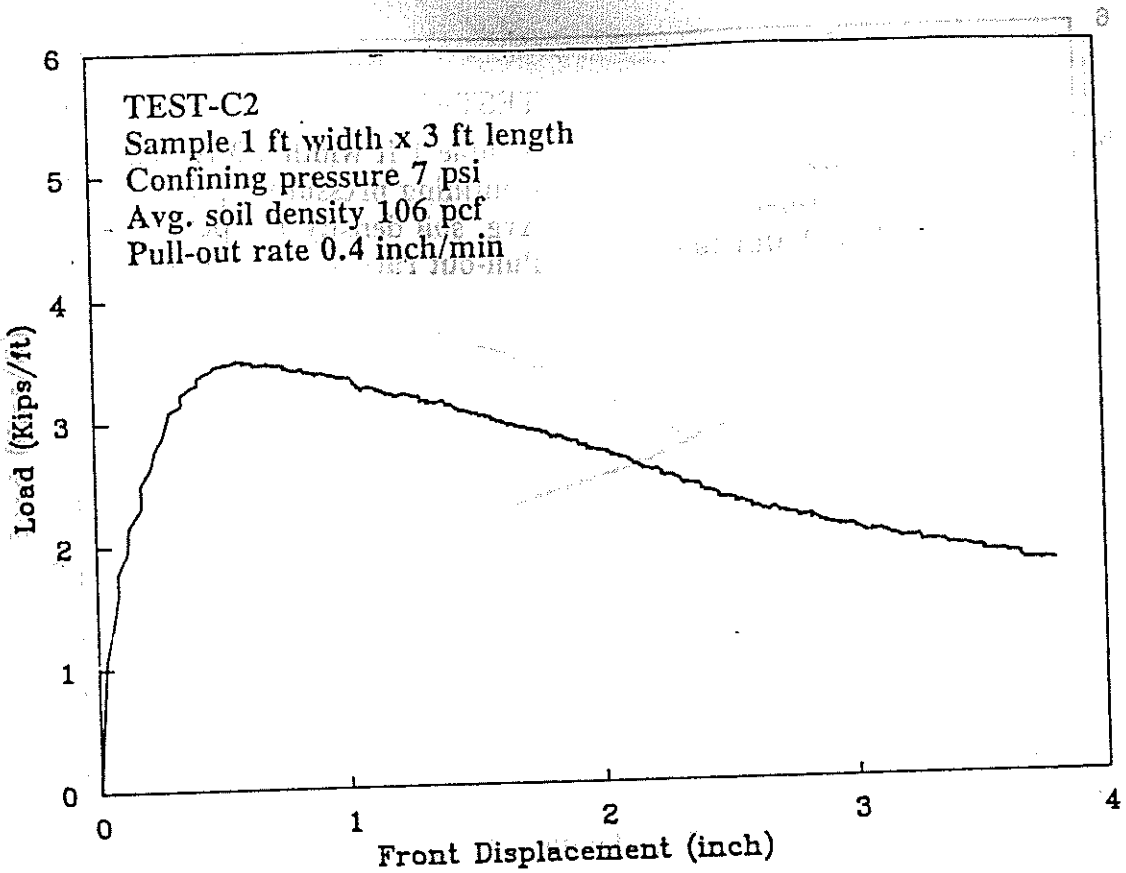
TEST-C2
Sample 1 ft width x 3 ft length
Confining pressure 7 psi
Avg. soil density 106 pcf
Pull-out rate 0.4 inch/min
Load (Kips/ft)
Front Displacement (inch)
0
1
2
3
4
5
6

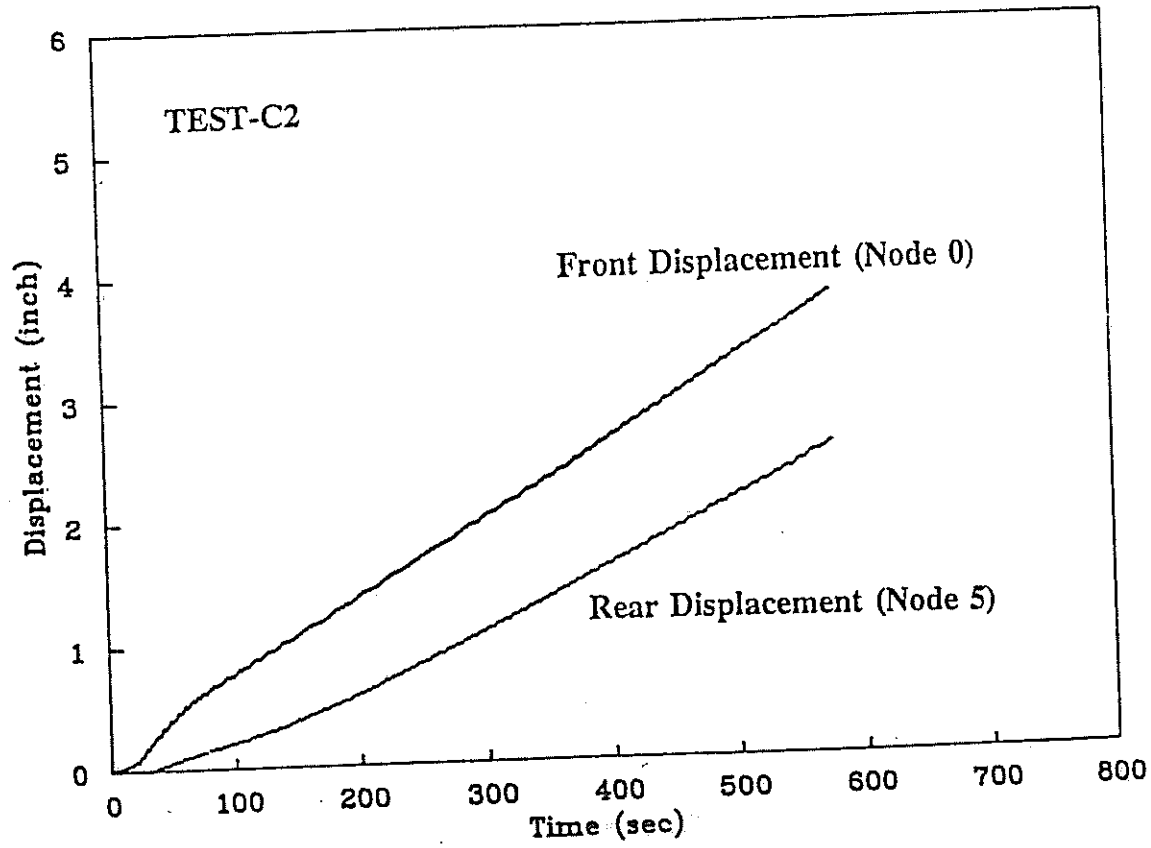
TEST-C2
Front Displacement (Node 0)
Rear Displacement (Node 5)
Displacement (inch)
Time (sec)
0
100
200
300
400
500
600
700
800

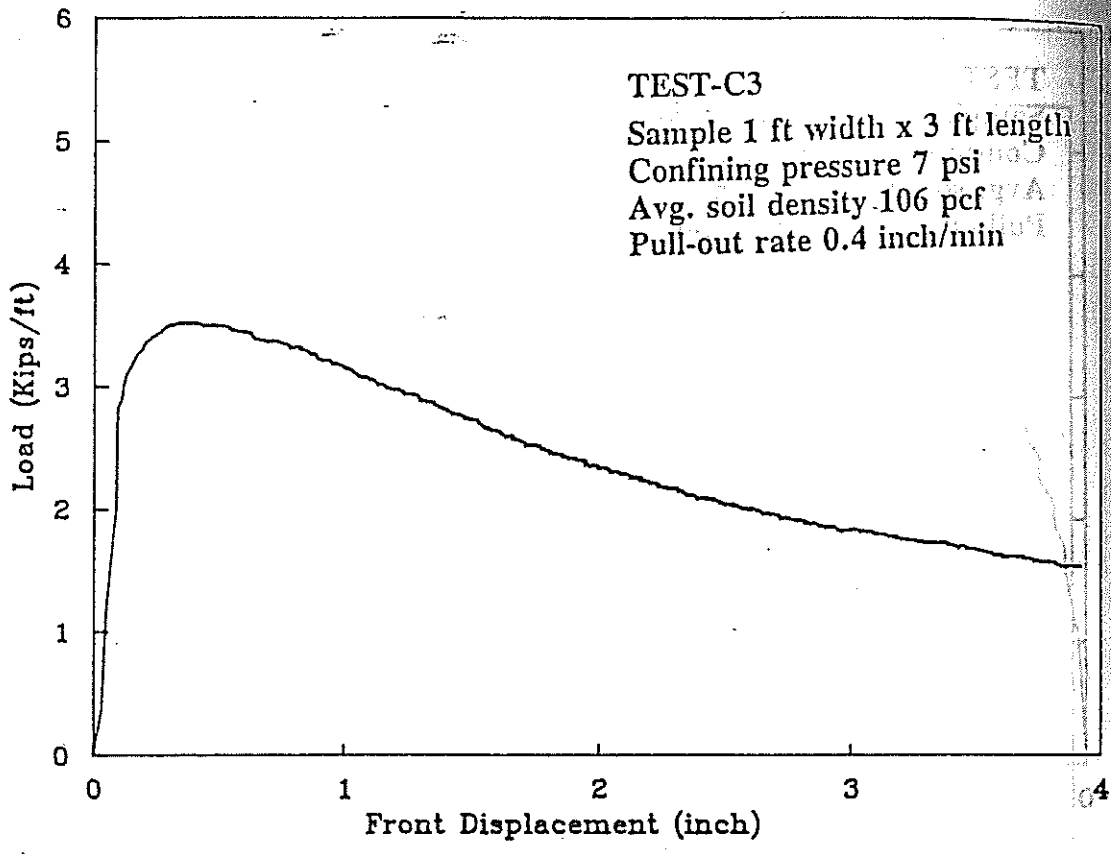
TEST-C3
Sample 1 ft width x 3 ft length
Confining pressure 7 psi
Avg. soil density 106 pcf
Pull-out rate 0.4 inch/min
Load (Kips/ft)
Front Displacement (inch)
0
1
2
3
4
5
6

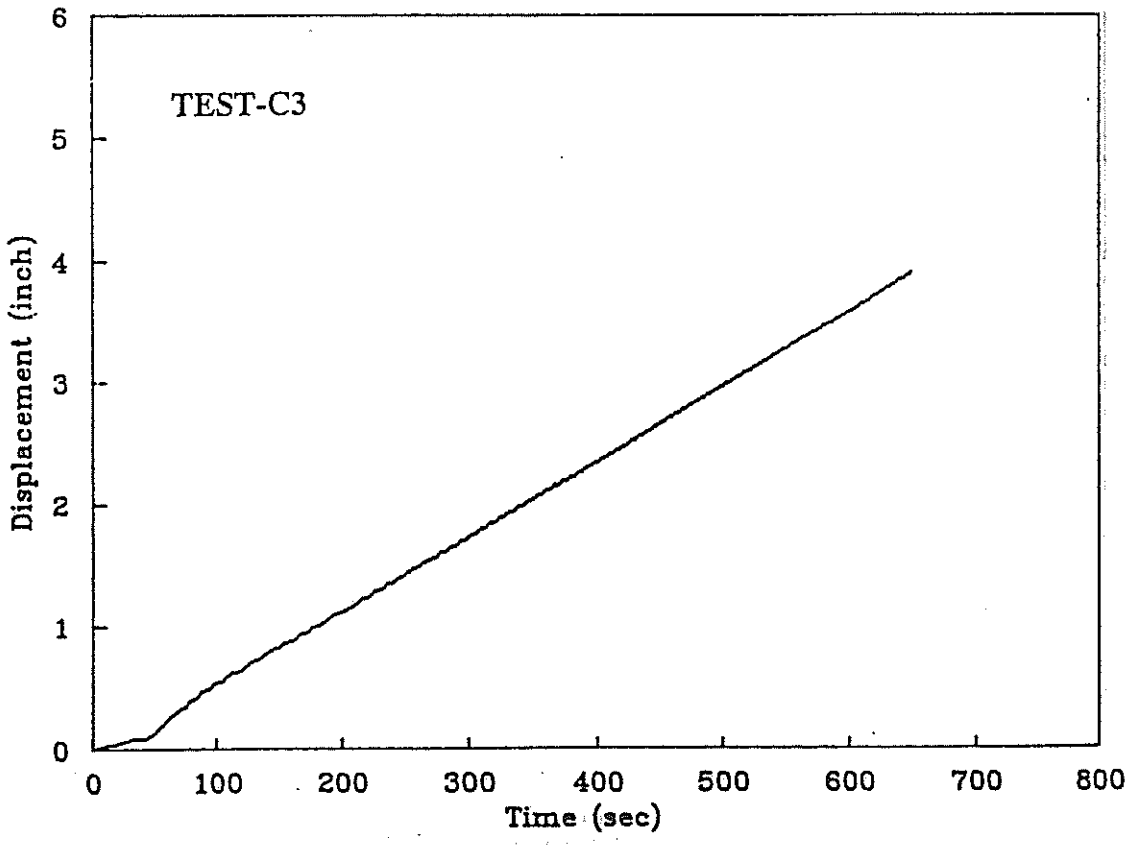
TEST-C3
Displacement (inch)
Time (sec)
0
100
200
300
400
500
600
700
800
1
2
3
4
5
6

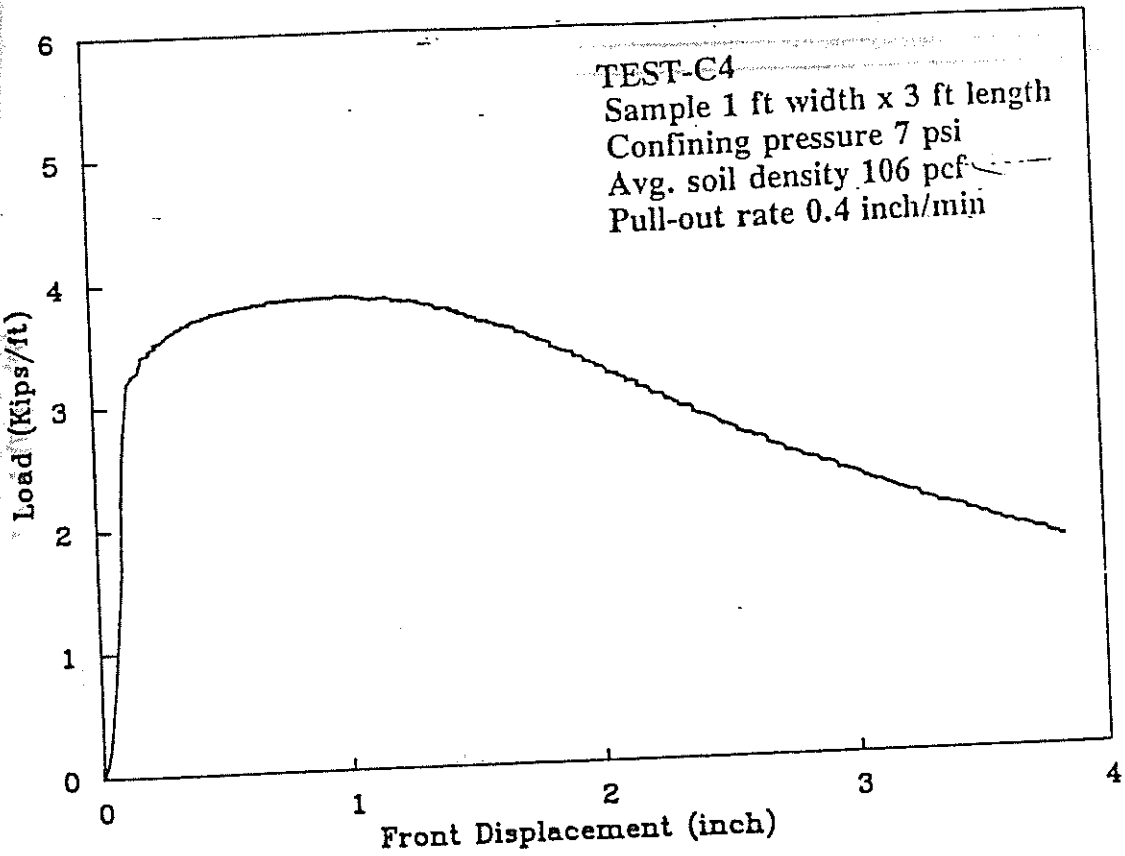
TEST-C4
Sample 1 ft width x 3 ft length
Confining pressure 7 psi
Avg. soil density 106 pcf
Pull-out rate 0.4 inch/min
Load (Kips/ft)
Front Displacement (inch)
0
1
2
3
4
5
6

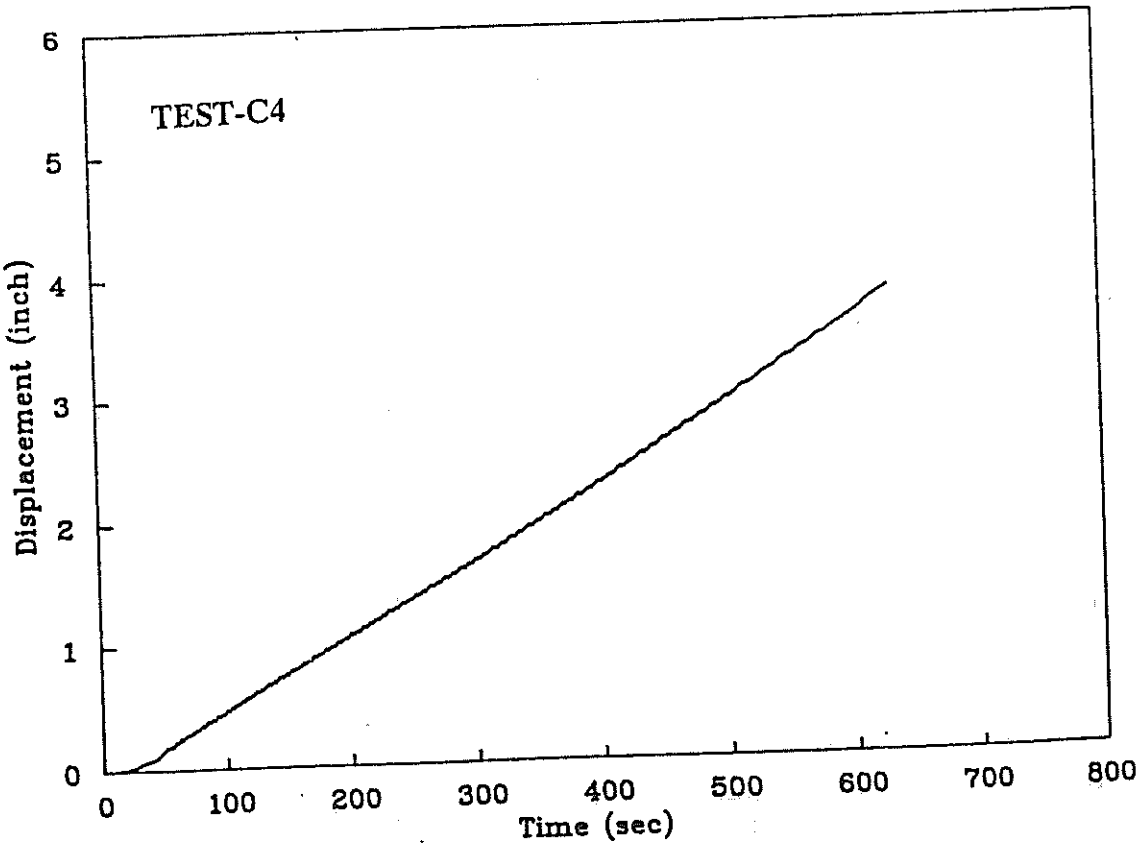
TEST-C4
Displacement (inch)
Time (sec)
0
100
200
300
400
500
600
700
800
1
2
3
4
5
6

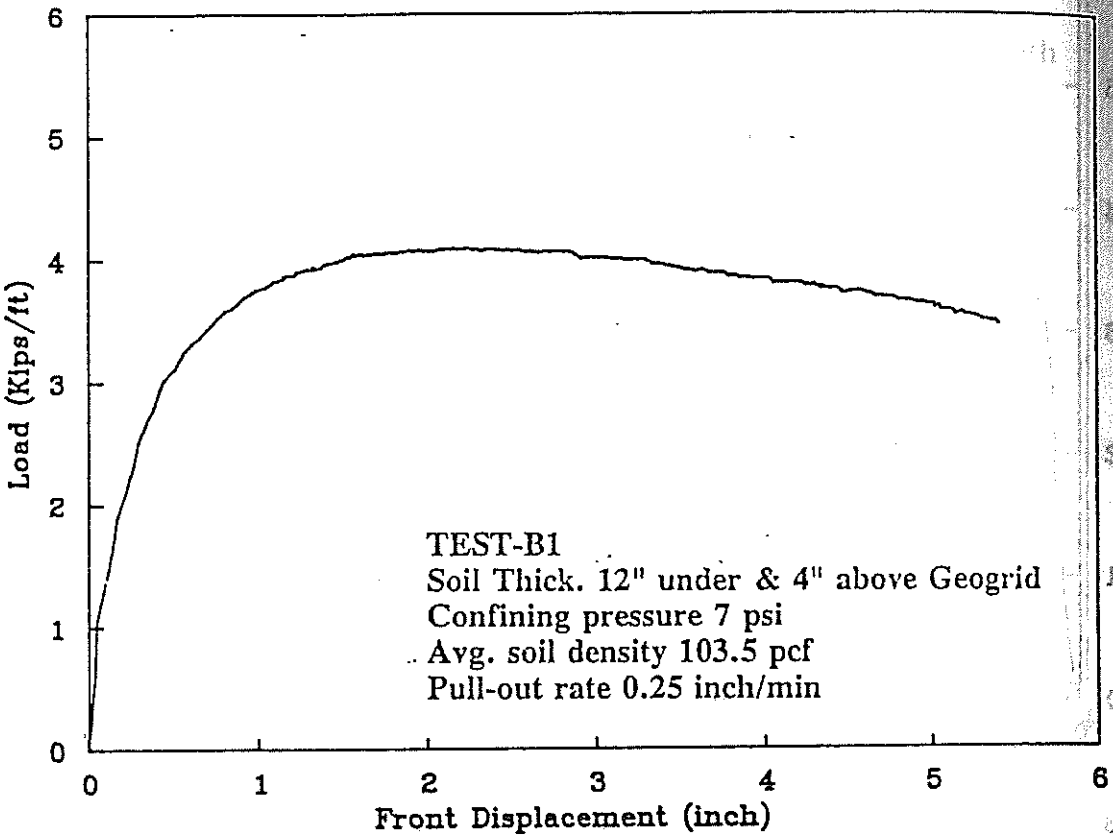
Load (Kips/ft)
Front Displacement (inch)
TEST-B1
Soil Thick. 12" under & 4" above Geogrid
Confining pressure 7 psi
Avg. soil density 103.5 pcf
Pull-out rate 0.25 inch/min

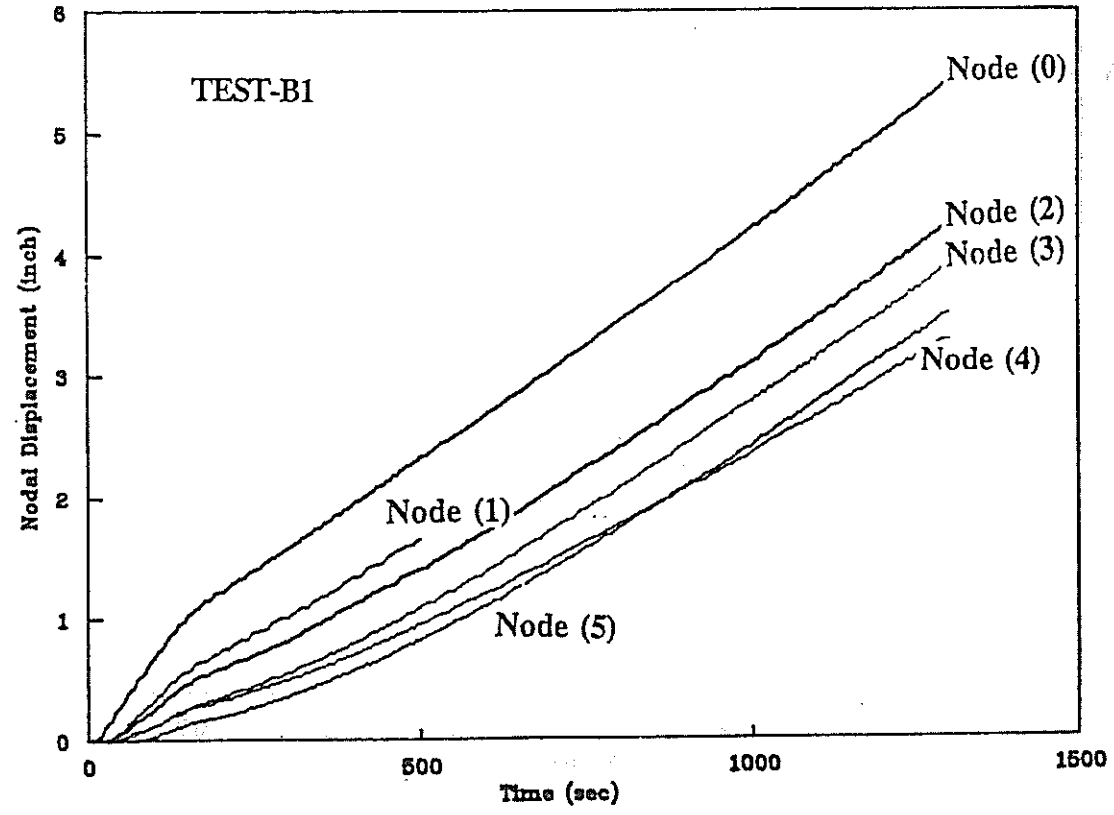
TEST-B1
Nodal Displacement (inch)
Time (sec)
Node (0)
Node (1)
Node (2)
Node (3)
Node (4)
Node (5)

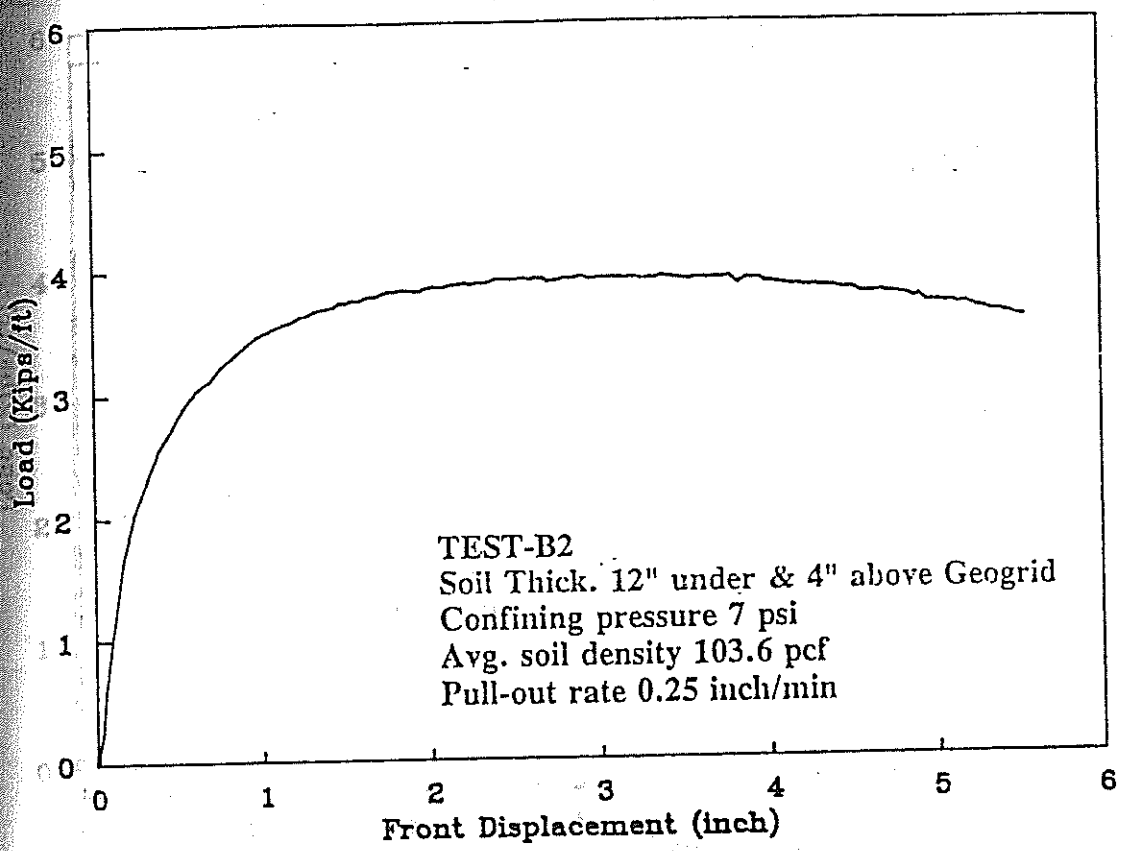
Load (Kips/ft)
Front Displacement (inch)
TEST-B2
Soil Thick. 12" under & 4" above Geogrid
Confining pressure 7 psi
Avg. soil density 103.6 pcf
Pull-out rate 0.25 inch/min

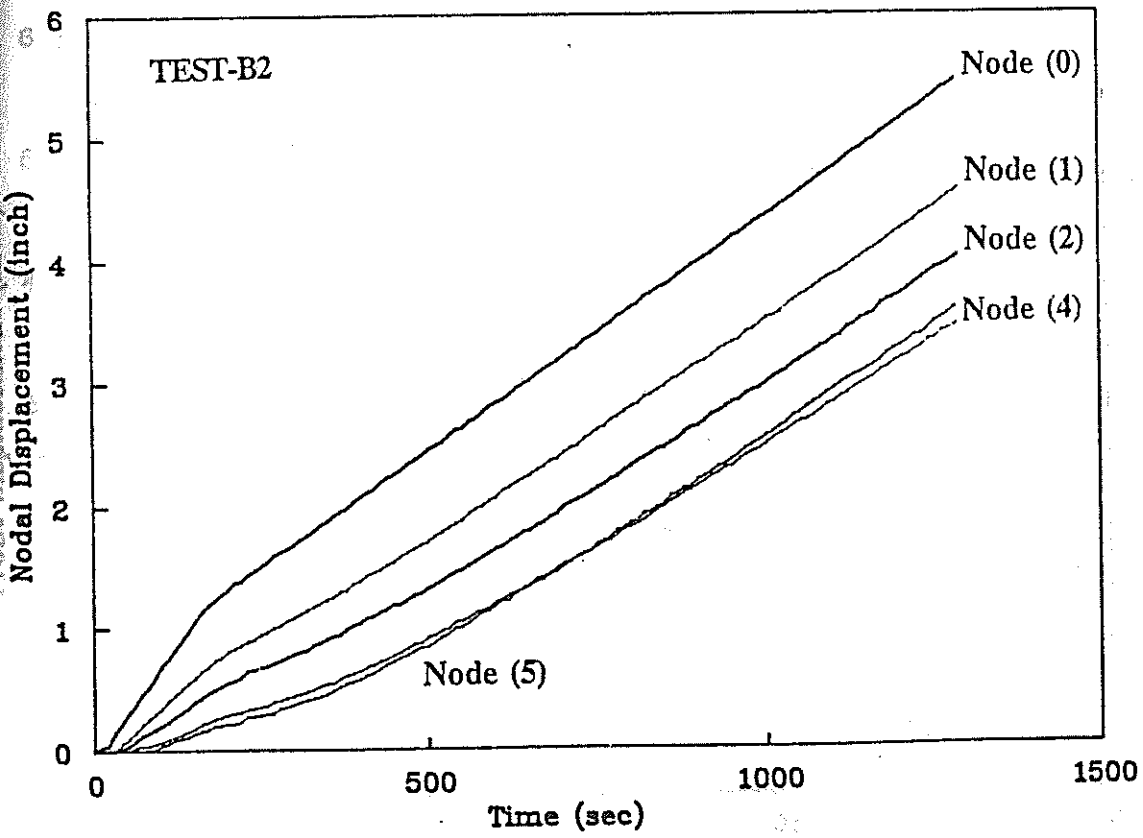
TEST-B2
Node (0)
Node (1)
Node (2)
Node (4)
Node (5)
Nodal Displacement (inch)
Time (sec)

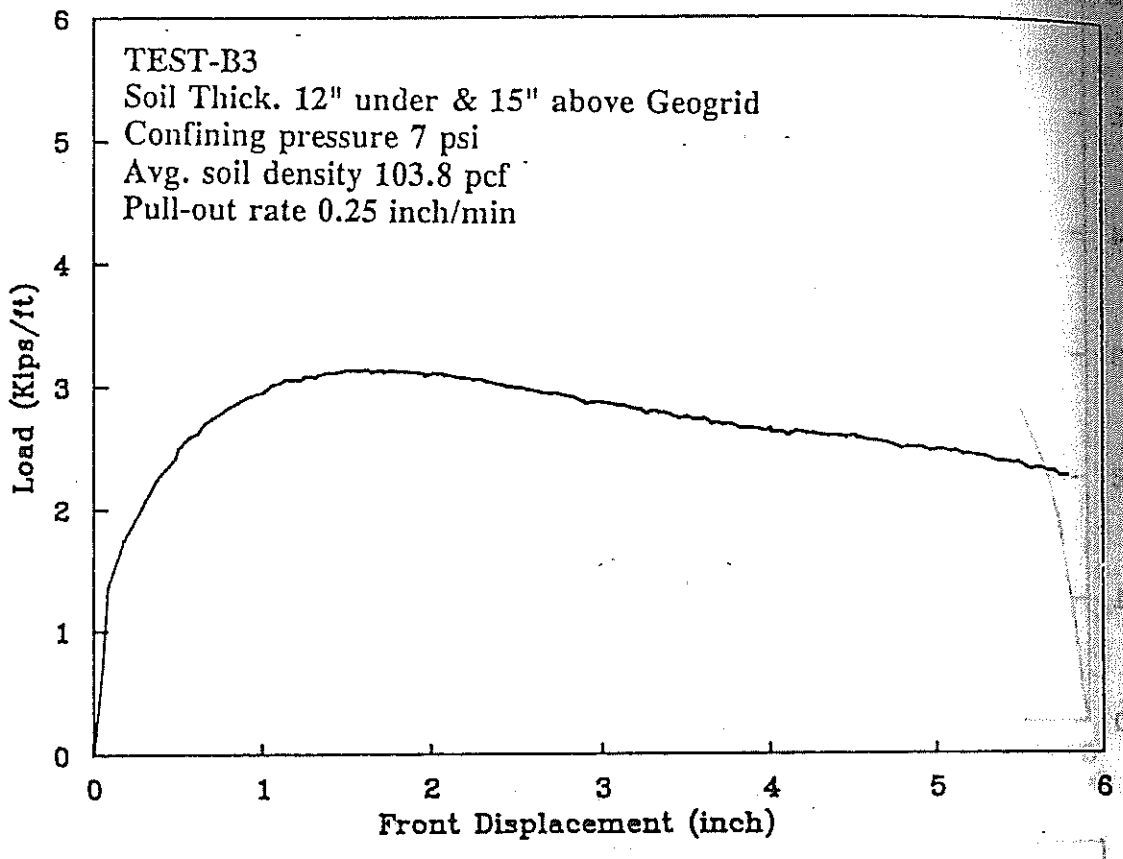
TEST-B3
Soil Thick. 12" under & 15" above Geogrid
Confining pressure 7 psi
Avg. soil density 103.8 pcf
Pull-out rate 0.25 inch/min
Load (Kips/ft)
Front Displacement (inch)
0
1
2
3
4
5
6

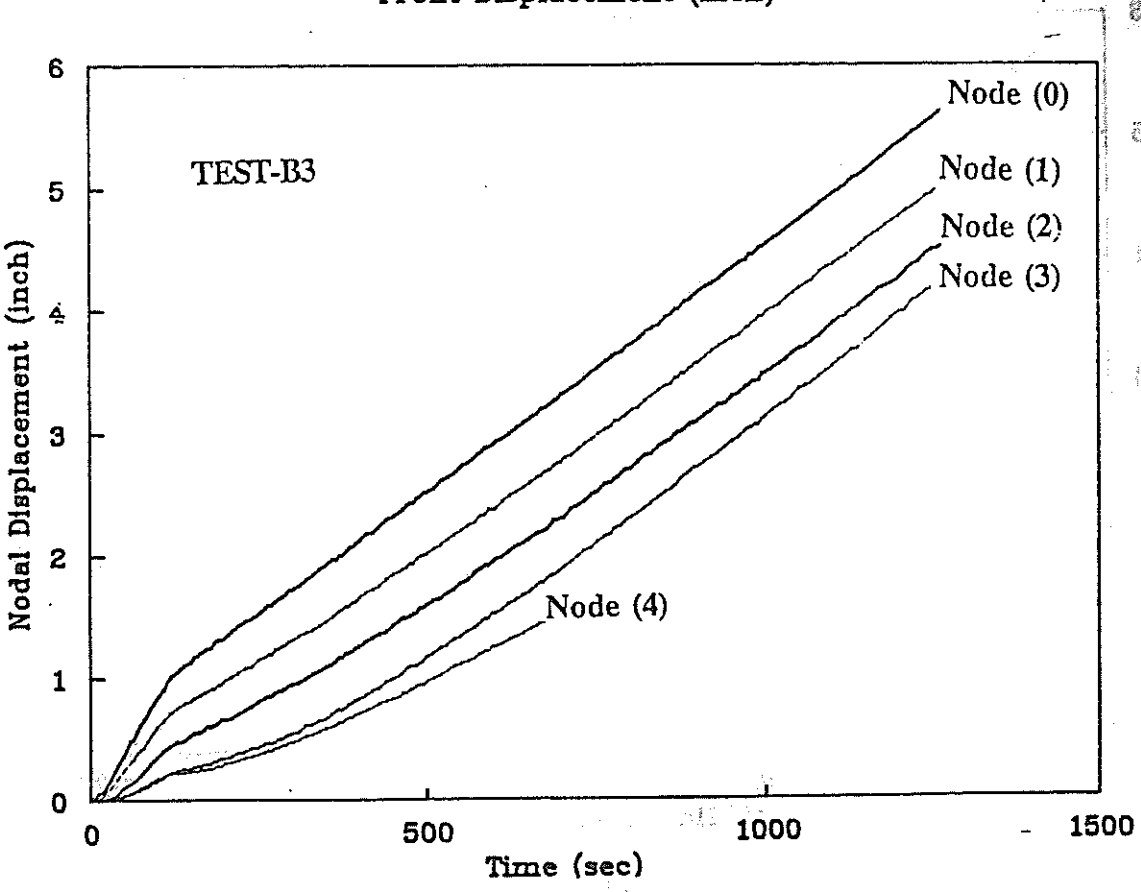
TEST-B3
Node (0)
Node (1)
Node (2)
Node (3)
Node (4)
Nodal Displacement (inch)
Time (sec)
0
500
1000
1500
1
2
3
4
5
6

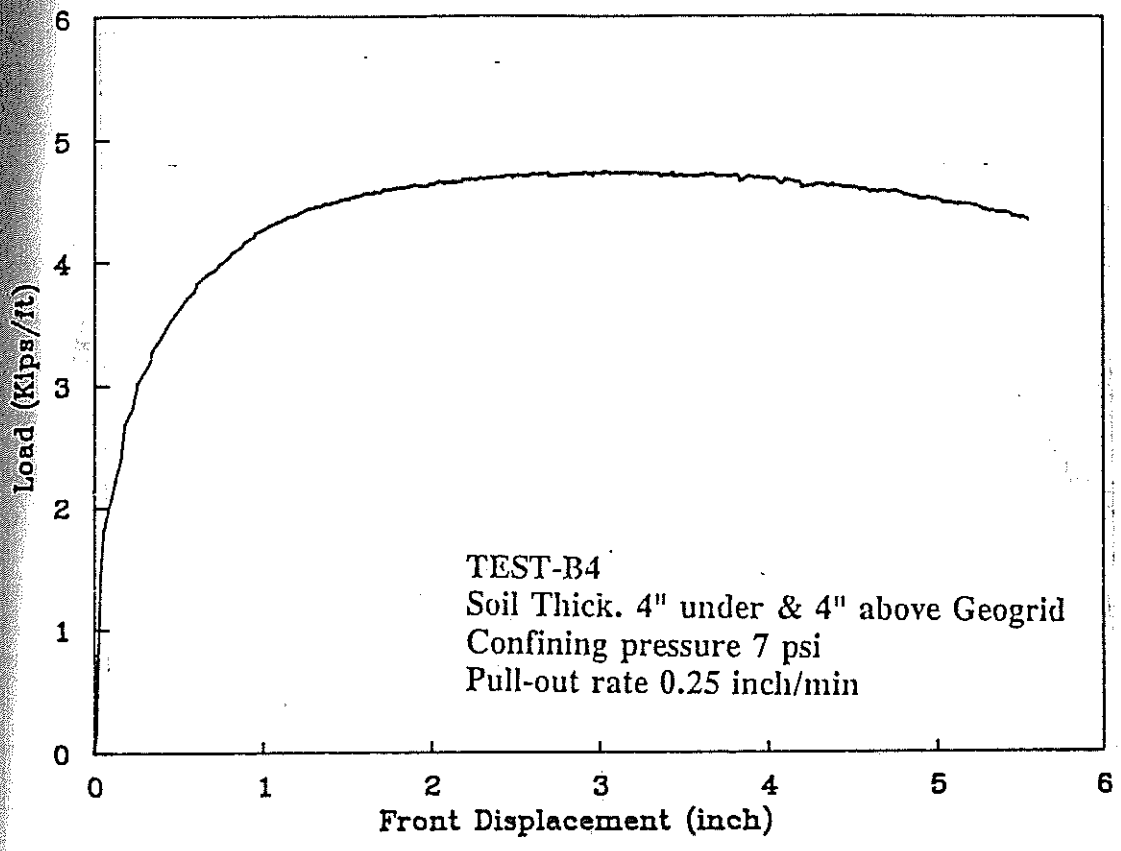
Load (Kips/ft)
Front Displacement (inch)
TEST-B4
Soil Thick. 4" under & 4" above Geogrid
Confining pressure 7 psi
Pull-out rate 0.25 inch/min

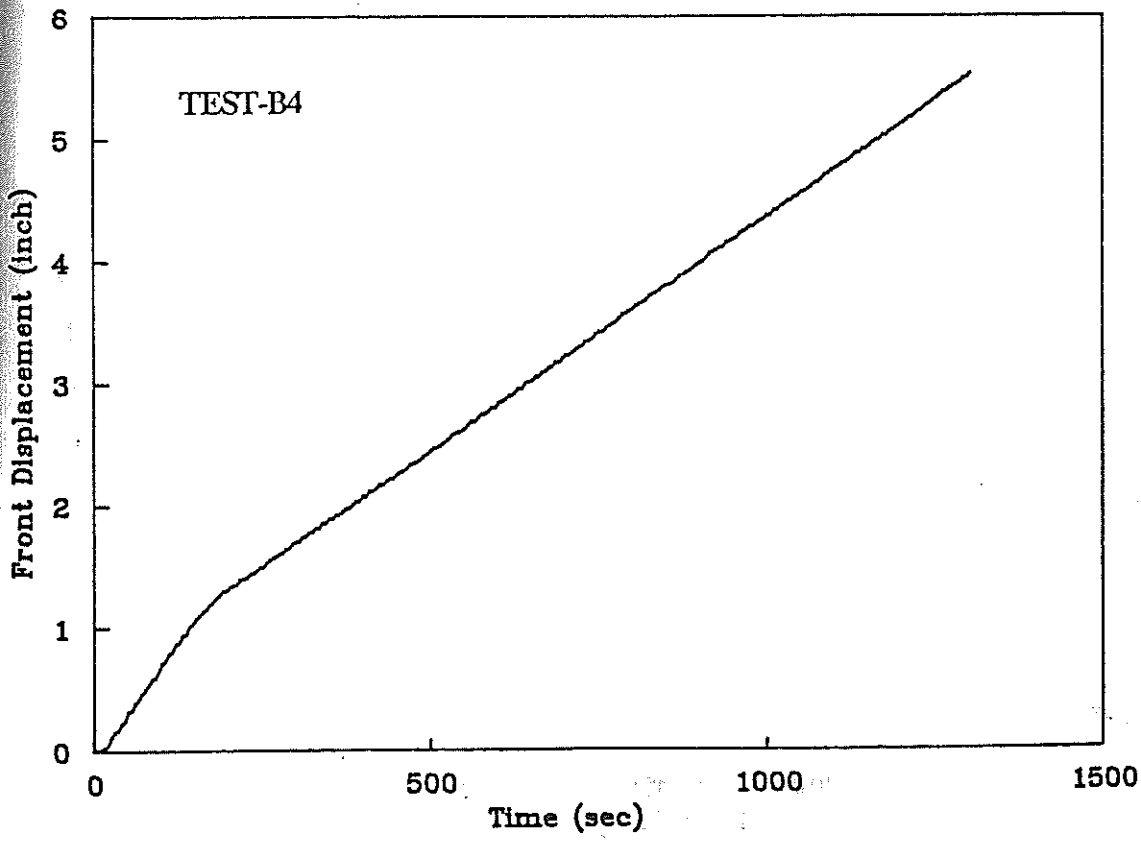
TEST-B4
Front Displacement (inch)
Time (sec)

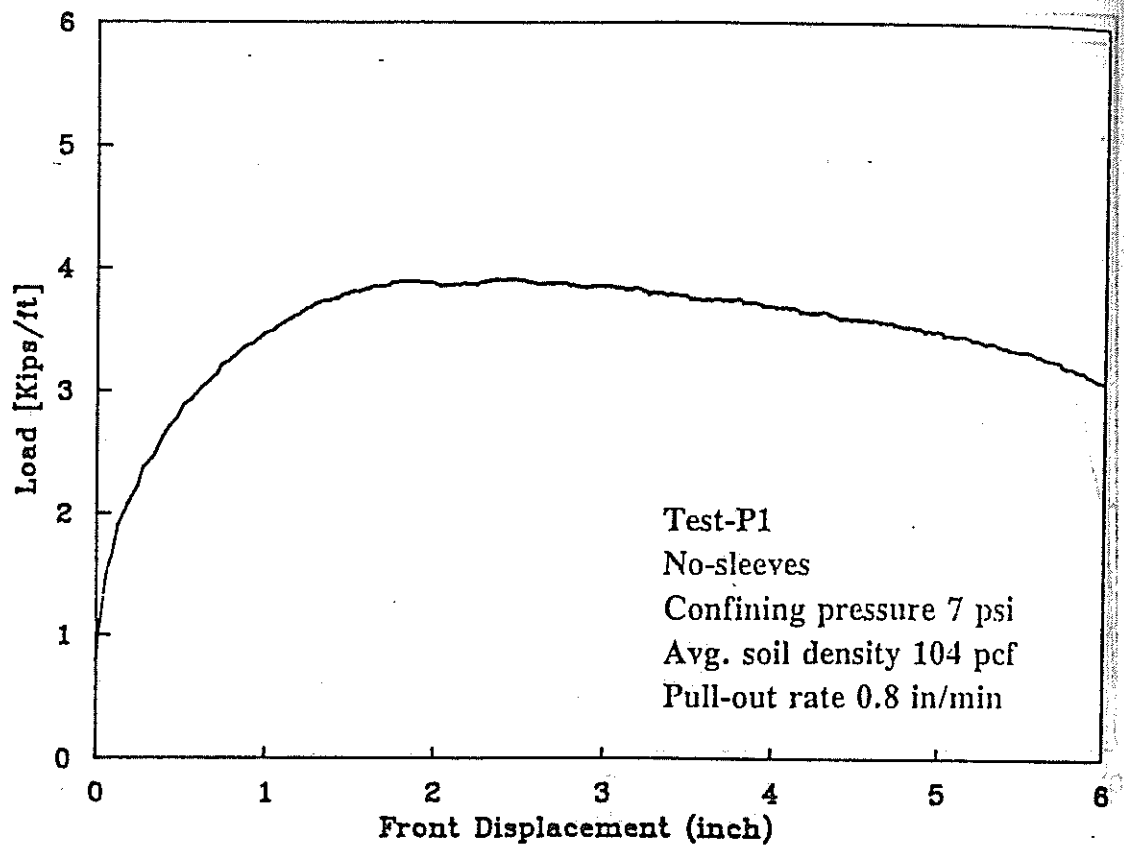
Load [Kips/ft]
Front Displacement (inch)
Test-P1
No-sleeves
Confining pressure 7 psi
Avg. soil density 104 pcf
Pull-out rate 0.8 in/min

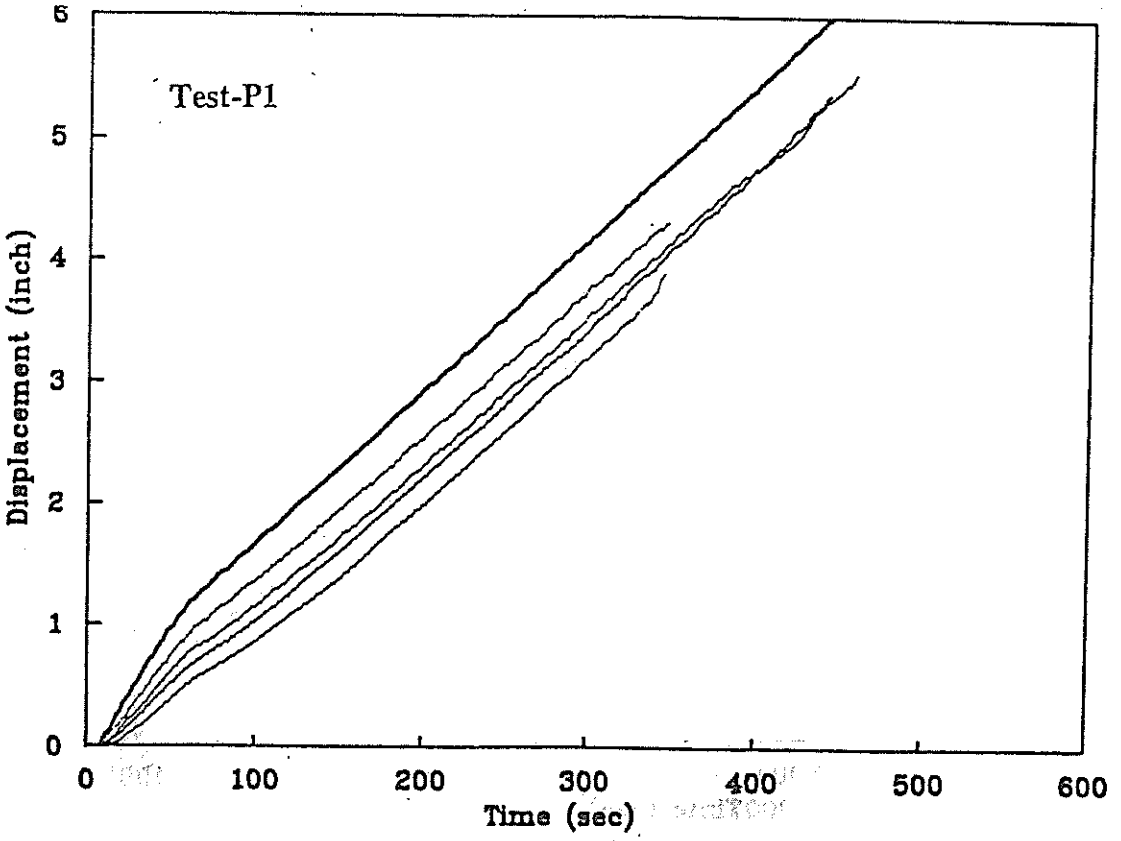
Displacement (inch)
Time (sec)
Test-P1

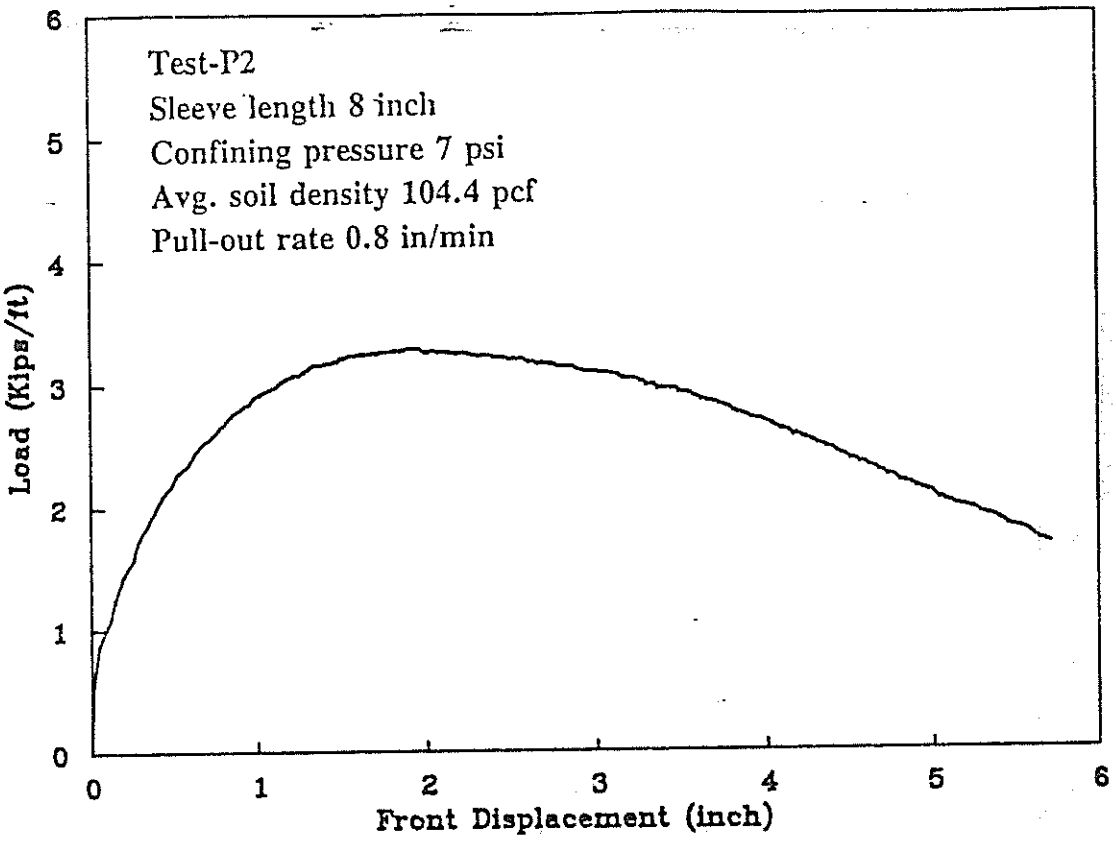
Test-P2
Sleeve length 8 inch
Confining pressure 7 psi
Avg. soil density 104.4 pcf
Pull-out rate 0.8 in/min
Load (Kips/ft)
Front Displacement (inch)
0
1
2
3
4
5
6

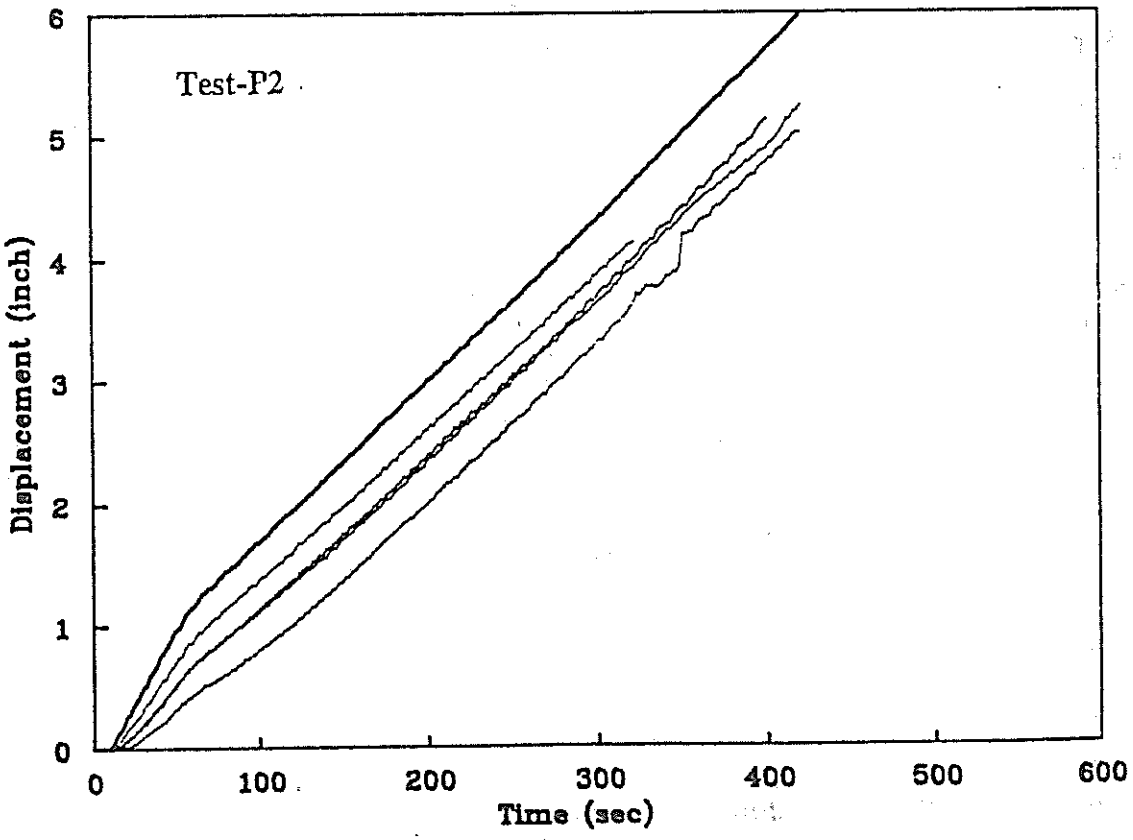
Test-P2
Displacement (inch)
Time (sec)
0
100
200
300
400
500
600

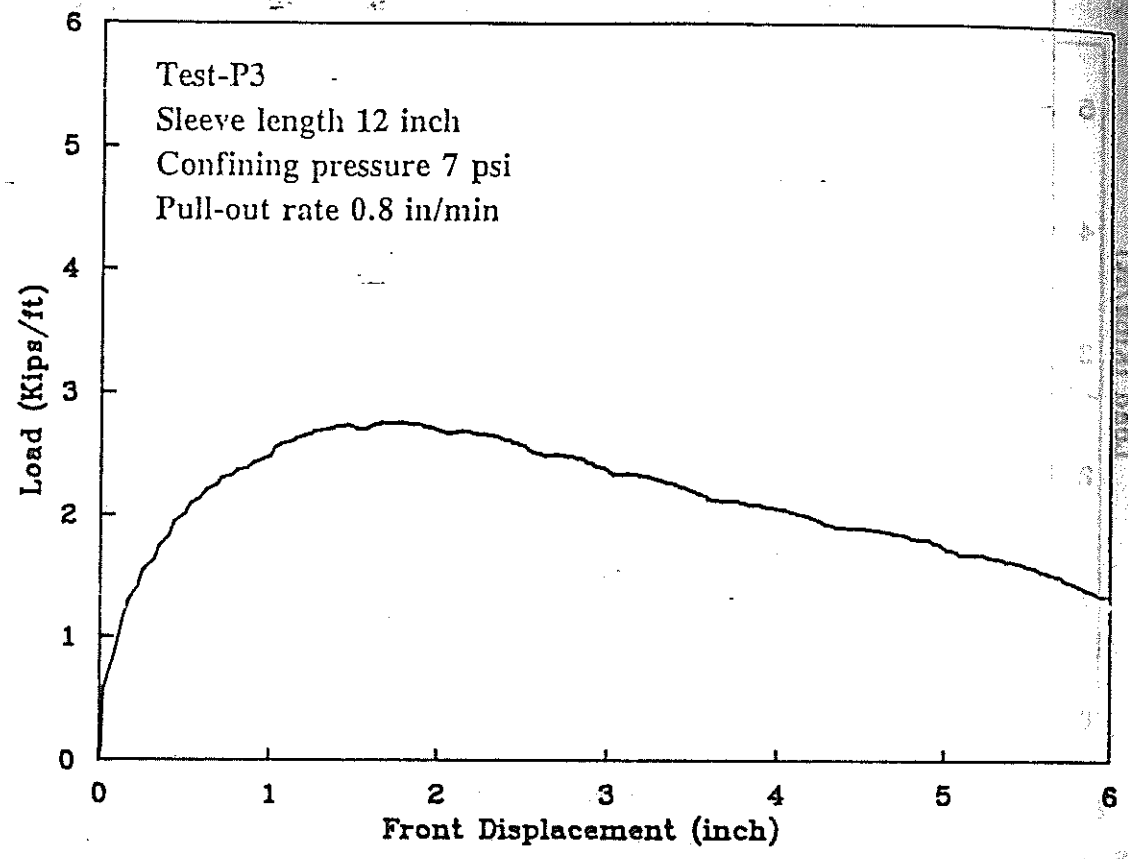
Test-P3
Sleeve length 12 inch
Confining pressure 7 psi
Pull-out rate 0.8 in/min
Load (Kips/ft)
Front Displacement (inch)
0
1
2
3
4
5
6

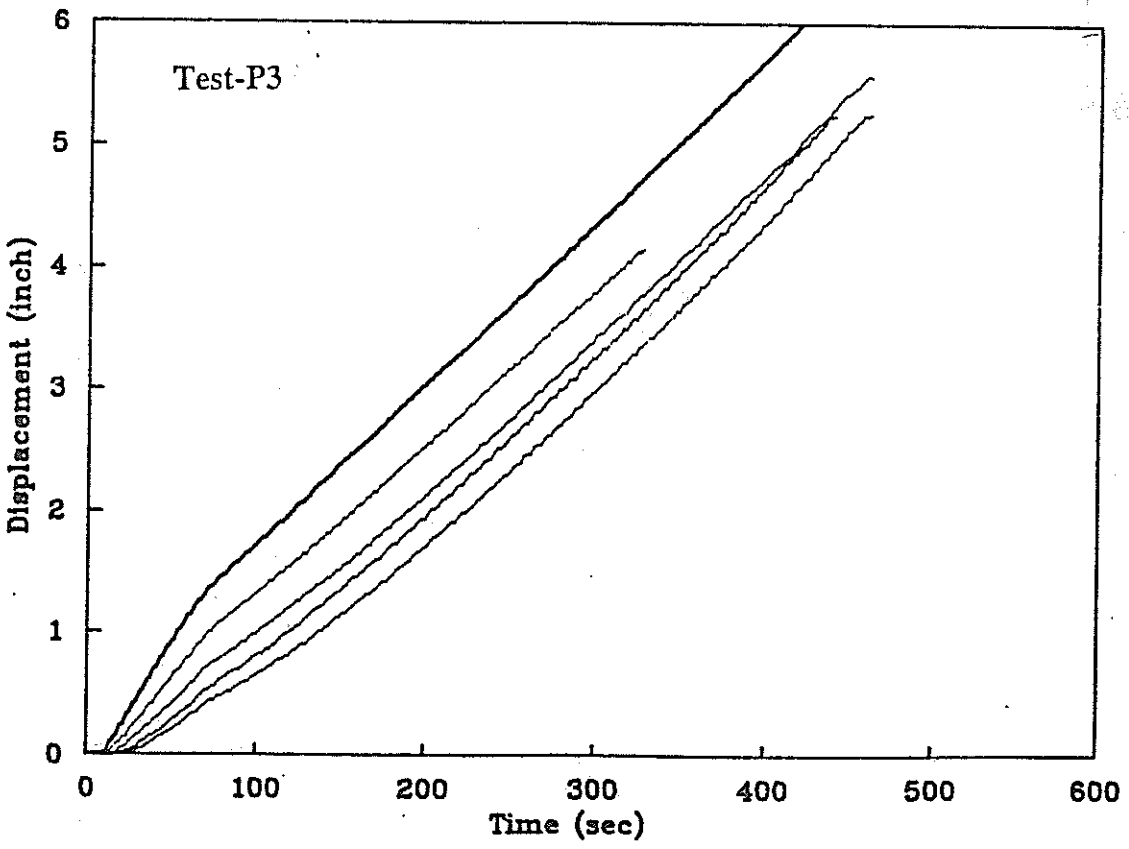
Test-P3
Displacement (inch)
Time (sec)
0
100
200
300
400
500
600
1
2
3
4
5
6

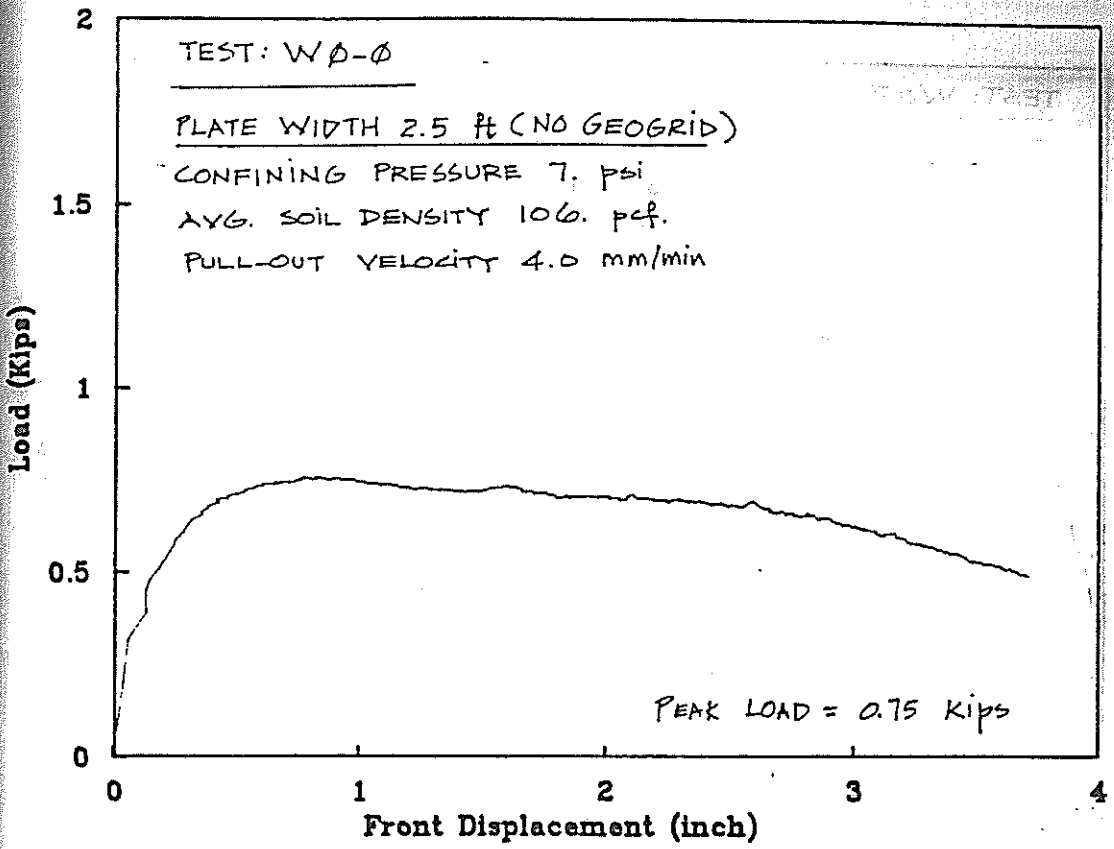
TEST: WØ-Ø
PLATE WIDTH 2.5 ft (NO GEOGRID)
CONFINING PRESSURE 7. psi
AVG. SOIL DENSITY 106. pcf.
PULL-OUT VELOCITY 4.0 mm/min
PEAK LOAD = 0.75 Kips
Load (Kips)
Front Displacement (inch)
0
0.5
1
1.5
2
0
1
2
3
4

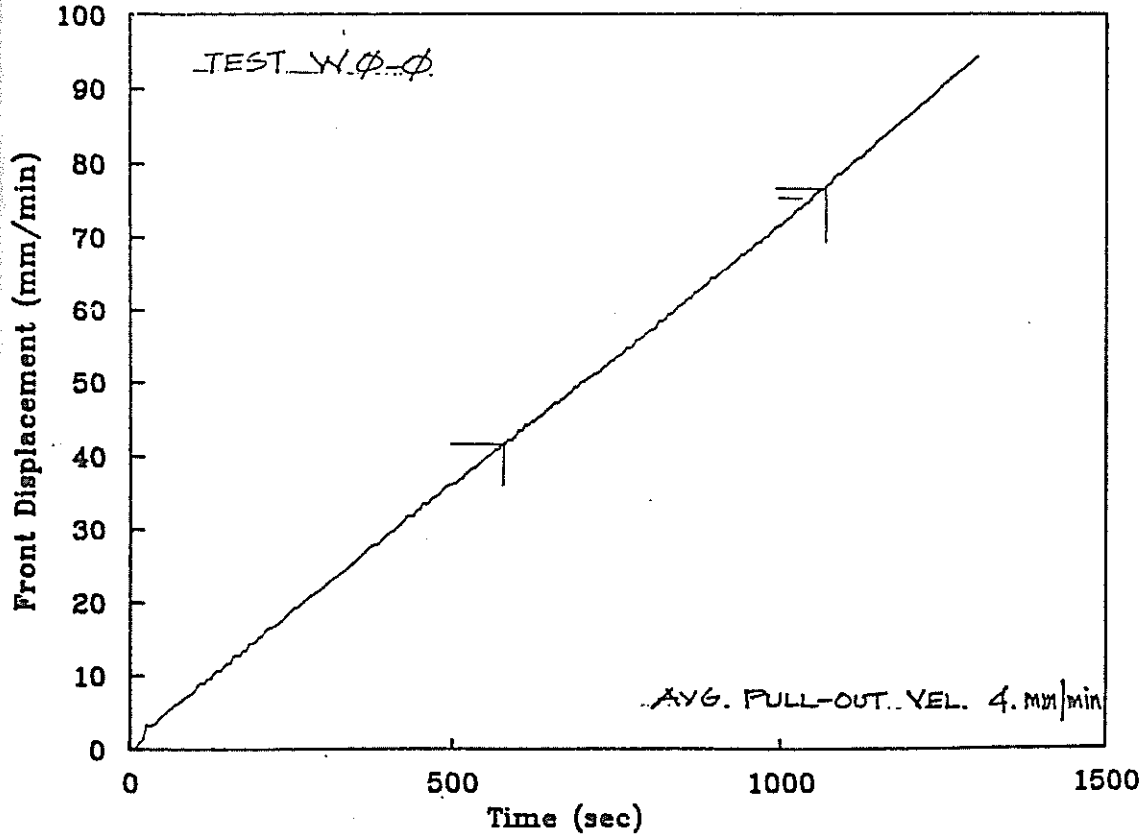
TEST W.Ø-Ø
AVG. PULL-OUT VEL. 4. mm/min
Front Displacement (mm/min)
Time (sec)
0
10
20
30
40
50
60
70
80
90
100
0
500
1000
1500

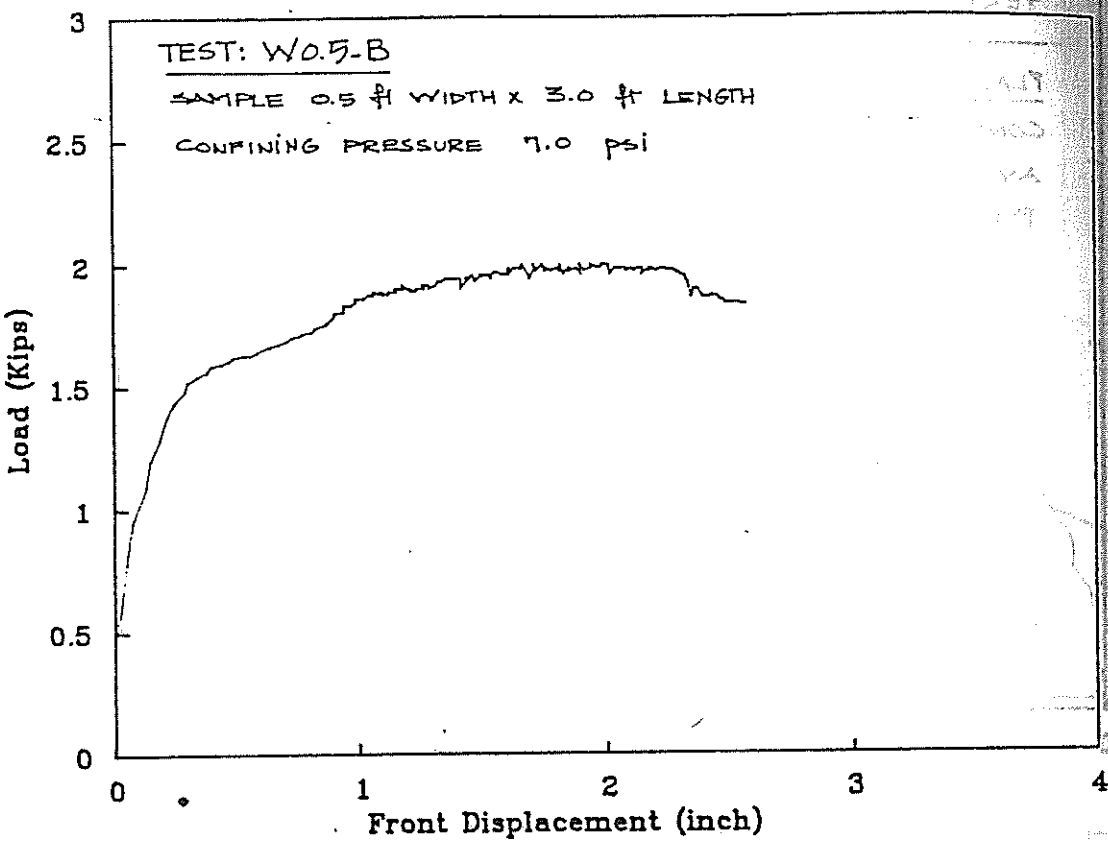
TEST: W0.5-B
SAMPLE 0.5 ft WIDTH x 3.0 ft LENGTH
CONFINING PRESSURE 7.0 psi
Load (Kips)
Front Displacement (inch)
0
0.5
1
1.5
2
2.5
3
0
1
2
3
4

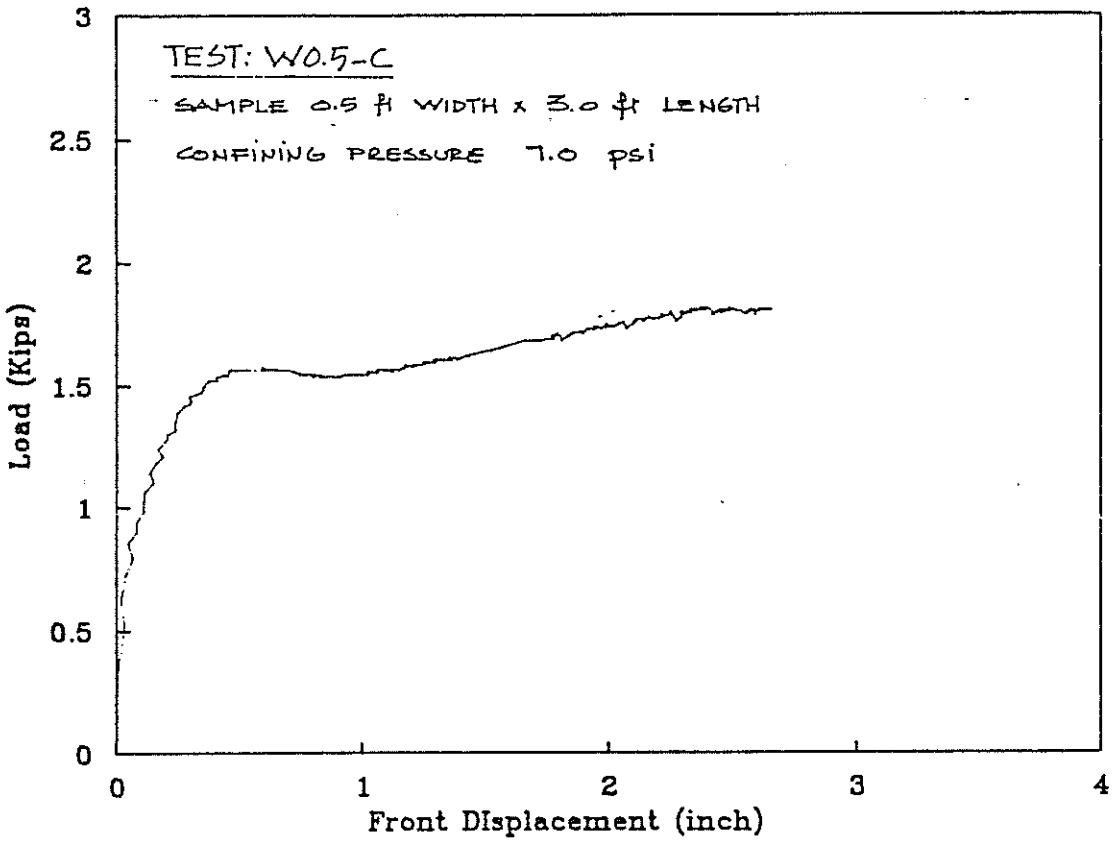
TEST: W0.5-C
SAMPLE 0.5 ft WIDTH x 3.0 ft LENGTH
CONFINING PRESSURE 7.0 psi
Load (Kips)
Front DIsplacement (inch)
0
0.5
1
1.5
2
2.5
3
0
1
2
3
4

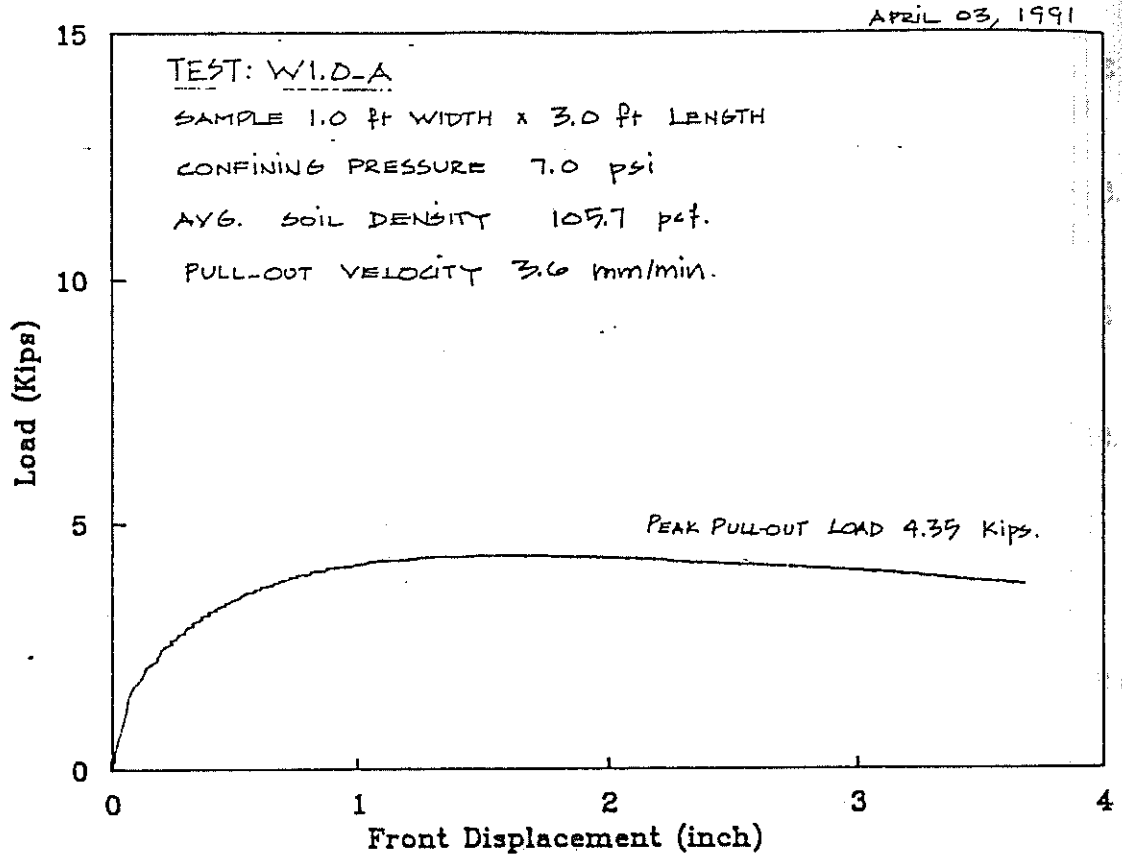
APRIL 03, 1991
TEST: W1.0-A
SAMPLE 1.0 ft WIDTH x 3.0 ft LENGTH
CONFINING PRESSURE 7.0 psi
AVG. SOIL DENSITY 105.7 pcf.
PULL-OUT VELOCITY 3.6 mm/min.
PEAK PULL-OUT LOAD 4.35 Kips.
Load (Kips)
Front Displacement (inch)
0
5
10
15
0
1
2
3
4

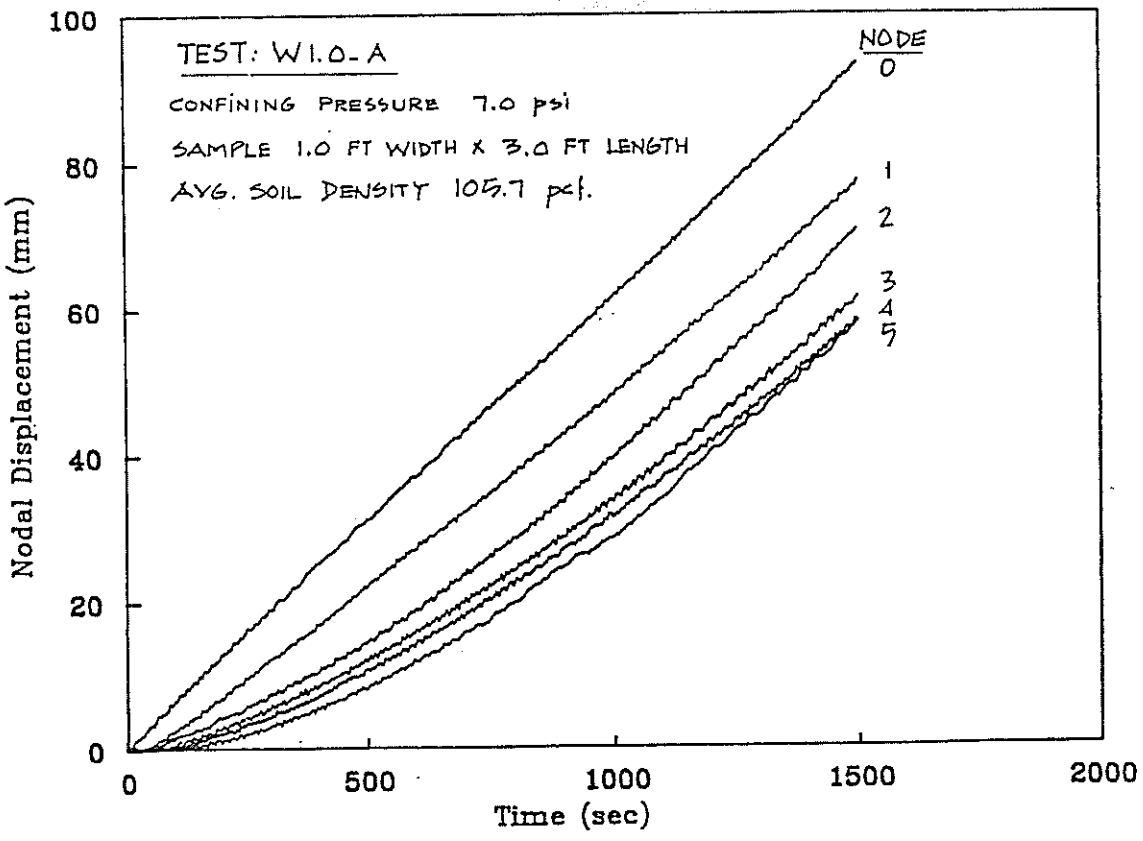
TEST: W1.0-A
CONFINING PRESSURE 7.0 psi
SAMPLE 1.0 FT WIDTH x 3.0 FT LENGTH
AVG. SOIL DENSITY 105.7 pcf.
NODE
0
1
2
3
4
5
Nodal Displacement (mm)
Time (sec)
0
20
40
60
80
100
0
500
1000
1500
2000

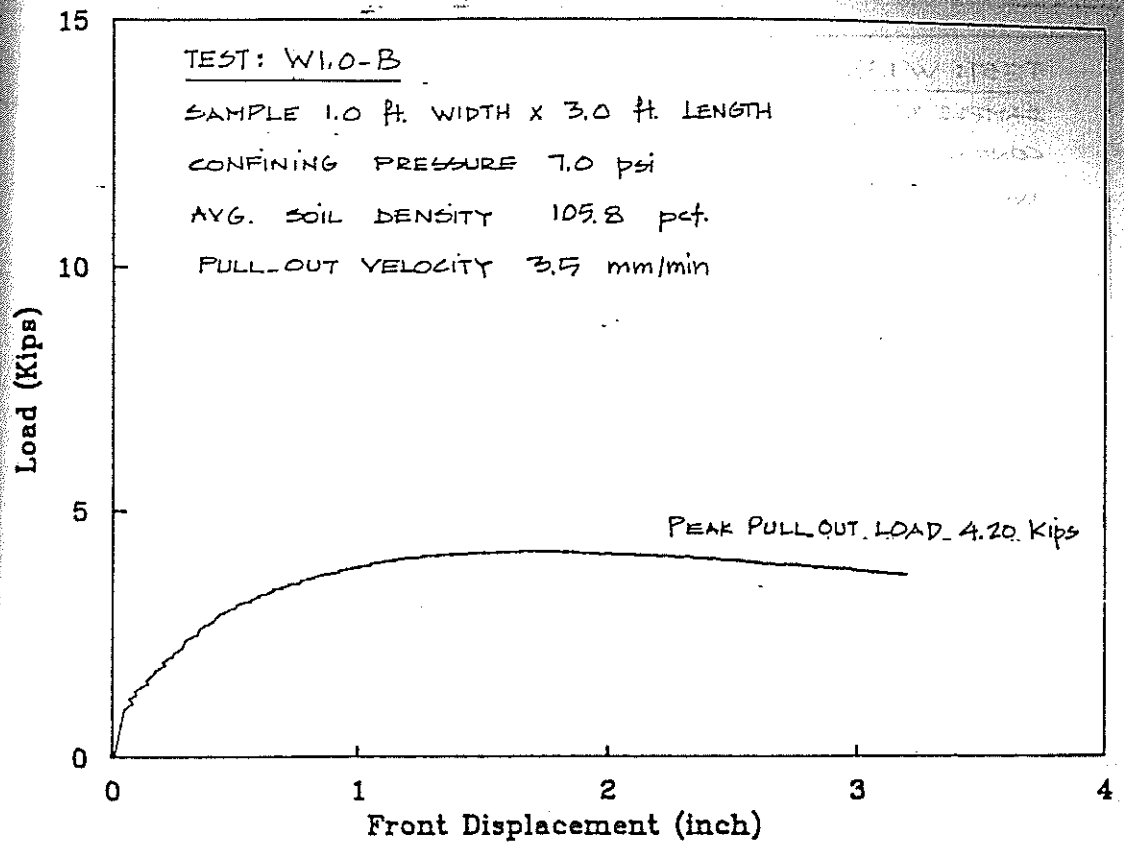
TEST: W1.0-B
SAMPLE 1.0 ft. WIDTH x 3.0 ft. LENGTH
CONFINING PRESSURE 7.0 psi
AVG. SOIL DENSITY 105.8 pcf.
PULL-OUT VELOCITY 3.5 mm/min
PEAK PULL-OUT LOAD 4.20 Kips
Load (Kips)
Front Displacement (inch)
0
5
10
15
0
1
2
3
4

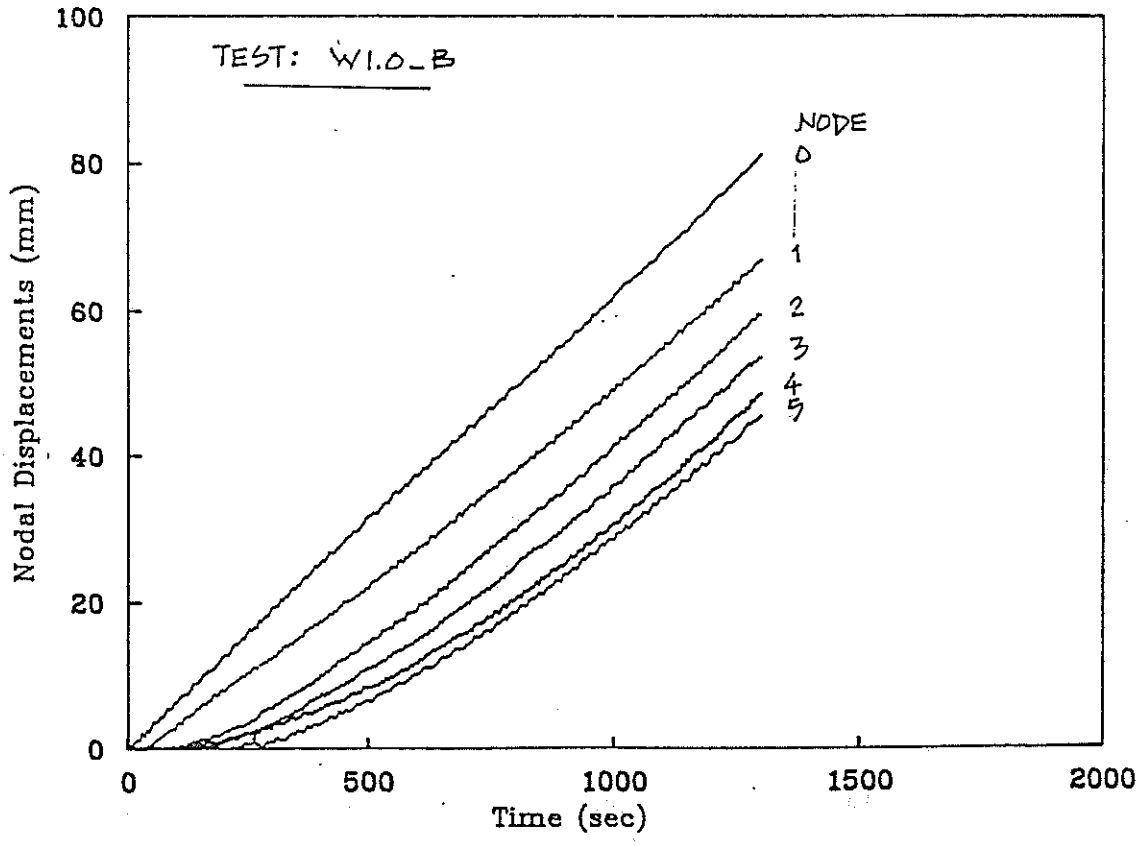
TEST: W1.0_B
NODE
0
1
2
3
4
5
Nodal Displacements (mm)
Time (sec)
0
20
40
60
80
100
0
500
1000
1500
2000

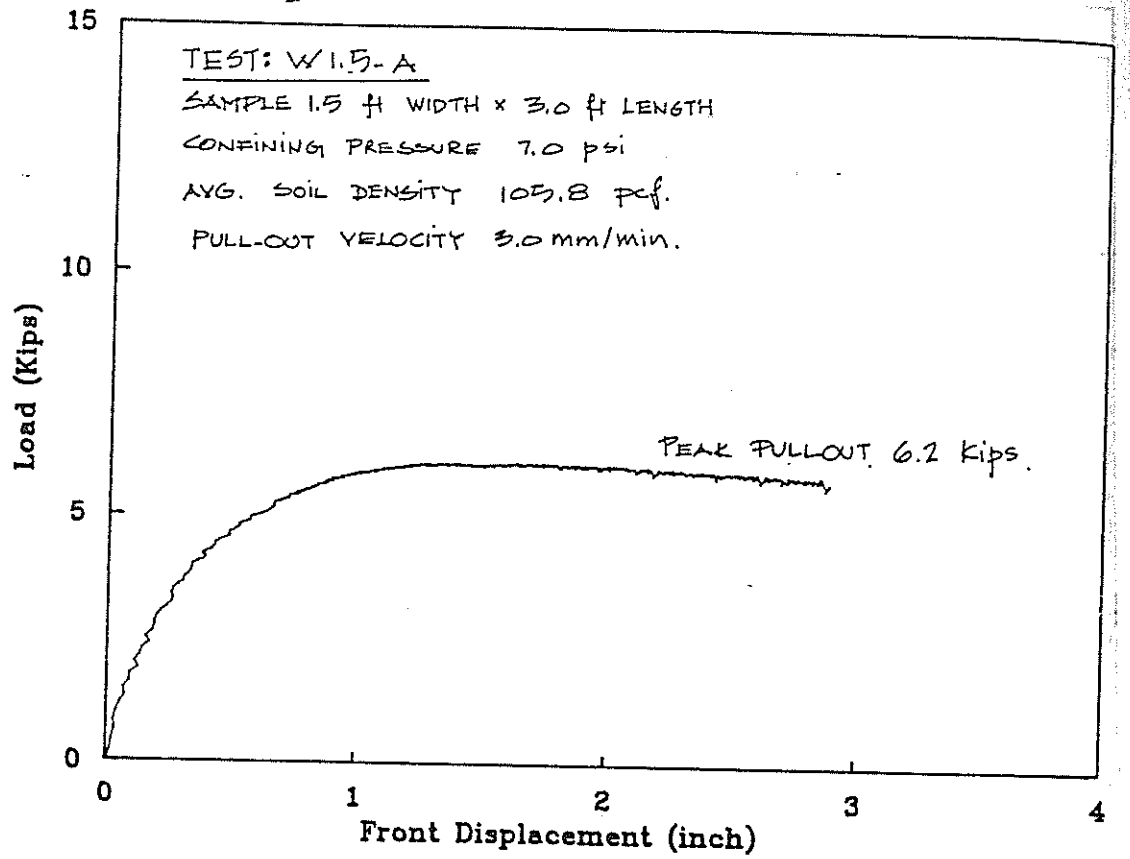
TEST: W1.5-A
SAMPLE 1.5 ft WIDTH x 3.0 ft LENGTH
CONFINING PRESSURE 7.0 psi
AVG. SOIL DENSITY 105.8 pcf.
PULL-OUT VELOCITY 3.0 mm/min.
PEAK PULLOUT 6.2 Kips.
Load (Kips)
Front Displacement (inch)
0
5
10
15
0
1
2
3
4

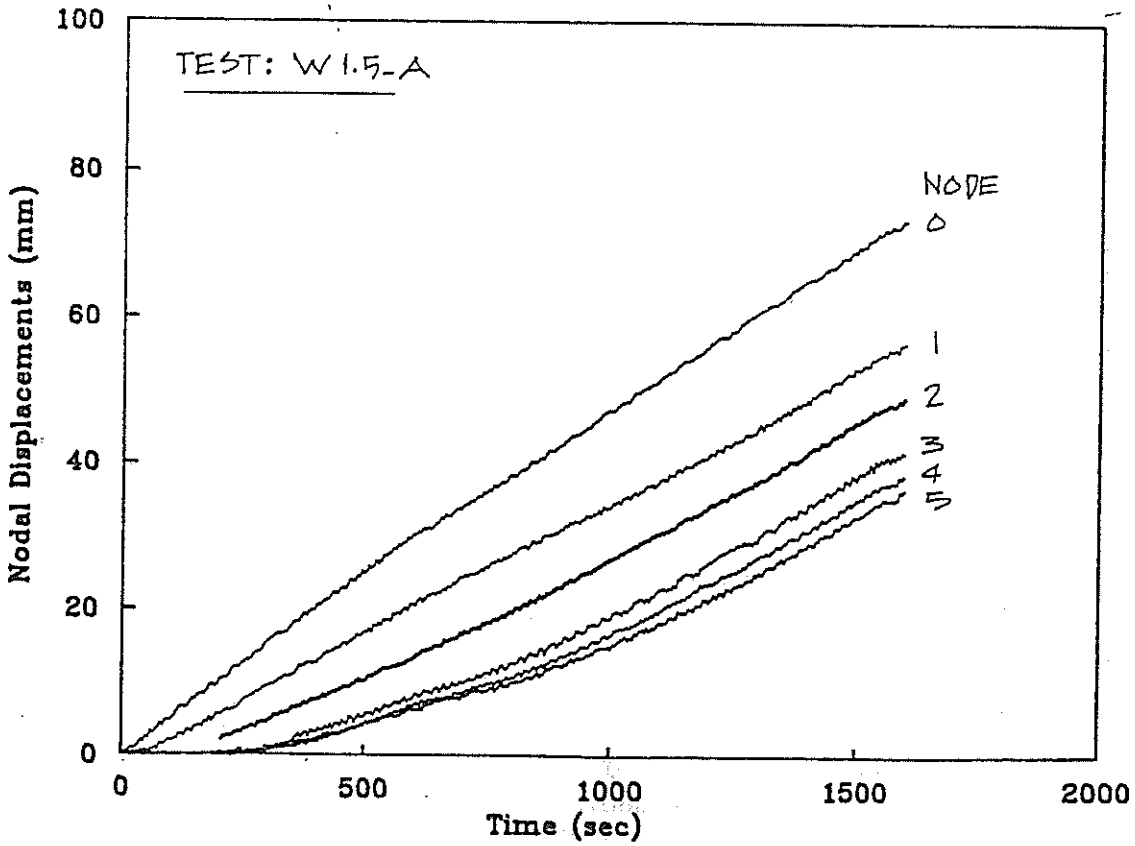
TEST: W1.5-A
NODE
0
1
2
3
4
5
Nodal Displacements (mm)
Time (sec)
0
20
40
60
80
100
0
500
1000
1500
2000

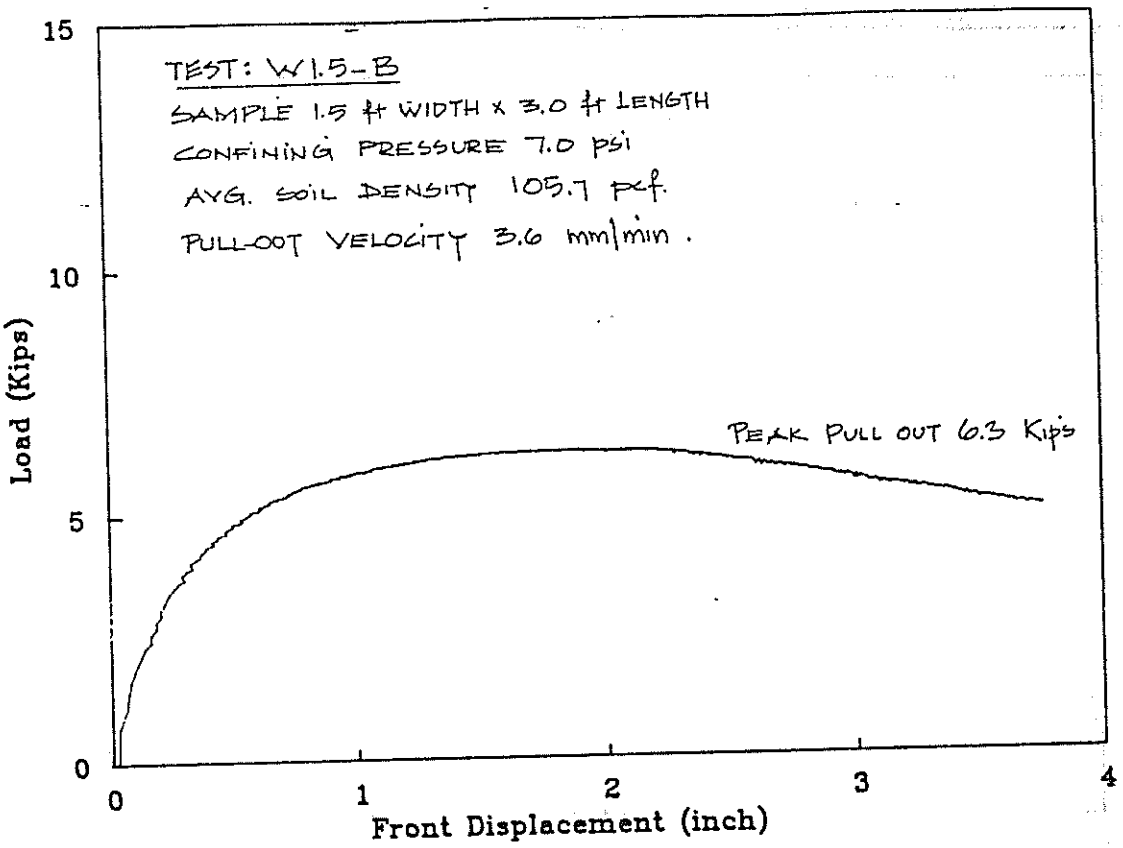
TEST: W1.5-B
SAMPLE 1.5 ft WIDTH x 3.0 ft LENGTH
CONFINING PRESSURE 7.0 psi
AVG. SOIL DENSITY 105.7 pcf.
PULL-OUT VELOCITY 3.6 mm/min.
PEAK PULL OUT 6.3 Kips
Load (Kips)
Front Displacement (inch)
0
5
10
15
0
1
2
3
4

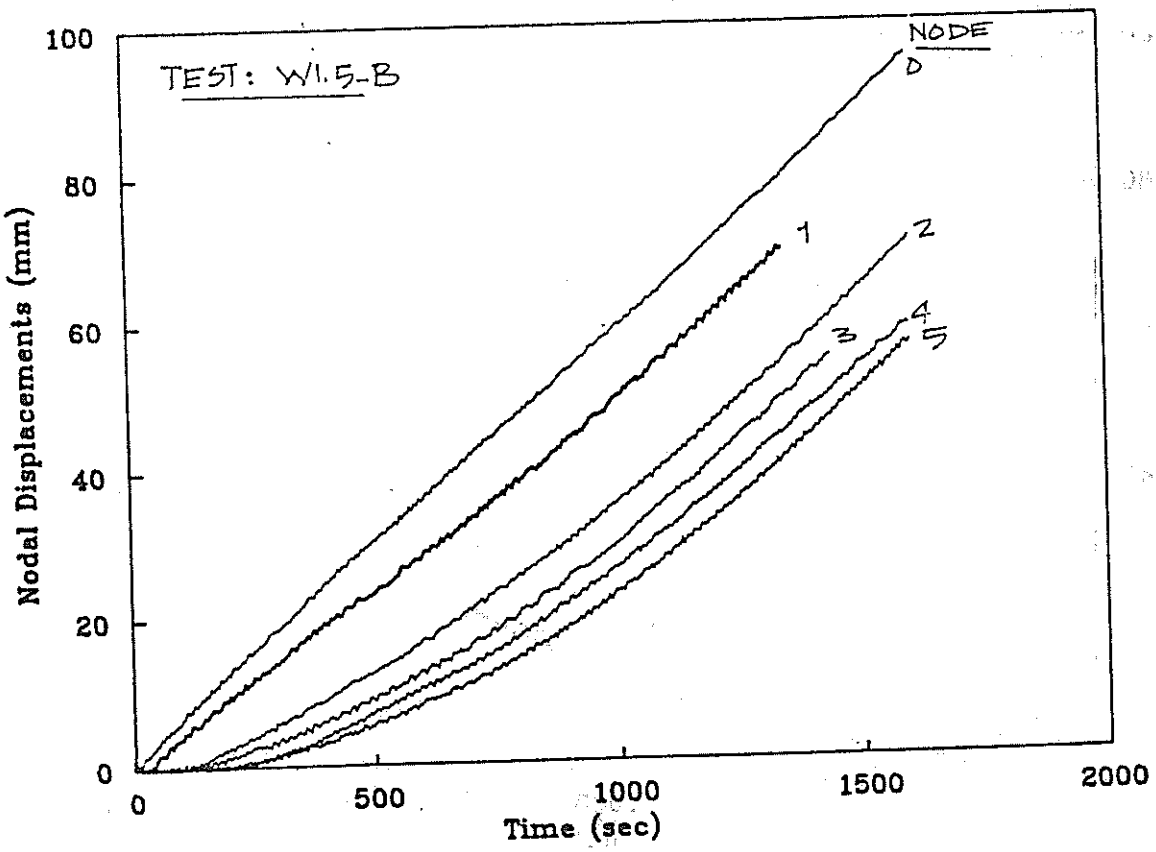
TEST: W1.5-B
NODE
0
1
2
3
4
5
Nodal Displacements (mm)
Time (sec)
0
20
40
60
80
100
0
500
1000
1500
2000

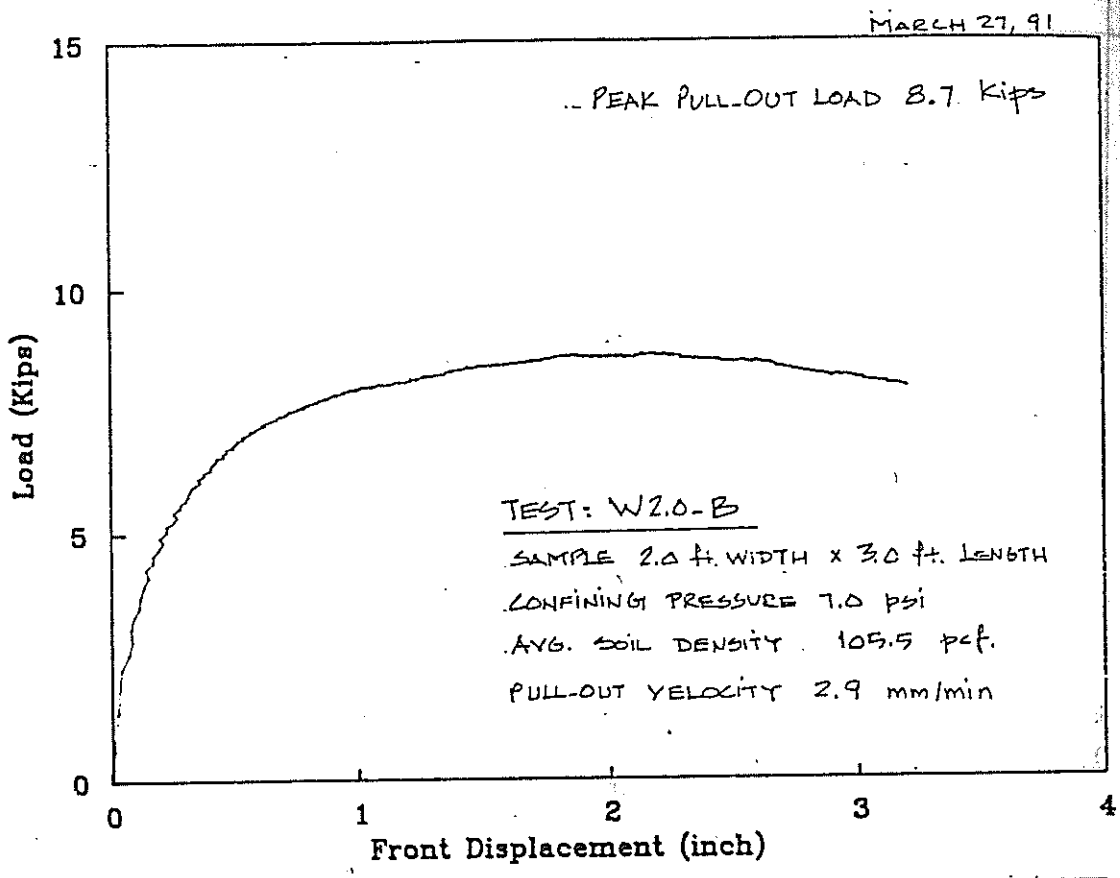
MARCH 27, 91
PEAK PULL-OUT LOAD 8.7 Kips
TEST: W2.0-B
SAMPLE 2.0 ft. WIDTH x 3.0 ft. LENGTH
CONFINING PRESSURE 7.0 psi
AVG. SOIL DENSITY 105.5 pcf.
PULL-OUT VELOCITY 2.9 mm/min
Load (Kips)
Front Displacement (inch)
0
5
10
15
0
1
2
3
4

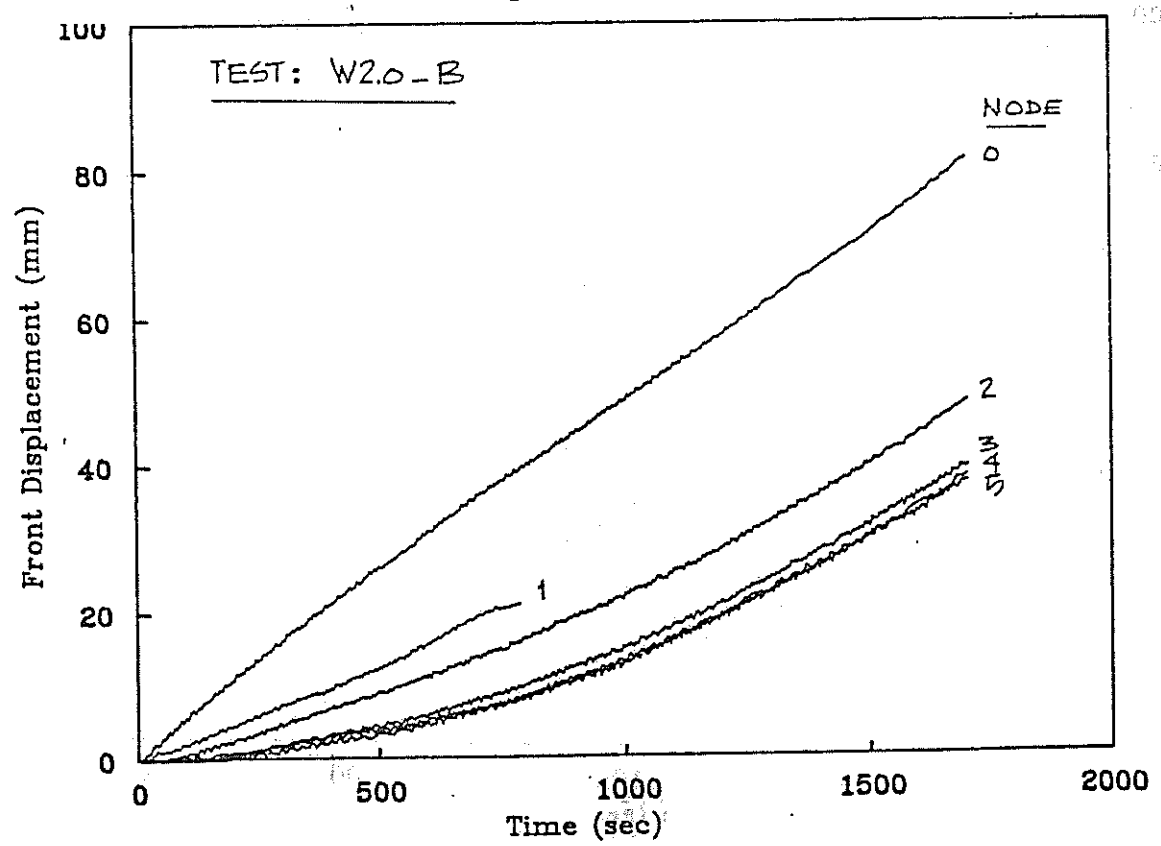
TEST: W2.0-B
NODE
0
1
2
3
4
Front Displacement (mm)
Time (sec)
0
20
40
60
80
100
0
500
1000
1500
2000

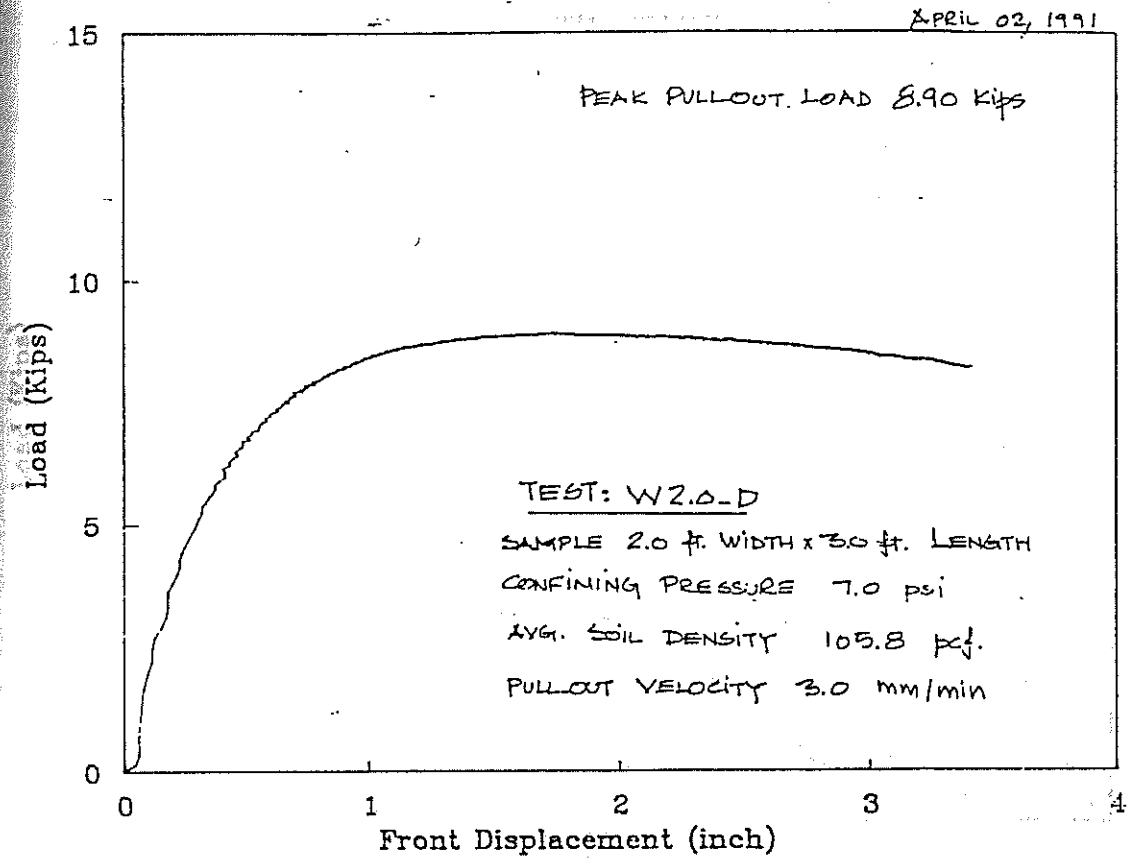
APRIL 02, 1991
PEAK PULLOUT LOAD 8.90 Kips
TEST: W2.0_D
SAMPLE 2.0 ft. WIDTH x 3.0 ft. LENGTH
CONFINING PRESSURE 7.0 psi
AVG. SOIL DENSITY 105.8 pcf.
PULLOUT VELOCITY 3.0 mm/min
Load (Kips)
Front Displacement (inch)
0
5
10
15
0
1
2
3
4

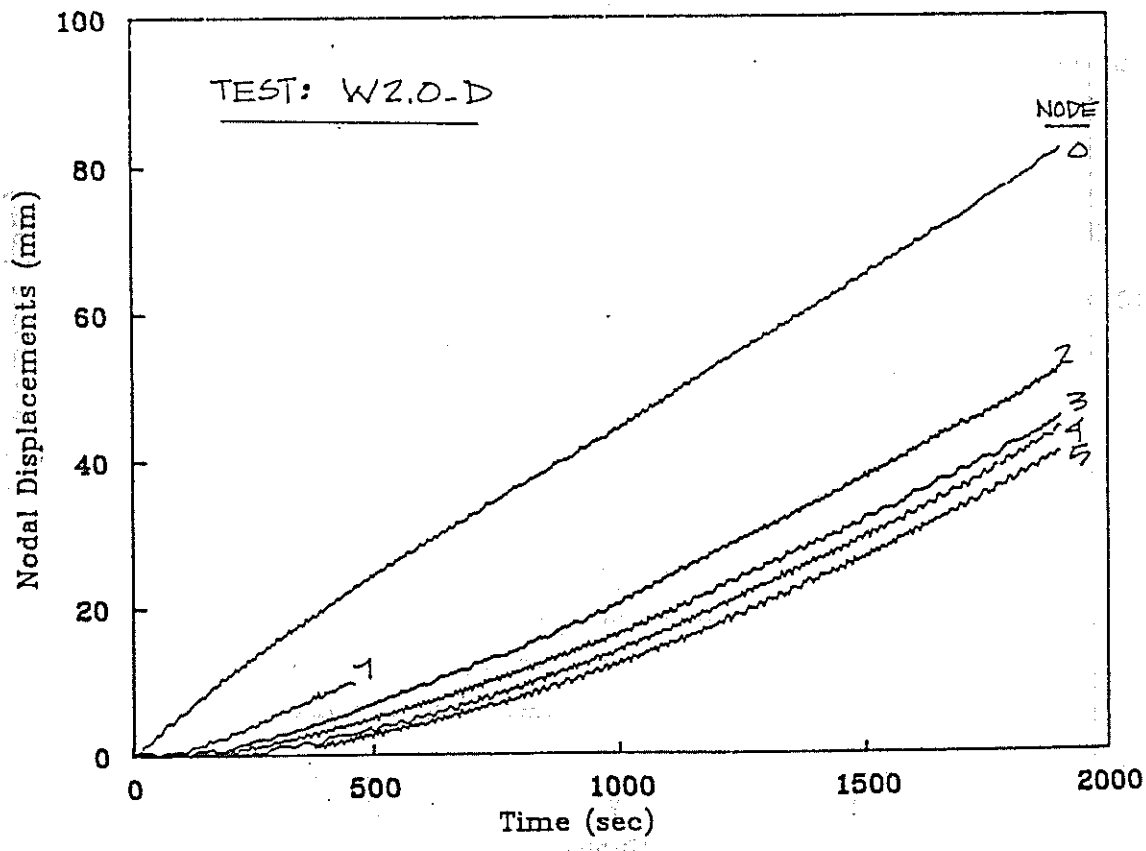
TEST: W2.0_D
NODE
0
2
3
4
5
1
Nodal Displacements (mm)
Time (sec)
0
20
40
60
80
100
0
500
1000
1500
2000

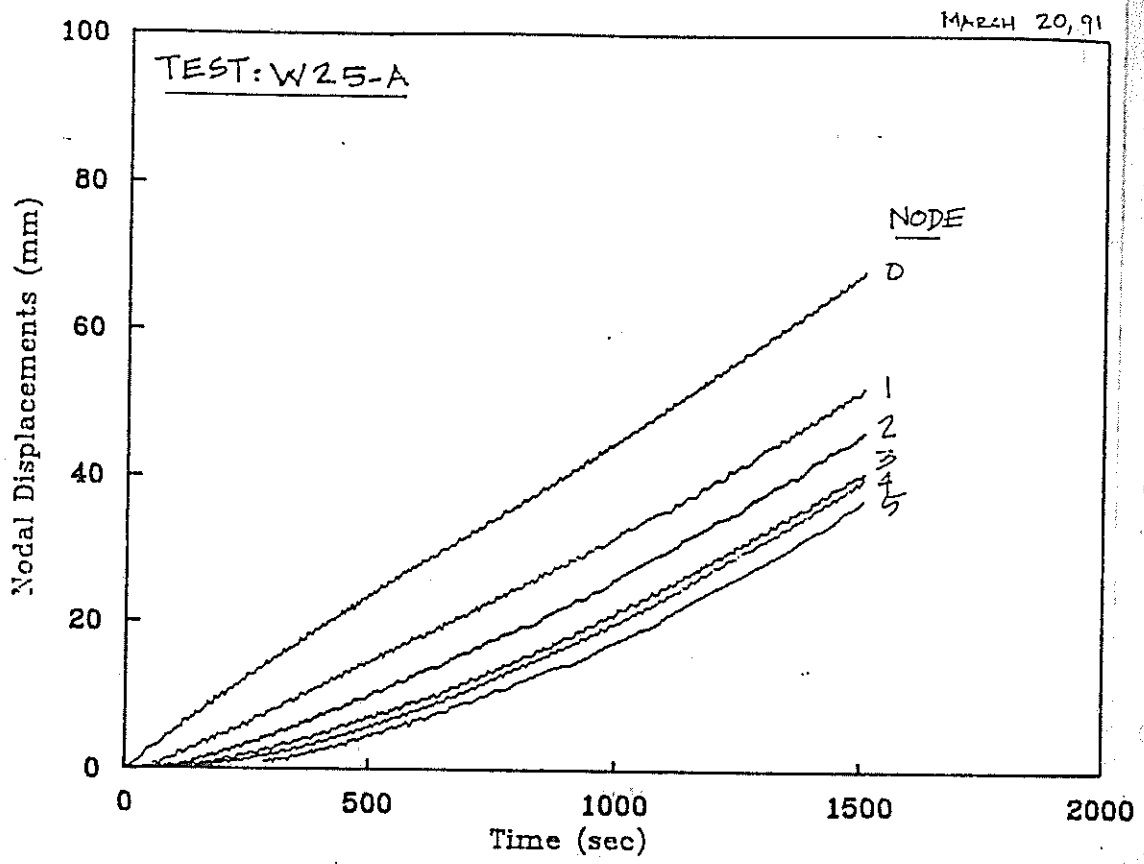
MARCH 20, 91
TEST: W2.5-A
NODE
D
1
2
3
4
5
Nodal Displacements (mm)
Time (sec)
0
20
40
60
80
100
0
500
1000
1500
2000

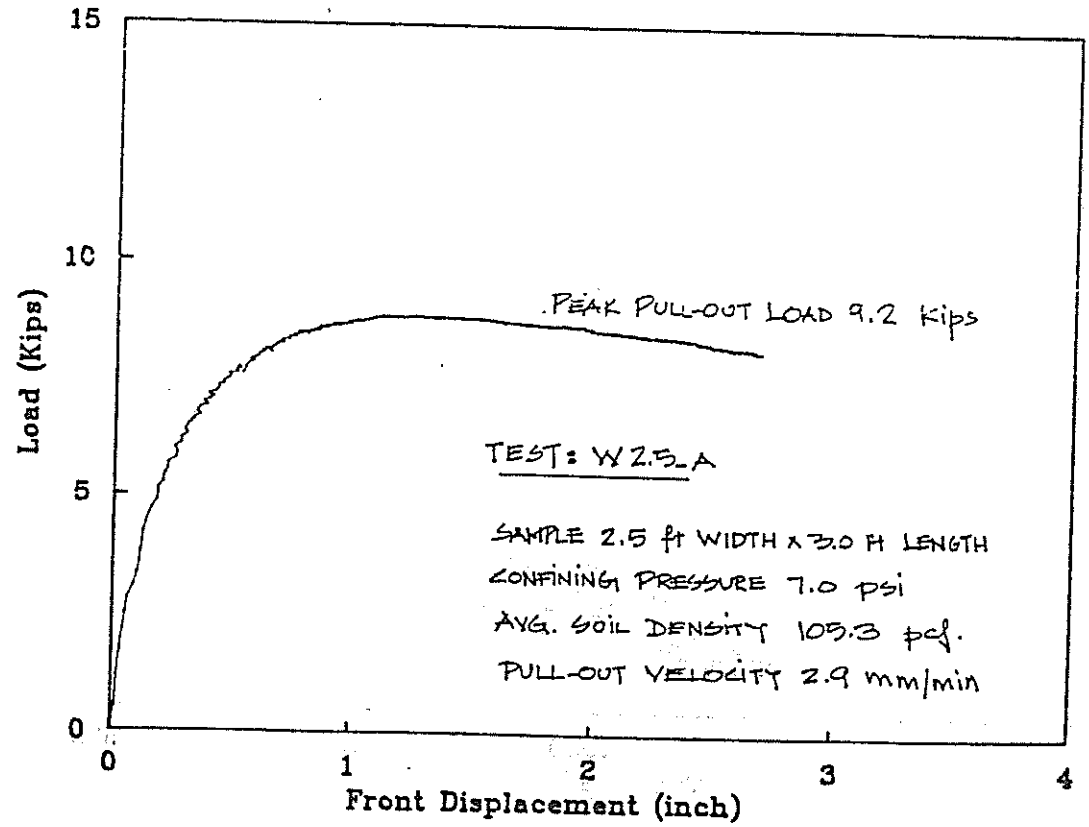
PEAK PULL-OUT LOAD 9.2 kips
TEST: W2.5_A
SAMPLE 2.5 ft WIDTH x 3.0 ft LENGTH
CONFINING PRESSURE 7.0 psi
AVG. SOIL DENSITY 105.3 pcf.
PULL-OUT VELOCITY 2.9 mm/min
Load (Kips)
Front Displacement (inch)
0
5
10
15
0
1
2
3
4

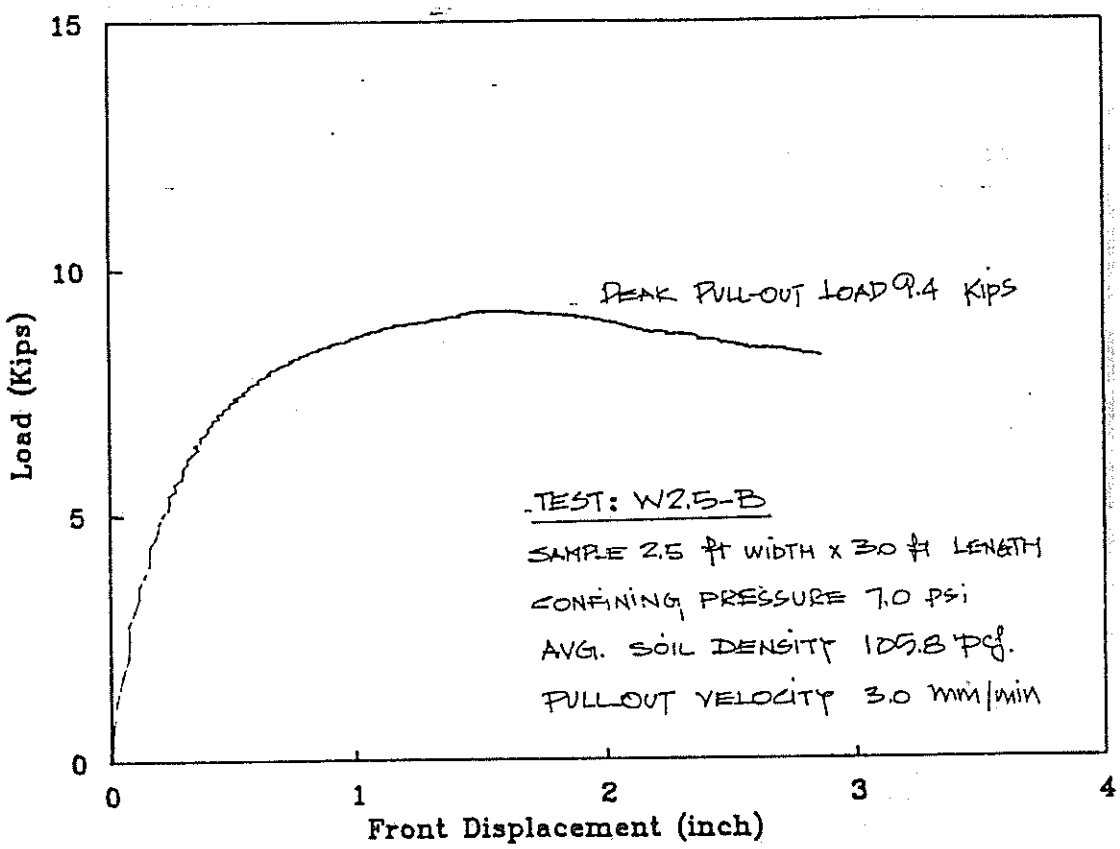
15
10
5
0
Load (Kips)
PEAK PULL-OUT LOAD 9.4 KIPS
TEST: W2.5-B
SAMPLE 2.5 ft WIDTH x 30 ft LENGTH
CONFINING PRESSURE 7.0 psi
AVG. SOIL DENSITY 109.8 pcf.
PULLOUT VELOCITY 3.0 mm/min
0
1
2
3
4
Front Displacement (inch)

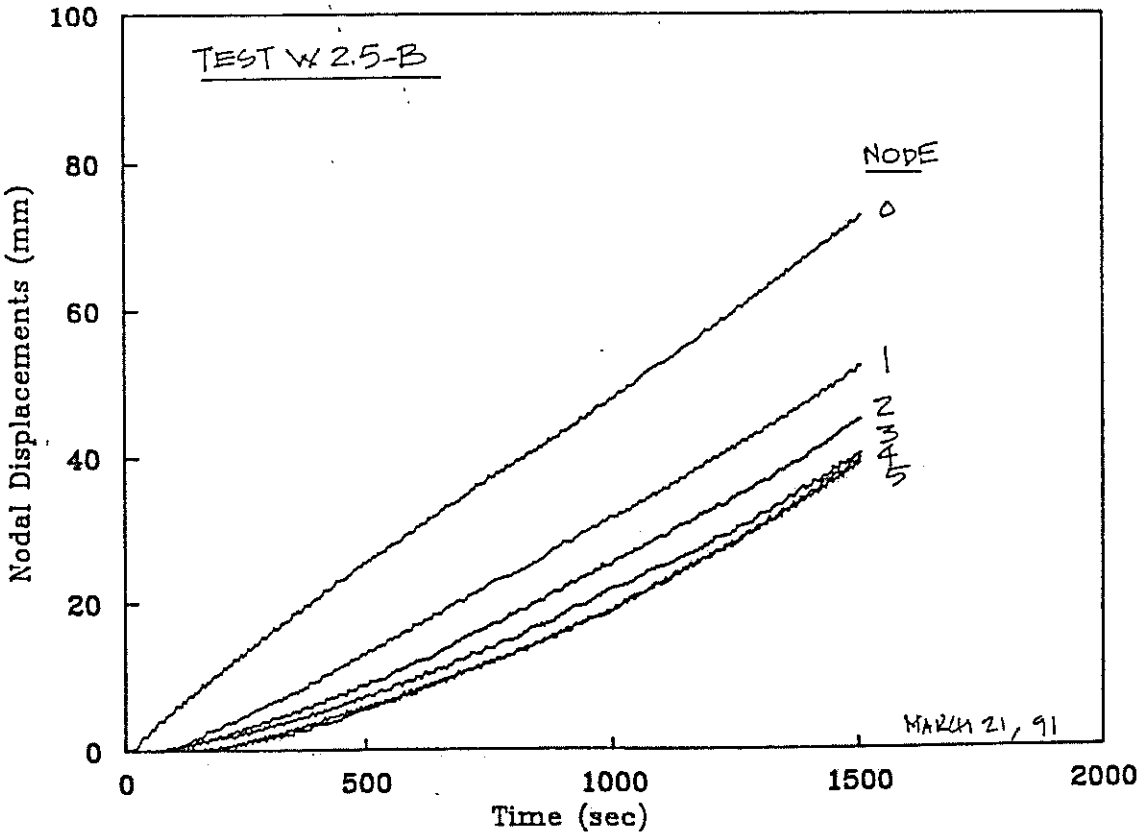
100
80
60
40
20
0
Nodal Displacements (mm)
TEST W 2.5-B
NODE
0
1
2
3
4
5
MARCH 21, 91
0
500
1000
1500
2000
Time (sec)

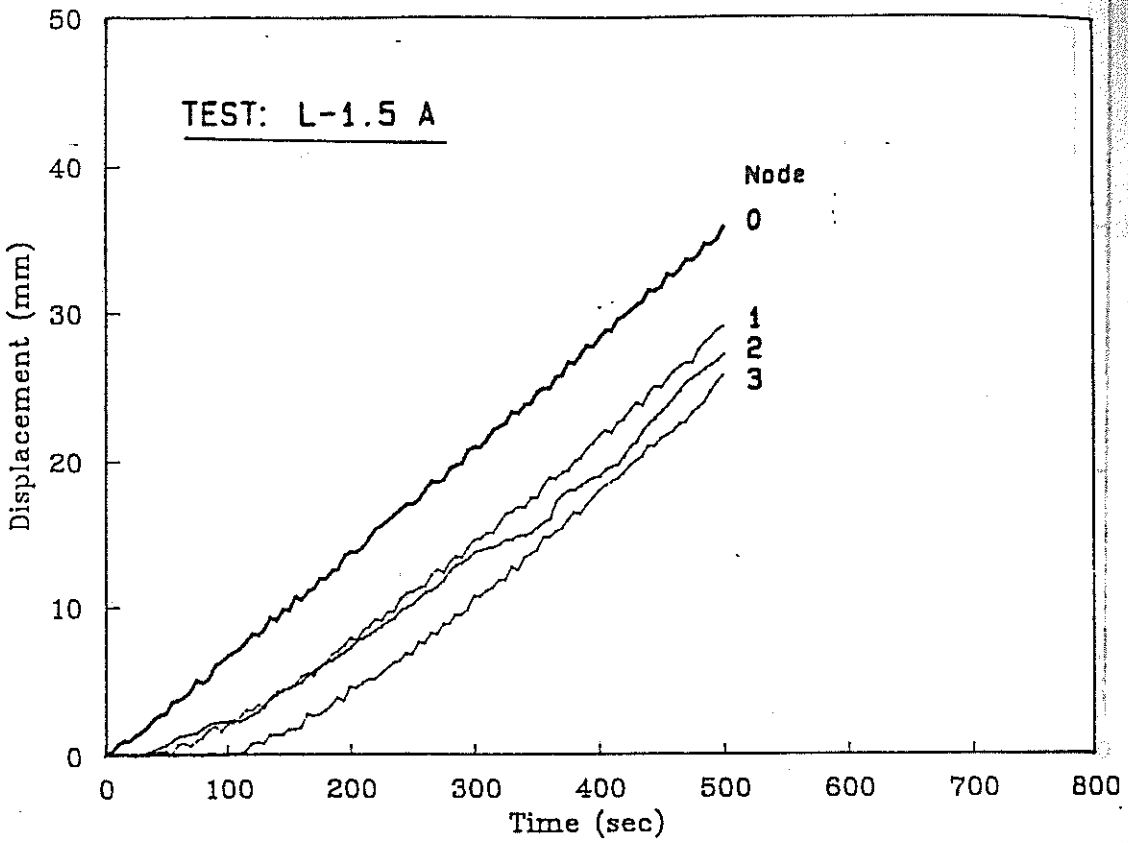
TEST: L-1.5 A
Node
0
1
2
3
Displacement (mm)
Time (sec)
0
10
20
30
40
50
0
100
200
300
400
500
600
700
800

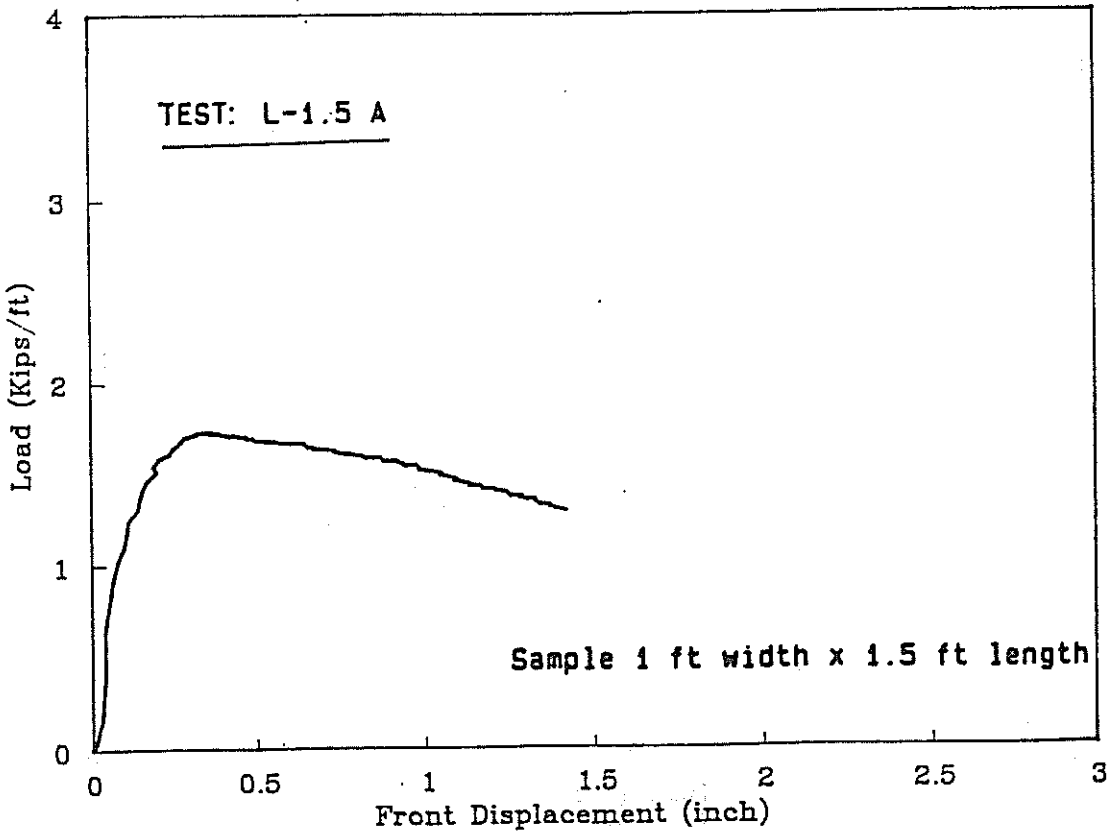
TEST: L-1.5 A
Load (Kips/ft)
Front Displacement (inch)
Sample 1 ft width x 1.5 ft length
0
1
2
3
4
0
0.5
1
1.5
2
2.5
3

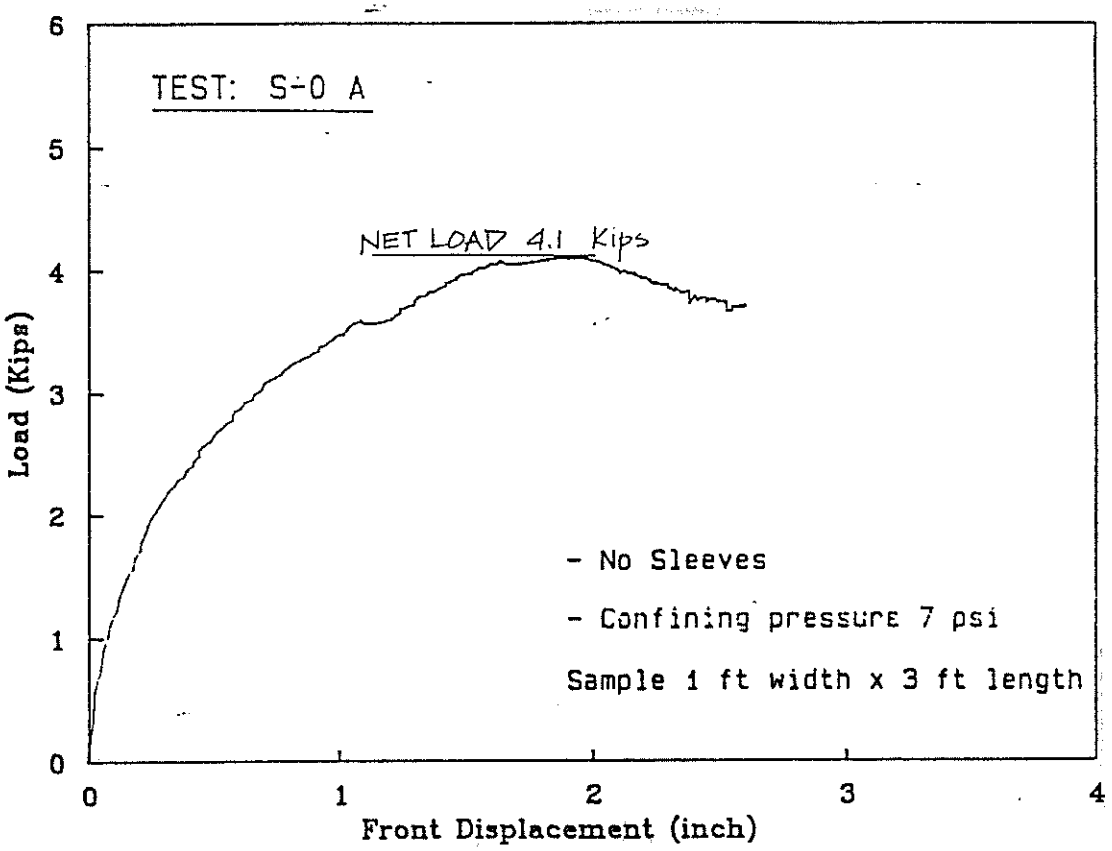
TEST: S-0 A
NET LOAD 4.1 Kips
- No Sleeves
- Confining pressure 7 psi
Sample 1 ft width x 3 ft length
Load (Kips)
Front Displacement (inch)
0
1
2
3
4
5
6

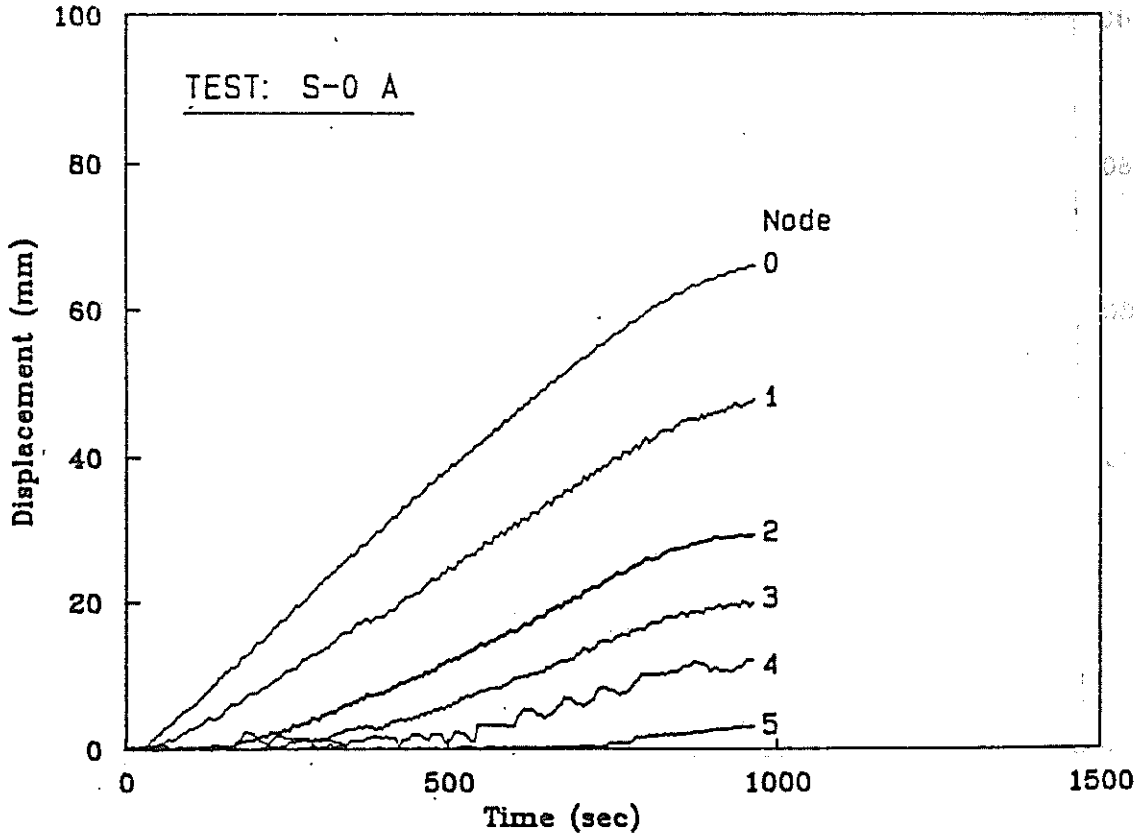
TEST: S-0 A
Node
0
1
2
3
4
5
Displacement (mm)
Time (sec)
0
20
40
60
80
100
500
1000
1500

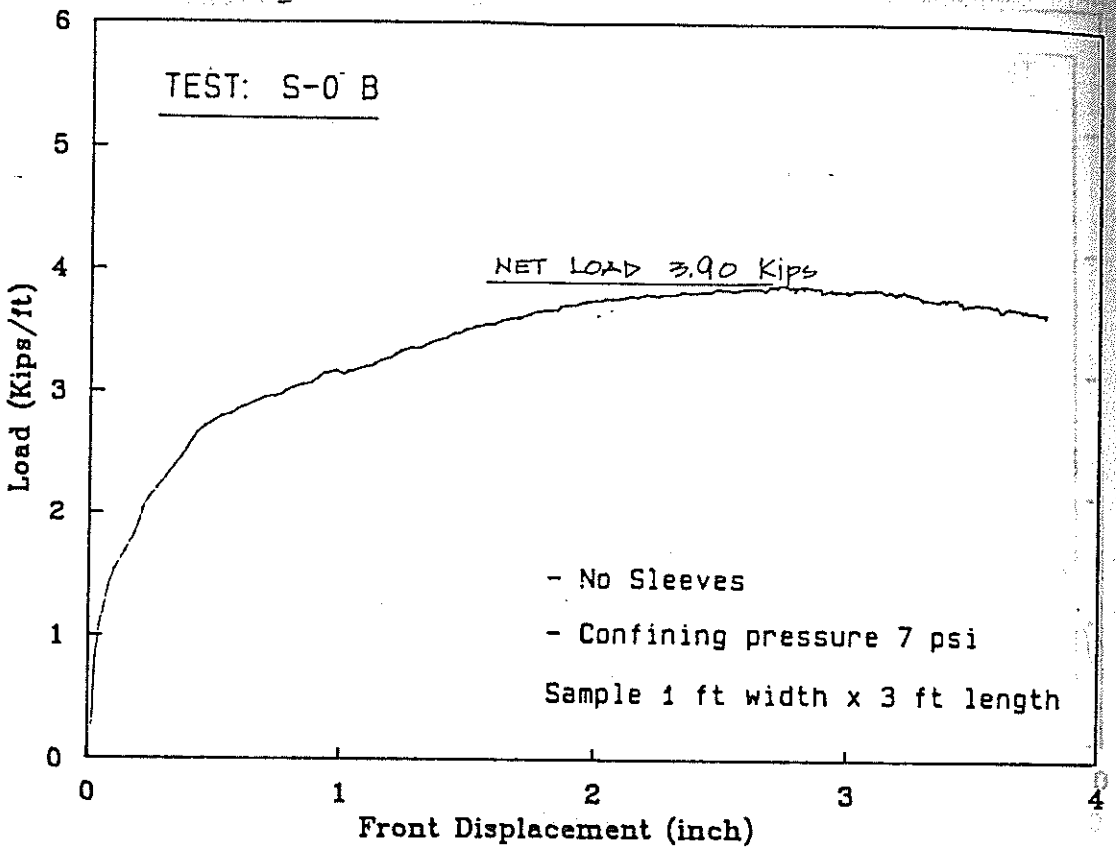
TEST: S-0 B
NET LOAD 3.90 Kips
- No Sleeves
- Confining pressure 7 psi
Sample 1 ft width x 3 ft length
Load (Kips/ft)
Front Displacement (inch)
0
1
2
3
4
5
6

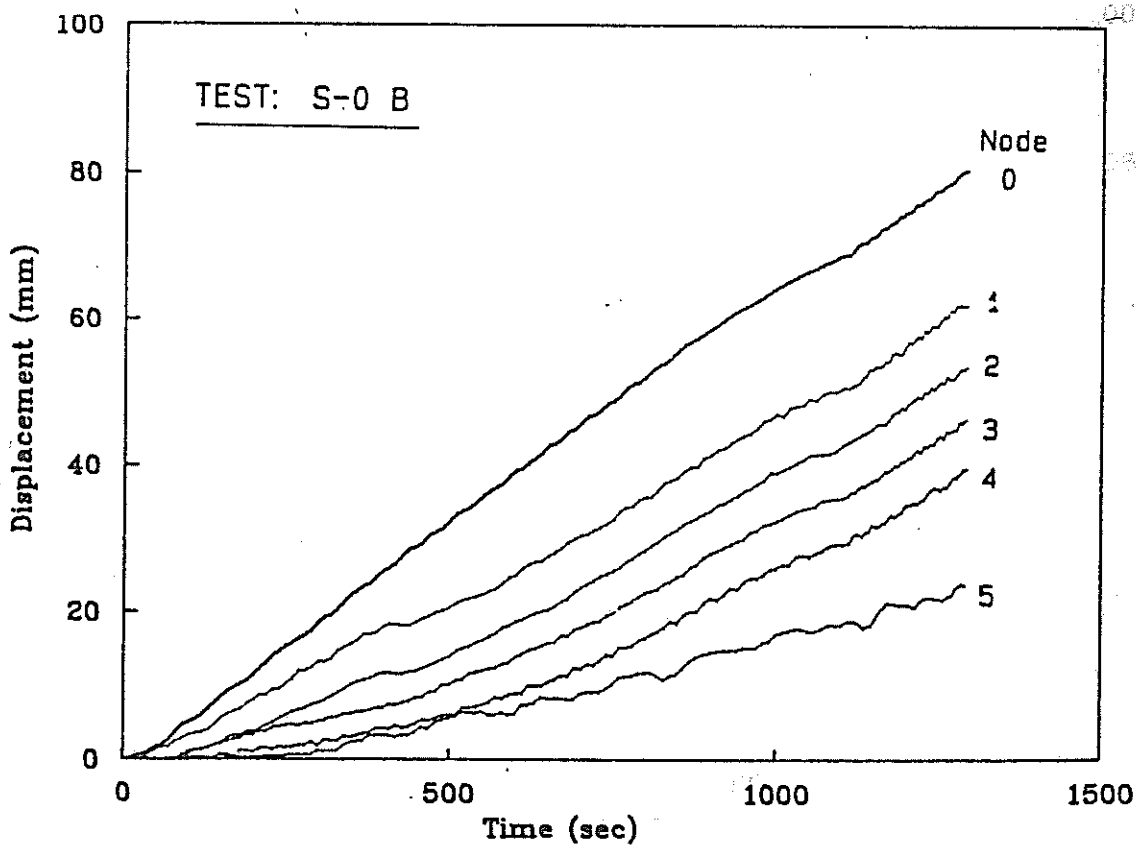
TEST: S-0 B
Node
0
1
2
3
4
5
Displacement (mm)
Time (sec)
0
20
40
60
80
100
500
1000
1500

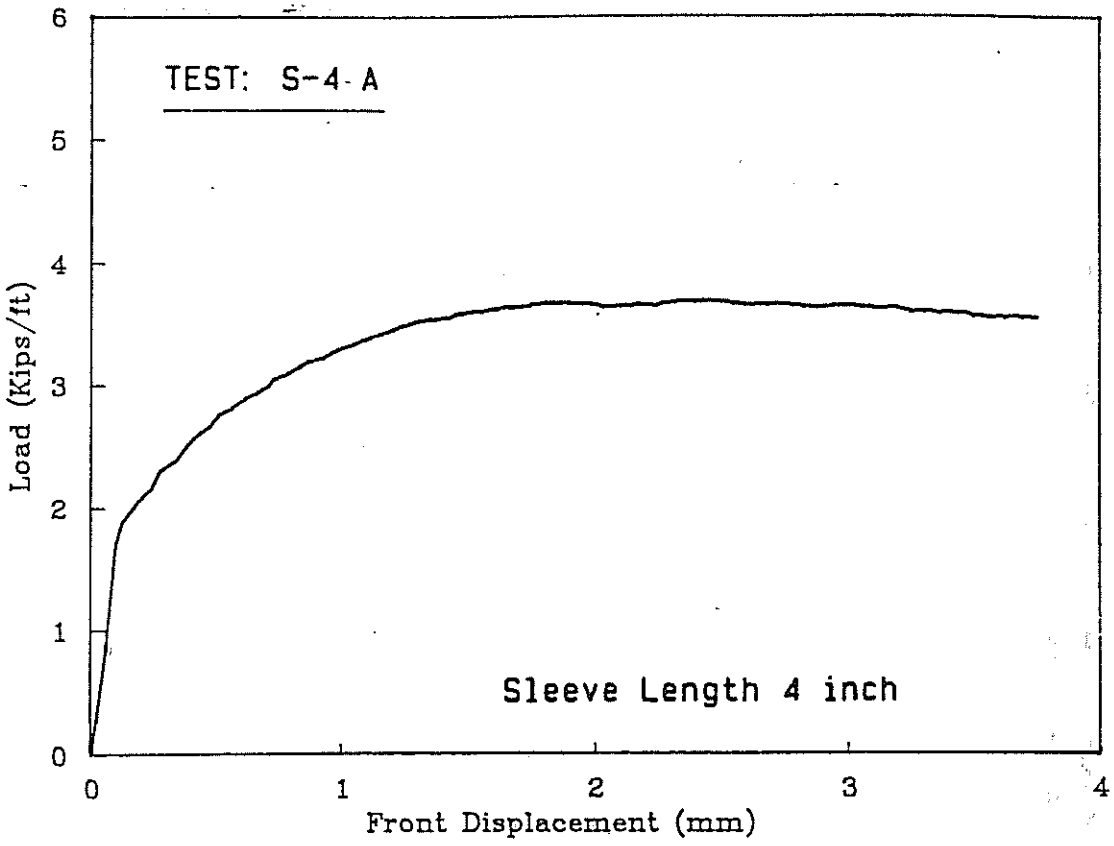
TEST: S-4-A
Load (Kips/ft)
Front Displacement (mm)
Sleeve Length 4 inch
0
1
2
3
4
5
6

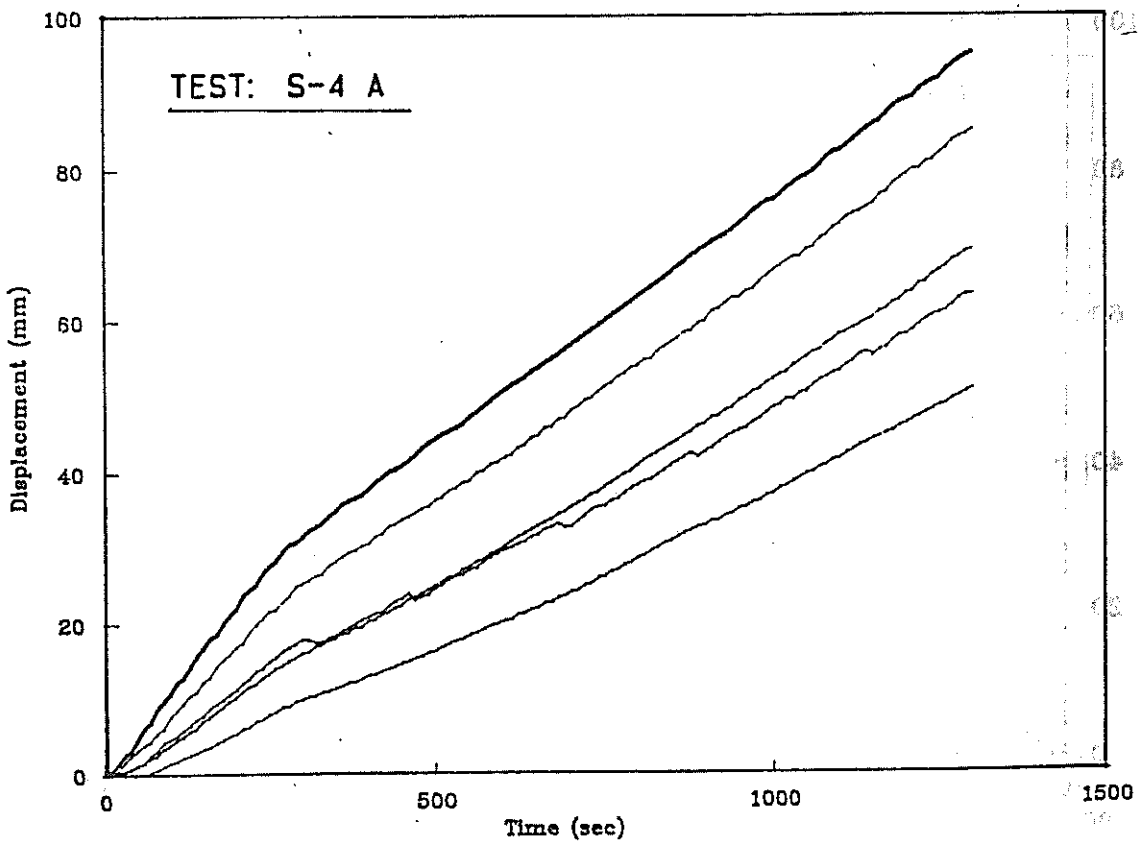
TEST: S-4 A
Displacement (mm)
Time (sec)
0
20
40
60
80
100
500
1000
1500

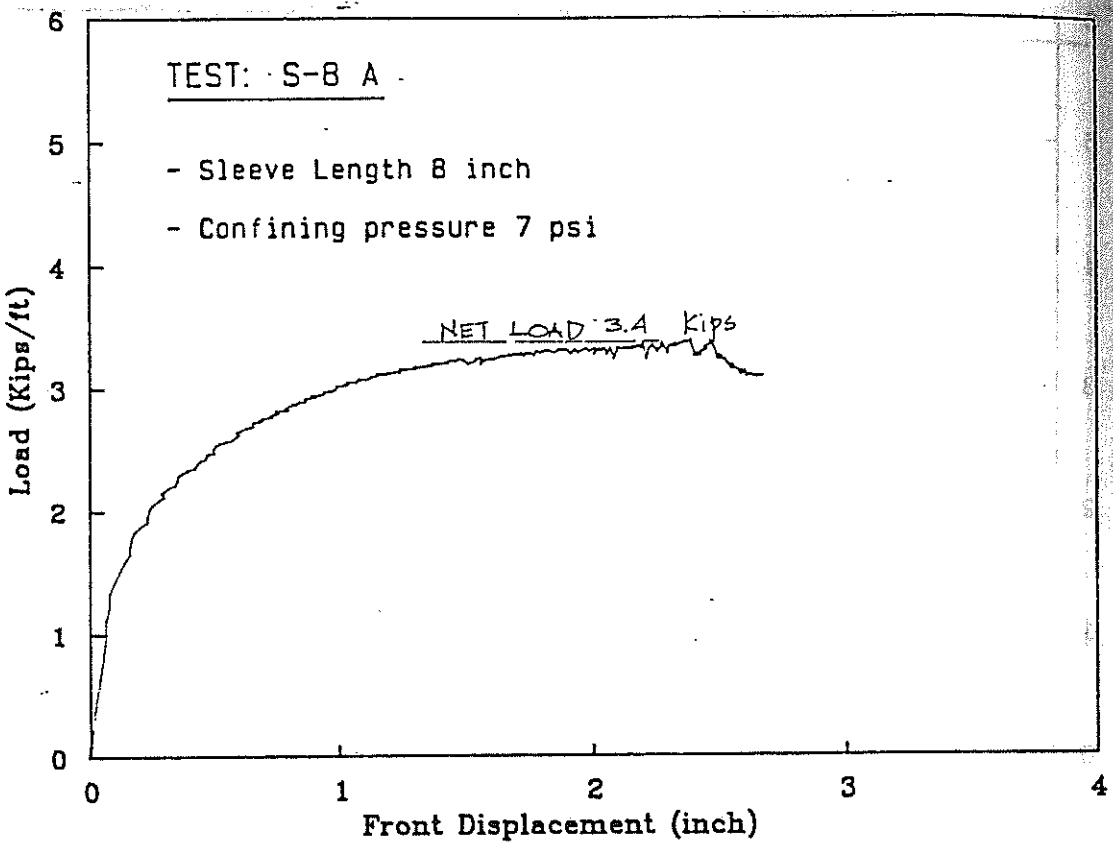
TEST: S-8 A
- Sleeve Length 8 inch
- Confining pressure 7 psi
NET LOAD 3.4 Kips
Load (Kips/ft)
Front Displacement (inch)
0
1
2
3
4
5
6

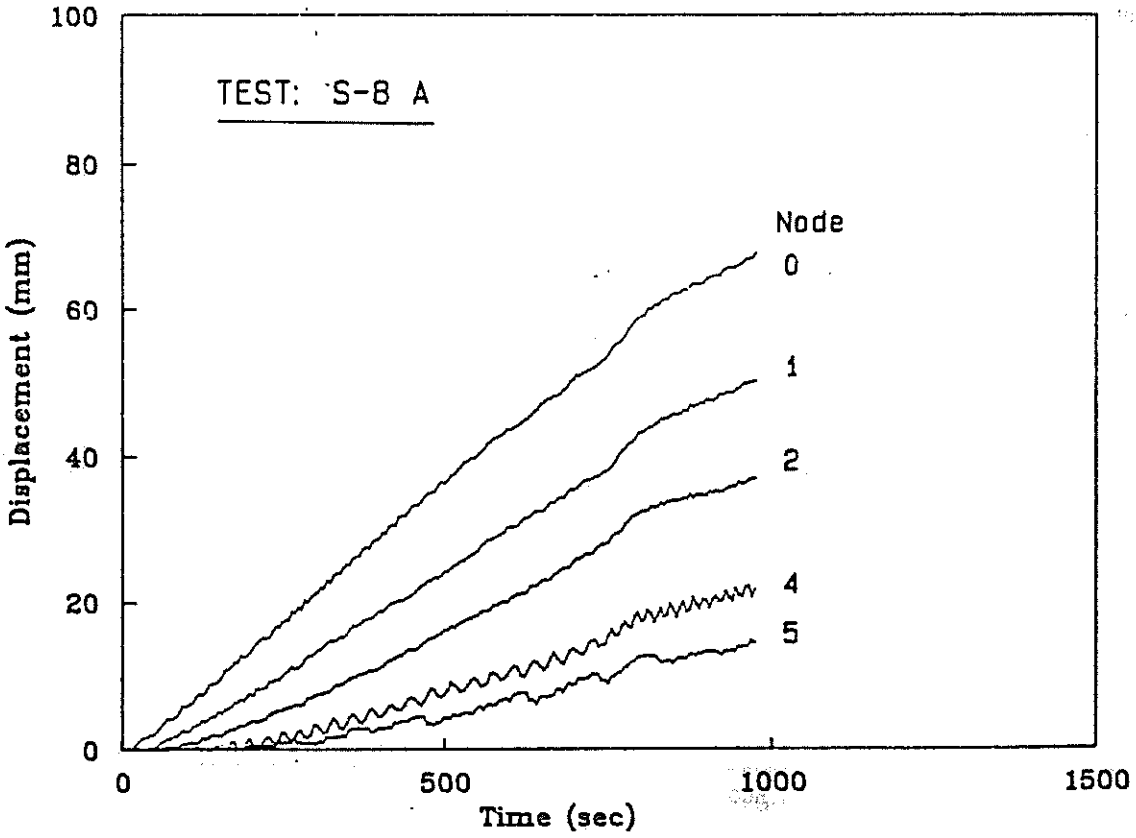
TEST: S-8 A
Node
0
1
2
4
5
Displacement (mm)
Time (sec)
0
20
40
60
80
100
500
1000
1500

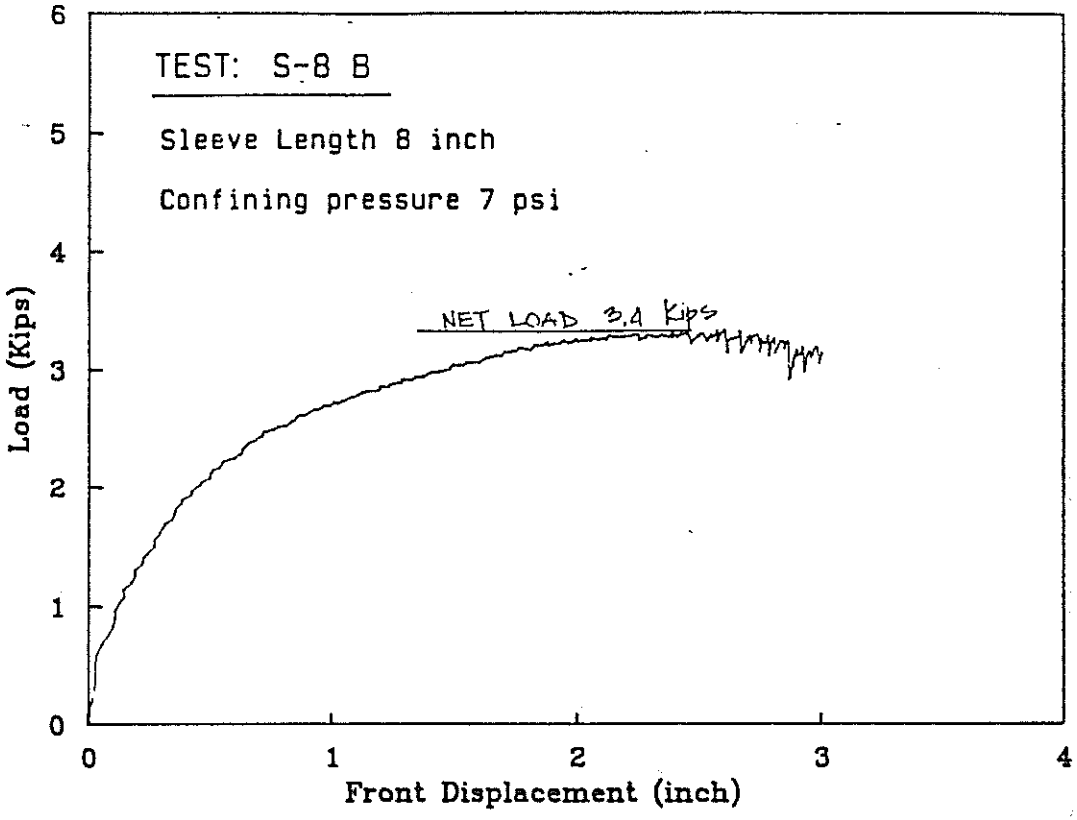
TEST: S-8 B
Sleeve Length 8 inch
Confining pressure 7 psi
NET LOAD 3.4 Kips
Load (Kips)
Front Displacement (inch)
0
1
2
3
4
5
6

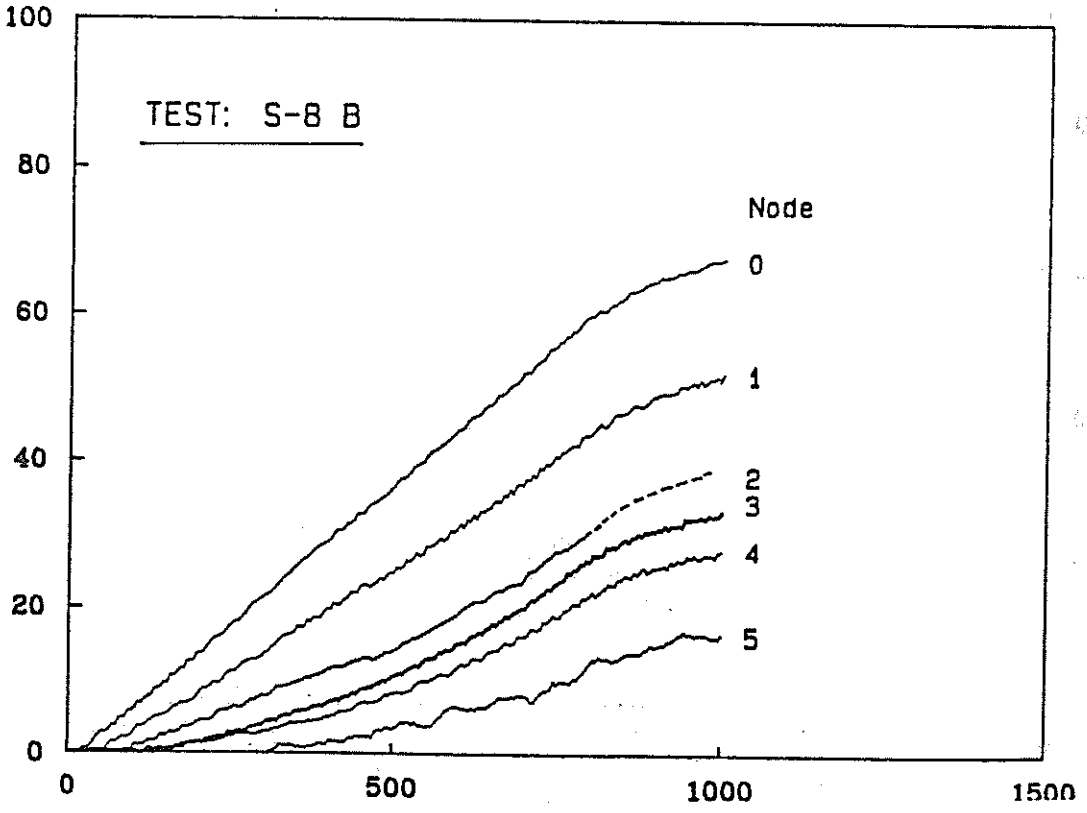
TEST: S-8 B
Node
0
1
2
3
4
5
0
20
40
60
80
100
500
1000
1500

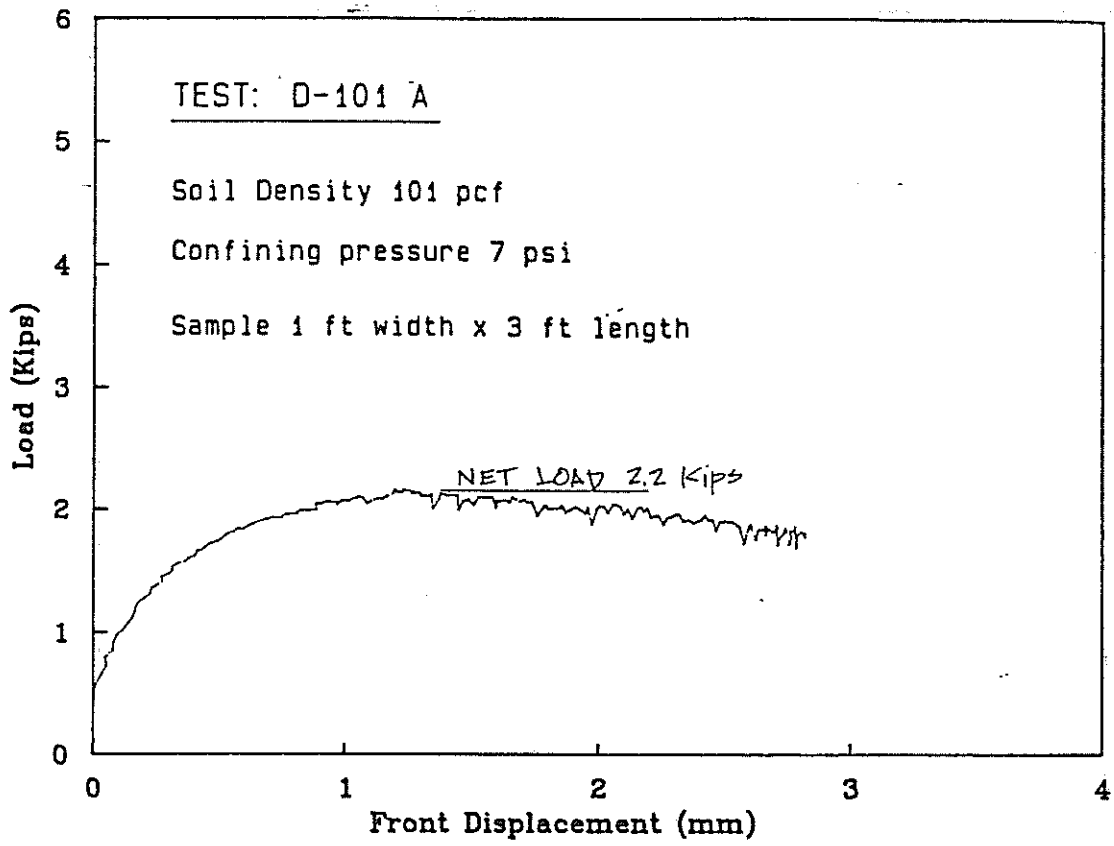
TEST: D-101 A
Soil Density 101 pcf
Confining pressure 7 psi
Sample 1 ft width x 3 ft length
NET LOAD 2.2 Kips
Load (Kips)
Front Displacement (mm)
0
1
2
3
4
5
6

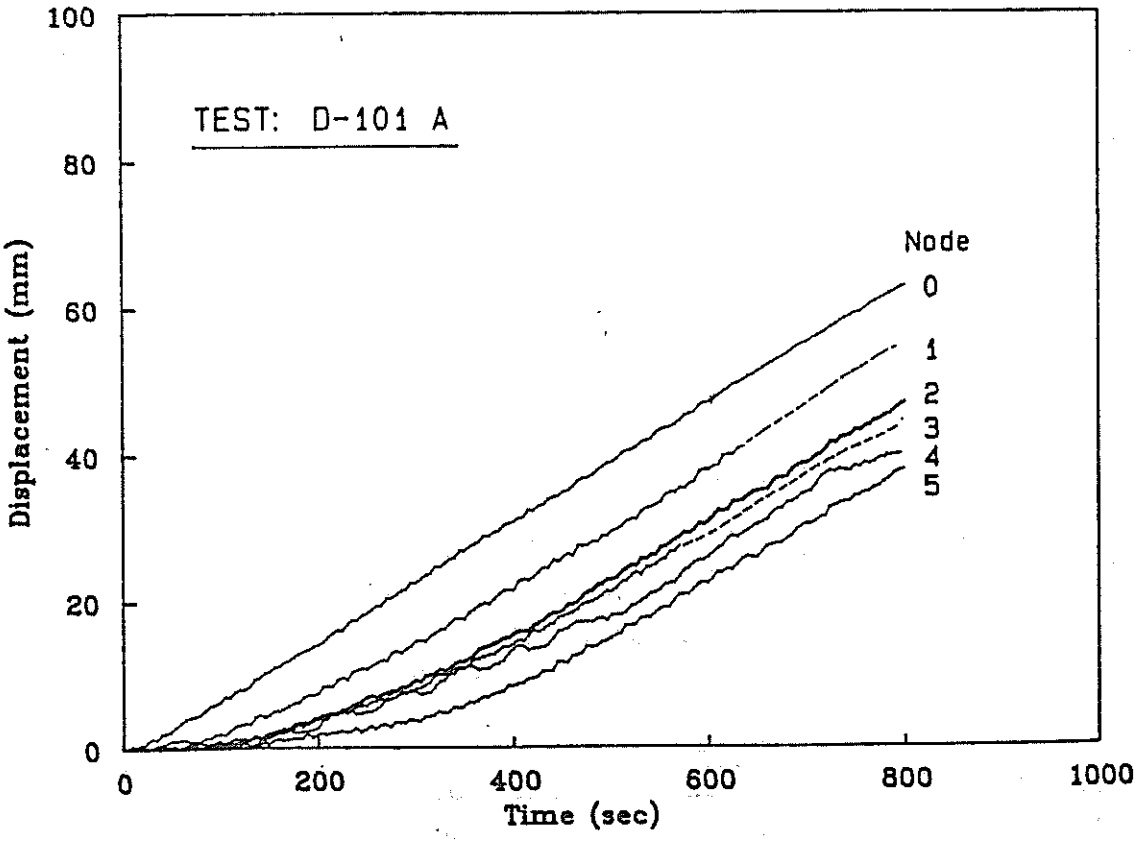
TEST: D-101 A
Node
0
1
2
3
4
5
Displacement (mm)
Time (sec)
0
20
40
60
80
100
200
400
600
800
1000

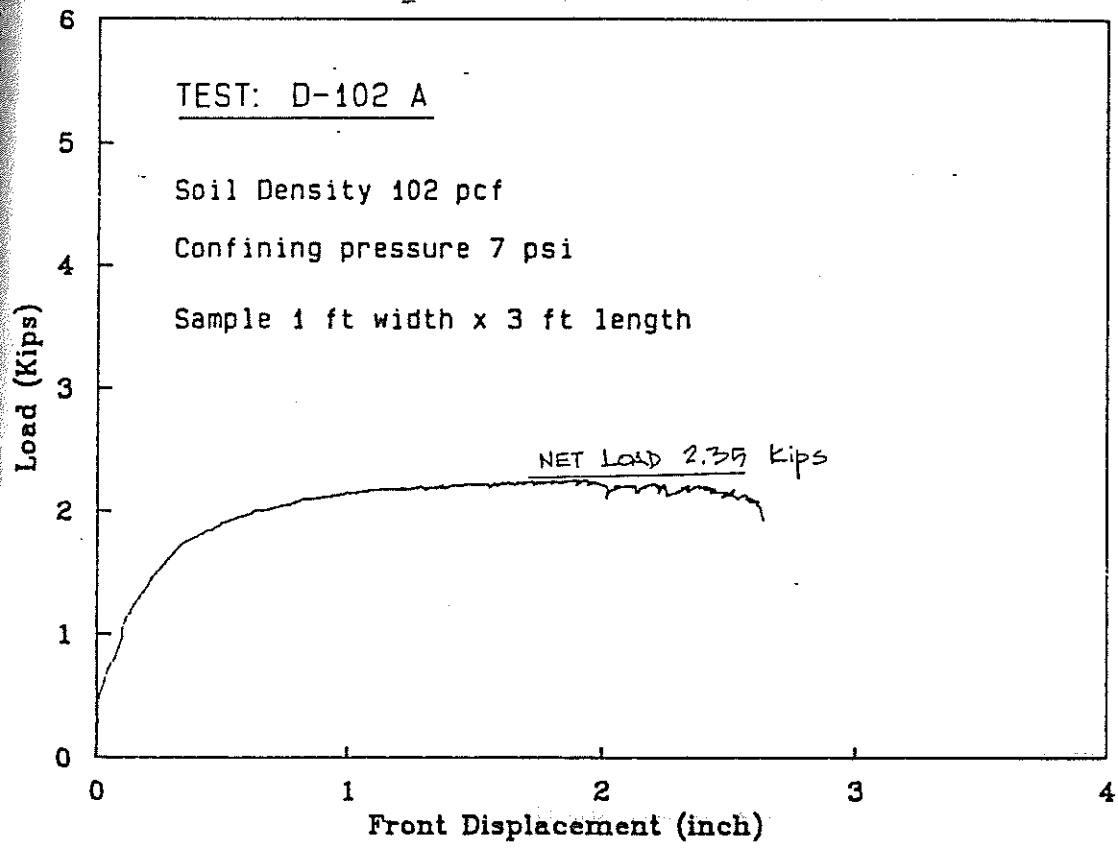
TEST: D-102 A
Soil Density 102 pcf
Confining pressure 7 psi
Sample 1 ft width x 3 ft length
NET Load 2.39 Kips
Load (Kips)
Front Displacement (inch)
0
1
2
3
4
5
6

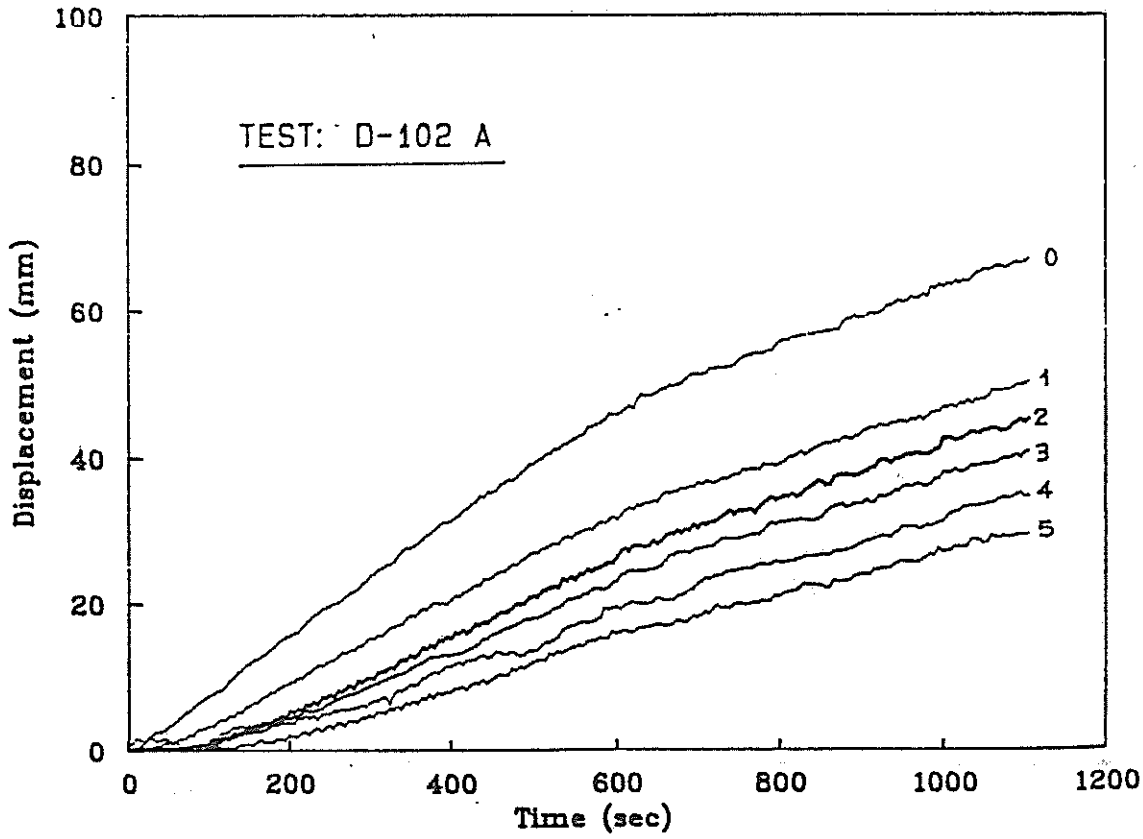
TEST: D-102 A
Displacement (mm)
Time (sec)
0
200
400
600
800
1000
1200
20
40
60
80
100
0
1
2
3
4
5

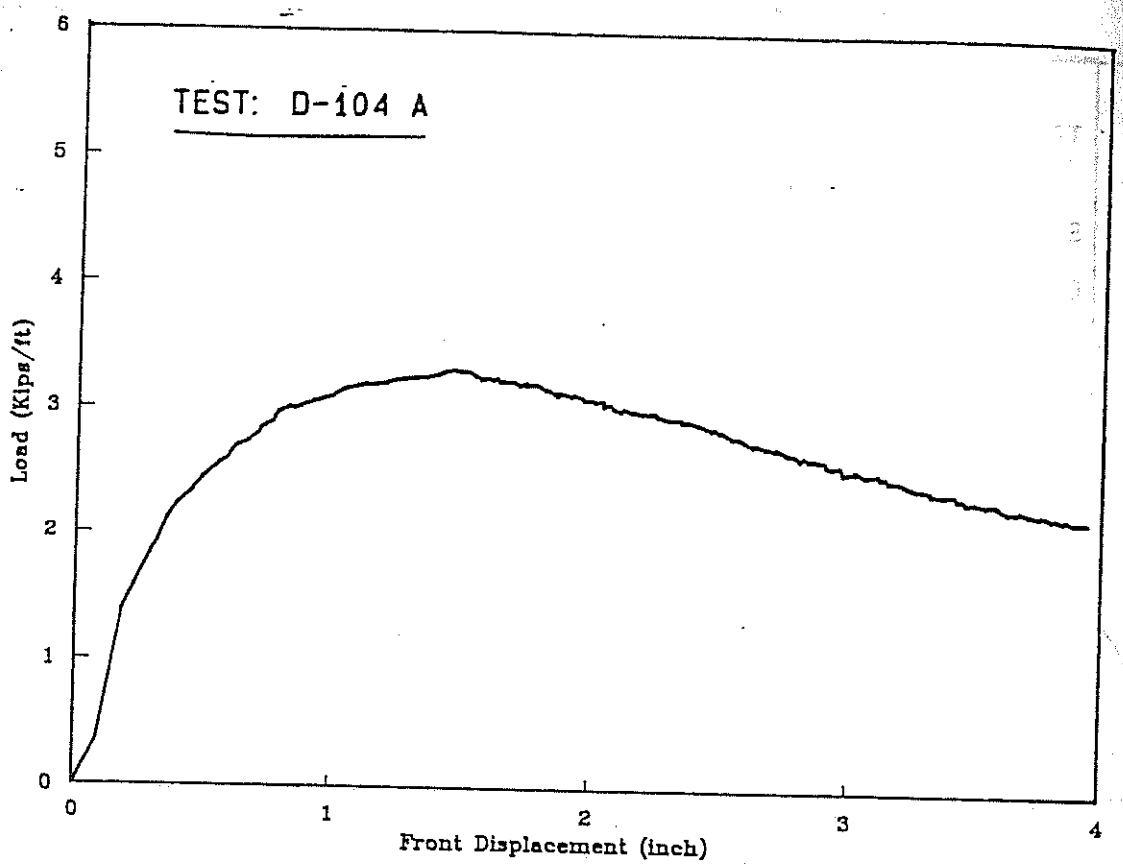
TEST: D-104 A
Load (Kips/ft)
Front Displacement (inch)
0
1
2
3
4
5
6

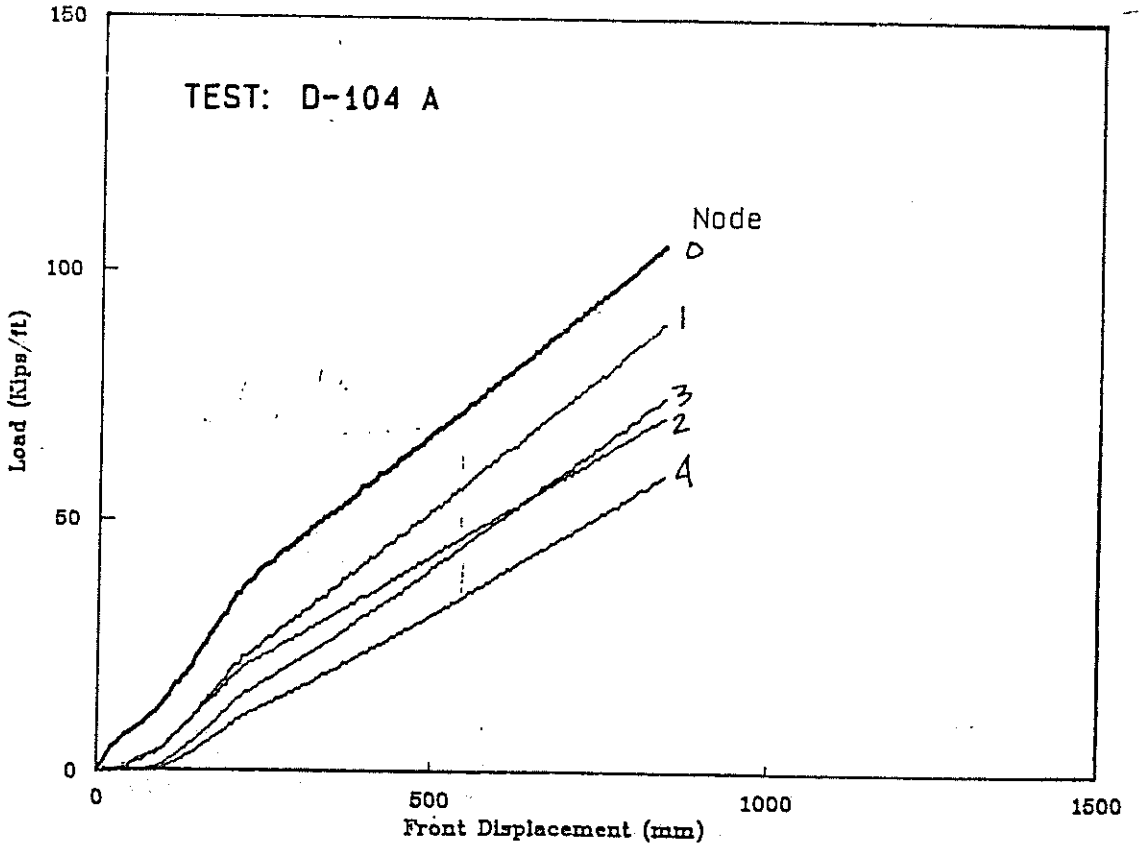
TEST: D-104 A
Node
0
1
2
3
4
Load (Kips/ft)
Front Displacement (mm)
0
50
100
150
500
1000
1500

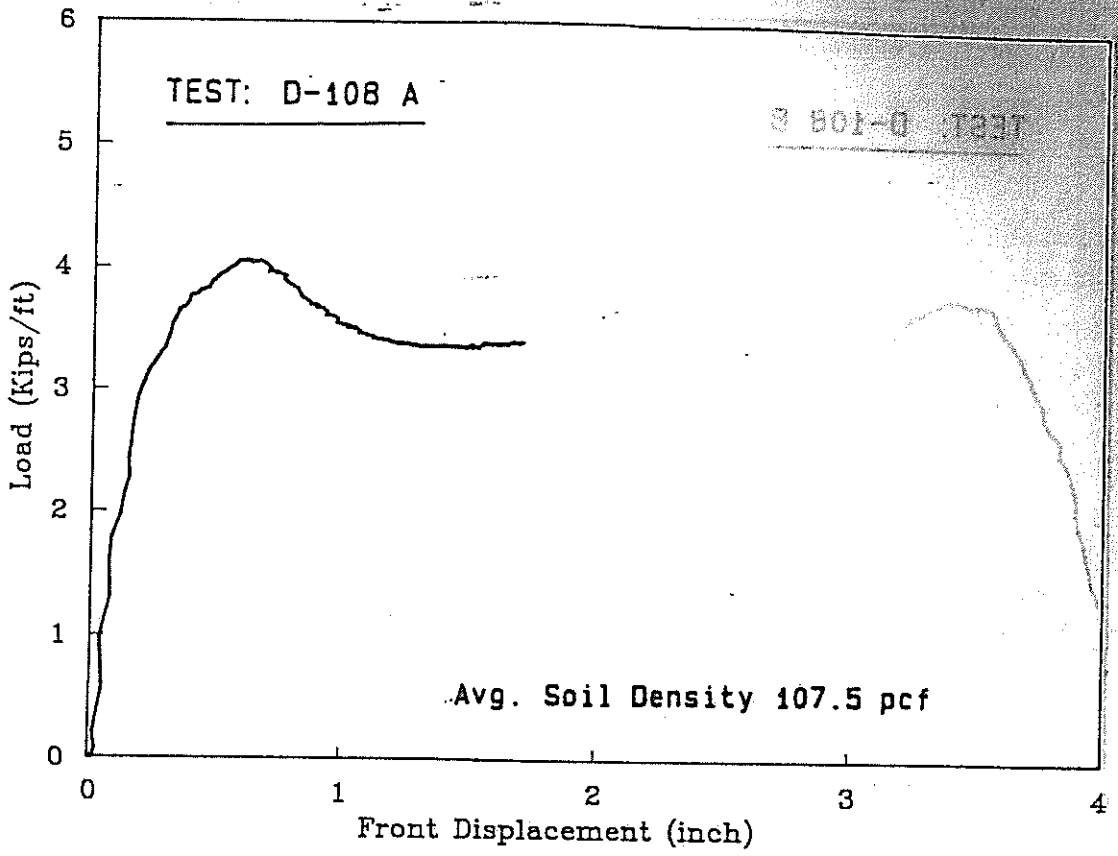
TEST: D-108 A
Load (Kips/ft)
Front Displacement (inch)
Avg. Soil Density 107.5 pcf
0
1
2
3
4
5
6

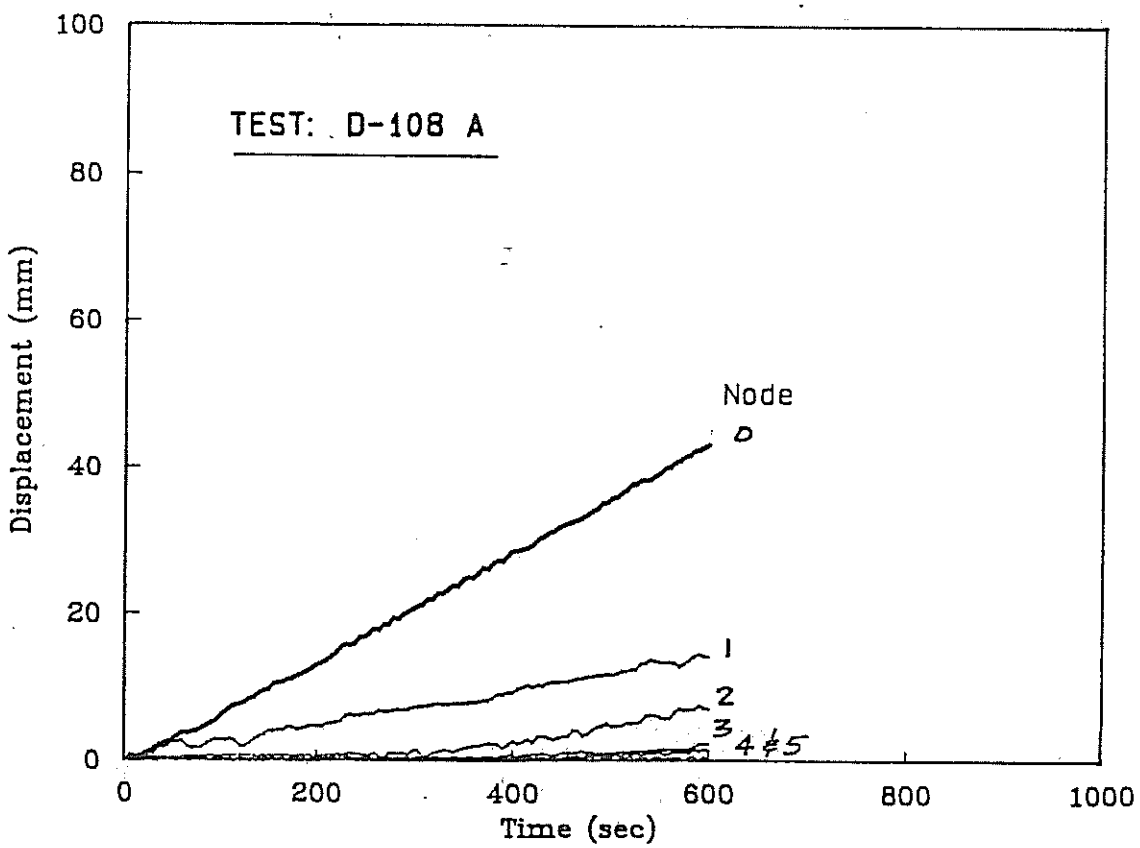
TEST: D-108 A
Displacement (mm)
Time (sec)
Node
0
1
2
3
4&5
0
20
40
60
80
100
200
400
600
800
1000

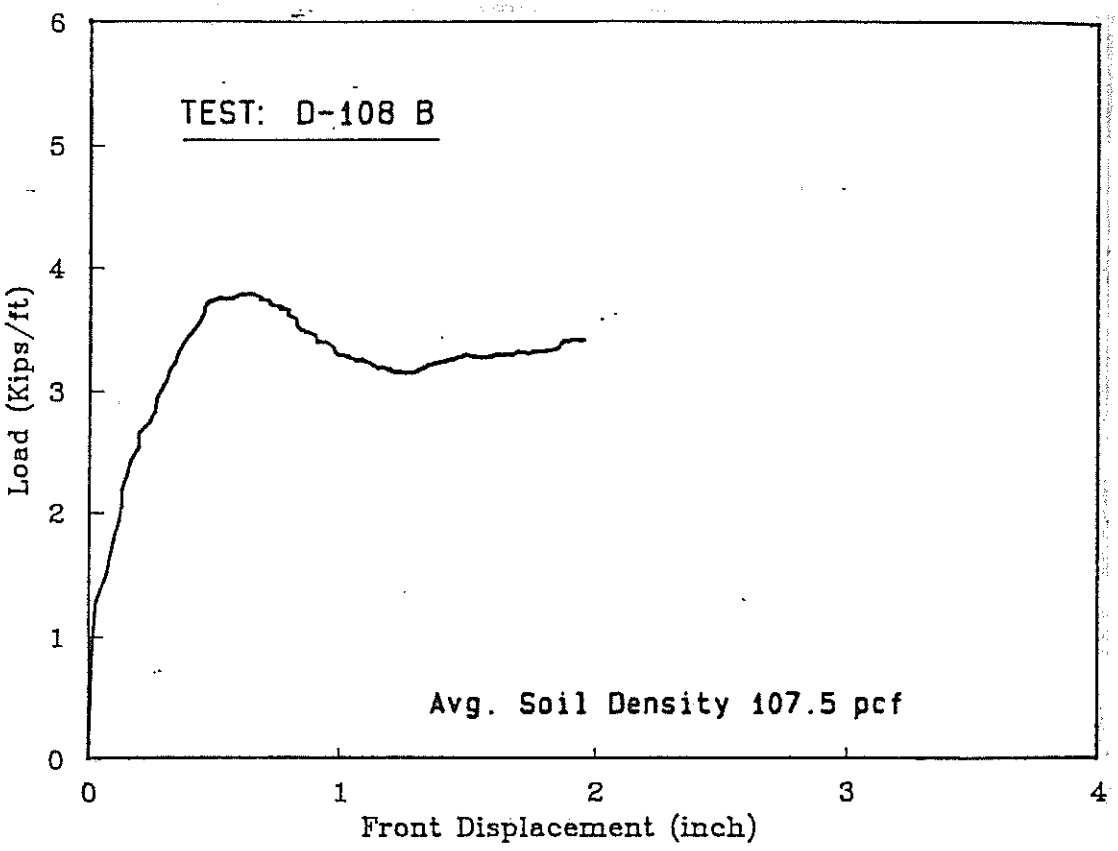
TEST: D-108 B
Load (Kips/ft)
Front Displacement (inch)
Avg. Soil Density 107.5 pcf
0
1
2
3
4
5
6

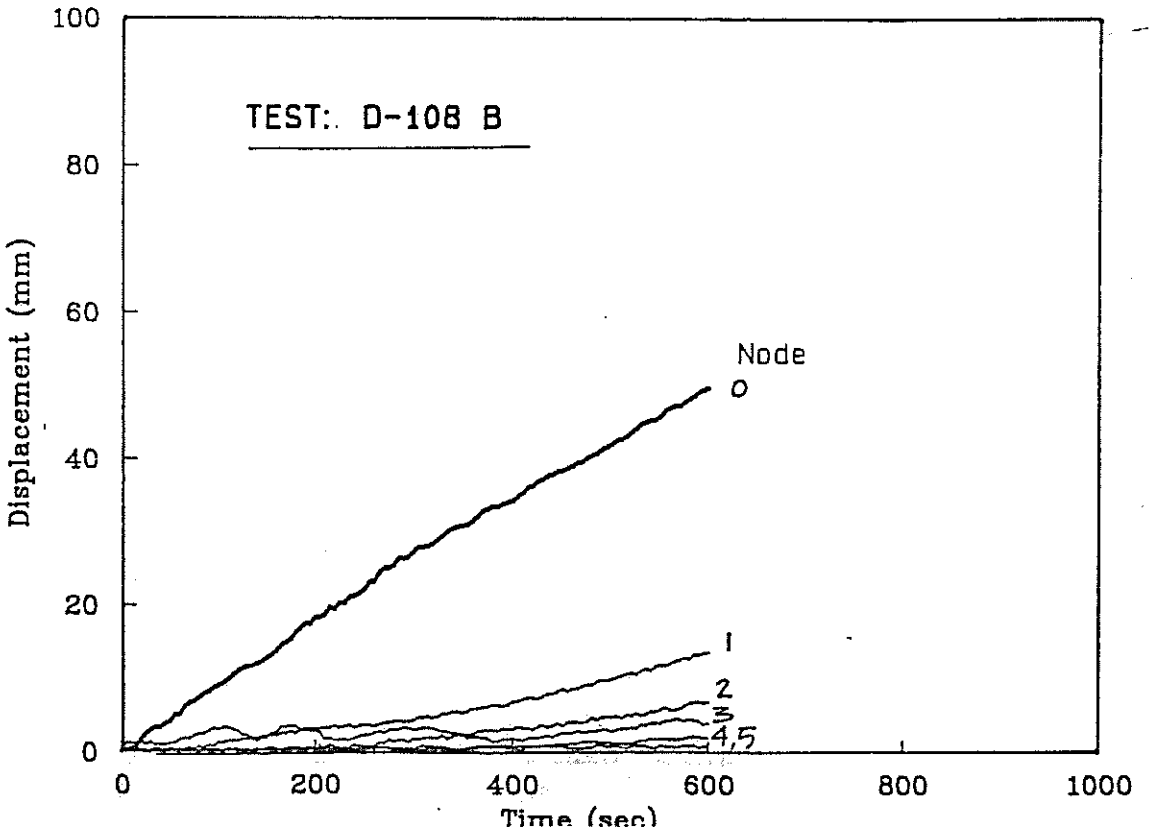
TEST: D-108 B
Displacement (mm)
Time (sec)
Node
0
1
2
3
4,5
0
20
40
60
80
100
200
400
600
800
1000

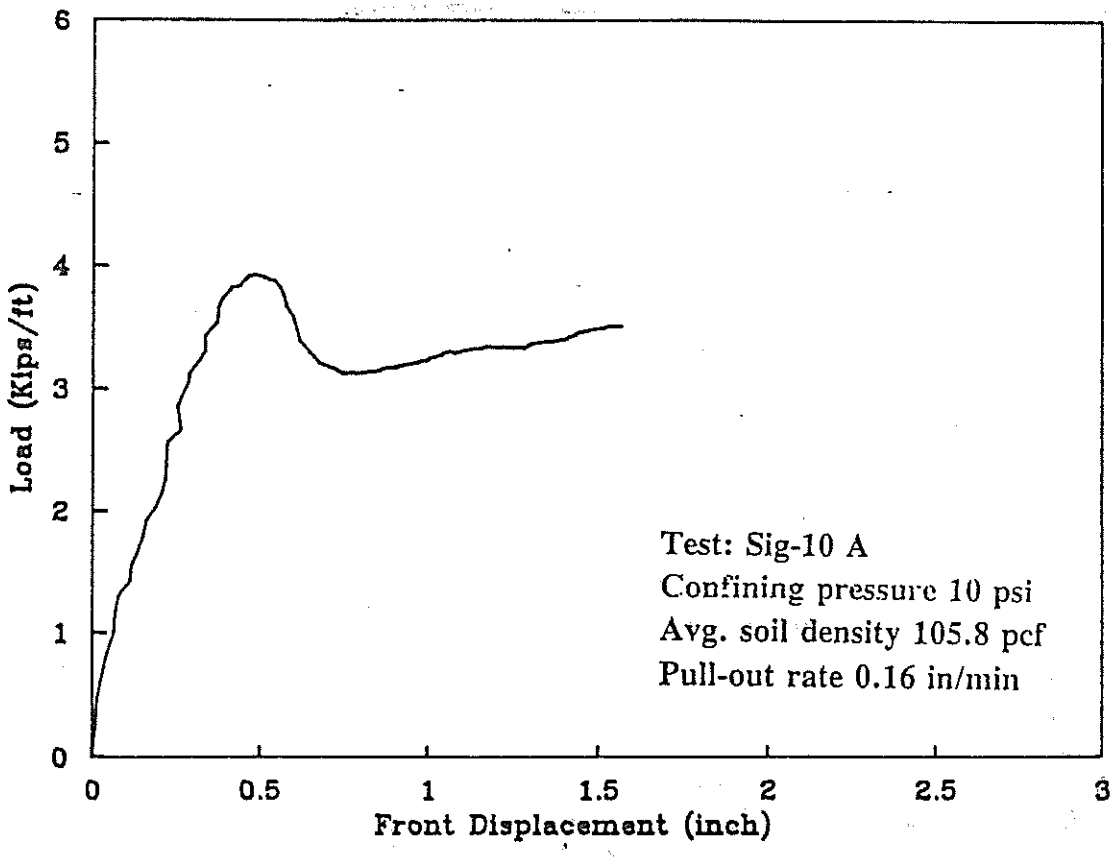
Load (Kips/ft)
Front Displacement (inch)
Test: Sig-10 A
Confining pressure 10 psi
Avg. soil density 105.8 pcf
Pull-out rate 0.16 in/min

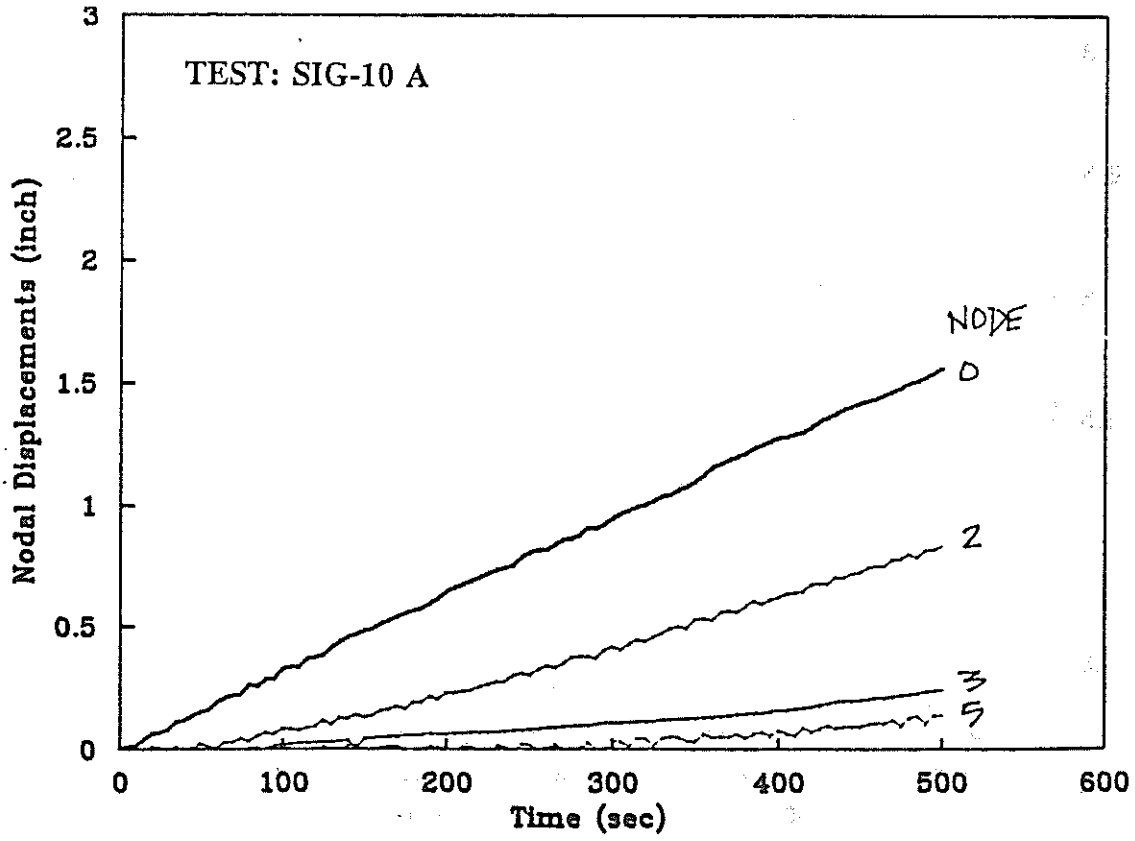
TEST: SIG-10 A
Nodal Displacements (inch)
Time (sec)
NODE
0
2
3
5

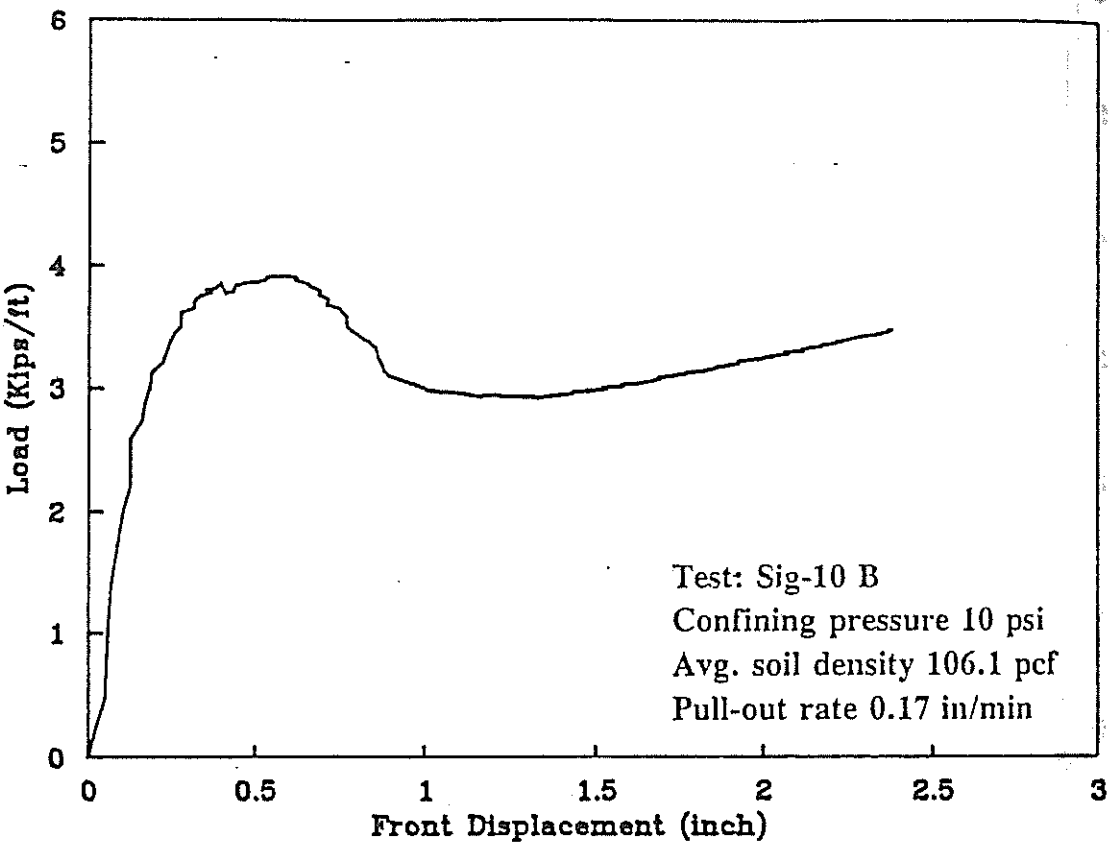
Load (Kips/ft)
Front Displacement (inch)
Test: Sig-10 B
Confining pressure 10 psi
Avg. soil density 106.1 pcf
Pull-out rate 0.17 in/min

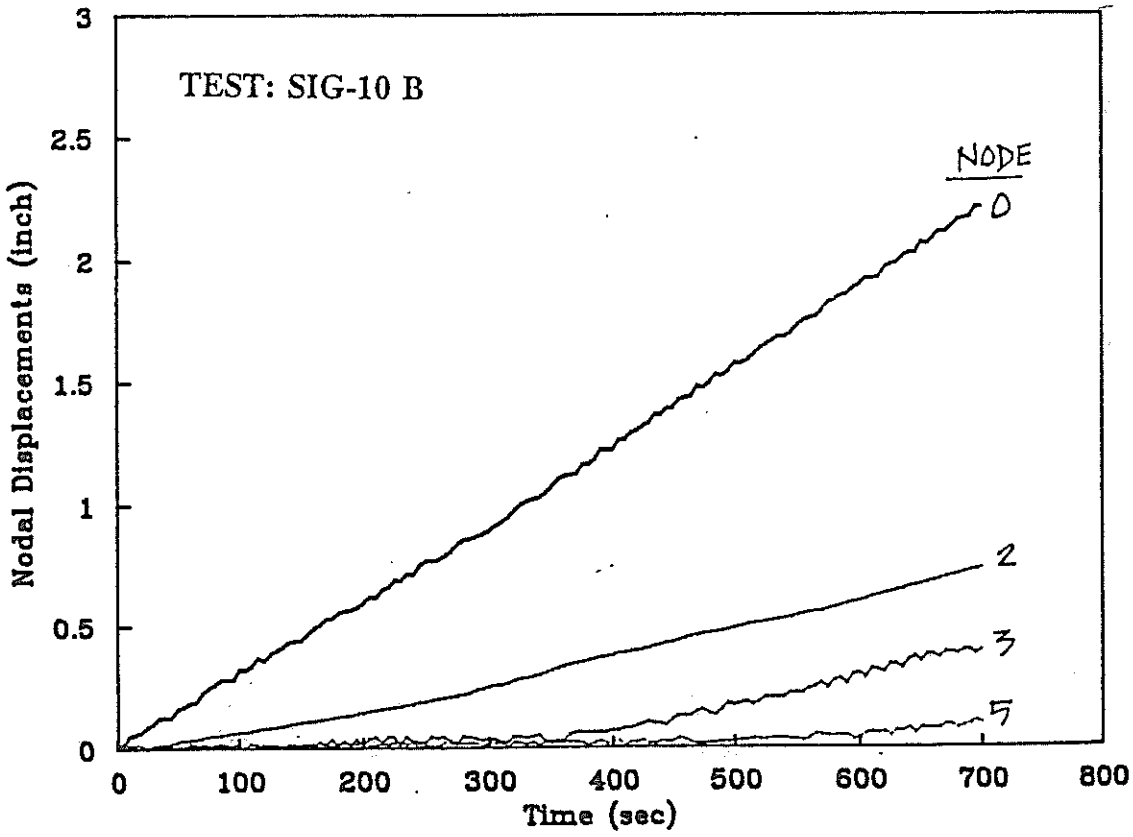
TEST: SIG-10 B
NODE
0
2
3
5
Nodal Displacements (inch)
Time (sec)

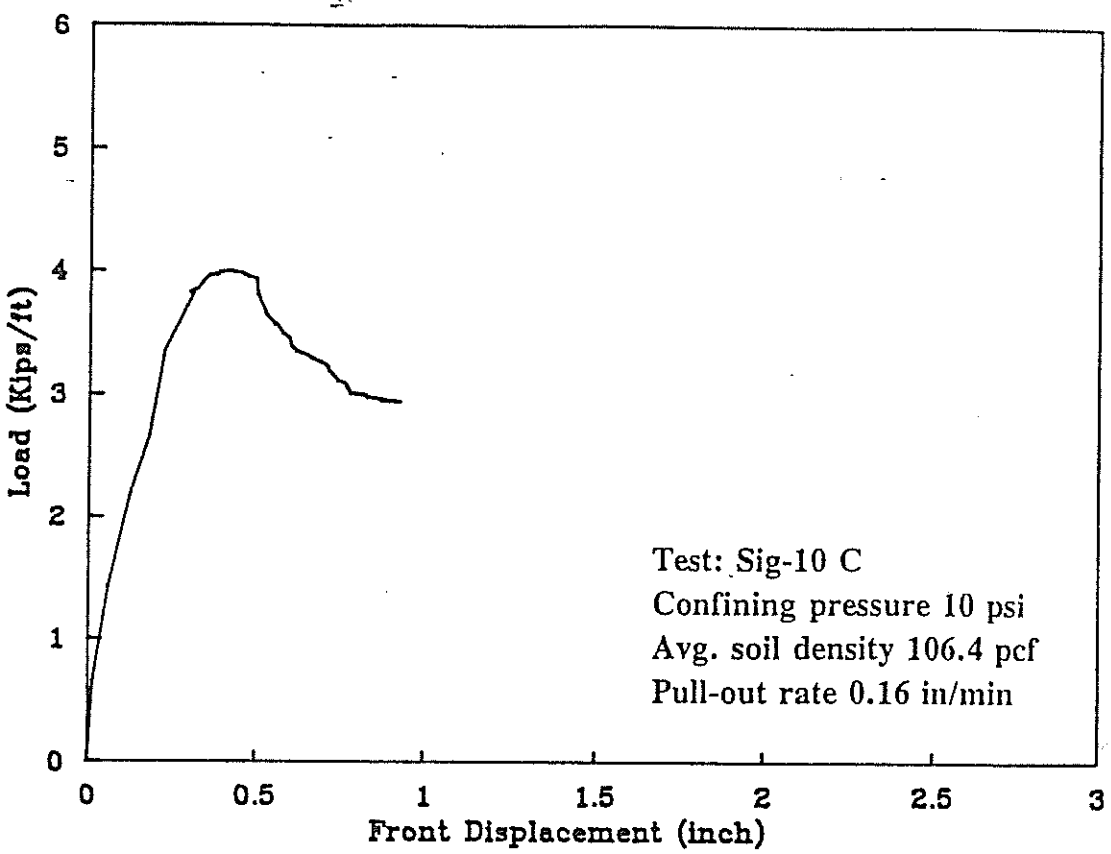
Load (Kips/ft)
Front Displacement (inch)
0
1
2
3
4
5
6
0
0.5
1
1.5
2
2.5
3
Test: Sig-10 C
Confining pressure 10 psi
Avg. soil density 106.4 pcf
Pull-out rate 0.16 in/min

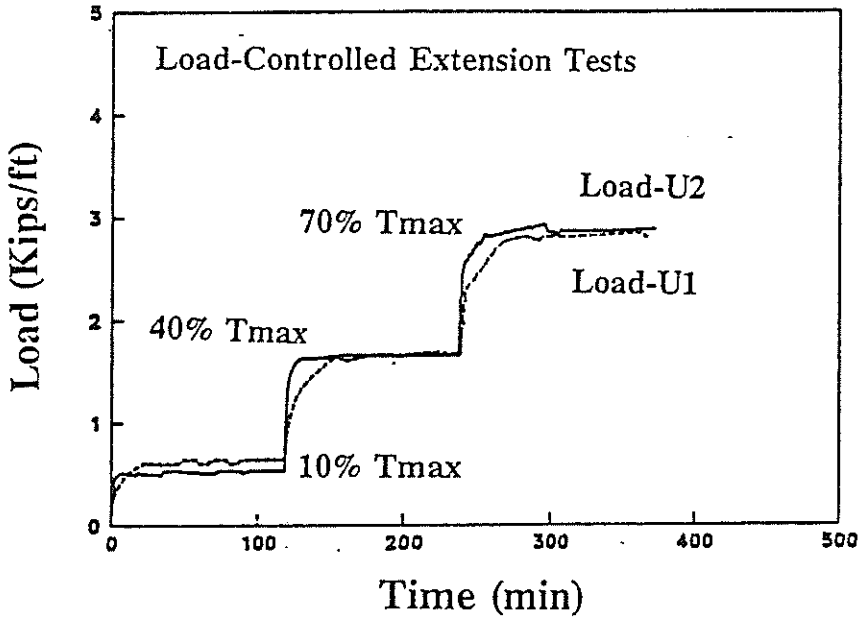
Load-Controlled Extension Tests
Load (Kips/ft)
Time (min)
Load-U2
Load-U1
70% Tmax
40% Tmax
10% Tmax
0
1
2
3
4
5
0
100
200
300
400
500

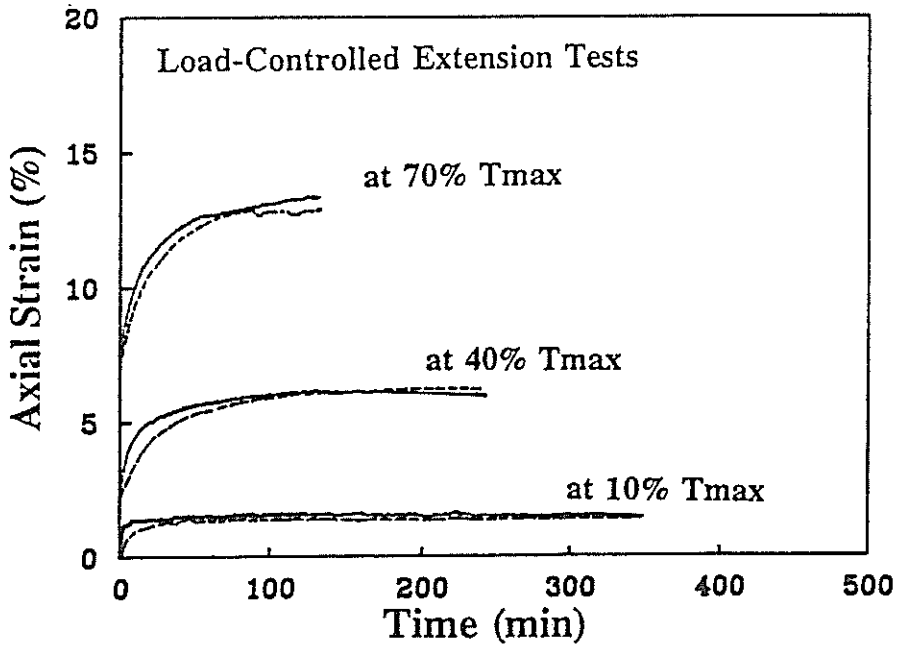
Load-Controlled Extension Tests
Axial Strain (%)
Time (min)
at 70% Tmax
at 40% Tmax
at 10% Tmax
0
5
10
15
20
0
100
200
300
400
500

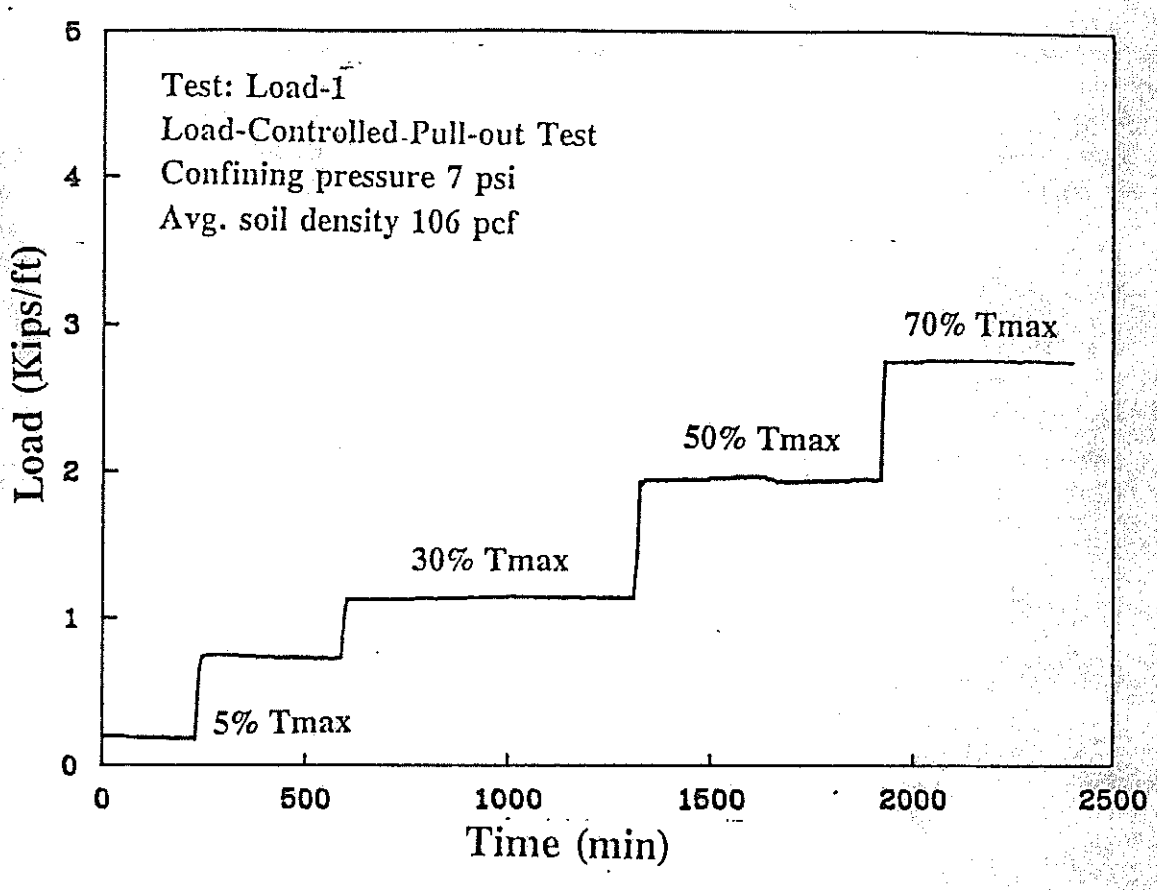
Test: Load-1
Load-Controlled Pull-out Test
Confining pressure 7 psi
Avg. soil density 106 pcf
70% Tmax
50% Tmax
30% Tmax
5% Tmax
Load (Kips/ft)
Time (min)
0
1
2
3
4
5
0
500
1000
1500
2000
2500

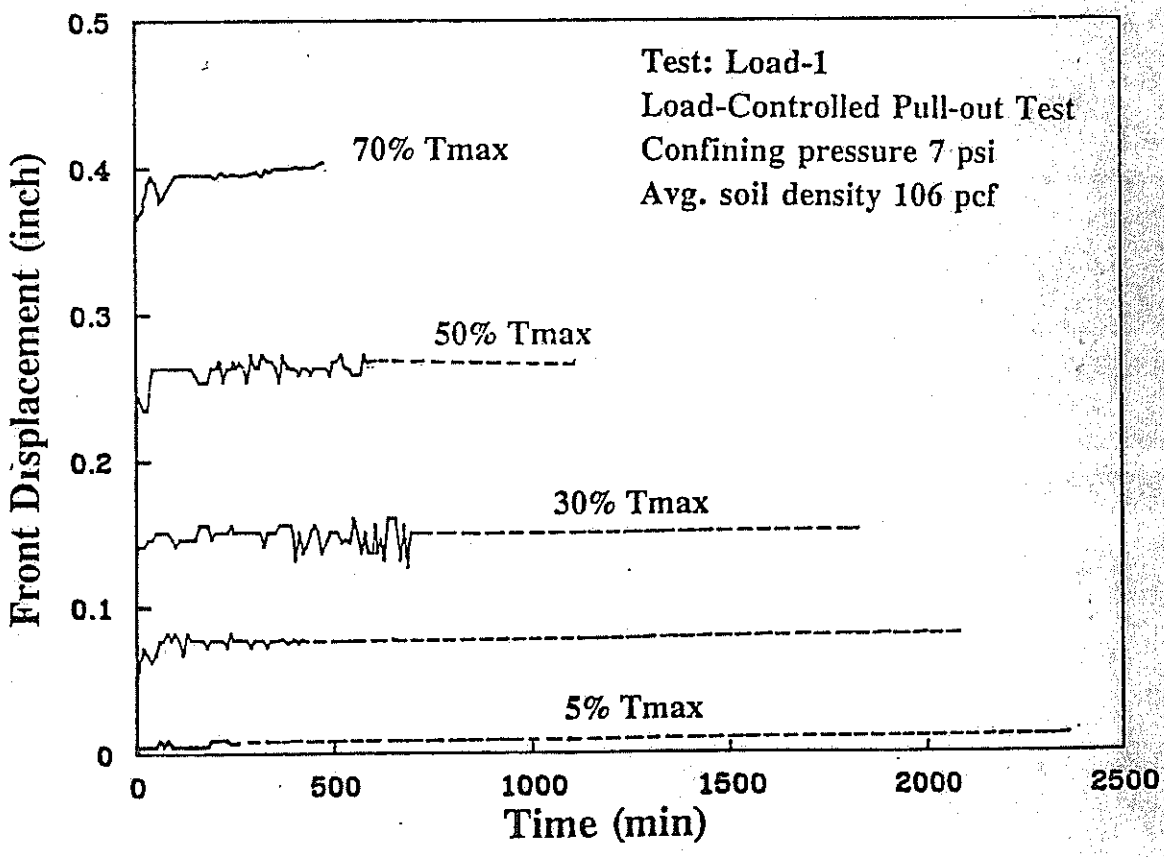
Test: Load-1
Load-Controlled Pull-out Test
Confining pressure 7 psi
Avg. soil density 106 pcf
70% Tmax
50% Tmax
30% Tmax
5% Tmax
Front Displacement (inch)
Time (min)
0
0.1
0.2
0.3
0.4
0.5
0
500
1000
1500
2000
2500